NAVAL FACILITIES ENGINEERING SERVICE CENTER
Port Hueneme, California 93043-4370

TECHNICAL REPORT
TR-2093-ENV

PERFORMANCE EVALUATION OF A PILOT-SCALE PERMEABLE REACTIVE BARRIER AT FORMER NAVAL AIR STATION MOFFETT FIELD, MOUNTAIN VIEW, CALIFORNIA (VOLUME I)

by

Charles Reeter, NFESC
Arun Gavaskar, Battelle
Bruce Sass, Battelle
Neeraj Gupta, Battelle
James Hicks, Battelle
Sam Yoon, Battelle
Tad Fox, Battelle
Joel Sminchak, Battelle

November 1998

REPORT DOCUMENTATION PAGE

Form Approved
OMB No. 0704-018

1. AGENCY USE ONLY *(Leave blank)*	2. REPORT DATE	3. REPORT TYPE AND DATES COVERED
	November 1998	Final: April 1996 - November 1998

4. TITLE AND SUBTITLE
PERFORMANCE EVALUATION OF A PILOT-SCALE PERMEABLE REACTIVE BARRIER AT FORMER NAVAL AIR STATION MOFFETT FIELD, MOUNTAIN VIEW, CALIFORNIA (VOLUME I)

5. FUNDING NUMBERS
Contract No. N47408-95-D-0730/DO 0014

6. AUTHOR(S)
Charles Reeter - NFESC
Arun Gavaskar, Bruce Sass, Neeraj Gupta, James Hicks, Sam Yoon, Tad Fox, and Joel Sminchak - Battelle

7. PERFORMING ORGANIZATION NAME(S) AND ADDRESSE(S)
Naval Facilities Engineering Service Center
1100 23rd Ave
Port Hueneme, CA 93043-4370

8. PERFORMING ORGANIZATION REPORT NUMBER
TR-2093-ENV

9. SPONSORING/MONITORING AGENCY NAME(S) AND ADDRESSES
Department of Defense
Environmental Security Technology Certification Program (ESTCP)
1725 Jefferson Davis Highway, Suite 1100
Arlington, VA 22202

10. SPONSORING/MONITORING AGENCY REPORT NUMBER

11. SUPPLEMENTARY NOTES

12a. DISTRIBUTION/AVAILABILITY STATEMENT
Approved for public release; distribution is unlimited.

12b. DISTRIBUTION CODE

13. ABSTRACT *(Maximum 200 words)*

A pilot scale permeable reactive barrier (PRB) or treatment wall demonstration project was initiated by the US Navy EFA West at the former Naval Air Station Moffett Field site in Mountain View, California about 3 years ago. Performance evaluations and cost-benefit analyses were performed by the US Naval Facilities Engineering Service Center (NFESC) and were sponsored by the Department of Defense (DoD) Environmental Security Technology Certification Program (ESTCP). The Moffett Field PRB uses a funnel-and-gate design, where the funnel is made of interlocking steel sheet piles and the gate consists of a reactive cell filled with zero-valent granular iron. Since its construction in April 1996, groundwater monitoring was conducted on a quarterly basis to demonstrate the effectiveness of the barrier technology in capturing and remediating groundwater that contained dissolved chlorinated hydrocarbon compounds. The primary contaminants of concern at Moffett Field in the vicinity of the PRB are trichloroethene (TCE), cis-1,2 dichloroethene (cDCE), and perchloroethene (PCE) at upgradient concentrations of about 2900 micrograms per liter (ug/L), 280 ug/L, and 26 ug/L, respectively. Quarterly monitoring events included water level measurements, field parameter testing, and groundwater sampling at about 75 monitoring points. Two tracer tests using bromide solutions and flow meter testing were also completed in April and August 1997 at the site. Iron cell coring samples were collected and analyzed in December 1997 for use as indicators of reactivity and longevity. Data from the quarterly monitoring, tracer testing, and iron cell coring have been used to determine the overall barrier performance. Since the first sampling event in June 1996, concentrations of all chlorinated compounds were either reduced to non-detect (ND) or to below the drinking water maximum contaminant levels (MCLs) within the first 2-3 feet of the permeable iron cell (gate).

The iron cell coring analyses and geochemical modeling from Moffett Field indicated that changes in the inorganic chemistry were caused by precipitation of calcite, carbonates, iron-sulfide, and hydroxide compounds. Chemical precipitates are a concern because of the potential loss of reactivity and permeability in the iron cell. In general, long-term performance and life expectancies at PRB sites are unknown. The DoD ESTCP, Environmental Protection Agency, and Department of Energy are sponsoring additional performance and longevity evaluations at multiple PRB sites across the country. This is being accomplished in partnership with the RTDF PRB Action Team in an effort to gain widespread regulatory acceptance and remedial project manager confidence in using the reactive barrier technology.

14. SUBJECT TERMS
Permeable reactive barrier; groundwater; remediation; zero-valent iron; treatment wall; chlorinated hydrocarbons; CVOC; TCE; PCE; DCE; VC; pump-and-treat alternative

15. NUMBER OF PAGES
191

16. PRICE CODE

17. SECURITY CLASSIFICATION OF REPORT	18. SECURITY CLASSIFICATION OF THIS PAGE	19. SECURITY CLASSIFICATION OF ABSTRACT	20. LIMITATION OF ABSTRACT
Unclassified	Unclassified	Unclassified	UL

Performance Evaluation of a Pilot-Scale Permeable Reactive Barrier at Former Naval Air Station Moffett Field, Mountain View, California

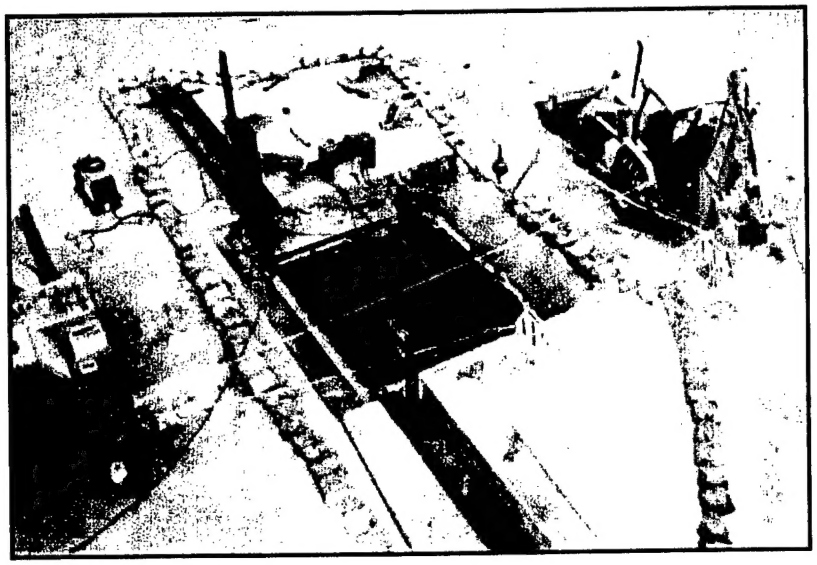

Prepared for

Naval Facilities Engineering Service Center
Port Hueneme, California

by

Battelle
. . . Putting Technology To Work

Columbus, Ohio
November 20, 1998

Project sponsored by

ESTCP

Performance Evaluation of a Pilot-Scale Permeable Reactive Barrier at Former Naval Air Station Moffett Field, Mountain View, California

Prepared for

NFESC
Port Hueneme, California
Project Officer: Charles Reeter

Prepared by

Battelle
Columbus, Ohio

Arun Gavaskar
Bruce Sass
Neeraj Gupta
James Hicks
Sam Yoon
Tad Fox
Joel Sminchak

November 20, 1998

Project Sponsored by

Executive Summary

A pilot-scale permeable reactive barrier was installed at Moffett Field in April 1996 and its performance was monitored over the following 16 months on a quarterly basis. The objective was to capture and treat a small portion of the West Side Plume that contains chlorinated volatile organic compound (CVOC) contaminants, primarily trichloroethene (TCE), *cis*-1,2-dichloroethylene (*cis*-1,2-DCE), and perchloroethene (PCE). The reactive cell in the funnel-and-gate type barrier is composed of granular zero-valent iron, a strong reducing agent.

The lowering of groundwater redox potential (Eh) and dissolved oxygen (DO), and the presence of nonchlorinated hydrocarbon products in the reactive cell, indicated conditions conducive to abiotic reductive dechlorination. Over the 16-month period after construction, the barrier consistently reduced groundwater concentrations of TCE, *cis*-1,2-DCE, and vinyl chloride to well below their respective maximum contaminant levels (MCLs). The range of degradation half-lives of these compounds observed in the field system conformed well with the half-lives predicted during bench-scale column tests. The reactive cell did not contribute any significant levels of dissolved iron to the groundwater and the water exiting the cell contained below 0.3 mg/L of iron, the secondary drinking water standard.

Water levels, a down-hole groundwater velocity meter, and tracer tests were used to evaluate the hydraulic flow characteristics of the barrier. The hydraulic capture zone of the barrier appears to be about 30 feet wide and extends about midway along each funnel wing. The dimensions of the barrier itself are 10 feet wide by 10 feet long, and it extends from approximately 5 to 22 feet below ground surface. The combined width of the funnel-and-gate section is 50 feet. The estimated groundwater velocity in the reactive cell ranges between 0.2 to 2 feet/day, providing a minimum residence time of 3 days in the reactive medium; the design requirement for contaminant degradation to desired levels was 2 days. The flow through the aquifer and the gate is heterogeneous and there appears to be more flow through the deeper portions of the reactive cell than in the shallower portions.

The geochemical evaluation included analysis of inorganic parameters in the barrier and its vicinity, as well as analysis of core samples of the iron collected at the end of 16 months of operation. Calcium and iron compounds appear to be precipitating out in the reactive cell. However, the actual calcium precipitate mass found on the iron cores was much lower than the loss of dissolved calcium in the groundwater flowing through the reactive cell. This may indicate that not all the precipitates formed stay in the gate; colloidal-sized precipitates could be flowing out with the groundwater. There were no indications, at the end of 16 months, of any impending decline in the reactivity or hydraulic performance of the barrier.

The barrier operated unattended and without maintenance after construction. The only recurring cost would be for compliance monitoring. If the barrier retains its performance over approximately 8 years, indications are that it will be more cost-effective than a groundwater pump-and-treat system.

Acknowledgments

Several organizations and individuals cooperated to make this demonstration possible. Jeff Marqusee of the Department of Defense Environmental Security Technology Certification Program (ESTCP) was instrumental in providing the funding for the technology performance evaluation. Charles Reeter of the U.S. Navy (NFESC) contributed substantially at the design stage of this study and throughout its implementation. Stephen Chao at Engineering Field Activity (EFA) West was primarily responsible for initiating the implementation of the pilot-scale permeable barrier at Moffett Field as an alternative for a conventional pump-and-treat system. Deirdre O'Dwyer, Jim Wulff, and Dave Berestka at Tetra Tech EMI played a major role in ensuring that the field activities associated with the performance evaluation were carried out with great diligence and competence. Steve Fann at the U.S. Navy Naval Facilities Engineering Service Center (NFESC) contributed significantly to the scale-up cost estimation process and comparison with the conventional pump-and-treat system. John Vogan, Robert Focht, and Stephanie O'Hannesin from Envirometal Technologies, Inc. provided review and advisory support. Several members of the U.S. Environmental Protection Agency (EPA) Remediation Technologies Development Forum (RTDF) Permeable Reactive Barriers Action Team also provided report reviews.

Contents

Contents
(Continued)

Page

Contents
(Continued)

Page

Contents
(Continued)

Contents
(Continued)

Page

Figures

Contents
(Continued)

Page

Contents
(Continued)

Tables

Contents
(Continued)

Page

Abbreviations and Acronyms

2-D	two-dimensional
3-D	three-dimensional
AFB	Air Force Base
ASF	Anderson-Schulz-Flory
Battelle	Battelle Memorial Institute
BEI	backscatter electron images
BFM	bromofluorobenzene
bgs	below ground surface
Br	bromine
BRAC	Base Realignment and Closure
BTEX	benzene, toluene, ethylbenzene, and xylenes
CCD	charged coupled device
CERCLA	Comprehensive Environmental Response, Compensation, and Liability Act
CFC	chlorofluorocarbon
CFU	colony forming units
cis-1,2-DCE	*cis*-1,2-dichloroethene
CPT	cone penetrometer test
CRQL	contract-required quantitation limit
CVOC	chlorinated volatile organic compound
DBFM	dibromofluoromethane
DCA	dichloroethane
DCE	dichloroethene
DNAPL	dense, nonaqueous-phase liquid
DO	dissolved oxygen
DOC	dissolved organic carbon
DoD	Department of Defense
DOE	Department of Energy
EDS	energy dispersive spectroscopy
EFA	Engineering Field Activity
Eh	redox potential relative to standard hydrogen electrode
EPA	Environmental Protection Agency
ESTCP	Environmental Security Technology Certification Program
GC-FAME	gas chromatograph-fatty acid methyl ester
GC/MS	gas chromatography/mass spectrometry

HAZWOPER	hazardous waste operations
HFB	horizontal flow barriers
ID	inside diameter
IRP	Installation Restoration Program
ITRC	Interstate Technology & Regulatory Cooperation
K	hydraulic conductivity
KBr	potassium bromide
LNAPL	light, nonaqueous-phase liquid
MCL	maximum contaminant level
meq	milliequivalencies
mg/L	milligrams per liter
mmol/L	millimoles per liter
MS	matrix spike
MSD	matrix spike duplicate
msl	mean sea level
MW	Montgomery Watson
NA	not applicable; not available
ND	not detected
NFESC	Naval Facilities Engineering Service Center
NPDES	National Pollutant Discharge Elimination System
NPL	National Priorities List
O&M	operations and maintenance
OD	outside diameter
ORP	oxidation-reduction potential
OSHA	Occupational Safety and Health Administration
PCE	perchloroethene
POTW	publicly owned treatment works
PPE	personal protective equipment
PRB	Permeable Reactive Barriers (Action Team)
PRP	potentially responsible party
PTZ	pretreatment zone
PVC	polyvinyl chloride
QA	quality assurance
QC	quality control

RCRA	Resource Conservation and Recovery Act
RFI	RCRA Facility Investigation
RI/FS	Remedial Investigation/Feasibility Study
ROD	Record of Decision
RPD	relative percent difference
RTDF	Remediation Technologies Development Forum
SEI	secondary electron images
SEM	scanning electron microscopy
SI	saturation index
S/O	sulfur to oxygen ratio
$t_{1/2}$	half-life
TCA	trichloroethane
TCE	trichloroethene
TDS	total dissolved solids
TOC	total organic carbon
TSA	trypticase-soy agar
TSS	total suspended solids
U.S. EPA	United States Environmental Protection Agency
VOA	volatile organic analysis
VOC	volatile organic compound
XRD	x-ray diffraction

Performance Evaluation of a Pilot-Scale Permeable Reactive Barrier at Former Naval Air Station Moffett Field, Mountain View, California

Battelle
Columbus, Ohio

November 20, 1998

1. Introduction

Several investigations at the former Naval Air Station, Moffett Field in Mountain View, California, have identified extensive groundwater contamination by chlorinated solvents. Contaminants of primary concern include trichloroethene (TCE); *cis*-1,2-dichloroethene (*cis*-1,2-DCE); 1,1-dichloroethene (1,1-DCE); 1,1-dichloroethane (1,1-DCA); and perchloroethene (PCE). Remediation of groundwater contaminated with chlorinated hydrocarbons by conventional pump-and-treat systems is difficult, costly, and generally ineffective. Therefore, the U.S. Navy's Engineering Field Activity (EFA) West and the Naval Facilities Engineering Service Center (NFESC) began investigating alternative technologies that have potential technical and cost advantages over pump-and-treat systems. One such alternative technology is the permeable reactive barrier, which has been identified by the U.S. Environmental Protection Agency (U.S. EPA, 1995) as an emerging technology for in situ cleanup of groundwater contaminated with chlorinated solvents.

A pilot-scale permeable reactive barrier was installed at Moffett Field in April 1996, primarily to study the application of this technology for remediation of the large regional chlorinated solvent plume on the west side of Moffett Field. A secondary objective of the pilot-scale permeable barrier was to improve the understanding of this technology for potential application to other Navy sites. The permeable barrier at Moffett Field uses a funnel-and-gate design, where the wings of the funnel are interlocked sheet piles and the gate consists of a reactive cell composed of granular iron with adjoining sections of pea gravel upgradient and downgradient to the direction of groundwater flow. Initial monitoring took place in June 1996, approximately 6 weeks after installation. Altogether, the investigation continued for six consecutive quarters, during which time chemical and hydrogeologic data pertaining to the performance of the reactive barrier were collected. This report discusses the scientific basis for reactive barrier technology and its implementation, documents the design and construction of the pilot-scale barrier at Moffett Field, identifies performance evaluation objectives and monitoring procedures, and provides detailed technology performance and cost assessments. Cost estimation, design recommendations, and implementation issues for a full-scale design are discussed in the final two sections of this report.

2. Technology Description

A permeable reactive barrier in its simplest form can be visualized as a trench filled with porous reactive material, placed in the path of a groundwater plume (Figure 2-1 a and b) (Gavaskar et al., 1998a, 1997a; Gillham, 1996). As the plume passes through the reactive material, the target contaminants are degraded to potentially nontoxic compounds. Several variations of this simple

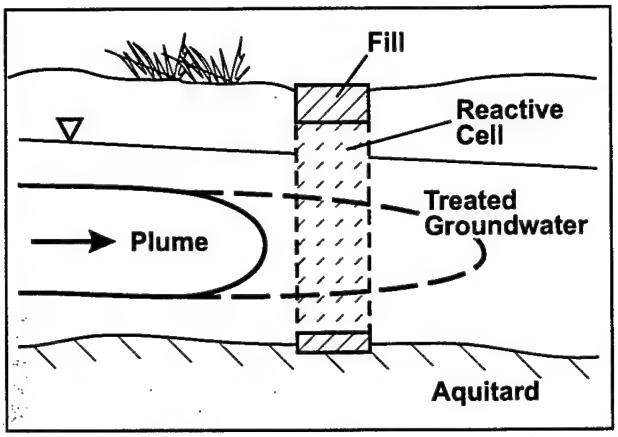

(a) Elevation view of a permeable barrier

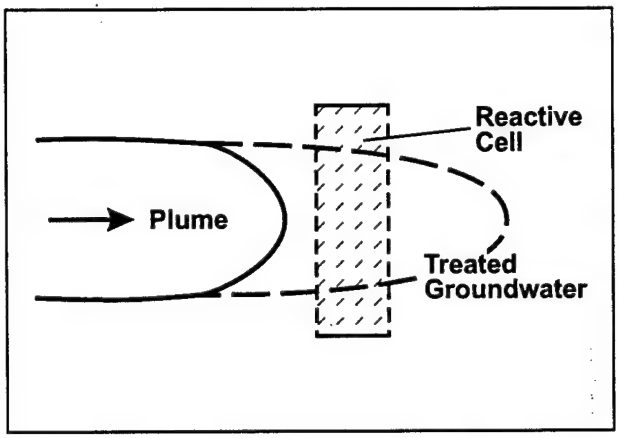

(b) Plan view of a continuous reactive barrier configuration

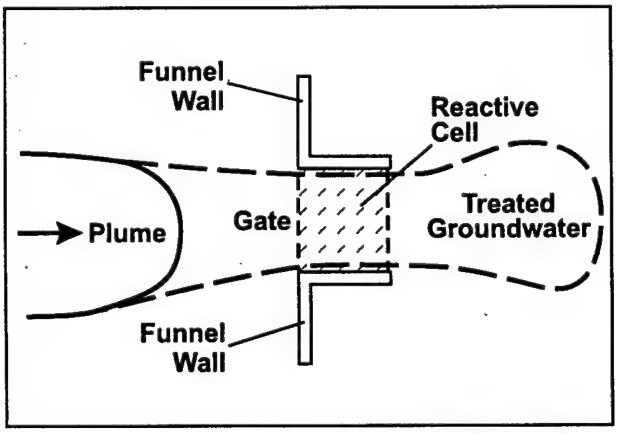

(c) Funnel-and-gate system (plan view)

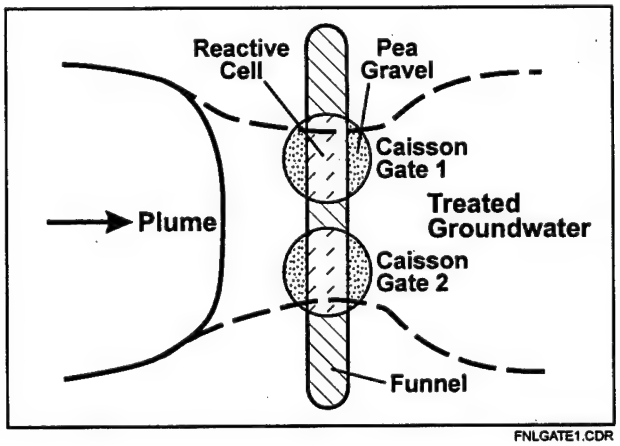

(d) Funnel-and-gate system with two caisson gates (plan view)

Figure 2-1. Schematic Illustrations of Some Permeable Barrier Configurations (Gavaskar et al., 1998a)

configuration are possible depending on individual site characteristics (Figure 2-1 a through d). One common variation shown in Figure 2-1c is the funnel-and-gate system, which combines permeable (gate) and impermeable (funnel) sections of the barrier to capture increased flow and better distribute the contaminant loading on the reactive medium. Multiple gates can be used for wider plumes. A simple gate could consist of a reactive cell or trench filled with the reactive medium (e.g., granular iron). The gate also could be divided into a reactive cell and other components. For example, pea gravel sections could be installed along the upgradient and downgradient edges of the reactive cell to improve porosity and mixing of the influent and effluent through the gate.

2.1 Technology Background

Permeable reactive barriers have emerged over the last 5 years as a promising alternative to pump-and-treat systems for treating dissolved groundwater contamination. The main advantage of a reactive barrier is the passive nature of the treatment. That is, for the most part, its operation does not depend on any external labor or energy input. Once installed, the barrier takes advantage of the in-situ groundwater flow to bring the contaminants in contact with the reactive material. A passive treatment system is especially desirable for contaminants such as chlorinated solvents, where the plume is likely to persist for several decades or hundreds of years. Considerable research (15 field pilot tests and 5 full-scale applications) has been conducted over the last 5 years to demonstrate variations of this technology.

The reactive material used in the barrier may vary depending on the type of contaminants being treated. The most common reactive medium used so far has been granular zero-valent iron, the use of which was patented by the University of Waterloo, Ontario (Gillham, 1993). Other reactive materials, such as bimetals and magnesium dioxide, are also being researched by the scientific community.

2.2 Theory of Operation and Limitations

Zero-valent iron is a strong reducing agent that can abiotically reduce dissolved contaminants, such as PCE, TCE, and other chlorinated solvents.

$$3Fe^0 + C_2HCl_3 + 3H^+ \rightarrow 3Fe^{2+} + C_2H_4 + 3Cl^- \quad (1)$$

Ethene and ethane are the main products of TCE degradation. However, indications are that these final reaction products are generated through multiple pathways. By the hydrogenolysis pathway, TCE degrades to *cis*-1,2-DCE, which in turn degrades to vinyl chloride. Both *cis*-1,2-DCE and vinyl chloride are fairly persistent under the reducing conditions of the iron medium and degrade to ethene and ethane more slowly than TCE or PCE. Fortunately, only 5% or less of TCE appears to take this pathway. Most of the TCE appears to degrade to ethene and ethane by the beta-elimination pathway (Roberts et al., 1996) through the formation of intermediates such as acetylene. These intermediates are short-lived and quickly degrade to ethene and ethane.

Other contaminants such as dissolved chromium and uranium, which are amenable to reduction by iron, also can be treated by precipitating them out of the groundwater. For example, results of a field study at a U.S. Cost Guard site in Elizabeth City, North Carolina demonstrated the effectiveness of zero-valent iron for remediating a plume containing chlorinated hydrocarbons and chromium (Puls et al., 1995). Full-scale permeable barriers also are being used to remediate uranium and technetium at the Y-12 site at Oak Ridge National Laboratory in Tennessee, and to remediate a uranium plume at Fry Canyon, Utah (RTDF, 1998). In general, the redox behavior of metals in solution is well understood, so that amenability of certain toxic metals for treatment by a reactive barrier can be predicted. Further discussion of the behavior of metals in solution is provided in Sections 4.4.4 (Inorganic Chemical Reactions in the Reactive Cell) and 4.4.5 (Geochemical Modeling).

The groundwater may have some native constituents, such as dissolved oxygen or carbonates, that react with and consume the reactive medium. Water itself is reduced, although slowly, by zero-valent metals such as iron.

$$2Fe^0 + O_2 + 2H_2O \rightarrow 2Fe^{2+} + 4OH^- \quad (2)$$

$$HCO_3^- + OH^- \rightarrow CO_3^{2-} + H_2O \quad (3)$$

$$Fe^0 + 2H_2O \rightarrow Fe^{2+} + H_2 + 2OH^- \quad (4)$$

These inorganic constituents could potentially affect the reactive and hydrologic properties of the reactive medium. Because several of these reactions generate hydroxyl ions, the pH of the water generally increases as it progresses through the iron. A possible scenario can be envisioned whereby precipitation of hydroxides and carbonates eventually causes loss of reactive surfaces and reduction in porosity and hydraulic conductivity of the reactive medium. This could affect the operation of the barrier by causing the plume to break through or bypass the reactive medium. A reactive iron barrier that has been operational for over 7 years at Borden, Ontario has yet to show any significant effects from such precipitation reactions. With new research underway to regenerate the reactivity and hydrologic characteristics of a reactive barrier without resorting to excavation and replacement of the reactive medium, it is hoped that any maintenance required in the future will be relatively infrequent and inexpensive.

Not all contaminated groundwater sites may be suitable for permeable barrier application. Generally, a review of existing site documents, such as the Resource Conservation and Recovery Act (RCRA) Facility Investigation (RFI) or Remedial Investigation/Feasibility Study (RI/FS) reports, and a visual examination of the layout of the site form the basis for a preliminary assessment of the feasibility of a permeable reactive barrier for a given site. Existing site documents may be scrutinized to evaluate a site in terms of the following application limitations of permeable barriers:

- Types of contaminants. Are the contaminants suitable for degradation by materials, such as iron, that are usable in a permeable barrier? Dissolved chlorinated solvent, chromium, and uranium compounds appear to be treatable with zero-valent iron. Of course, newer reactive materials could be developed for specific contaminants. But so far, reactive metals (e.g., iron) and magnesium dioxide (oxygen provider to promote aerobic degradation of petroleum hydrocarbons) typically have been used in field barriers.

- Contaminant distribution. Although the plume and aquifer dimensions are not an insurmountable hurdle, very deep or very wide plumes can increase the barrier cost. Barriers have so far been applied to plumes that are as wide as 1,000 feet (at the Denver Federal Center, Colorado) and as deep as 40 to 50 feet (Dover Air Force Base, Delaware, and Somersworth Landfill Site, New Hampshire). Innovative installation techniques, such as jetting and hydrofracturing, are a possibility for overcoming depth limitations. A competent aquitard is desirable so that the barrier can be keyed in. Hanging barriers (barriers that are not keyed into the aquitard) have been modeled, but great caution would be necessary in the field to ensure that the plume does not find a way under the barrier.

- Groundwater velocity. Extremely fast-moving groundwater may require a thicker barrier to ensure adequate residence time (contact time between the contaminants and the reactive medium) and this would increase cost. Extremely slow-moving or stationary groundwater may prevent contaminants from coming into contact with the reactive medium in any reasonable timeframe. Most sites are likely to be between these two extremes.

- Aquifer geochemistry. The inorganic composition of the contaminated groundwater may be an important factor in determining long-term performance of the permeable reactive barrier. Dissolved inorganic constituents can precipitate within the reactive cell, due to changes in pH and redox potential brought about by the interaction of groundwater with zero-valent iron. A potential concern, but undocumented result, is that extensive precipitation or oxidation of the iron may reduce both permeability and chemical reactivity of the reactive cell. Therefore, aquifer mineralogy and the concomitant inorganic chemistry of the groundwater (e.g., total dissolved solids content) may be an indicator of barrier longevity.

- Geotechnical considerations. Access to the plume is a major consideration for application of a permeable barrier. Overlying buildings and/or a plume that has moved off property boundaries are factors that may limit access to the plume. Underground utility lines also can make installation of a barrier difficult. The presence of cobbles or highly consolidated sediments in the subsurface also may impede installation equipment.

None of these limitations are insurmountable, but it is important to consider them so that a realistic preliminary assessment of the technical, economic, and administrative feasibility of a permeable barrier is obtained for the site. Prospective locations for the barrier are generally established at this stage.

2.3 Technology Specifications

The technology performance specifications for the permeable reactive barrier technology usually involve the following:

- Treating the contaminants in the captured groundwater to below their respective maximum contaminant levels (MCLs), drinking water standards, or to a risk-based alternative level. Table 2-1 contains the MCLs for various chlorinated contaminants, a common contaminant category at several U.S. Department of Defense (DoD) and U.S. Department of Energy (DOE) sites, in relation to their solubilities in water. There are special cases when administrative and/or resource constraints may allow the groundwater to be treated to above the MCLs, as long as a significant reduction in concentrations can be achieved and the remaining downgradient contamination is allowed to attenuate naturally.

Table 2-1. Properties of Common Chlorinated Organic Compounds

Compound	MCL (mg/L)	Water Solubility (mg/L at 25°C)	Density (g/cm3 at 20°C)	Vapor Pressure (pascals at 25°C)
Carbon tetrachloride	0.005	800	1.59	15,097
1,2-dichloroethane	0.005	8,600	1.26	9,000
Methylene chloride	0.005	20,000	1.33	46,522 (20°C)
Perchloroethene	0.005	150	1.63	2,415
1,1,1-trichloroethane	0.2	1,250	1.34	13,300
Trichloroethene	0.005	1,100	1.46	9,910
cis-1,2-dichloroethene	0.07	3,500	1.28	26,700
trans-1,2-dichloroethene	0.1	6,300	1.26	45,300
Vinyl chloride	0.002	2,000	0.91	350,000

- Ensuring that the interaction between the barrier materials and the groundwater constituents does not cause environmentally deleterious materials to be released in the downgradient aquifer. An example, in the case of reactive iron barriers, would be the release of dissolved iron into the downgradient aquifer. Iron is subject to a secondary drinking water standard of 0.3 mg/L. This standard is based on aesthetic rather than health considerations and many groundwaters naturally exceed this level. However, it is of interest to see how much the permeable barrier contributes to this parameter. Other groundwater parameters that could potentially undergo change as the groundwater passes through the aquifer are dissolved oxygen (DO), pH, and redox potential

(Eh). Elimination of DO and reduction in Eh may create downgradient anaerobic conditions that could potentially stimulate microbial growth.

- Achieving the desired hydraulic capture efficiency. The barrier should capture the entire plume or the targeted portion of the plume depending on the objectives of the installation. If any portion of the targeted contamination flows around, over, or under the barrier, the risk reduction potential of the barrier is compromised.

- Ensuring that the barrier retains its reactivity and hydraulic capture efficiency in the long term. Precipitation caused by the interaction of inorganic groundwater constituents (such as DO, alkalinity, calcium, and magnesium) and the reactive medium can deposit on the reactive medium surfaces over time and cause a reduction in the degradation rates of the contaminants and the volume of groundwater captured.

- Ensuring that the barrier represents a cost-effective option for the treatment of the targeted contamination at the site. The capital cost of the barrier can be directly compared with the capital cost of a pump-and-treat system (the conventional alternative). Historical experience with pump-and-treat systems generally enables a reasonable estimation of their average annual operations and maintenance (O&M) costs, which are expected to remain fairly constant over the long term. With the new barrier technology, estimation of annual O&M costs over the long term is a challenge mainly because the longevity of field reactive barriers has not been established. One rule of thumb suggests that if a reactive barrier were to retain its performance at the desired level for at least 10 to 15 years, it would be more cost-effective than a pump-and-treat system. Another unknown is the type of maintenance that would be required if the barrier loses its performance. Replacement of the reactive medium can be a relatively expensive option; flushing the reactive medium with a chemical that removes the precipitates formed potentially would be a relatively inexpensive option. More research is needed in these areas to obtain a better estimate of O&M costs.

A permeable barrier is generally constructed by qualified geotechnical contractors, several of whom now have experience with such installations. Construction crew members typically have general construction training and the specific Occupational Safety and Health Administration (OSHA) Hazardous Waste Operations (HAZWOPER) training. Depending on the types of contaminant and equipment involved, protective equipment may be required for certain activities. For example, when sheet piles are being driven in to form the funnel sections, a vibratory hammer is used, mandating use of hard hat, safety shoes, and safety glasses. Hearing protection may be required for those working close to this activity.

One safety concern at some sites has come from the necessity to send personnel into the excavated trench. Entry into the trench may be required to excavate around corners, install shoring or cross bracing, install monitoring wells, or to ensure that the reactive medium is well packed. Confined space entry rules require that a registered professional engineer examine the trench

prior to personnel entry. At more recent barrier installations, such as at Elizabeth City and Dover Air Force Base, specialized construction techniques (using a continuous horizontal trencher or caissons) have reduced or eliminated the need for entering the excavation.

Being a passive technology, ease of operation is the main advantage of the permeable barrier. Once the barrier is installed, operator involvement is limited to the relatively infrequent monitoring required to ensure that the barrier is performing as designed. Any maintenance required also is likely to be relatively infrequent, judging by the performance of the Moffett Field barrier so far and the performance of the barrier at Borden, which was installed in 1991 and has now been operational for more than 7 years without signs of decline in performance.

2.4 Key Design Steps

Figure 2-2 shows the steps in the design of a permeable reactive barrier. These steps involve the determination of the following:

- Site characteristics affecting barrier design
- Reaction rates or half-lives (through column testing)
- Location, configuration, and dimensions of the barrier (through hydrogeologic modeling)
- Longevity (through a geochemical evaluation)
- Emplacement options
- Cost

Some of the design steps are interrelated. Adequate site characterization provides the contaminant distribution and hydrogeologic parameters required for designing the location, configuration, and dimensions of the barrier. Column tests are used to determine the reaction rates of the contaminants, which are then used to determine the residence time or contact time required, which in turn is used (along with the groundwater velocity determined during site characterization) to determine the thickness of the reactive cell. The width of the reactive cell or gate depends upon the relative permeabilities of the aquifer and reactive medium, as well as the width of the plume targeted for capture. The depth of the barrier is determined by the depth of the aquitard. In most cases, especially for chlorinated solvent contamination, the barrier is expected to be keyed into the aquitard. Hanging barriers (those completed to a depth above the aquitard) have been proposed but they may be more suitable for plumes emanating from light, nonaqueous-phase liquid (LNAPL), rather than dense, nonaqueous-phase liquid (DNAPL) sources. There is always a possibility that some contamination may eventually find its way below the hanging barrier. Similarly, the top of the reactive barrier should be completed to a foot or more above the seasonal, or preferably historical, high water table level. This prevents the water from periodically flowing over the top of the barrier.

Evaluation of the inorganic constituents of the site groundwater provides an indication of the barrier's expected longevity and of the safety factors that may be required in the barrier dimensions to account for eventual decline in performance. The monitoring strategy includes regulatory compliance monitoring and engineering evaluation of the barrier performance. The

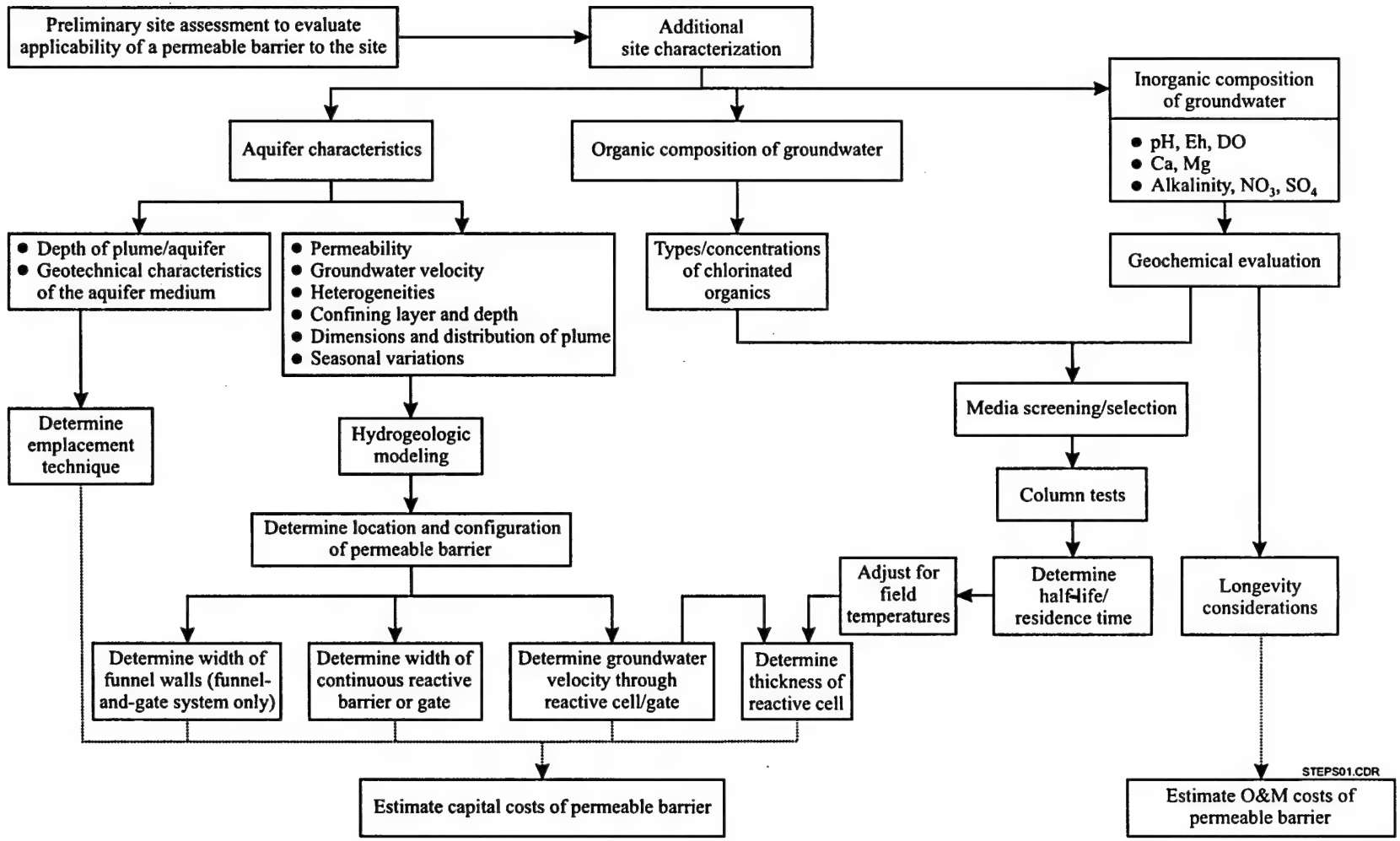

Figure 2-2. Steps in the Design of a Permeable Barrier System

monitoring strategy used at Moffett Field and the resulting evaluation of barrier performance are the main focus of this report. Cost is a consequence of the dimensions of the barrier, the reactive medium selected, the construction techniques used, and the longevity of the barrier.

2.5 Mobilization, Construction, and Operation

Once the location, configuration, and dimensions of the barrier have been designed, a qualified geotechnical contractor is hired to construct the barrier. Most qualified geotechnical contractors have standard construction equipment (such as a backhoe, crane, vibratory hammer, front-end loader, etc.) that can be used for the job. Generally, at least 6 weeks are required for mobilization, including 4 to 5 weeks for readying the equipment and transporting it to the site. Once at the site, the equipment can be set up relatively quickly and construction usually starts within a week. Most of the equipment can be set up in a 50- by 50-foot area that has no overhead utilities. The iron or other reactive medium has to be purchased and transported to the site as well. The iron is generally sold in 3,000-pound waterproof bags and is in a form ready to be installed. Monitoring wells within the barrier are installed during barrier construction. Monitoring wells in the surrounding aquifer can be installed at any time with standard well drilling equipment. Once the barrier is installed and the ground surface has been restored, the barrier operates on its own using the natural groundwater flow to bring the contaminants in contact with the reactive medium.

2.6 Advantages over Conventional Technologies

The permeable barrier technology has five main advantages over conventional pump-and-treat systems:

1. It is passive in nature (no external energy is consumed).

2. It has the potential for treating dissolved chlorinated solvents in a groundwater plume to very low levels.

3. No aboveground structures are required, making the property suitable for more uses.

4. No hazardous waste byproducts requiring disposal are generated, and discharge of treated effluent to a National Pollutant Discharge Elimination System (NPDES) outfall or publicly owned treatment works (POTW) is not needed.

5. It has potential for long-term unattended operation.

3. Demonstration Design

This section describes the strategy and planning leading to the construction of the pilot barrier at Moffett Field and the subsequent performance evaluation.

3.1 Demonstration Site/Facility Background

As part of the Installation Restoration Program (IRP), the U.S. Navy has been identifying and evaluating past hazardous waste sites at the former Naval Air Station, Moffett Field (now referred to as Moffett Federal Airfield) in an effort to control the spread of contamination from these sites. Moffett Field, as it is still commonly called, is located in Mountain View, California (see Figure 3-1). Moffett Field appeared on the Superfund's National Priorities List (NPL) in June 1987. As a result, the RI/FS process was initiated as required by the Comprehensive Environmental Response, Compensation, and Liability Act (CERCLA).

Several investigations at Moffett Field have identified extensive groundwater contamination by chlorinated solvents. The primary contaminants of concern are TCE; *cis*-1,2-DCE; 1,1-DCE; 1,1-DCA; and PCE. Remediation of groundwater contaminated with chlorinated volatile organic compounds (CVOCs) by pump-and-treat systems is difficult, costly, and generally ineffective. NFESC and the U.S. Navy's EFA West are therefore investigating alternative technologies that have potential technical and cost advantages over conventional pump-and-treat systems. The permeable barrier technology has been identified by the U.S. Environmental Protection Agency (U.S. EPA, 1995) as an emerging technology for cleanup of groundwater contaminated with chlorinated solvents, and was the technology of choice for this pilot demonstration in the West Side Plume (the large regional chlorinated solvent plume on the west side of Moffett Field) (Figure 3-2). The pilot barrier is located in the aquifer region underlying a parking lot at the intersection of Severyns Avenue and South Akron Road (Figure 3-3).

3.2 Physical Setup and Operation

Table 3-1 shows the schedule of events leading to the completion of the demonstration. After completion of the bench-scale testing and design activities at Moffett Field, a pilot-scale permeable barrier was installed in April 1996, primarily to study the application of this technology for remediation of the West Side Plume (see Figure 3-2). Another objective of the pilot-scale permeable barrier was to improve the understanding of this technology for potential application to other Navy sites.

Battelle Memorial Institute (Battelle) was contracted by NFESC in Port Hueneme, California, under delivery order N47408-95-D-0730/DO 0014, to develop a Performance Monitoring Plan (Battelle, 1997a) for evaluating the pilot-scale permeable barrier at Moffett Field. This plan was developed with funding provided by the U.S. DoD Environmental Security Technology Certification Program (ESTCP) for establishing a framework to evaluate the technical performance and cost-effectiveness of the pilot barrier. The results of this permeable barrier technology

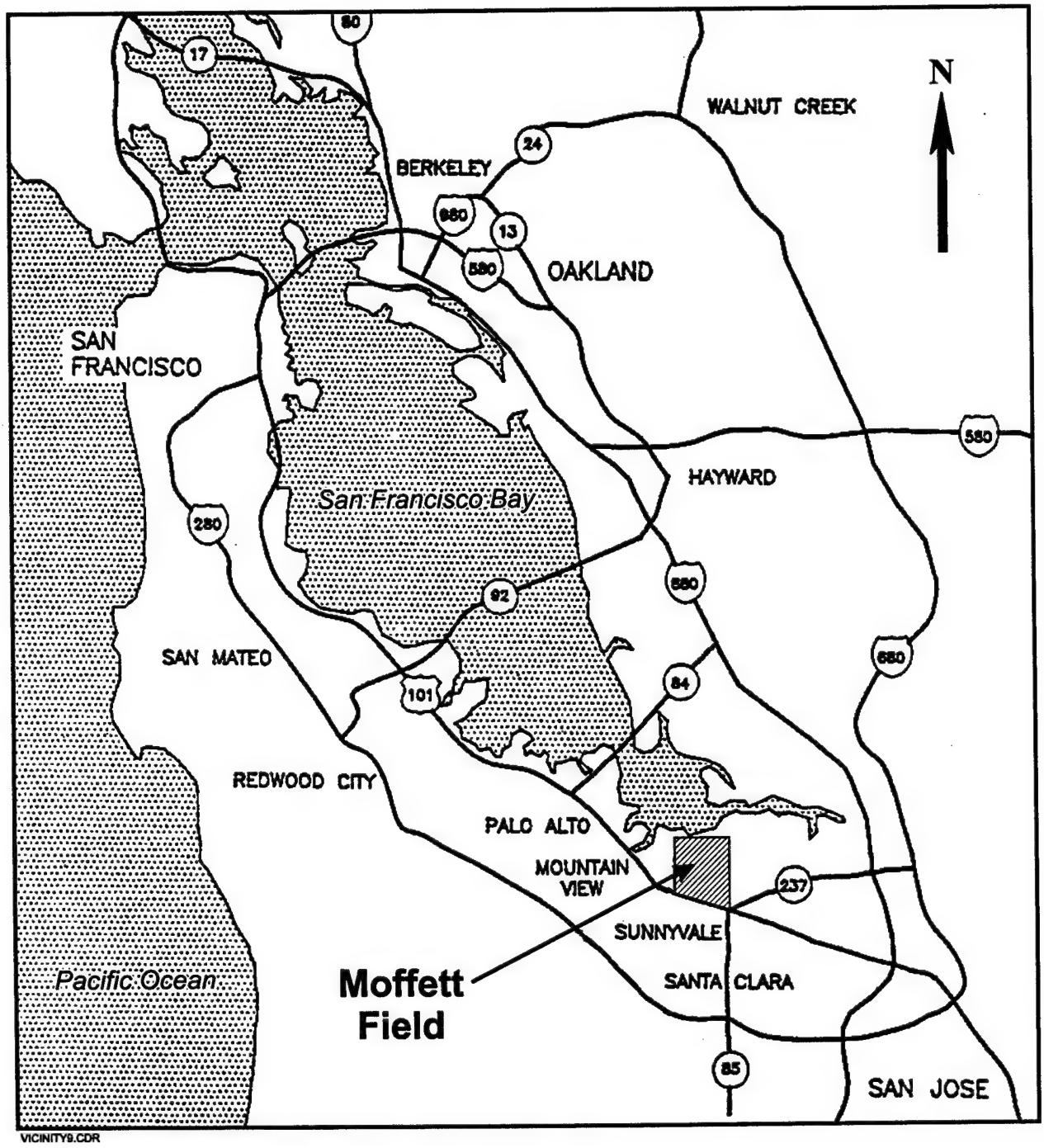

Figure 3-1. Map of San Francisco Bay and Vicinity

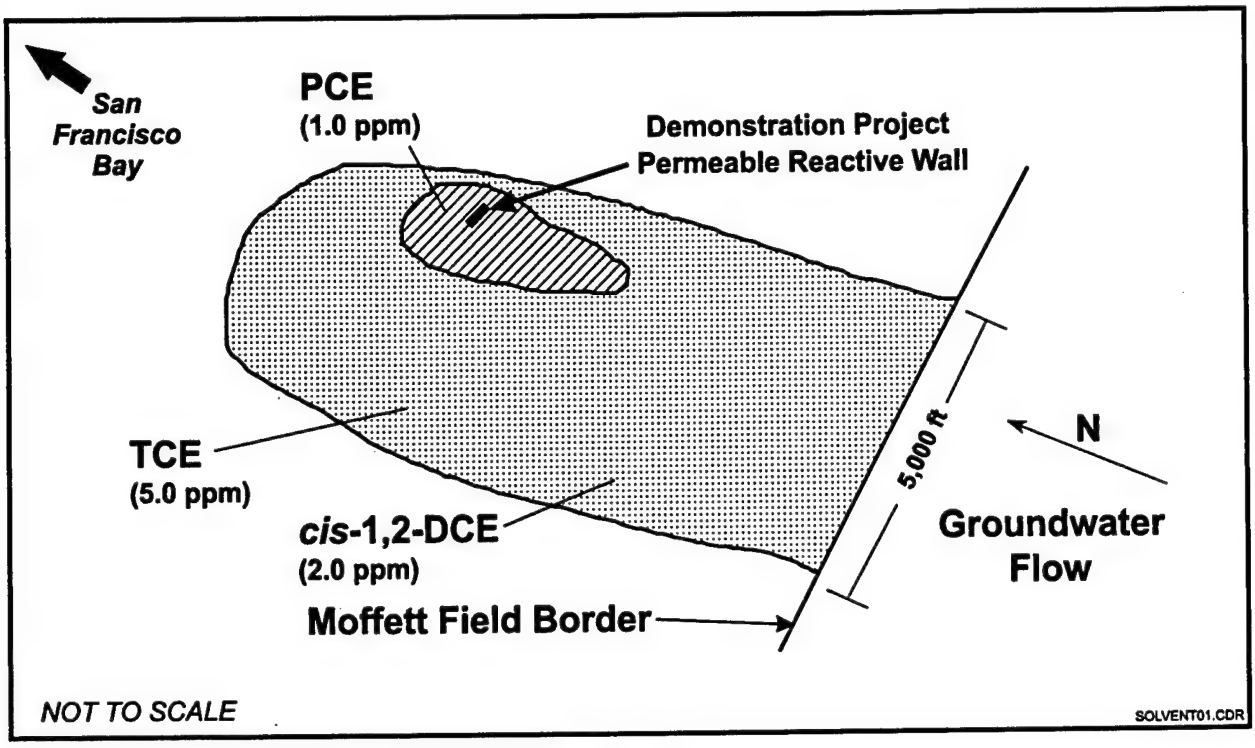

Figure 3-2. Moffett Field Solvent Plume

demonstration project are being documented in this report to assist in the potential use of this technology at Moffett Field and other DoD sites contaminated with chlorinated solvents.

The pilot barrier was constructed at Moffett Field in April 1996. Preliminary monitoring of groundwater conditions in and around the Moffett Field permeable barrier was conducted in June 1996, about 6 weeks after installation, to establish that the barrier was functioning as designed. The results of this preliminary monitoring event showed that the TCE and PCE concentrations in the groundwater flowing through the barrier were being significantly reduced.

Subsequent quarterly monitoring (five quarters) has enabled the evaluation of barrier performance under seasonal changes in contaminant and flow characteristics. Quarterly monitoring also allowed an estimation of the length of time it takes the barrier to reach steady-state performance. In addition, two tracer tests and down-hole groundwater velocity measurements were conducted. At the end of approximately 1.5 years, core samples of the reactive medium from the barrier and a core sample of the downgradient aquifer were collected and analyzed to evaluate potential precipitation and biofouling effects on the barrier and aquifer media, respectively.

Table 3-2 shows the various participants involved in the demonstration. Battelle, under contract to NFESC, prepared the performance monitoring plan for the demonstration, coordinated its implementation, conducted the hydrogeologic and geochemical modeling, evaluated the

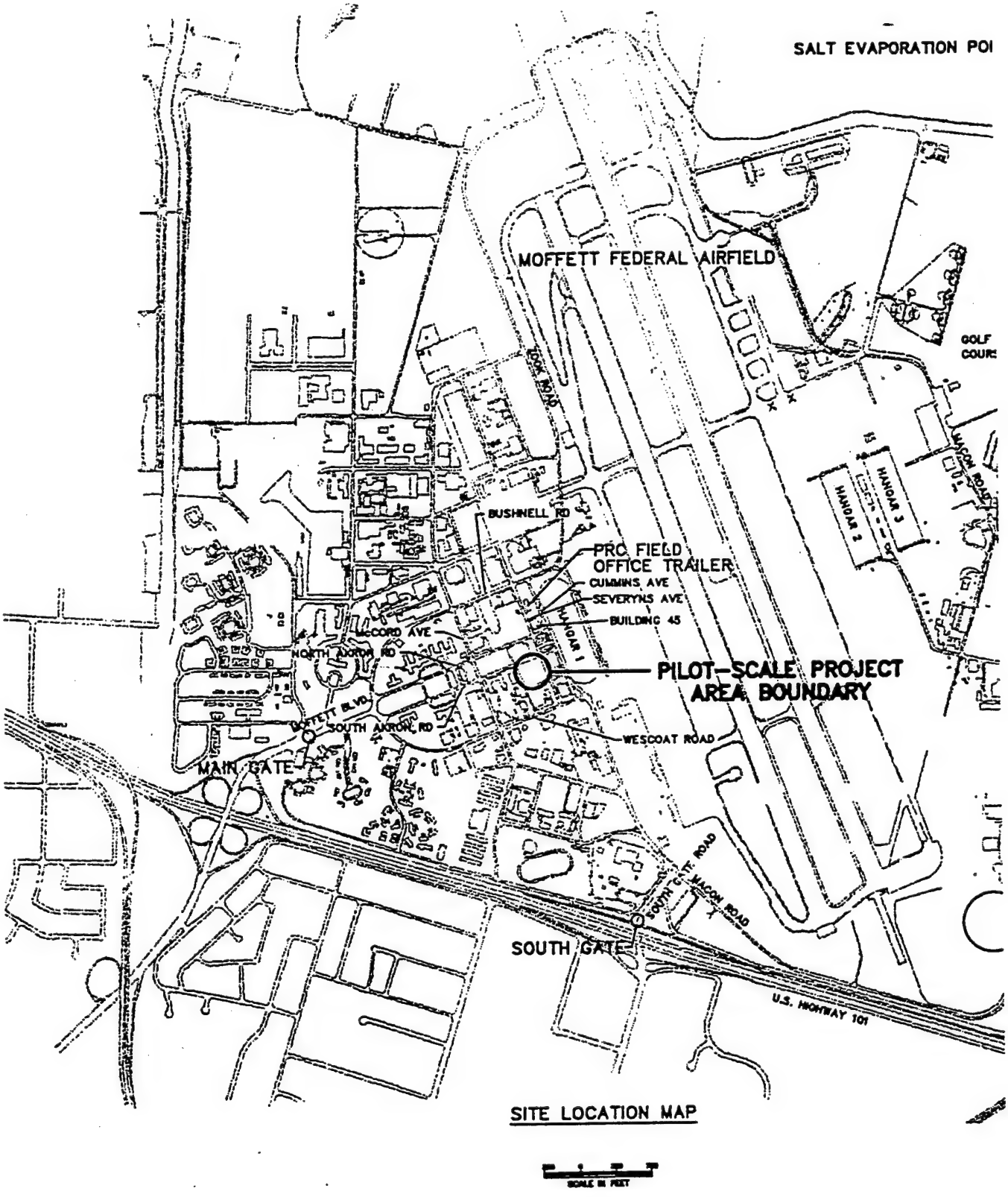

Figure 3-3. Moffett Local Map

Table 3-1. Demonstration Activities Schedule

Activity	Date Completed
Site characterization	December 1995
Bench-scale tests	October 1995
Preliminary groundwater modeling report	June 1996
Performance Monitoring Plan (draft)	September 1996
Updated groundwater modeling report	November 1996
Performance Monitoring Plan (final)	July 1997
Pilot barrier construction	April 1996
First quarterly monitoring event	June 1996
Second quarterly monitoring event	September 1996
Third quarterly monitoring event	January 1997
Fourth quarterly monitoring event	April 1997
Fifth quarterly monitoring event	October 1997
First tracer test	April 1997
Second tracer test	August 1997
Iron cores collection	December 1997
Draft Performance Evaluation Report	June 1998
Final Performance Evaluation Report	November 1998

Table 3-2. List of Project Participants

Funding for Demonstration	
ESTCP	**BRAC**
NFESC Evaluation of barrier performance	**EFA West** Design and construction
Battelle Performance evaluation plan Field monitoring Data evaluation, modeling Report preparation **Tetra Tech EMI** Field monitoring **Subcontract laboratories** Analysis of iron cores **Precision Sampling Inc.** Drilling for iron cores	**Tetra Tech EMI** Bench-scale tests Barrier design Oversee construction **EnviroMetal Technologies, Inc.** Design guidance **Slurry Systems Inc.** Construction subcontractor **Subcontract laboratories** Groundwater analysis

monitoring and modeling results, and prepared this demonstration report. TetraTech EMI (formerly PRC Environmental Management, Inc.), under contract to EFA West, conducted the bench-scale tests, coordinated the design, supervised the construction of the pilot barrier, and conducted the sampling and analysis for the field effort outlined in the performance monitoring plan.

3.3 Demonstration Site/Facility Characteristics

This section describes the results of the site characterization conducted to determine the physical characteristics of the aquifer underlying the pilot barrier site.

3.3.1 Site Geology and Hydrogeology

A discussion of the subsurface characteristics of the Moffett Field site that influence the performance of the permeable barrier is presented below.

3.3.1.1 Site Geology

Sediments in the Moffett Field area have been described in previous technical reports (PRC, 1995; IT Corp., 1993) as a complex mixture of fluvial-alluvial clay, silt, sand, and gravel that slopes toward San Francisco Bay in the northeast. The deposits are Holocene/Pleistocene in age and generally are associated with flood events. Sands and gravels form interbraided channel structures that are incised into silt and clay deposits. These channels are divided into layered aquifers designated as A, B, and C aquifers. These aquifers extend more than 200 feet below land surface. Multiple channels of sand and gravel have been delineated at various elevation intervals within the aquifer zones (PRC, 1995).

The major region of interest for this study is the near-surface A aquifer. This zone is not laterally homogeneous due to the interbraided channel nature of the sediments. In the immediate vicinity of the permeable barrier, well logs, cone penetrometer tests, and geophysical logs were used to characterize sand channels and surrounding interchannel deposits. Several individual channels were mapped in the A aquifer and the permeable barrier was located in one of these sand channels. Figure 3-4 shows the location of the permeable barrier relative to the lithologic variations at the site. As shown on this figure, the channel is oriented north/south and consists of high conductivity sand and gravel surrounded by interchannel deposits of lower conductivity silt and clay. Based on the channel maps, the permeable barrier is roughly perpendicular to the length of the channel. The reactive gate and the funnel walls cover the whole width of the channel and are keyed into low-permeability sediments east and west of the target channel. These heterogeneities are likely to have a significant impact on groundwater flow through and around the barrier wall.

In the vertical direction, the A aquifer can be further divided into two zones, A1 and A2, separated by a silty-clay zone called the A1/A2 confining layer (aquitard) (Figure 3-5). The A1 aquifer zone is up to 20 feet thick and is overlain by a clayey surface layer of varying thicknesses. Well logs and paleochannel maps suggest that the confining layer underlying the A1 aquifer zone is relatively thin in some areas and discontinuous. The A1 and A2 aquifer zones are interconnected in some areas. The A2 aquifer zone is 0 to 20 feet thick and extends to 40 feet below mean sea level (msl). Although both A1 and A2 aquifer zones are contaminated, the pilot-scale reactive barrier penetrates only the A1 zone. Further, the barrier does not penetrate the A1/A2

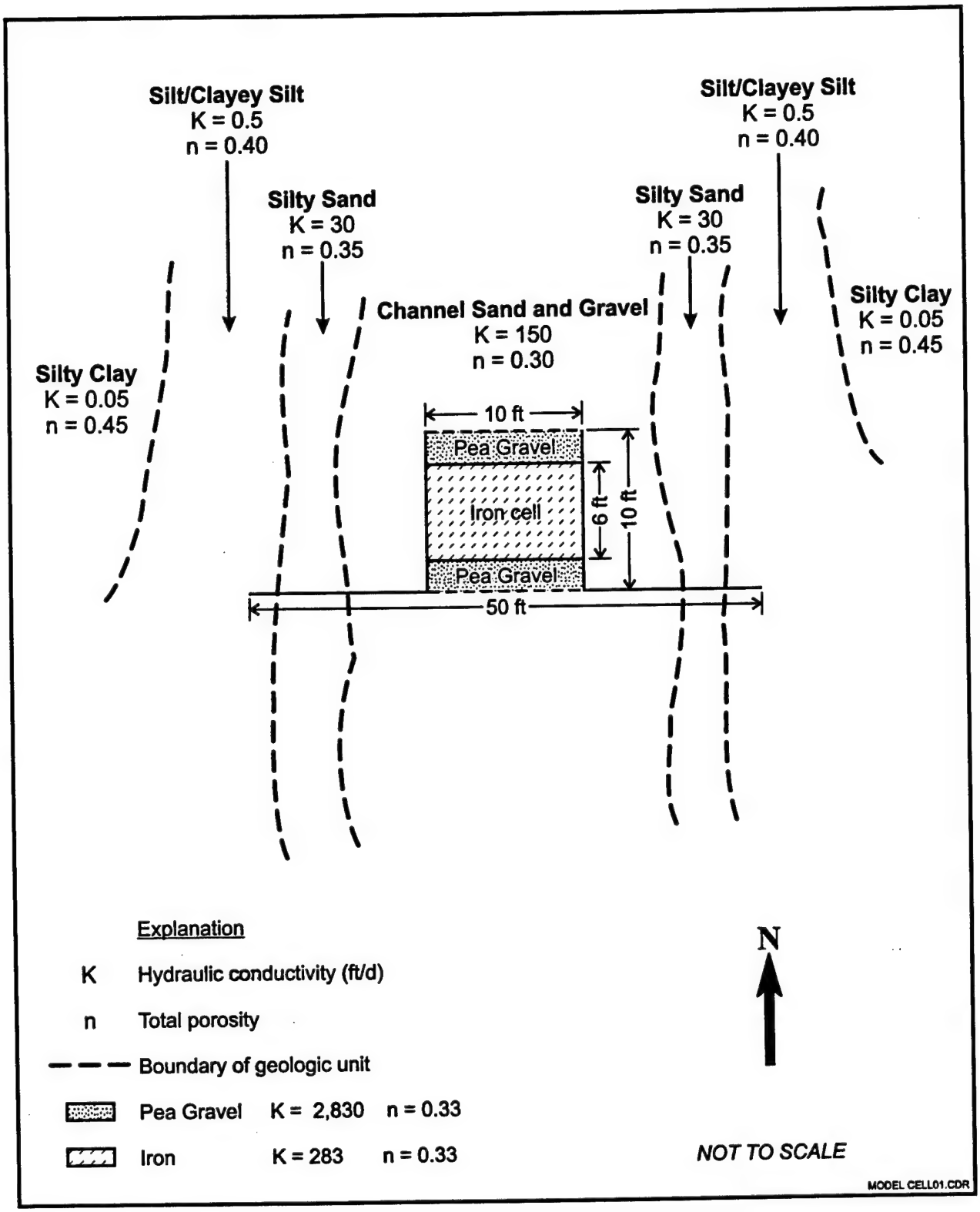

Figure 3-4. Permeable Barrier Location Relative to Lithologic Variations in Surrounding A1 Aquifer Zone (Adapted from PRC, 1996a)

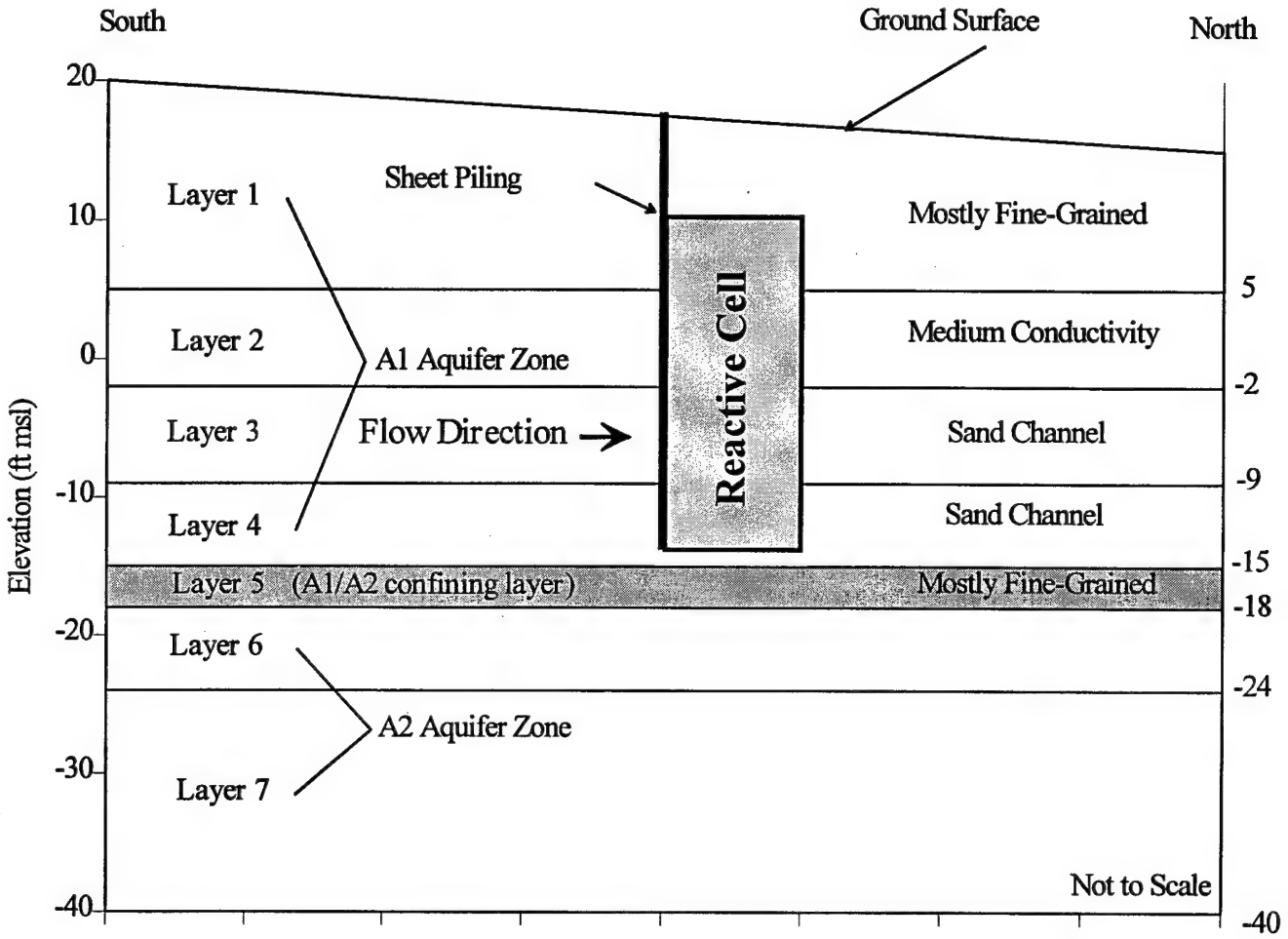

Figure 3-5. Schematic Depiction of Sediment Layers and Model Layers Along a North-South Vertical Section Through the Permeable Barrier (Based on Battelle, 1996a)

aquitard because of concern over breaching the thin aquitard. Instead, the bottom of the permeable barrier lies 1 to 2 feet above the top of the aquitard, creating a permeable gap at the bottom of the barrier. Thus, there is the potential for some underflow through this gap. Again, the main zone of interest for this study is the A1 aquifer zone.

3.3.1.2 Site Hydrology

Water levels and pumping tests indicate that the A1 aquifer zone behaves as a semi-confined aquifer at this site. Figure 3-6 shows observed preconstruction (January 1996) water levels as measured in the A1 aquifer zone. In the vicinity of the permeable barrier location, the observed hydraulic gradient varies from 0.005 to 0.009. This is also a representative range for historic hydraulic gradient at the site. Although there are some small-scale local variations due to heterogeneities, the overall flow direction is roughly from south to north toward the San Francisco Bay. An IT (1993) report notes a slight upward gradient from A2 to A1 in the area, suggesting that the A2 aquifer zone is not fully confined. The connection between the two aquifers is also suggested by the presence of groundwater contamination in both the aquifers. Historic water level information from the site indicates that there is a strong correlation between the water levels in shallow aquifers and the rainfall. Thus, the groundwater levels are usually the highest during winter months when most of the rainfall occurs and lowest during late summer.

Four pumping tests were conducted by IT to determine the hydraulic properties of sediments in the area (IT Corp., 1993). Hydraulic conductivity (K) estimates from well tests range from 13 to 461 feet/day in the A1 aquifer zone and from 9 to 576 feet/day in the A2 aquifer zone. These tests show that there is a strong variability in the hydraulic conductivity at the site. Porosity values from 23 samples (PRC, 1993) ranged from 0.30 for sand and gravel to 0.45 for silty clay. Slug tests and pumping tests in the A1/A2 confining layer showed K of 0.1 to 0.3 foot/day.

As part of this demonstration, an attempt was made to improve the K determination at the site. Slug tests were conducted in February 1997 within the reactive cell and in the aquifer wells (Battelle, 1997c). The tests within the reactive cell were inconclusive because recoveries were rapid and good time series profiles of water levels were unachievable due to the high K of the granular iron. Better results were obtained in the slug tests conducted in the aquifer. K values ranged from 0.04 foot/day to 633 feet/day and were related to lithologic variations as expected from previous site characterizations. The higher K values were observed in wells WIC-7, WIC-8, PIC-31, and WIC-3. These wells are located in the sand channel that runs through the deeper regions of the A1 aquifer zone containing the pilot gate (see Section 3.8.2). The lower K values were observed in PIC-27 and PIC-24 wells located in the interchannel silty and clayey deposits that run through the location of the funnel walls.

Based on the observed K of about 30 feet/day at WIC-7 and WIC-8, a representative hydraulic gradient of 0.007 and aquifer porosity of 0.30, the average linear velocity in the sand channel is calculated to be about 0.7 foot/day. This is lower than the estimated preconstruction velocity of 3.3 feet/day, which was based on a K of 150 feet/day and a lower gradient. Due to the spatial

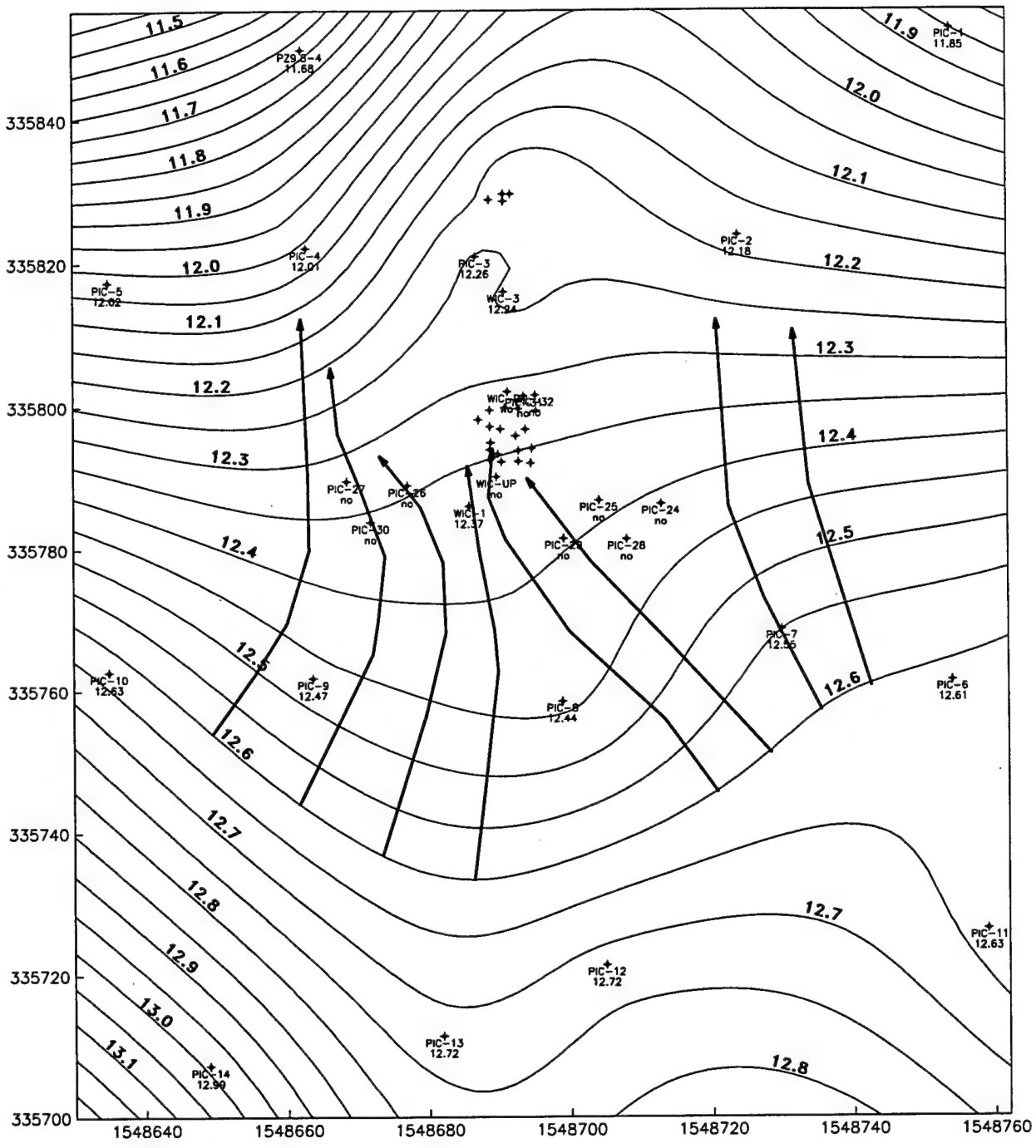

Figure 3-6. Observed Preconstruction (January 1996) Water Levels Near the Permeable Barrier

variations in aquifer parameters, the actual velocity may be anywhere within an order of magnitude of this value. A representative range of groundwater velocity in the A1 aquifer zone is 0.2 to 5.0 feet/day. However, the true range of velocities is probably at the lower end of the representative range when considered on a site-wide scale. In summary, based on the site characterization information, the groundwater flow velocity in the A1 aquifer zone varies depending on the hydraulic properties of the sediments in very localized settings.

3.3.2 Description of Contaminant Plume

The permeable reactive barrier lies within a regional groundwater plume of chlorinated volatile organic compounds (CVOCs). Cleanup and contaminant identification activities have been underway at Moffett Field since 1987. Contaminants at Moffett Field include waste oils, solvents, cleaners, and jet fuels. Among many possible sources of contamination on the site are several underground storage tanks, aboveground storage tanks, a dry cleaning facility, and sumps. CVOCs found in the vicinity of the barrier include TCE; PCE; *cis*-1,2-DCE; 1,1-DCE; 1,1-DCA; and other chlorinated hydrocarbons. TCE is the most prevalent contaminant on the site. Nonchlorinated volatile organic compounds (VOCs), such as benzene, toluene, ethylbenzene, and xylene (BTEX) compounds, are mostly absent in the vicinity of the current barrier demonstration project.

Routine groundwater sampling was already underway between January 1991 and January 1995. For this demonstration, groundwater chemical data were obtained for wells within the hydrogeologic evaluation zone; that is, within 1,500 feet of the permeable barrier. Figure 3-7 presents a map of the 17 aquifer wells that are within the evaluation zone. Table C-1 (in Appendix C) contains a list of the well location coordinates, the top of casing elevations, casing diameters, and well screen intervals for the wells inside the permeable barrier and its vicinity.

The CVOC plume exists mainly in the A aquifer (IT Corp., 1993). The plume is more than 10,000 feet long, about 5,000 feet wide, oriented north/northeast, and tapers to the north. TCE levels reported by IT Corp. (1992) exceeded 20 mg/L, and PCE levels were about 0.5 mg/L in the A aquifer. The distribution of TCE in the West Side Plume is shown in Figure 3-8.

Table 3-3 contains historical data for the eight most prevalent CVOCs in Well W9-35, an A1 aquifer zone well near the current barrier location. The highest concentrations are for TCE, *cis*-1,2-DCE, and PCE. Fluctuations in concentrations of these three contaminants in Well W9-35 are plotted against time over a 6-year period in Figure 3-9. For the most part, historical TCE concentrations have fluctuated over a wide range up to 7,000 µg/L in W9-35; *cis*-1,2-DCE concentrations have ranged from 230 to 740 µg/L; and PCE concentrations have ranged from 72 to 180 µg/L.

Although the A2 aquifer zone was not studied in this investigation, some background data concerning the A2 zone are worth noting because of the potential for upward migration of contaminants into the A1 zone, as explained in Section 4.1.2 of this report. Table 3-4 contains historical CVOC data for well W9-20, an A2 aquifer zone well also located close to the current permeable barrier location. Concentrations of TCE, *cis*-1,2-DCE, and PCE in well W9-20 are

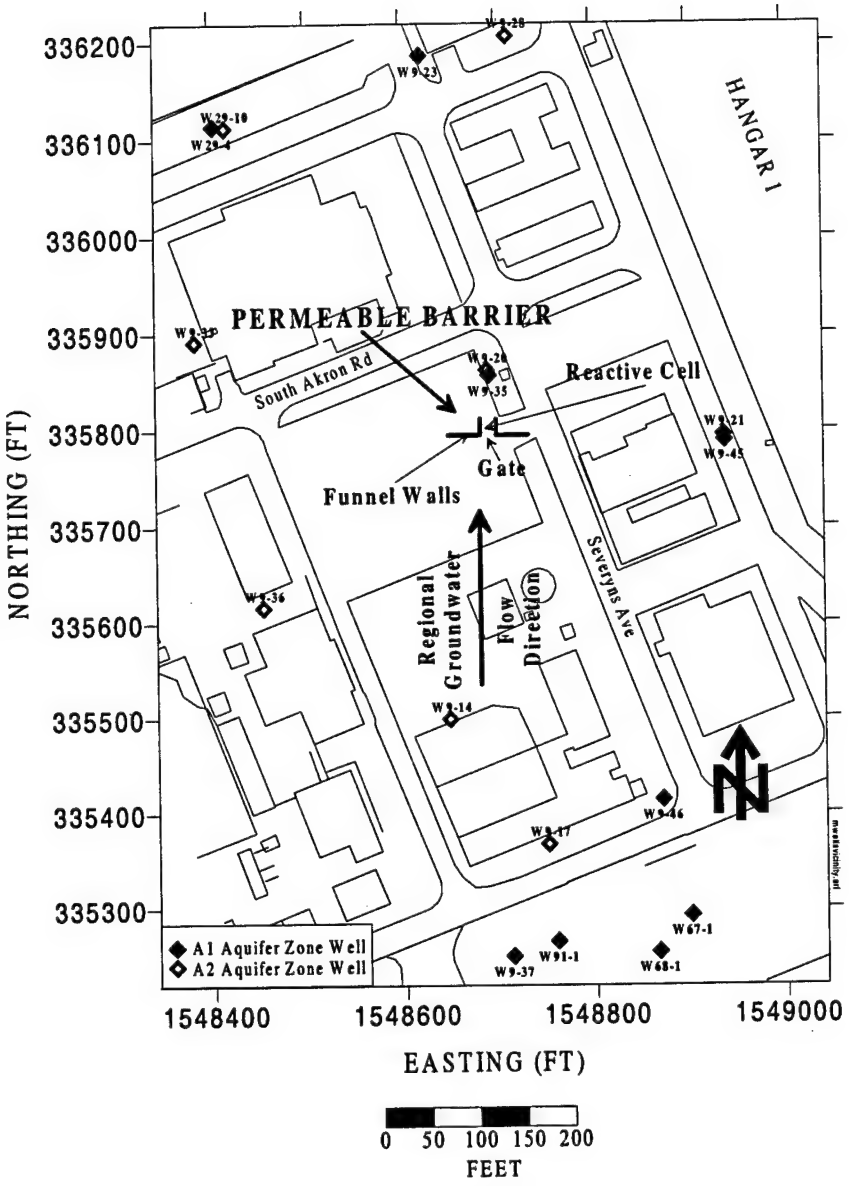

* Easting and Northing coordinates correspond to the California State Plane Coordinate System for zone 403.

Figure 3-7. Location Map for Monitoring Wells in the Vicinity of the Current Permeable Barrier Location

plotted against time over a 6-year period in Figure 3-10. By comparing the data presented in either the tables or figures, it can be seen that TCE levels are several times higher in the A2 aquifer zone than in the A1 aquifer zone near the permeable barrier. However, due to resource limitations and the pilot nature of the demonstration, the permeable barrier was installed only in the A1 aquifer zone.

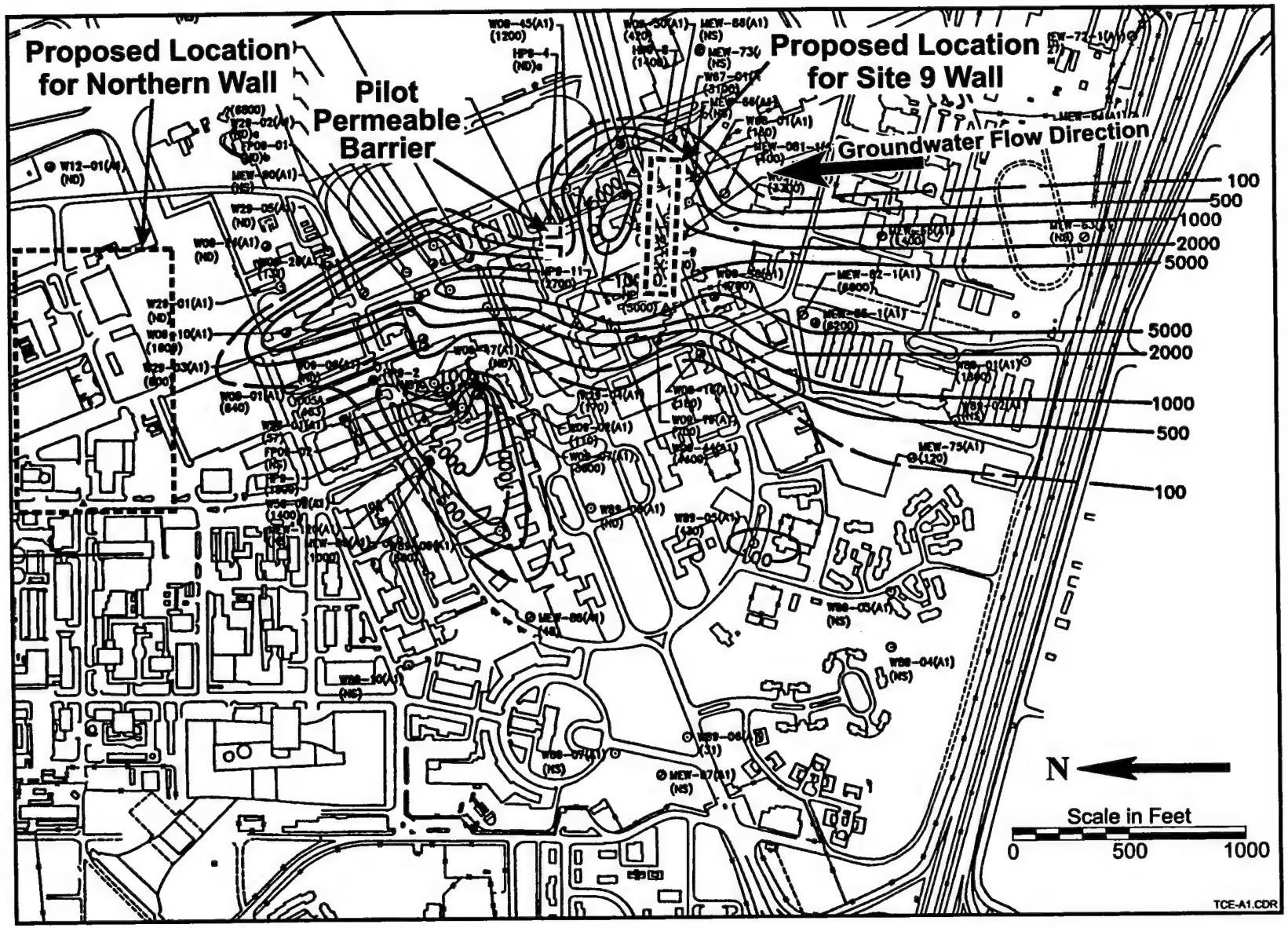

Figure 3-8. TCE Concentration Contour Map for A1 Aquifer Zone, 2nd Quarter 1991 (Source: IT Corp., 1991)

Table 3-3. Historical CVOC Data for Well W9-35 in the A1 Aquifer Zone (concentration unit is µg/L)

Sampling Date	PCE	TCE	*cis*-1,2-DCE	Vinyl Chloride
07-Jun-90	130 J	6000	490	500 U
13-Jul-90	130 J	5600	500	500 U
07-Aug-90	170 J	7000	570	500 U
09-Nov-90	72 J	3300	480	250 U
06-Feb-91	140 J	5200	740	400 U
13-May-91	120 J	120 J	430	250 U
01-Sep-92	86	3800 D	380	50 U
19-May-93	87	3600 D	380 D	20 U
17-Sep-93	78 J	4200	330	250 U
23-Feb-94	110 J	4600 B	410	250 U
24-Aug-94	180 J-H	4500 J-H	400 J-H	330 UJ-H
28-Feb-95	83 U	1300	230	83 UJ-K

Sampling Date	1,1-DCA	1,2-DCA	1,1,1-TCA	1,1-DCE
07-Jun-90	ND	ND	ND	ND
13-Jul-90	ND	ND	ND	ND
07-Aug-90	ND	ND	ND	ND
09-Nov-90	ND	ND	ND	ND
06-Feb-91	ND	ND	ND	ND
13-May-91	ND	ND	ND	ND
01-Sep-92	37 J-G	50 U	50 U	66 J-K
19-May-93	34	20 U	14 J	67
17-Sep-93	250 U	250 U	250 U	60 J
23-Feb-94	35 J	250 U	250 U	70 J
24-Aug-94	330 UJ-H	330 UJ-H	330 UJ-H	76 J-H
28-Feb-95	83 U	83 U	83 U	11 J

Source: PRC and MW (1996).
ND = No data.
1,1,1-TCA = 1,1,1-trichloroethane.

Qualifiers

B Used when a given target compound was detected in the associated method blank as well as in the sample. It indicates that there was possible/probable blank contamination.
D Indicates that all compounds were identified in an analysis at a secondary dilution factor.
J Indicates that the value was qualitatively identified but was reported at an estimated quantity.
J-G Value was estimated due to result being below the contract-required quantitation limit (CRQL) but above the 5 or 10 times rule for blank contamination.
U Indicates that the analyte was not detected at the reported quantity.
UJ-H/J-H Detection limit or value was estimated due to method holding time violation.
UJ-K/J-K Value was estimated due to calibration or gas chromatography/mass spectrometry (GC/MS) tuning criteria being out of quality control (QC) limits.

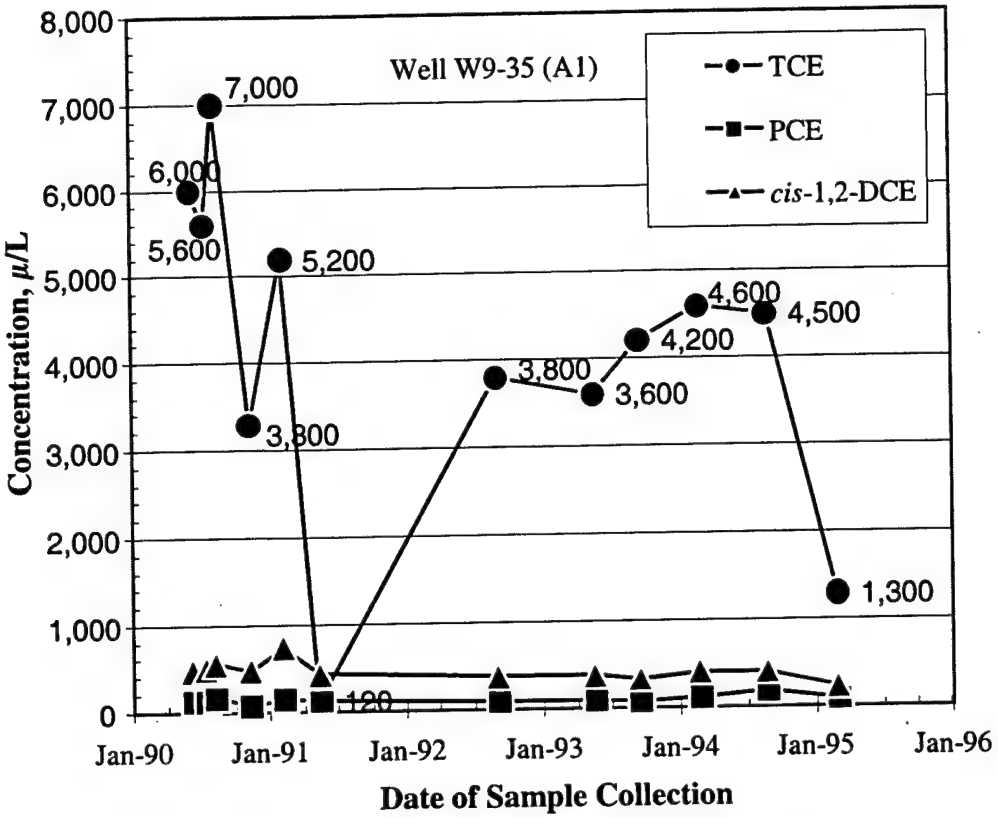

Figure 3-9. Historical TCE, PCE, and *cis*-1,2-DCE Data for Well W9-35

Table 3-4. Historical CVOC Data for Well W9-20 in the A2 Aquifer Zone (concentration unit is µg/L)

Sampling Date	PCE	TCE	*cis*-1,2-DCE	Vinyl Chloride
07-Jun-90	340 J	18,000	300 J	1,200 U
13-Jul-90	380 J	20,000	370 J	1,200 U
08-Aug-90	400 J	22,000 B	1,000 U	2,000 U
09-Nov-90	340	9,500	440	620 U
08-Feb-91	450 J	13,000	500 J	1,200 U
13-May-91	480 J	18,000	420 J	1,200 U
01-Sep-92	360	10,000 D	420	50 U
19-May-93	420	9,900 D	560	50 U
23-Feb-94	200 J	13,000 B	260 J	1,000 U
24-Aug-94	220 J	18,000	390 J	1,000 U
03-Mar-95	1,000 U	13,000	330 J	1,000 U

Source: PRC and MW (1996).

Qualifiers
- B Used when a given target compound was detected in the associated method blank as well as in the sample. It indicates that there was possible/probable blank contamination.
- D Indicates that all compounds were identified in an analysis at a secondary dilution factor.
- J Indicates that the value was qualitatively identified, but was reported at an estimated quantity.
- U Indicates that the analyte was not detected at the reported quantity.

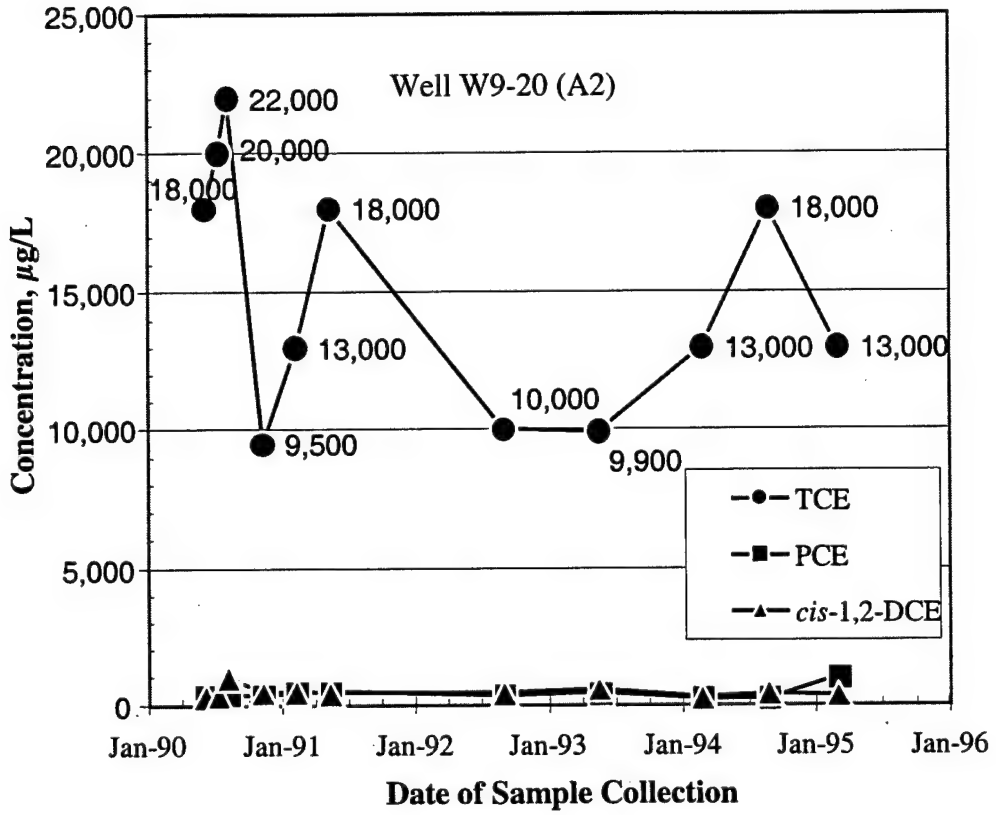

Figure 3-10. Historical TCE, PCE, and *cis*-1,2-DCE Data for Well W9-20

3.3.3 Description of Groundwater Geochemistry

Historical data collected prior to construction of the permeable barrier were reviewed for inorganic chemical parameter measurements. Considerably less inorganic chemical data were available than for the organic compounds. Fewer than six measurements of bicarbonate, chloride, nitrate, nitrite, sulfate, and bromide were taken at all 17 wells in the vicinity of the barrier. Calcium was sampled more extensively; DO and pH were sampled at all 17 wells, but never at more than three time points per well. Therefore, spatial or temporal variability for the water quality parameters is hard to determine from historical data. Table 3-5 presents the estimated geometric means based on a log-normal assumption for the observed inorganic data, by parameter and by well.

The inorganic component data in Table 3-5 show that the groundwater in the vicinity of the permeable barrier is moderately high in total dissolved solids (TDS), at approximately 800 to 1,000 mg/L. The predominant anions are bicarbonate and sulfate, while calcium is the only reported cation. The relatively high concentrations of calcium and bicarbonate and near neutrality of the pH are indicative of groundwater interaction with carbonate minerals in the

Table 3-5. Estimated Geometric Means of Historical Inorganic and Field Parameters in Wells in the Vicinity of the Proposed Permeable Barrier

Well	Aquifer	Bicarbonate (mg/L)	Chloride (mg/L)	Nitrate (mg/L)	Sulfate (mg/L)	Bromide (mg/L)	Calcium (mg/L)	pH	DO (mg/L)
W29-4	A1	250	41	1.8	230	0.62	129	7.05	1.1
W67-1	A1	NA	NA	NA	NA	NA	225	6.76	NA
W68-1	A1	NA	NA	NA	NA	NA	170	6.79	NA
W9-23	A1	NA	NA	NA	NA	NA	153	7.6	1.2
W9-35	A1	380	40	3.5	350	1.38	193	7.07	3.4
W9-37	A1	280	32	2.6	250	NA	206	7.44	0.1
W9-45	A1	NA	NA	NA	NA	NA	135	7.17	3.2
W9-46	A1	390	40	3.6	360	NA	186	6.99	1.0
W91-1	A1	410	38	2.1	380	2.76	196	7.05	NA
W29-10	A2	NA	NA	NA	NA	NA	75	7.54	0.3
W9-14	A2	NA	NA	NA	NA	NA	149	7.05	2.0
W9-17	A2	NA	NA	NA	NA	NA	167	7.14	1.2
W9-20	A2	NA	NA	NA	NA	NA	159	6.88	1.9
W9-21	A2	NA	NA	NA	NA	NA	145	7.8	0.2
W9-28	A2	NA	NA	NA	NA	NA	172	7.43	1.5
W9-33	A2	NA	NA	NA	NA	NA	178	7.32	0.0
W9-36	A2	NA	NA	NA	NA	NA	157	7.71	1.1
All A1 Wells	A1	336	38	2.6	308	1.25	169	7.09	1.3
All A2 Wells	A2	NA	NA	NA	NA	NA	120	7.26	0.8

NA = not available.

aquifer matrix. Precipitation of iron and calcium as carbonates in the reactive cell is a possibility. The DO levels of 0.0 to 3.4 indicate that the groundwater is anoxic to slightly oxic. DO is of concern in the reactive iron barriers because of its potential to form ferric hydroxide precipitates. No data were available to assess silicate chemistry. The mineralogy of the sediments at the permeable barrier site has not been fully investigated; however, they have been characterized as a complex mixture of alluvial-fluvial clay, silt, sand, and gravel. The relatively high level of inorganic chloride (approximately 40 mg/L) compared with chlorinated organics makes mass balance for CVOC degradation based on chloride infeasible. The low level of bromide (<3 mg/L) indicated that bromide could be used as a conservative tracer for evaluating the barrier.

3.4 Design of the Pilot Permeable Reactive Barrier at Moffett Field

The pilot barrier was designed with the help of the site characterization results (described above), bench-scale testing, and modeling.

3.4.1 Bench-Scale Test Results

Prior to installing the pilot-scale permeable barrier, a bench-scale study was conducted to evaluate the treatability of the site groundwater with granular iron (PRC, 1995). In both batch and column tests, a mixture of reactive iron and sand was used. Because of its relatively low cost compared to other reactive metals, only iron was tested, using iron samples from four different iron fabrication processes. Both laboratory-prepared water solutions and contaminated Moffett

Field site groundwater were used. The laboratory water solution had concentrations of 2.5 mg/L of TCE and 2.5 mg/L of PCE. The Moffett Field site groundwater used for the tests contained 1.2 mg/L of TCE and 0.12 mg/L of PCE.

Batch tests were performed by mixing the reactive iron samples with both types of contaminated water. An iron sample from Peerless Metal Powders, Inc. was found to have the greatest sustained treatment efficiency for TCE and PCE and was the only sample used in the column tests. Altogether, five batch tests were performed to evaluate the effects of the iron on field parameters (pH, Eh, and DO) and to determine its efficiency for removing TCE and PCE. One set of batch tests was conducted both with and without buffers [apatite, $Ca_5(PO_4)_3OH$] in the solutions to determine the correlation between pH and degradation rate (or half-life). After 117 hours contact time, the pH of laboratory-prepared solutions ranged from 7.1 (unbuffered) to 6.5 (buffered), and the pH of solutions prepared with site groundwater ranged from 7.9 (unbuffered) to 7.4 (buffered). The buffered and unbuffered solutions did not significantly affect reaction rates. Therefore, it was decided that the permeable barrier system at Moffett Field would be left unbuffered.

The column tests were performed with a 4-foot-long, 4-inch-diameter, ported glass column filled with mixtures of construction-grade sand and the one reactive iron sample from Peerless. With a 90% sand and 10% iron mixture, calculated permeabilities through the apparatus averaged 216 feet/day. Porosities in the mixture were reported to be about 0.38. The flowrate through the column was calibrated to about 7.7 feet/day, which is faster than natural conditions at Moffett Field. Water samples were collected from the inflow port, the outflow port, and seven intermediate ports along the length of the column at timed intervals.

The column tests were run with 50:50 mixtures (by mass) of iron and sand. The column tests indicated that the iron removed TCE and PCE under Moffett Field conditions. Calculated half-lives were about 0.87 to 1.0 hour for TCE, and 0.29 to 0.81 hour for PCE. Half-lives were 3.1 hours for *cis*-1,2-DCE, 4.7 hours for vinyl chloride, and 9.9 hours for 1,1-DCA. Adsorption was not significant in the samples. Consistent pH values were observed along the column, and Eh decreased along the column in the tests.

The bench-scale study concluded that the iron sample from Peerless was suitable for the Moffett Field site. The half-lives from the bench-scale study and the assumed seepage velocities from the groundwater model (PRC, 1996a) indicated that a reactive cell thickness of 6 feet with no buffering would be adequate to treat TCE, PCE, and other chlorinated compounds. In the final field design, a reactive cell consisting of 100% granular iron (instead of an iron/sand mixture) was used as a safety factor to promote complete and rapid degradation of PCE and TCE. The contaminant half-lives obtained from the column tests and the projections for 100% iron are listed in Table 3-6. For comparison with the field performance of the permeable barrier, it is assumed that the bench-scale reaction rates would be approximately 2.3 times higher when 100% iron was used instead of 50% iron (by weight), based on the expected increase in surface area and porosity. This calculation was based on measured densities for sand (2.67 g/cm^3) and iron

Table 3-6. Bench-Scale Test Results and Design Projections

Contaminant	Half-Life in Bench-Scale Test (50:50) Iron-Sand Mixture)	Projected Half-Life For 100% Iron Medium[a]
PCE	0.29 to 0.81 hour	0.13 to 0.35 hour
TCE	0.87 to 1.0 hour	0.38 to 0.43 hour
cis-1,2-DCE	3.1 hours	1.35 hours
Vinyl chloride	4.7 hours	2.04 hours
1,1-DCA	9.9 hours	4.3 hours

(a) Half-lives were reduced by a factor of 2.3 to account for the higher surface area and porosity in 100% iron medium versus in a 50:50 iron-sand (by mass) mixture.

(7.90 g/cm^3) (PRC, 1995), which gives a volume ratio for sand/iron of 2.96/1 in the column tests. The net porosity in the column tests was 0.38, according to PRC (1995). This value implies more efficient packing in the columns than in the 100% iron permeable barrier, for which porosity was estimated to be 0.66. This information shows that the ratio of pore water in the column tests to a unit volume of iron is 2.3 times greater than in the permeable barrier. No temperature correction was given to the reaction rates because the temperature of the site groundwater ranges between 19 and 23°C annually, which is close to the presumed laboratory temperature where the column tests were run.

3.4.2 Groundwater Modeling and Design

A three-dimensional numerical groundwater model was used to evaluate the ability of the permeable barrier to capture contaminated groundwater and to predict the flowrate of water through the barrier (Battelle, 1996a). This groundwater model is an updated version of a previous model by PRC (1996a) for the same site. The original model was modified to include more detailed information on the heterogeneities and hydraulic variability near the barrier by reducing the cell sizes and by using the horizontal flow barrier feature. The MODFLOW finite difference numerical flow model code (McDonald and Harbaugh, 1988) was used in order to maintain consistency with the PRC study. MODFLOW has several flexible features that allowed for detailed simulation of the barrier. RWLK3D (Naymik and Gantos, 1995), a groundwater transport code, was used to simulate particle pathways near the barrier.

The groundwater model addressed several scenarios, such as changes in permeability within the iron cell and the existence of a preferential pathway in the gap layer under the permeable barrier. The scenarios were used to determine the detectable changes in the flow system that could serve as indicators of changing conditions within the cell itself. A groundwater transport model was used to delineate capture zones of the gate and the treatment zone downgradient of the permeable barrier. Several other aspects, such as volumetric budgets through the barrier and travel times within the gate, also were examined. More details on the use of models for permeable barrier design and modeling methodologies may be found in Gavaskar et al. (1998a).

Specific parameters for the updated model were the same as for the original model, except for changes in the final design of the funnel-and-gate system and in grid resolution near the gate. The updated model domain was 1,000 feet long in the north/south direction and 700 feet wide in the east/west direction. The finite difference grid had 7 layers, 137 rows, and 130 columns. The cell size was 20 feet by 20 feet at its maximum, and 0.5 by 0.5 foot in the iron cell itself to provide high resolution around the permeable barrier. The A1 aquifer zone was represented by four layers (Figure 3-5) from ground surface to 15 feet below msl (Layers 3 and 4 represent the target channels for the permeable barrier). The confining layer between A1 and A2 was Layer 5, which was 3 feet thick. Layers 6 and 7 comprised the A2 aquifer zone and were at an elevation interval of −18 to −40 feet msl. The sand channels were represented as high K zones surrounded by low K silt and clay. Thus, most of the heterogeneities in the subsurface were represented in the model.

Boundary conditions were no-flow on the east and west sides of the model and constant head nodes at the northern and southern boundaries. These conditions allowed flow to be predominantly from south to north in the model area. Lithologic variations determined from site characterization efforts were incorporated into the model as four distinct sediment facies: silty clay, clayey silt, silty sand, and channel sand and gravel. Permeability and porosity values for these facies were based on previous slug and pumping tests in the area (IT, 1993) and are shown in Table 3-7. The distribution of sedimentary facies in the model (heterogeneities) was based on the paleochannel maps and cone penetrometry test logs. Recharge was set as 2.2 inches per year throughout the area.

Table 3-7. Aquifer Parameters

Hydrofacies	Permeability (feet/day)	Porosity
Silty Clay	0.05	0.45
Silt/Clayey Silt	0.5	0.40
Silty Sand	30	0.35
Sand and Gravel	150	0.30

All barrier walls penetrated through the top four layers in the model. The barrier walls were included in the model as 20-foot-long lines of horizontal flow barriers (HFBs) oriented east/west, and the walls bounding the east and west side of the reactive cell were assigned HFB lengths of 10 feet oriented north/south. Within the gate itself, the pea gravel was represented with a 2-foot-thick zone on each side of the iron cell with a permeability of 2,830 feet/day and porosity of 0.33. The reactive cell was depicted as a 6-foot-thick by 25-foot-deep cell with a permeability of 283 feet/day and porosity of 0.33. The permeability and porosity of the iron medium were based on column tests (PRC, 1995). The reactive cell and pea gravel both penetrated model Layers 2 to 4.

The model was calibrated to January 1996 preconstruction water levels in piezometers at the site. The simulated water levels and the particle tracking results for preconstruction and post-construction scenarios are shown in Figure 3-11a and 3-11b respectively. This figure shows the capture zone width for the permeable barrier. It is clear that the placement of a high-K gate and the funnel walls resulted in a significant increase in flow through the volume occupied by the reactive cell compared to the preconstruction scenario. It is also evident that the aquifer heterogeneities had a significant impact on the flow system. The particles in the sand channel area showed a very rapid movement through the reactive cell. However, particles starting in the lower K media showed very little movement even in 50 days. This also shows that most of the groundwater flow and contamination transport at the site is occurring in the high K sand channels.

The effect of the vertical heterogeneities in the A1 aquifer zone can be seen in Figure 3-12. This figure shows the movement of particles backward in time for 40 to 50 days, starting at the permeable cell interface. In the shallow lower K Layers 1 and 2 there is almost no particle movement. However, in the higher K Layers 3 and 4 there is rapid particle movement in the sand channel areas and slow movement in the interchannel areas. This figure again shows the influence of heterogeneities on water and contaminant movement toward the iron cell.

Finally, the simulated water levels through the iron barrier for two different reactive cell permeability scenarios are shown in Figure 3-13. The main feature of this figure is that the water levels in the reactive cell are flatter than in the surrounding aquifer. This is most likely due to the high conductivity of the iron and pea gravel. As shown later in the report, this trend in simulated water levels was confirmed by field observations. The simulated flow velocity in the reactive cell, based on the porosity of 0.66 and geometric mean K for iron and pea gravel, ranges from 1.5 to 2.5 feet/day for the two scenarios, resulting in the residence time range of 2.4 to 4.0 days.

3.5 Moffett Field Barrier Design

Figure 3-14 shows a plan and elevation view of the funnel-and-gate type barrier at Moffett Field. This pilot barrier was located in the CVOC plume as shown in Figure 3-2 (in Section 3.1) and targets only a part of the plume. The groundwater level marker indicates the approximate annual maximum. As shown in Figure 3-12 (in Section 3.4.2), the gate was placed in the sand channel to capture the bulk of the flow. Additional capture from the interchannel deposits is affected by the funnel. The heterogeneities in the aquifer formation, as determined during site characterization and modeled in the design, indicate that the capture zone is likely to be asymmetric with more flow coming in from the west side of the barrier than the east. The gate is 10 feet wide and 10 feet thick (in the direction of flow), and includes two pea gravel zones, each of which is 2 feet thick. The funnel is 20 feet on either side and extends in a straight line with the gate and is perpendicular to the flow.

The barrier extends down to a depth of 25 feet below ground surface (bgs), which covers most of the A1 aquifer zone. The base of the gate is lined with concrete, and a geosynthetic liner on top and bottom covers the reactive medium. The sides of the gate parallel to the flow are sealed with

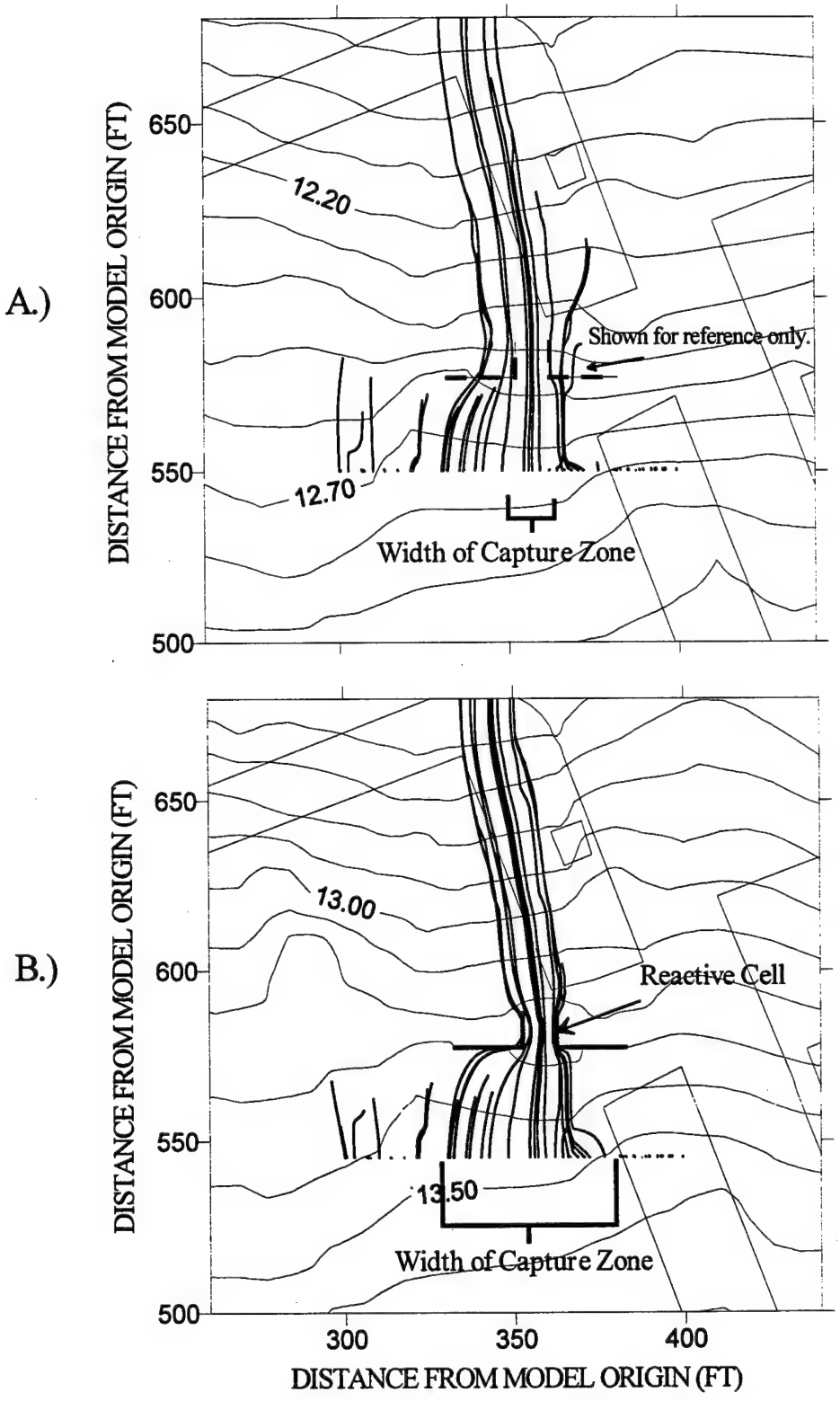

Figure 3-11. Simulated Water Levels and Forward Particle Flow Paths for (A) Preconstruction and (B) Post-Construction Model Scenarios

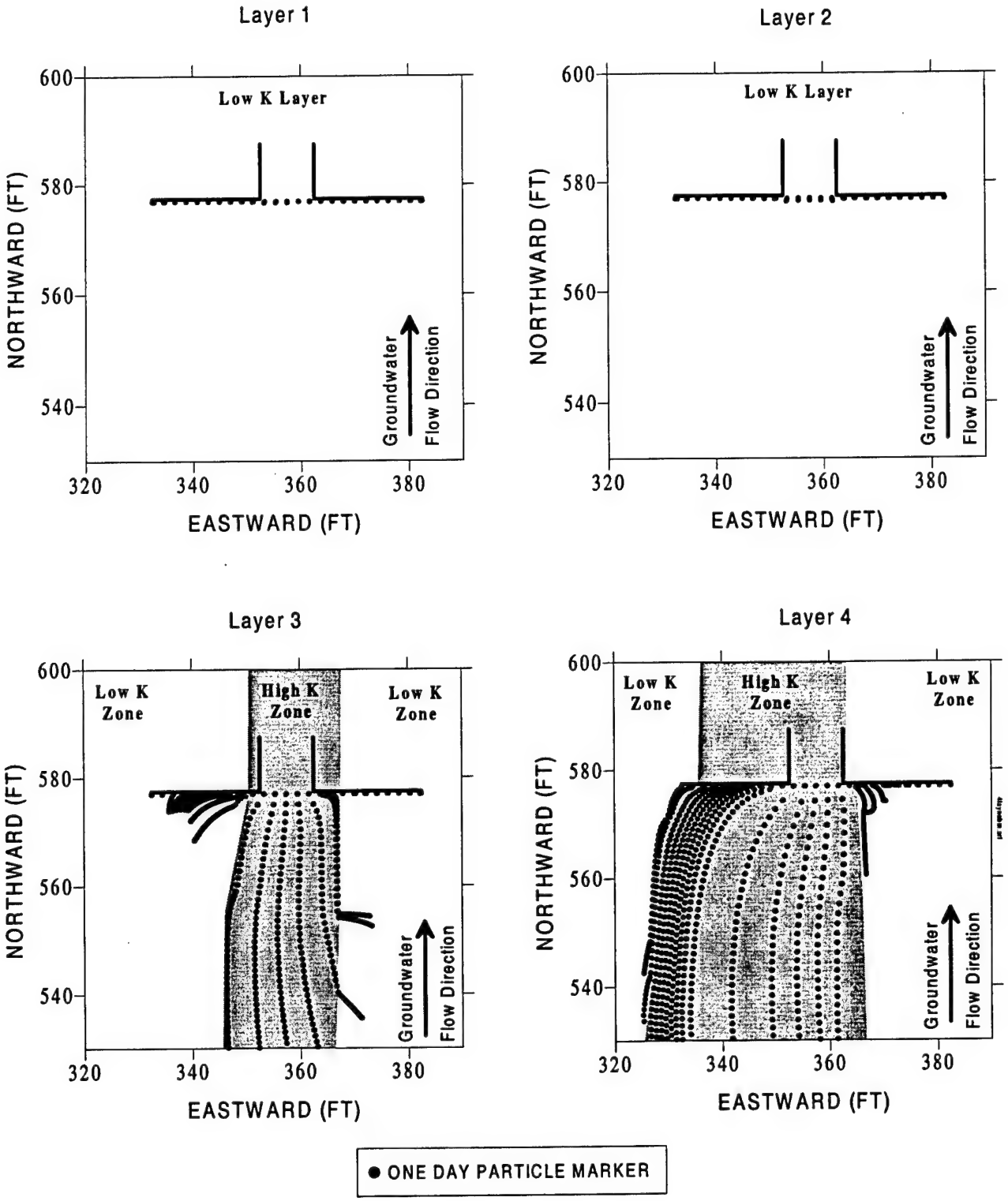

Figure 3-12. Simulation Backward Particle Tracking Results for Model Layers 1 Through 4 Showing Effect of Lithologic Heterogeneities

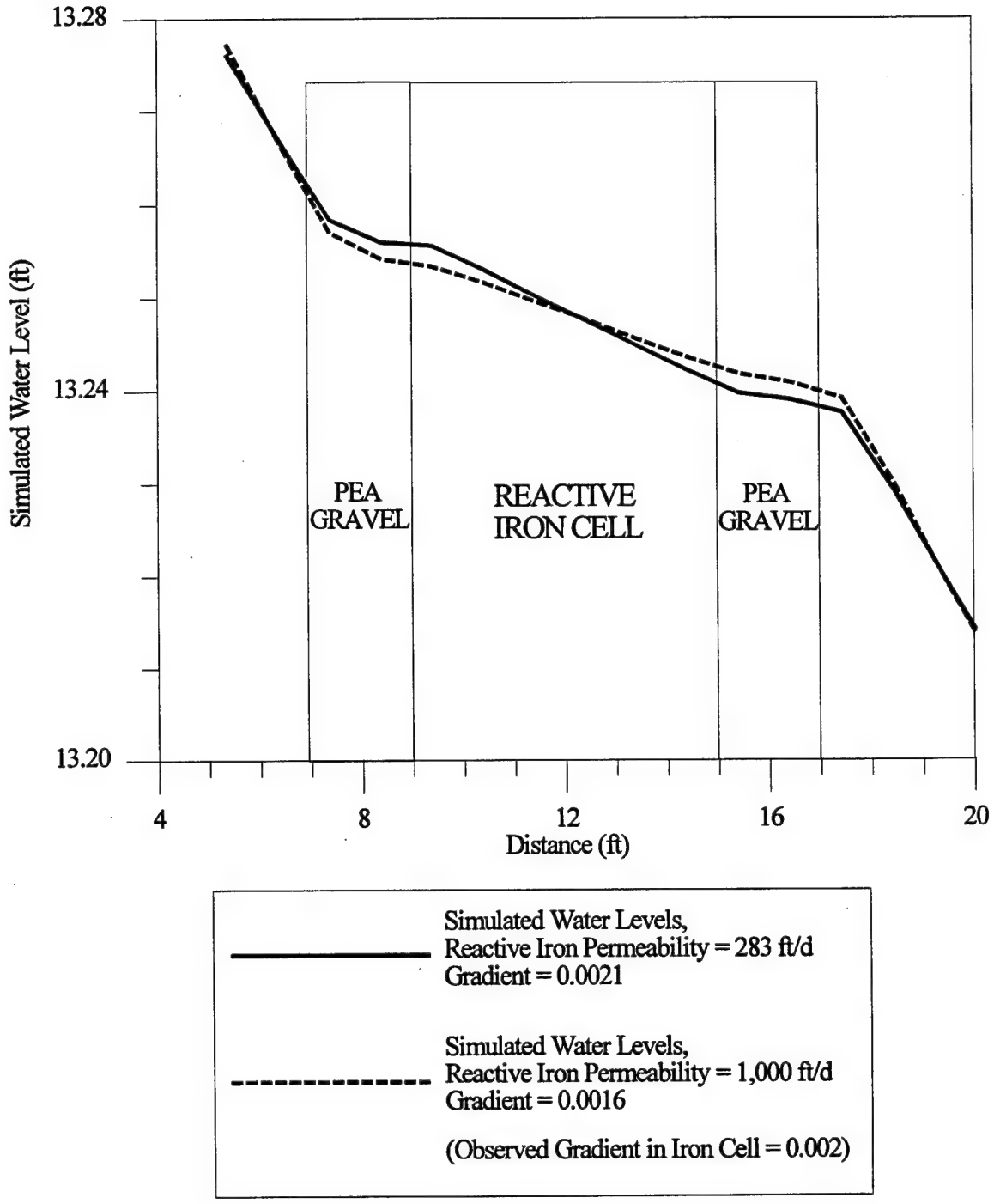

Figure 3-13. Simulated Water Level Profile Through the Permeable Barrier for Low and High Iron Conductivity Scenarios

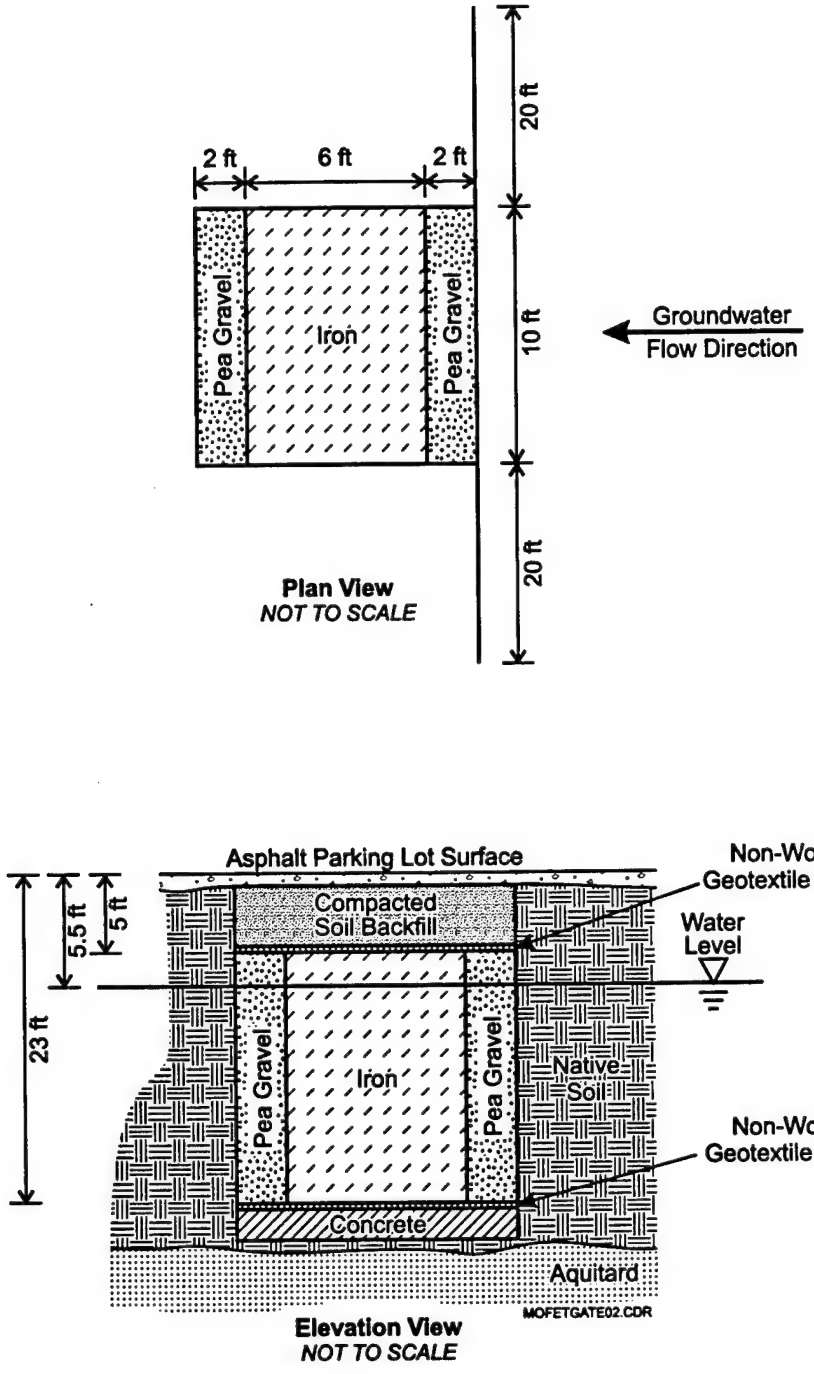

Figure 3-14. Permeable Reactive Barrier Plan and Elevation View at Moffett Field

sheet piles. This ensures that the groundwater flows into and out of the reactive cell only through its upgradient and downgradient faces, respectively.

Unfortunately, geotechnical concerns prevented the barrier from being keyed into the aquitard. The A1/A2 aquitard is variable in thickness and was suspected of being only 6 inches thick at the location of the barrier. For fear of breaching the thin aquitard, its exact location could not be determined during the site characterization, and site representatives did not want to risk breaching it during construction. Therefore, the pilot barrier was constructed with a suspected gap of a few inches between the base of the barrier and the aquitard. A1 and A2 aquifer zones are interconnected and the A2 aquifer zone is contaminated as well. Any future full-scale barrier would probably have to extend all the way down and key into the confining layer below A2.

3.6 Construction and Operation of the Moffett Field Barrier

Slurry Systems, Inc. was contracted by EFA West to construct the pilot barrier (Figure 3-15). A backhoe was used to excavate the trench. Sheet piles with sealable joints were used to form the funnel and to hold the sides of the excavation. Sheet piles were temporarily installed in the gate as dividers to separate the pea gravel and iron sections. The iron was obtained from Peerless Metal Products, Inc. and was in the −8 to +40 mesh particle-size range. After the excavated trench box was completed and the dividers had been installed, the monitoring wells in the gate were suspended with a frame. The iron and pea gravel were poured in their respective sections through a bag suspended on top of the gate. The iron and pea gravel were poured around the standing wells (see Figure 3-16) and packed into place by personnel inside the trench. A geosynthetic liner was placed on top and backfill was added to make up the grade. The ground surface was then repaved for continued use as a parking lot. The aquifer wells were drilled with standard drilling equipment and completed with flush mounts to maintain the parking lot grade. Figure 3-17 is a picture of the barrier site after construction was completed and the surface restored. This postconstruction picture shows that there are no aboveground structures remaining.

3.7 Performance Evaluation Objectives and the Associated Monitoring Strategy

The performance objectives (in order of priority) for the technology demonstration were as follows:

1. Ensuring reactivity of the barrier. This objective seeks to ensure that the portion of the CVOC plume flowing through the barrier is being remediated. Remediation at this site implies reduction of PCE, TCE, *cis*-1,2-DCE, and vinyl chloride concentrations to below their respective MCLs. The presence of byproducts of abiotic reduction, such as *cis*-1,2-DCE, vinyl chloride, ethene, ethane, and methane in the reactive cell were evaluated as evidence of degradation. Half-lives (or reaction rates) in the field barrier were estimated for the target contaminants and compared to the half-lives obtained during bench-scale tests.

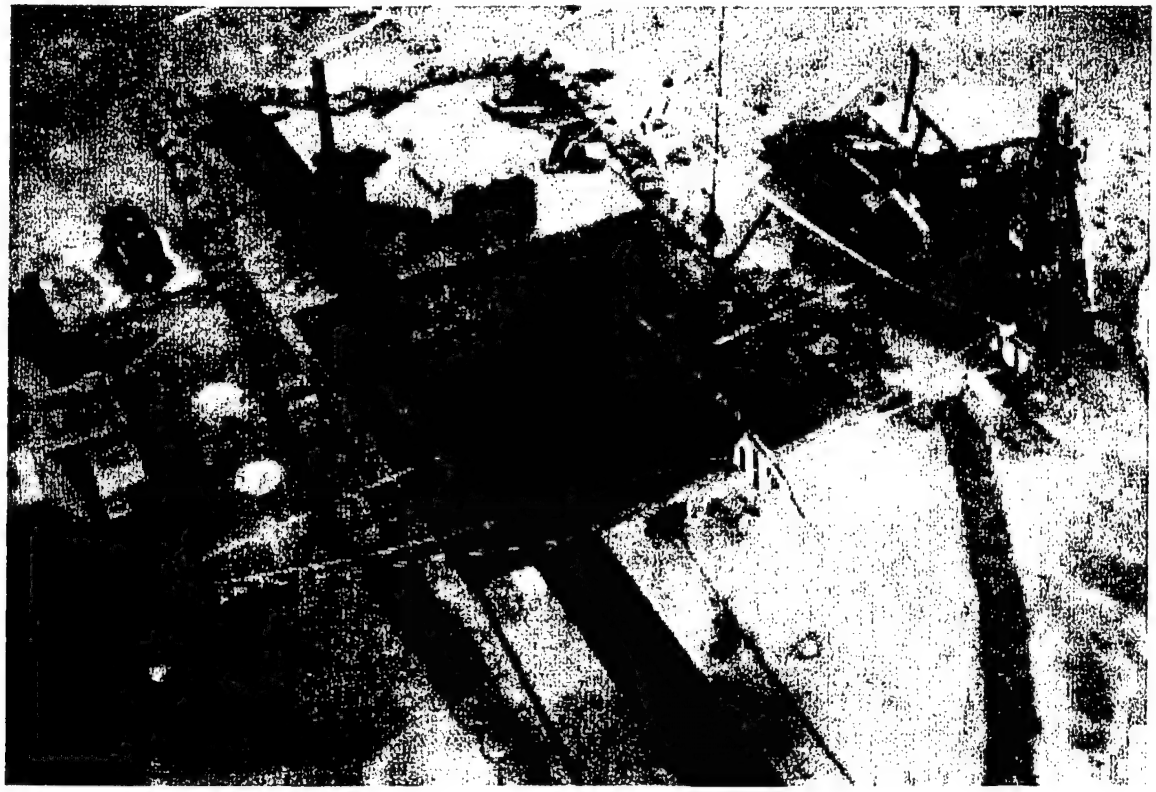

Figure 3-15. Funnel-and-Gate Construction

2. Assessing downgradient aquifer quality. This objective seeks to ensure that no environmentally deleterious materials are being introduced through the barrier into the downgradient aquifer. Potential materials of concern are dissolved iron (emanating from the reactive cell) and biological growth. Iron is subject to a secondary drinking water limit of 0.3 mg/L. Biological growth could be stimulated by the anaerobic conditions created in the downgradient aquifer by water flowing through the strongly reducing iron cell.

3. Assessing hydraulic capture efficiency of the barrier. This objective seeks to assess the efficiency of groundwater capture. Is the field barrier capturing the targeted portion of the groundwater in the design? This includes ensuring that the volume of water flowing through the barrier is equivalent to that estimated in the design, as well as ensuring that this volume of water is coming from the targeted portion of the aquifer.

4. Evaluating longevity of the barrier. Precipitates formed though the interaction between the iron medium and the native inorganic constituents (e.g., calcium, dissolved oxygen, and alkalinity) of the groundwater may, over a period of time, deposit on the iron surfaces in the reactive cell. Such deposits could potentially affect both the reactivity and hydraulic performance of the barrier. This objective seeks to evaluate the type and degree of such precipitation and its impact on the long-term performance of the barrier.

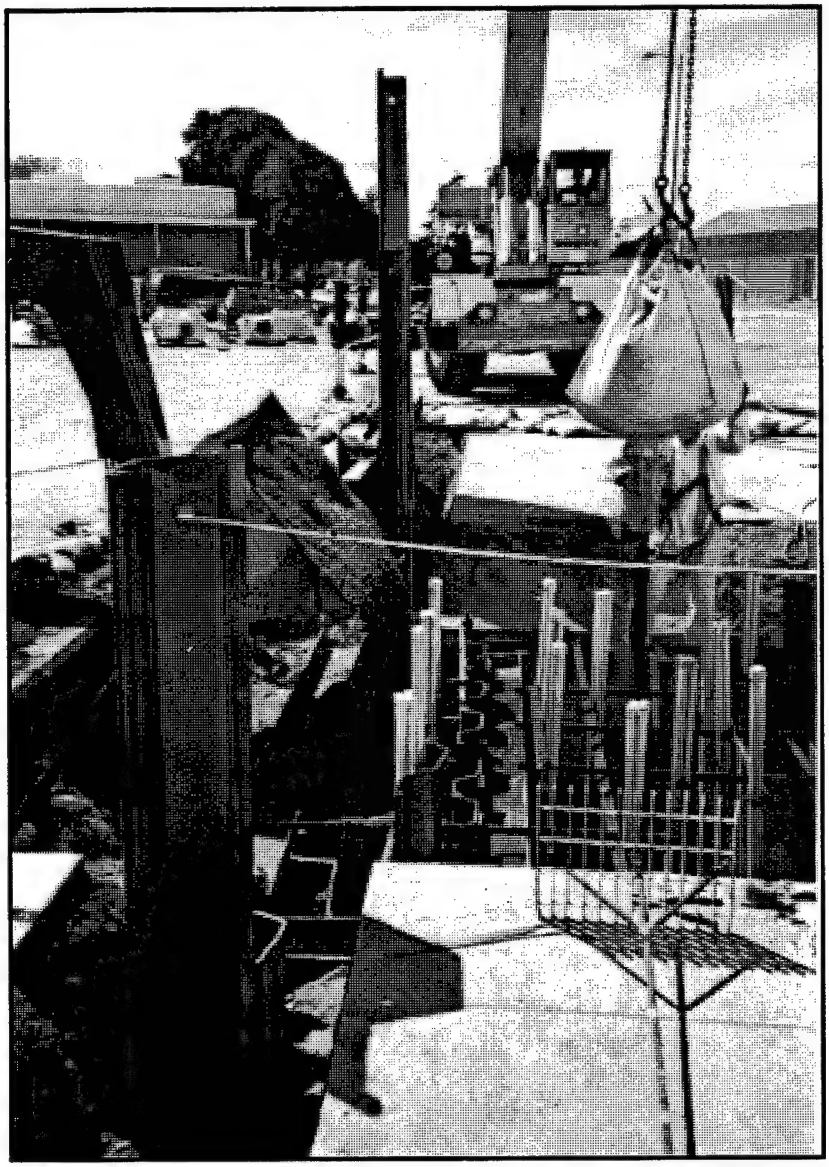

Figure 3-16. Installation of Monitoring Wells in the Reactive Cell and Pea Gravel for a Trench-Type Permeable Barrier

5. Estimating cost of the barrier application. The capital costs for the pilot barrier were noted during construction. The capital and O&M costs for a proposed full-scale application were estimated and compared to the costs of an equivalent pump-and-treat system.

Based on a discussion with site representatives, the first two objectives, evaluating the reactivity of the barrier and assessing the downgradient water quality, are considered critical for this demonstration. The other objectives are considered secondary. Objective 3, dealing with hydraulic

Figure 3-17. Surface Restoration after the Permeable Barrier Construction

capture efficiency, is secondary because this issue is location-specific for the heterogeneous Moffett Field site, and a potential full-scale barrier in the future may not be placed at the same location as the pilot barrier. Objective 4, evaluating the longevity of the barrier, is difficult to address in a 1-year timeframe and only preliminary indications of precipitation were obtained during the demonstration. Objective 5, estimating costs, is secondary because in the absence of long-term historical experience with permeable barriers, O&M costs can only be projected with some uncertainty.

A minor objective was to evaluate the effect of the gap under the barrier if any exists, because the barrier was not keyed into the aquitard.

The primary goal of the Moffett Field permeable barrier performance monitoring was to evaluate its technical performance, whereas several other goals were secondary. The performance monitoring objectives and associated monitoring strategy were detailed in the Performance Monitoring Plan (Battelle, 1997a) and are summarized below in order of priority determined during discussions with site representatives.

3.7.1 Objective 1: Evaluating Reactivity of the Permeable Barrier

This critical objective assesses the degradation rates of the target contaminants in the reactive cell, their residence time in the reactive cell, and the presence of byproducts. This objective was achieved through the following activities:

a. Quarterly sampling and analysis of CVOCs in groundwater samples from monitoring points (single wells and clusters) located within the reactive cell and the upgradient and downgradient pea gravel.
b. Determining the presence of potentially hazardous partially dechlorinated byproducts of degradation (e.g., vinyl chloride or *cis*-1,2-DCE) and examining their ultimate destruction in the reactive cell.
c. Determining the presence of potential hydrocarbon byproducts (e.g., ethene, ethane, etc.) in the reactive cell as indicators of degradation.
d. Measuring water levels in the pea gravel and reactive cell wells.
e. Conducting groundwater velocity vector measurements in the reactive cell and pea gravel.
f. Conducting slug tests in the reactive cell wells to determine conductivities at various points and to evaluate the homogeneity of flow through the cell.
g. Conducting a tracer test in the gate (pea gravel to pea gravel) to assess flow velocities (or residence times) through the reactive cell.

The first three activities relate to the determination of the presence and spatial and temporal distribution of CVOCs and their degradation products in the reactive cell. The last four activities relate to the determination of groundwater residence time in the reactive cell.

3.7.2 Objective 2: Assessing Downgradient Aquifer Quality

This critical objective was achieved through the following activities:

a. Quarterly monitoring of contaminants and inorganic parameters (Fe, DO, pH, etc.) in upgradient and downgradient pea gravel and aquifer wells.
b. Comparing upgradient and downgradient water quality in the aquifer wells.

3.7.3 Objective 3: Assessing Hydraulic Capture Efficiency of the Barrier

This was accomplished with the following activities:

a. Installing seven new monitoring wells upgradient of the permeable barrier to measure water levels in the upgradient vicinity of the barrier.
b. Installing two new four-well clusters, one immediately upgradient and one immediately downgradient of the gate along the centerline through the gate. The deepest well in each cluster was screened at the level of the suspected gap between the base of the barrier and the aquitard. Besides providing additional aquifer

monitoring points for water level and groundwater velocity measurements, these new clusters were installed to evaluate the effect of the gap under the barrier.

c. Conducting slug tests in several wells to determine the hydraulic conductivity distribution in the upgradient aquifer.
d. Conducting a tracer test in the upgradient aquifer to further ascertain hydraulic capture and measure groundwater velocity.
e. Using values of the measured aquifer parameters in the hydrogeologic model for the permeable barrier (Battelle, 1996a) to evaluate the capture zone.
f. Using in-situ groundwater velocity measurements to determine flow velocities and directions in the barrier and in the surrounding aquifer.

3.7.4 Objective 4: Evaluating the Longevity of the Permeable Barrier Application

The longevity of the barrier was assessed by evaluating the changes taking place in the inorganic constituents of the groundwater as it flowed through the reactive cell. The following activities were conducted:

a. The quarterly distribution of reactive inorganic parameters (e.g., DO, nitrate, sulfate) in the reactive cell and pea gravel were examined. These parameters had the potential to interact with the iron in the reactive cell and affect its reactivity.
b. Core samples of the iron in the reactive cell were collected at the end of 1.5 years (after installation) to look for qualitative signs of precipitation or microbial fouling.
c. A limited geochemical evaluation of the longevity of the barrier was performed by using the upgradient and downgradient inorganic constituent values (measured during quarterly monitoring events) in an inverse geochemical model.

3.7.5 Objective 5: Estimating Costs of the Barrier Application

Cost considerations involved in the application of permeable barrier technology were addressed in several ways. During the demonstration, data were compiled on cost of materials, cost of construction, and monitoring (the principal O&M cost). This information was used as a basis for estimating costs of a full-scale barrier at Moffett Field. Costs for a full-scale barrier include estimates of longevity, which were discussed in Objective 4.

3.8 Sampling and Analysis Procedures

The performance monitoring plan was designed such that sampling activities would correspond with each of the study's objectives. The following sections summarize the sampling and analysis activities.

3.8.1 Monitoring Frequency

Table 3-8 summarizes the sampling schedule for all of the analytes. Water samples were collected on approximately a quarterly basis (over six quarters) for chemical analysis. During each sampling event, the existing wells in the reactive cell, pea gravel, and in the immediate

Table 3-8. Monitoring Frequency

Parameter Type	Analytes	Sampling Schedule				
		Jun-96	Sep-96	Jan-97	Apr-97[a]	Oct-97
Field parameters	Water level, pH, groundwater temperature, Eh, DO	✓	✓	✓	✓	✓
Volatile organic compounds	CVOCs	✓	✓	✓	✓	✓
	Dissolved hydrocarbon gases			✓		✓
Inorganics and neutrals	Metals (K, Na, Ca, Mg, and Fe) Anions (NO_3, SO_4, Cl, Br, F, sulfide[c], alkalinity) Neutrals (TDS, TSS, TOC, DOC)	✓	✓	✓	✓	✓
Water elevations	Water level measurements (13 total events)	✓	✓	✓	✓	✓
Continuous monitoring	Water level, pH, temperature, Eh			✓	✓	
Reactive cell core samples	XRD, SEM, EDS, Raman spectroscopy, microbial analysis					✓[b]

(a) Water samples for certain wells sampled in April 1997 were repeated in July 1997 for reanalysis of CVOCs, which were below detection in the April 1997 monitoring event. Resampling and analysis was performed because the laboratory diluted the samples and detection limits were not within the requirements stated in the performance monitoring plan. Results from both April and July 1997 sampling events were reported. Continuous water level measurements were conducted in August and September 1997.

(b) Core samples were collected in December 1997.

(c) Sulfide was analyzed only in samples collected in April 1997 and October 1997.

TDS = total dissolved solids; TSS = total suspended solids; TOC = total organic carbon; DOC = dissolved organic carbon; XRD = x-ray diffraction; SEM = scanning electron microscopy; EDS = energy dispersive spectroscopy.

Vicinity of the aquifer were sampled. Measurements of field parameters were usually performed within 1 week of sample collection so that the various kinds of measurements could be gathered within a short period of time.

Water levels were measured a total of 13 times during the evaluation. Continuous water level monitoring was conducted twice during the study in events lasting approximately 3 to 4 weeks. The main purpose of continuous monitoring is to provide a frame of reference for the periodic water level and chemical measurements that may not capture possible short-term variations due to local recharge (e.g., rainfall) or other transient effects. Comparing the continuously measured parameters with quarterly monitoring (snapshot in time) events data showed whether the parameters in the wells at the time of sampling events were related to transient changes or to more permanent changes in the nature of the permeable barrier. Four wells were monitored for continuous analysis.

After the fifth quarter of water sampling, core samples of the iron in the reactive cell were collected. A core sample of soil from the downgradient aquifer was also collected to evaluate possible biological activity resulting from the anaerobic conditions created by the barrier.

3.8.2 Description of Monitoring Well Network

The monitoring well locations in the permeable barrier and vicinity are shown in Figures 3-18 and 3-19. Some of these wells (WIC-1 to WIC-4 and WW-1 to WW-18) were installed during the construction of the permeable barrier, and were sampled during the June and September 1996 and subsequent monitoring events. Additional aquifer wells were installed in December 1996 primarily to better evaluate the hydraulic performance of the barrier. These new wells were sampled in the January 1997 and subsequent monitoring events.

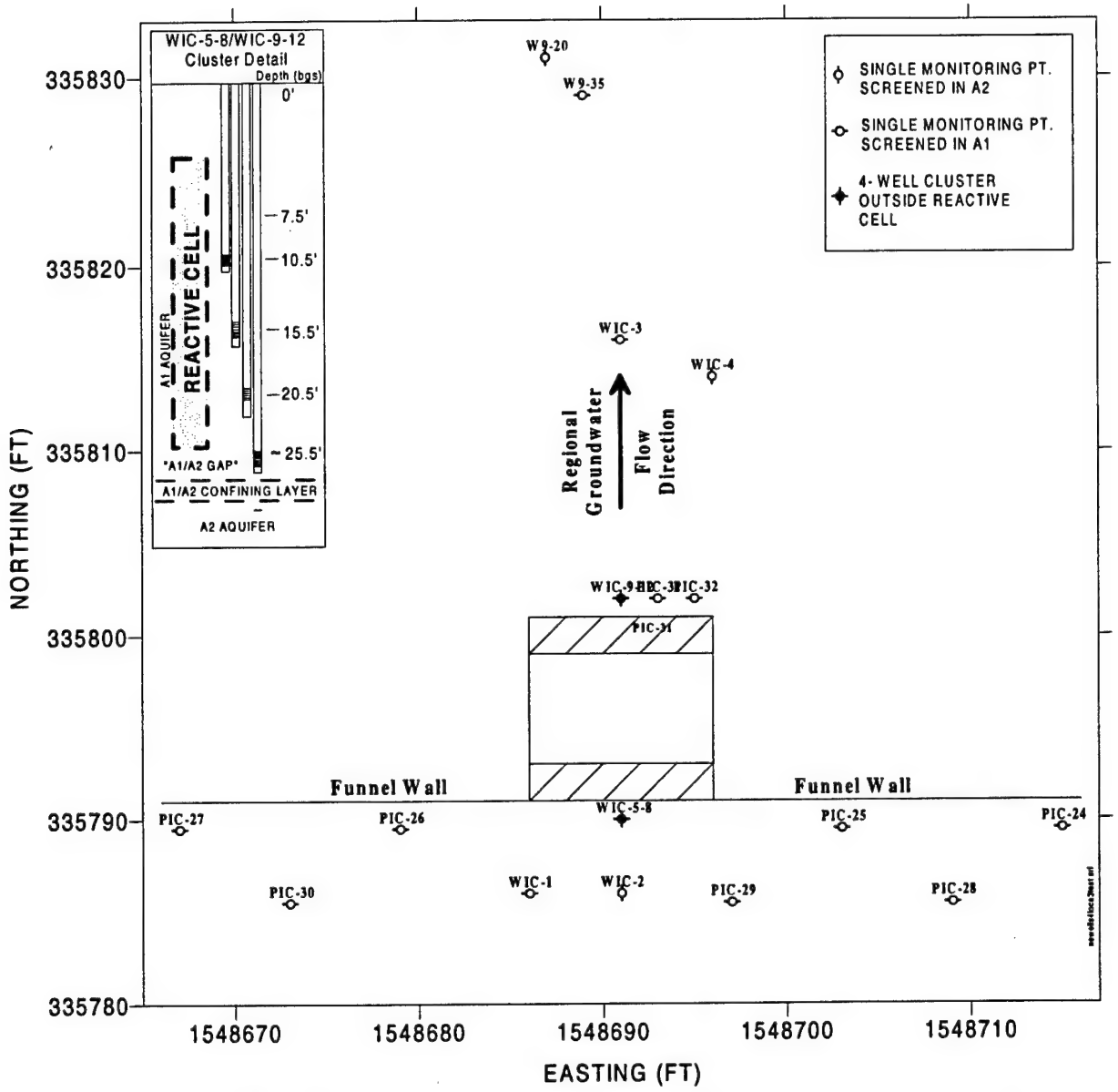

Figure 3-18. Location Map for Model Boundaries and Monitoring Wells in the Vicinity of the Permeable Barrier

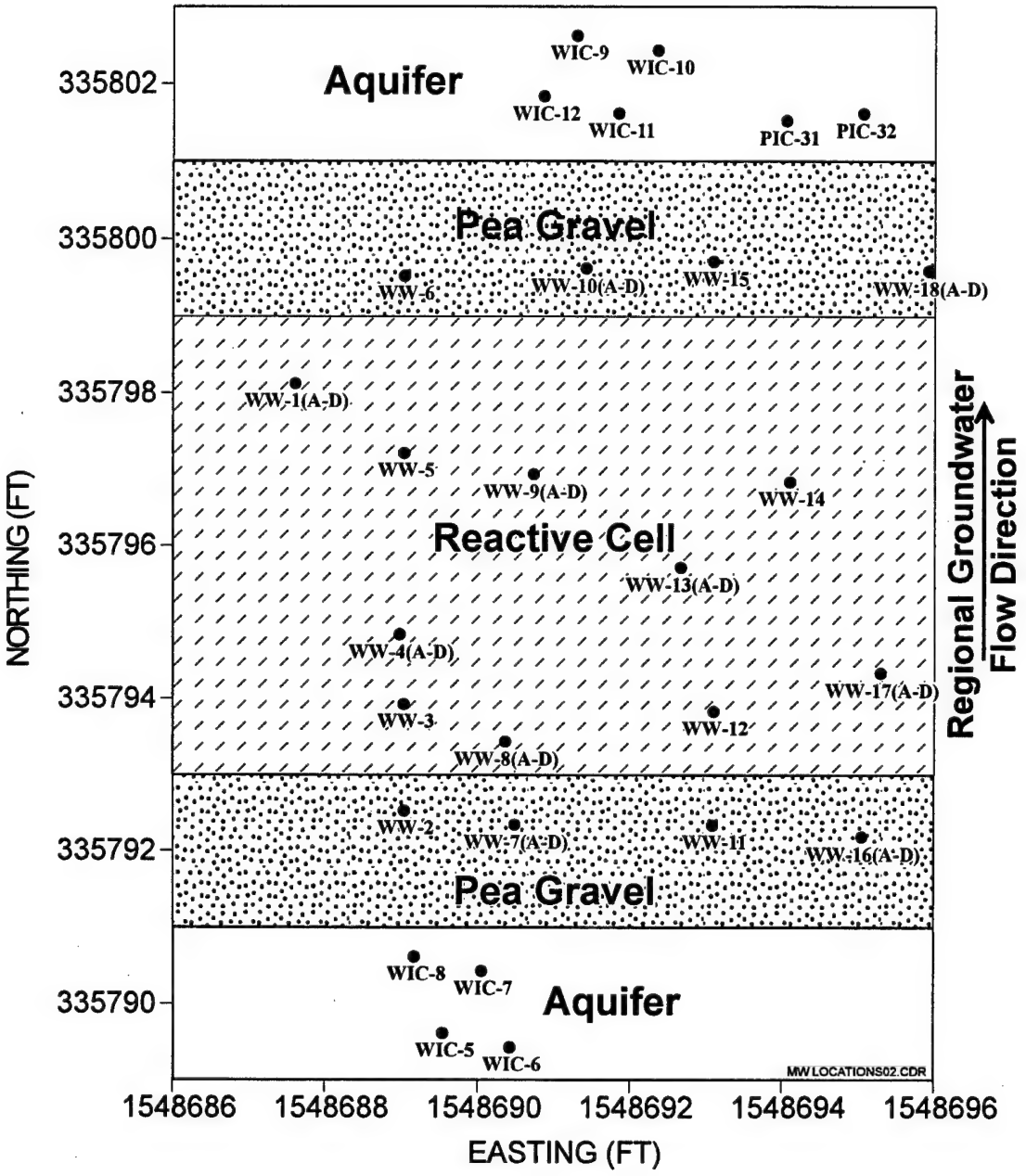

* Easting and Northing coordinates correspond to the California State Plane Coordinate System for zone 403.

Figure 3-19. Locations of Monitoring Wells Within and near the Permeable Barrier at Moffett Field

The newer wells installed in December 1996 consisted of two four-well clusters and nine single wells. Both new clusters are located along the centerline of the permeable barrier and have 12-inch screen lengths. The upgradient cluster was designated WIC-5 to WIC-8, and the downgradient cluster was designated WIC-9 to WIC-12. The deepest well in each cluster was screened at the level of the suspected gap between the base of the barrier and the aquitard. In addition, seven long-screen monitoring wells (PIC-24 to PIC-30) were installed upgradient of the permeable barrier to measure water levels in the upgradient vicinity of the barrier. To investigate the potential effect of backflow of groundwater and contamination on the downgradient side, two single-well monitoring wells (PIC-31 and PIC-32) were installed on the downgradient side of the barrier. Table C-1 (in Appendix C) contains a detailed list of well location coordinates, top of casing elevations, casing diameters, and well screen intervals.

3.8.3 Groundwater Sampling and Analysis

Groundwater sampling provides essential information on water movement, organic contaminant levels, and inorganic chemistry needed to understand and model the performance of the permeable barrier. Groundwater samples were collected and prepared for laboratory chemical analysis; field parameters were analyzed on site. Table 3-9 lists the parameters that were measured in the wells in and around the permeable barrier. Samples for determination of CVOCs, inorganic analytes, and field parameters were obtained from all wells in the permeable barrier and vicinity. Samples for determination of dissolved gases and certain additional analytes were obtained primarily from longer screened wells to reduce the total volume of water removed from the short-screen wells.

3.8.3.1 Groundwater Sampling Procedures

The main challenge in collecting groundwater samples was to minimize the impact of sampling on flow through the permeable barrier. Water withdrawal during sampling can lead to faster flow and reduced residence time of groundwater in the reactive medium. To prevent artificial gradients, water samples were extracted at low flowrates using an aboveground peristaltic pump. Also, to minimize disruption of normal flow through the barrier, successive samples were collected in different parts of the barrier, rather than from neighboring wells.

To minimize cross-contamination, dedicated sample tubing was used for each row of wells perpendicular to the flow direction. Seven lengths of tubing were used corresponding to seven row intervals. Also, each length of tubing was thoroughly decontaminated prior to collecting the next sample. Decontamination procedures are described in Appendix B.

Procedures for collecting groundwater samples for organic and inorganic analytes are described here and are presented in more detail in Appendix B. Teflon™ tubes of ¼-inch outside diameter (OD) were used to sample each multilevel monitoring well. The Teflon™ tube was connected to flexible tubing made of Viton™ for use with a peristaltic pump. Groundwater was withdrawn at a rate that causes water level drawdown at the well to be no greater than 0.05 foot. The water level within the wells was monitored using a down-hole water level sensor. Typically, a

Table 3-9. Groundwater Parameters Sampled on a Quarterly Basis

Parameters	Monitoring Wells Sampled					
	Upgradient A1 Aquifer Zone Wells	Upgradient Pea Gravel Wells	Reactive Cell Wells	Downgradient Pea Gravel Wells	Downgradient A1 Aquifer Zone Wells	A2 Aquifer Zone Wells
CVOCs[a]	WIC-1, WIC-5, 6 WIC-7, 8	WW-7A-D, WW-16A-D, WW-2, WW-11	WW-1A-D, WW-4A-D, WW-8A-D, WW-9A-D, WW-13A-D, WW-17A-D, WW-3, 5 WW-12, 14	WW-10A-D, WW-18A-D, WW-6, WW-15	W9-35, WIC-3, WIC-9, WIC-10, WIC-11, WIC-12	W-9-20, WIC-2, WIC-4
Dissolved Gases[b]	WIC-1, WIC-5, 6 WIC-7, 8	WW-2, WW-11	WW-3, 5 WW-12, 14	WW-6, WW-15	W9-35, WIC-3, WIC-9, 10, WIC-11, 12	WIC-2, WIC-4
Inorganic Cations (filtered)[c]	WIC-1, WIC-5, 6 WIC-7, 8	WW-7A-D, WW-16A-D, WW-2, WW-11	WW-1A-D, WW-4A-D, WW-8A-D, WW-9A-D, WW-13A-D, WW-17A-D, WW-3, 5 WW-12, 14	WW-10A-D, WW-18A-D, WW-6, WW-15	W9-35, WIC-3, WIC-9, 10, WIC-11, 12	W-9-20, WIC-2, WIC-4
Inorganic Anions (unfiltered)[c]	WIC-1, WIC-5, 6, WIC-7, 8	WW-7A-D, WW-16A-D, WW-2, WW-11	WW-1A-D, WW-4A-D, WW-8A-D, WW-9A-D, WW-13A-D, WW-17A-D, WW-3, 5, WW-12, 14	WW-10A-D, WW-18A-D, WW-6, WW-15	W9-35, WIC-3, WIC-9, 10, WIC-11, 12	W-9-20, WIC-2, WIC-4
Field Parameters[d]	WIC-1, WIC-5, 6, WIC-7, 8	WW-7A-D, W-16A-D, WW-2, WW-11	WW-1A-D, WW-4A-D, WW-8A-D, WW-9A-D, WW-13A-D, WW-17A-D, WW-3, 5, WW-12, 14	WW-10A-D, WW-18A-D, WW-6, WW-15	W9-35, WIC-3, WIC-9, 10, WIC-11, 12	W-9-20, WIC-2, WIC-4
Additional Analytes[e]	WIC-1, WIC-5, 6, WIC-7, 8	WW-2, WW-11	WW-3, 5, WW-12, 14	WW-6, WW-15	W9-35, WIC-3, WIC-9, 10, WIC-11, 12	WIC-2, WIC-4

(a) CVOCs determined by EPA Method 8260.
(b) Dissolved gases include volatile compounds such as hydrogen and C1-C5 hydrocarbons. In addition, N_2 and CO_2 were measured.
(c) Inorganics include the cations Ca, Mg, Na, K, Fe; anions Cl, F, Br, SO_4, NO_3, sulfide, and total alkalinity.
(d) Field parameters include T, pH, Eh, DO, and water level.
(e) Additional analytes include TOC, DOC, TDS, and TSS.

sampling rate of 40 mL per minute was used. Purging of wells before sample collection was kept to a minimum to restrict the sample to the water immediately surrounding the well. However, to assure that the water samples were representative, at least three volumes of the tubing were purged. For typical 3/16-inch inside diameter (ID), 25-foot tubing, three tubing volumes are equivalent to about 400 mL. After sample collection, all tubing was decontaminated as described in Appendix B. In addition, similar decontamination of any down-hole sampling equipment, such as down-hole groundwater velocity sensors, was performed prior to reuse.

3.8.3.2 Groundwater Analysis Methods

Table 3-10 lists the standard analytical methods used for the groundwater samples collected during the quarterly sampling events. Individual parameters are grouped according to field measurements, organic analytes, and inorganic analytes.

The primary purpose of taking field parameter measurements is to monitor chemical conditions within the reactive cell that can affect its performance. Therefore, temperature (T), pH, Eh, and DO were measured at every well location. To obtain accurate readings, the field parameters were measured using suitable down-hole probes.

The CVOCs of primary interest are the chlorinated hydrocarbons (EPA Method 8260) and light hydrocarbons (EPA Method 3810), including hydrogen gas, carbon dioxide, methane, ethane, ethene, acetylene, and propane. These CVOC analyses were performed to help identify the distribution of contaminants in and around the permeable barrier, as well as potential byproducts of degradation.

Samples were collected from each monitoring well for inorganic analysis as indicated in Table 3-10. Quarterly inorganic analyses were implemented to identify seasonal variations in parameters that have the potential to affect the long-term performance of the permeable barrier. Samples for analysis of cations were filtered and all samples were preserved immediately after collection as indicated in Table 3-10. The nominal filter pore size for cation analysis was 0.45 μm; however, filters of smaller pore sizes were occasionally used for comparison of results. In June 1996 and September 1996, several samples were collected and preserved without filtering to determine the metal content in the suspended matter. TDS and TSS were determined from filtered and unfiltered samples, respectively. In addition, organic carbon was measured in September 1996 using the method for TOC and DOC.

Because Moffett Field groundwater is moderately high in carbonate alkalinity (typically >350 mg/L), there was some concern over precipitation of carbonates inside the sample containers due to refrigeration and holding time. Precipitation would lead to underdetermining the alkalinity in laboratory samples. To verify whether accurate alkalinity measurements could be obtained in laboratory analyses, alkalinity was also determined in the field shortly after sample collection using a titration technique (Hach test kit).

Table 3-10. Analytical Requirements for Groundwater Samples

Parameter	Critical	Analysis Method	Sample Volume	Storage Container	Preservation	Sample Holding Time
Field Parameters						
Water Level	Yes	Down-hole probe	None	None	None	None
pH	Yes	Down-hole probe	None	None	None	None
Water Temperature	Yes	Down-hole probe	None	None	None	None
Eh	Yes	Down-hole probe	None	None	None	None
DO	No	Down-hole probe	None	None	None	None
Organic Analytes						
CVOCs	Yes	EPA 8260	2 x 40 mL	VOA Vial	4°C, pH<2 (HCl)	14 d
Dissolved Gases	No	EPA 3810	2 x 40 mL	VOA Vial	4°C, pH<2 (HCl)[a]	14 d
Inorganic Analytes						
Cations						
K, Na, Ca, Mg, Fe	Yes	200.7	100 mL	Polyethylene	Filter[b], 4°C, pH<2 (HNO_3)	180 d
Anions						
NO_3, SO_4, Cl, Br, F	Yes	300.0	100 mL	Polyethylene	4°C	7 d[c]
Alkalinity	Yes	310.1	100 mL	Polyethylene	4°C	14 d[d]
Sulfide	Yes	9030	100 mL	Polyethylene	4°C	14 d
Neutrals						
TDS	No	160.2	100 mL	Polyethylene	4°C	7 d
TSS	No	160.1	100 mL	Polyethylene	4°C	7 d
TOC	No	415.1	40 mL	Polyethylene	4°C, pH <2 (H_2SO_4)	7 d
DOC	No	415.1	40 mL	Polyethylene	4°C, pH <2 (H_2SO_4)	7 d

(a) Samples for CO_2 and H_2 analysis should not be acidified.
(b) The primary filter pore size will be 0.45 µm. In addition, several samples will be filtered using different pore-size filters, and unfiltered samples will be collected for comparison.
(c) Holding time for nitrate is 48 hours when unpreserved; holding time can be extended to 7 days when preserved with sulfuric acid.
(d) Determination of alkalinity in the field using a titration method is preferred whenever there is concern over precipitation in the sample container during storage.
VOA = volatile organic analysis.

3.8.4 Water Level Measurements

The water levels were monitored periodically in all the monitoring wells at the site to evaluate the hydraulic behavior of the permeable barrier. Water level data are available from a total of 12 monitoring events between June 1996 and February 1998. In addition, preconstruction water

levels are available for December 1995 and January 1996. These provide the background water levels and assist in determining the effect of permeable barrier placement on the flow system. In general, the water level measurements were used to evaluate the capture zone and flow patterns for the system. These data are also useful in determining the seasonal fluctuations in the flow patterns and in ensuring that the permeable barrier meets the design criteria under all conditions. Because the evaluation of hydraulic capture efficiency was a secondary objective for this study, only a few wells were placed behind the upgradient funnel walls to delineate the capture zones. Therefore, only an approximate determination of the capture zone is possible. Similarly, no wells were placed at the edges and immediately downgradient of the funnel walls. Therefore, the flow patterns in and around the funnel walls could not be precisely mapped.

Continuous water level monitoring was conducted in wells WIC-6, WW-7C, and WW-8C for 3 weeks in January 1997. In addition, the same three wells and well PZ9.8-2 were monitored continuously for water levels in August-September 1997. Well WIC-6 is located just upgradient of the reactive cell, WW-7C is in the upgradient pea gravel, and WW-8C is in the reactive iron. PZ9.8-2 is located about 45 feet downgradient of the barrier. The main purpose of the continuous monitoring was to provide a frame of reference for periodic water level and chemical monitoring and to capture short-term fluctuations that may affect performance of the barrier.

3.8.5 Down-Hole Groundwater Velocity Measurement Procedures

Direct measurement of groundwater velocity in the wells was used to aid in the understanding of flow through the barrier and in planning and interpreting tracer tests. In recent years, significant advances have been made in development of techniques and down-hole instruments for such measurements. However, most of the techniques are still experimental and all have some limitations. Therefore, the results from these measurements were used with some discretion. Two types of groundwater velocity measurement devices are commonly used. One type uses an in-situ probe that is installed permanently in the aquifer (e.g., HydroTechnics sensors). The second type uses a down-hole probe that can be temporarily placed in screened monitoring wells. The down-hole probe type was used at the Moffett Field permeable barrier to determine flow direction and velocity prior to the tracer test.

The velocity meter used in this investigation (see Figure 3-20) was the Model 40L Geoflo Groundwater Flowmeter System manufactured by KVA Analytical Systems (Falmouth, MA). The system is a portable self-contained instrument consisting of a 2-inch-diameter velocity meter probe and associated packer assembly attached to 80 feet of electronic cable, aluminum suspension rods, and a control unit with battery packs (Figure 3-21). The submersible probe consists of a central heating element surrounded by four pairs of opposed thermistors (Figure 3-22). The heating element and thermistors are contained within a packer assembly that is filled with 2-mm-diameter glass beads. The measurement of groundwater velocity and direction by the velocity meter is based on initiating a short-term heat pulse at the center of the probe. The distribution of the resulting heat in the glass beads is measured by the thermistors and the relative difference between opposed thermistors is displayed. The values read from the display are resolved into the rate and direction of flow in the well through: (1) a process of vector resolution and

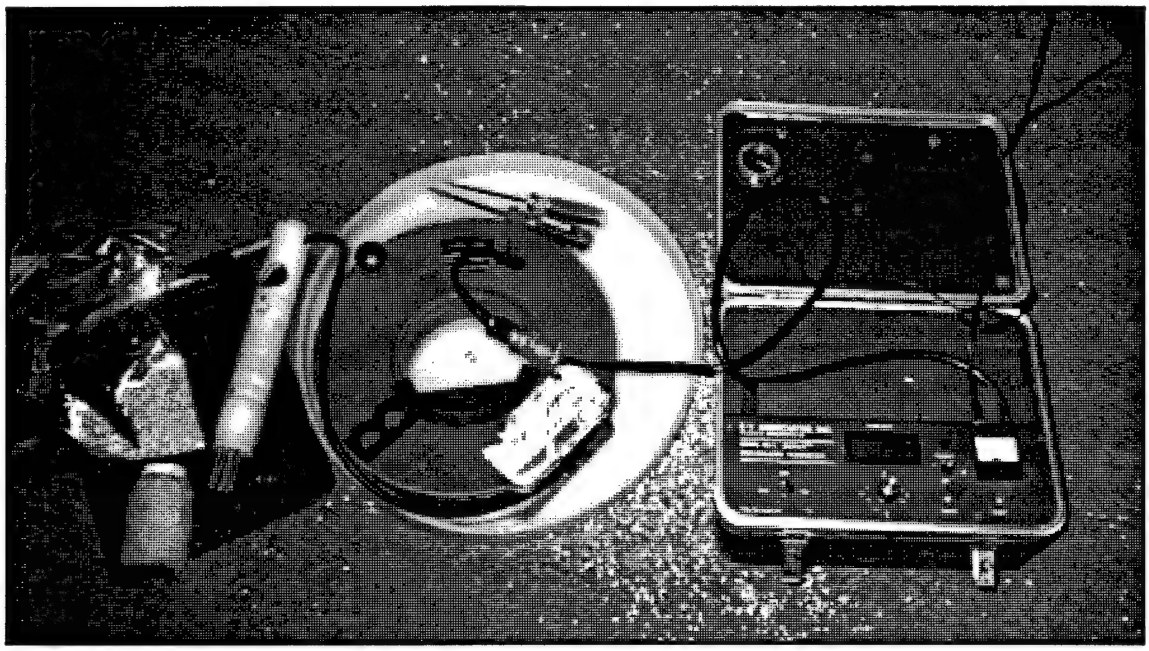

Figure 3-20. KVA Geoflow Groundwater Flowmeter System Model 40L

(2) computation with a flow velocity calibration equation. The quality of the tests can be evaluated by use of a cosine test as described in the user's manual. Hand calculations and graphical methods for vector resolution provided by the manufacturer are cumbersome. Therefore, a customized spreadsheet program using Microsoft® Excel was set up to perform vector resolution, velocity calculation, and cosine test for the Moffett Field permeable barrier site.

Calibration of the velocity meter instrument is required to ensure accurate results. Factors potentially affecting the instrument response include aquifer matrix, configuration and orientation of the well screen, size of the annular space of the well and fill material, adherence of uniform and horizontal groundwater flow through the well screen, and operator techniques. The velocity meter used at the Moffett Field permeable barrier site was rented from its manufacturer, K-V and Associates. Calibration was performed by the manufacturer prior to shipping based on the information about site-specific conditions. The calibration is based on measuring the instrument response in a laboratory tank with flow velocity, probe screen, and particle grain size similar to that expected at the site. The flow velocity calculated for several flowrates in the tank is plotted against the instrument reading, and the slope of the resulting calibration curve is used to calculate field velocity in the wells. Thus, a site-specific calibration equation is obtained for each site. Three tank flowrates (2.5, 5, and 10 feet/day) and a sensitivity range of 4X were used to construct the calibration curve for Moffett Field permeable barriers. The calculation sheets and the resulting calibration curve are presented in Battelle (1997e). The flow directions calculated from the vector resolution were further adjusted for magnetic declination at the site by adding 16.5 degrees to the calculated angle.

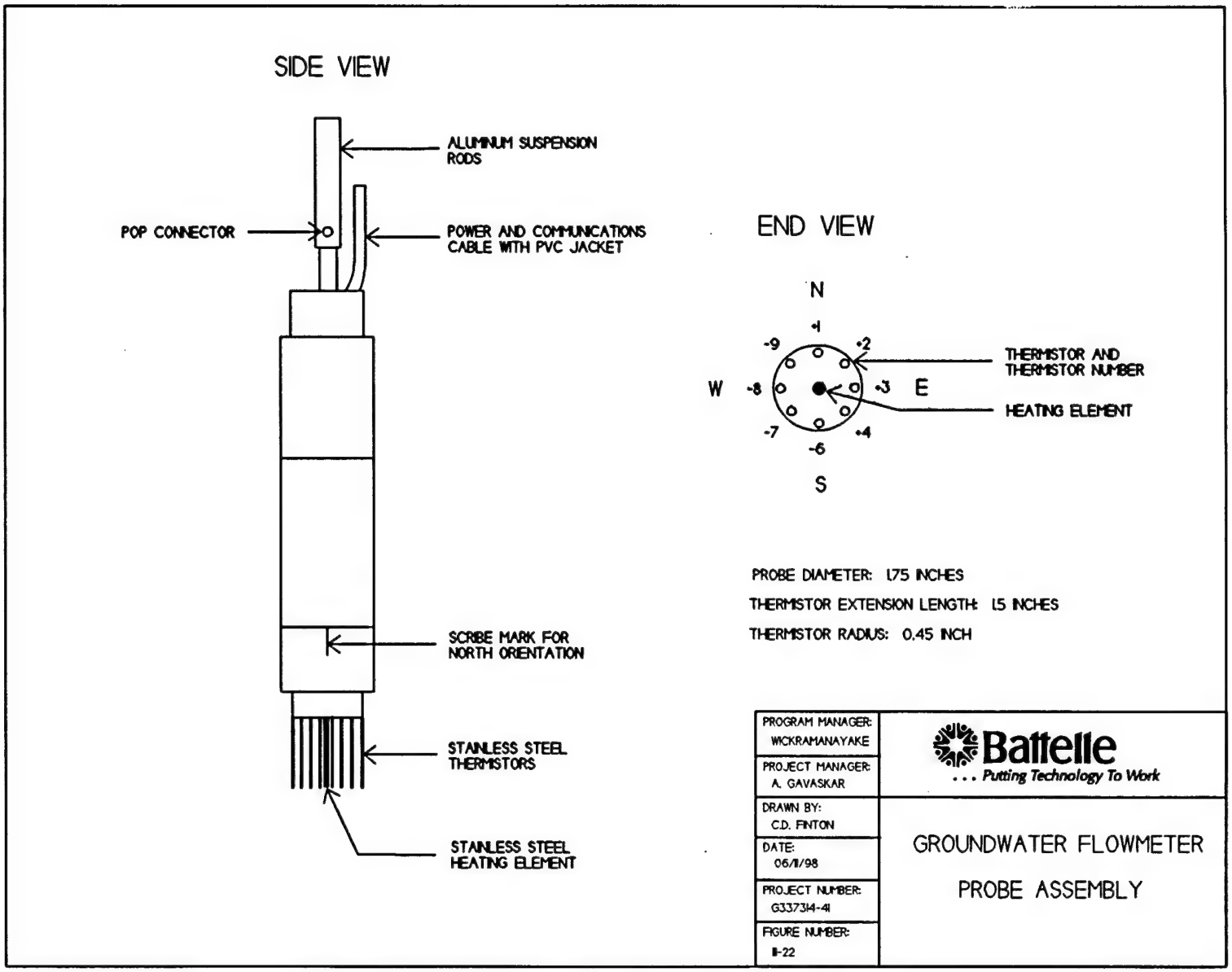

Figure 3-21. Groundwater Flowmeter Probe Assembly

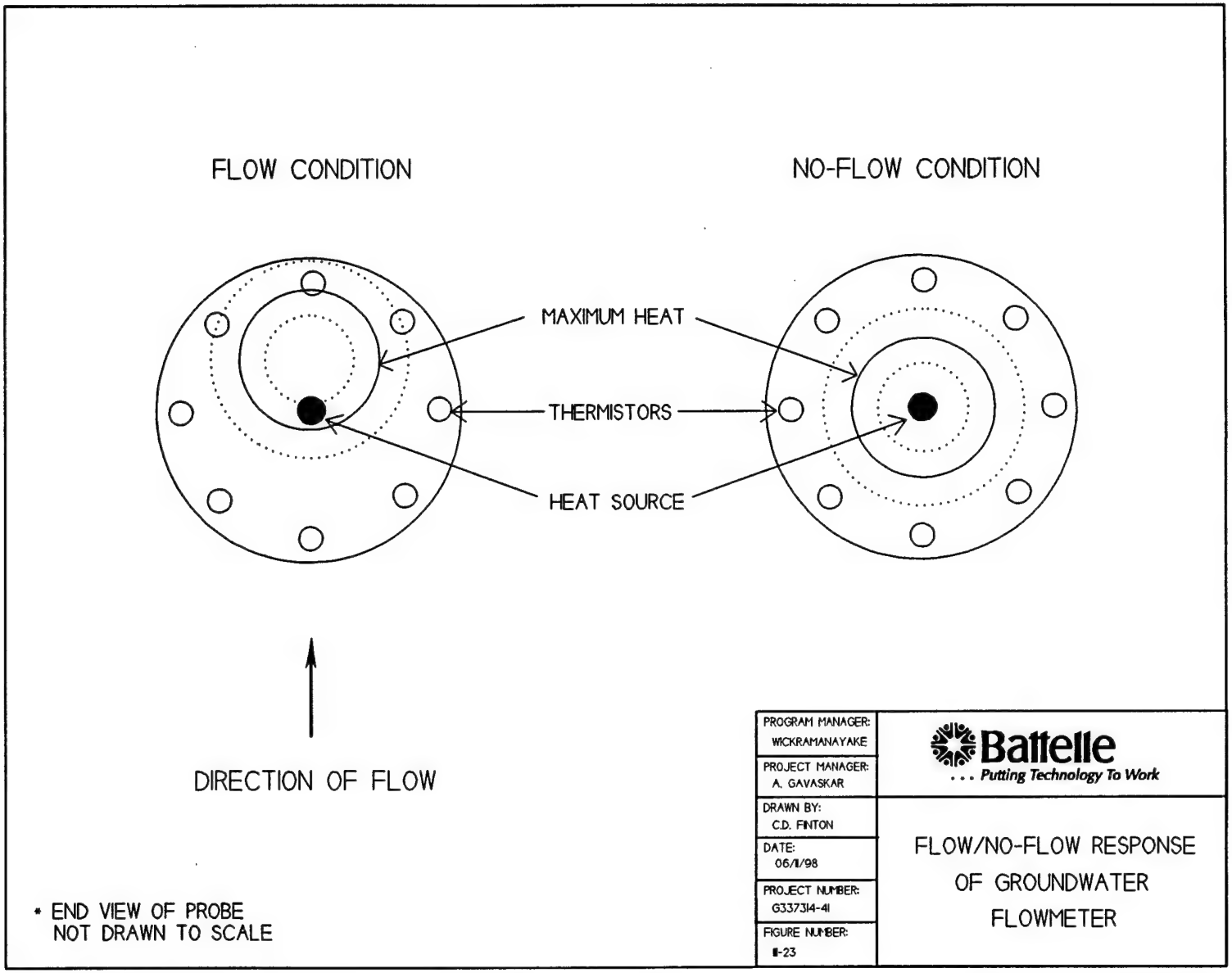

Figure 3-22. Flow/No-Flow Response of Groundwater Flowmeter

At Moffett Field, groundwater velocities in several wells in the upgradient and downgradient pea gravel, A1 aquifer zone, and the reactive media were measured. Only the 2-inch-diameter wells were tested due to the size of the probe. Testing was performed by lowering the probe attached to aluminum rods and electrical cable into the well and monitoring the heat pulse response with the probe aligned with the north and the south directions. The time needed for the probe to equilibrate with ambient groundwater flow was longer than expected. Therefore, all of the 2-inch wells at the site could not be tested. The probe and the aluminum rods were decontaminated with deionized water between successive tests. Several depths were tested in some of the wells.

3.8.6 Tracer Test Methods

Tracer testing was conducted to improve the understanding of flow through the barrier. Some key issues involved in tracer testing include selecting the tracer material, choosing the location of monitoring wells, and determining sampling frequency. Tracer selection for flow direction and velocity determination usually requires a conservative substance to avoid significant retardation of the tracer by sorption or chemical reactivity. The tracer must be monitored at multiple locations based on an initial approximate expectation of the flow patterns so that the monitoring points are placed downgradient of the injection points and most of the injected tracer can be detected as it passes. The sampling frequency is based on an approximation of the flow velocity, such that a large number of measurements are possible during the time the tracer passes through the monitoring locations. The tracer injection should be small enough that the injected volume does not have a large impact on the flow field, i.e., natural hydraulic gradients are not disturbed. However, the mass of the tracer needs to be large enough to obtain detectable concentrations in the monitoring wells.

3.8.6.1 Tracer Selection

Bromide was selected as the most advantageous tracer for the following reasons:

1. Bromide has been shown to be a relatively conservative tracer with respect to iron (a retardation factor of 1.2 in granular iron has been noted by General Electric) (Sivavec, 1997).

2. Potassium or sodium bromide is inexpensive and highly soluble in water.

3. Analytical costs associated with bromide concentration measurements using specific ion electrodes and automated data recorders are not excessive.

4. Bromide is nonhazardous in low concentrations and therefore may pass regulatory requirements easily.

5. Bromide concentration can be measured in real time, so there is less chance of missing the peak.

Based on these observations, potassium bromide (KBr) was selected as the tracer compound for this study.

3.8.6.2 Tracer Monitoring Method

Continuous real-time monitoring was chosen as the primary method of obtaining bromide concentration data. This method had several important advantages over traditional point-in-time groundwater sampling and analysis:

- Continuous monitoring provides a means of obtaining a large amount of data without creating a disturbance in the flow field associated with sample collection. This is especially relevant at this site because large numbers of samples needed to be collected from closely spaced wells.

- Continuous monitoring ensured that any of the concentration breakthroughs and peaks were not missed due to insufficient sampling frequency in this relatively high-velocity media.

- Less total expense was involved in continuous monitoring, compared to costs involved in setting up a field analytical facility and analyzing a large number of samples.

- There was significant savings in the labor costs because fewer people were needed to conduct the tracer test and samples did not need to be collected around the clock.

3.8.6.3 Field Tracer Test Planning

The tracer injection location and duration, as well as the location of the down-hole bromide probes obtained for the field study, were determined from previous modeling experience and the groundwater velocity vector measurements (see Section 3.8.5). The groundwater velocity vector measurements indicated that flow in the upgradient aquifer zone is predominantly eastward near WIC-1, but highly variable in the pea gravel and reactive cell wells. Based on an assessment of these data in the field, WW-2 was chosen as the tracer injection well for the first test (initiated 3/29/97) and WIC-1 was chosen for the second test (initiated 7/30/97). WW-2 is located in the west side of the upgradient pea gravel (Figure 3-19). The objective of the first injection (in WW-2) was to ensure that groundwater flowed from the upgradient pea gravel into the reactive cell. The objective of the second injection (in WIC-1; see Figure 3-18) was to ensure that groundwater in the immediate upgradient vicinity of the barrier flowed into the upgradient pea gravel.

3.8.6.4 Field Tracer Injection

The tracer injection solution for the first injection was prepared at a concentration of 3,000 mg/L bromide using reagent-grade KBr and groundwater from WW-7C. The solution was injected into WW-2, a 2-inch well in the upgradient pea gravel. A peristaltic pump was used to pump the solution through a ¼-inch Teflon™ tube that was slotted from 15 to 20 feet bgs and packed off at the top, as shown in Figure 3-23. This was done to distribute the tracer uniformly within the vertical section and help promote a larger bromide plume. Injection of tracer solution began at 1620 hours on 3/29/97. Tracer was injected at a rate of 100 mL/minute for approximately 2 hours. A total of 12 liters of tracer solution were injected, which is equivalent to 36 grams of bromide.

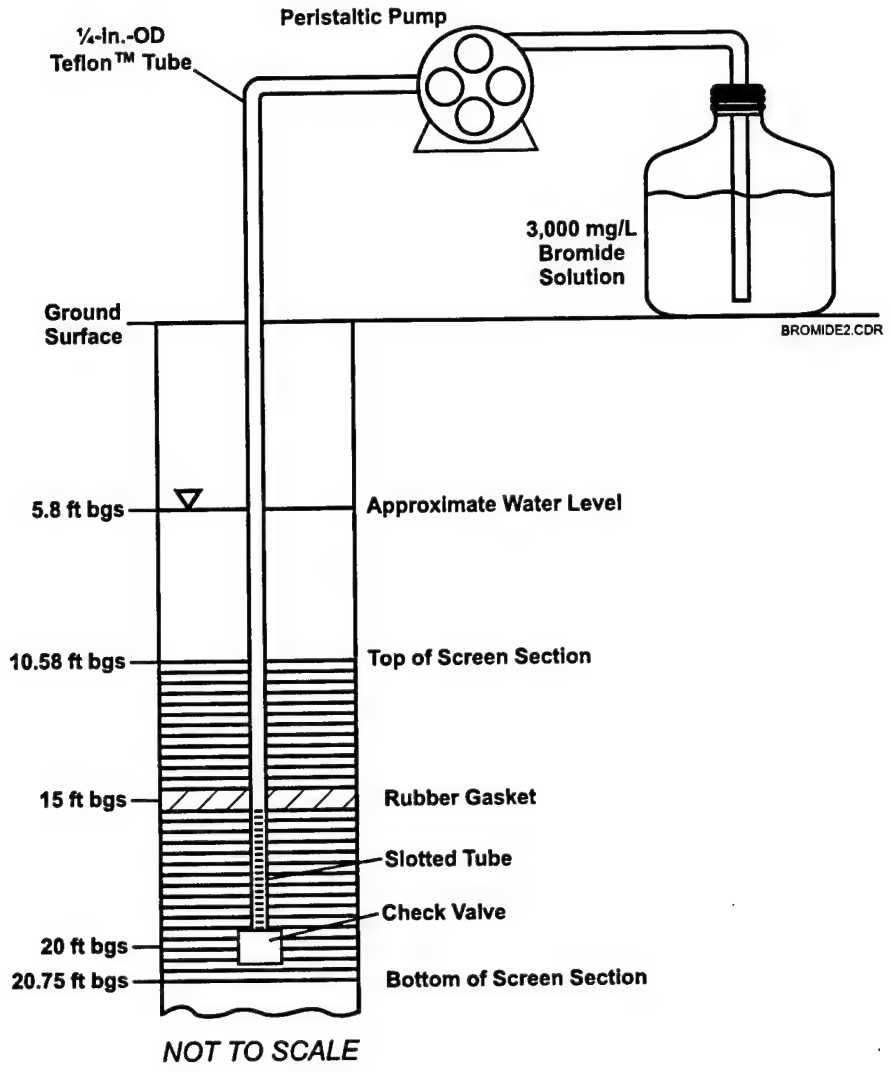

Figure 3-23. Configuration of Bromide Injection System at WW-2

The tracer injection solution for the second injection was prepared by dissolving 171 grams of reagent-grade KBr (equivalent to 115 grams bromide) with groundwater from the upgradient aquifer, to obtain a bromide concentration of 3,190 mg/L. The bromide solution was injected into WIC-1, a 2-inch monitoring well in the upgradient aquifer that is screened from 19 to 24 feet bgs. A peristaltic pump was used to pump the tracer solution through ¼-inch OD Teflon™ tubing that was slotted from 19 to 21 feet bgs and packed off at the top and bottom. The slotted tubing was employed to distribute the tracer solution uniformly within the 2-foot vertical section and help promote a larger bromide plume. Injection of tracer solution began at 1300 hours on 7/30/97 and

concluded approximately 10 hours later. A total of 36 liters of tracer solution was injected at a rate of 60 mL/minute.

3.8.6.5 Field Tracer Detection Equipment

Sixteen Temphion™ submersible water quality sensors (see Figure 3-24) were rented from Instrumentation Northwest, Inc. (Redmond, WA) for use in down-hole and aboveground detection of bromide. The sensors were equipped with a bromide-specific electrode, reference electrode, and temperature sensor, as shown in Figure 3-25 (the pH module was not used during tracer testing). The outside diameter of the sensor is 0.90 inch and could be installed in both the 1-inch and 2-inch-diameter wells in the permeable barrier. The bromide electrode consists of a silver ring plated with AgBr and is used in conjunction with the Ag/AgCl reference electrode. The body of the sensor is made of Delrin® and 300-series stainless steel. Sealants are composed of Viton® rubber and Teflon™. Each sensor was connected to a 6-conductor shielded electrical cable with an ether-based polyurethane jacket. The signal from the bromide electrode was conditioned by an amplifier circuit and noise-reducer prior to input to an 8-channel automatic data logger or handheld Orion meter.

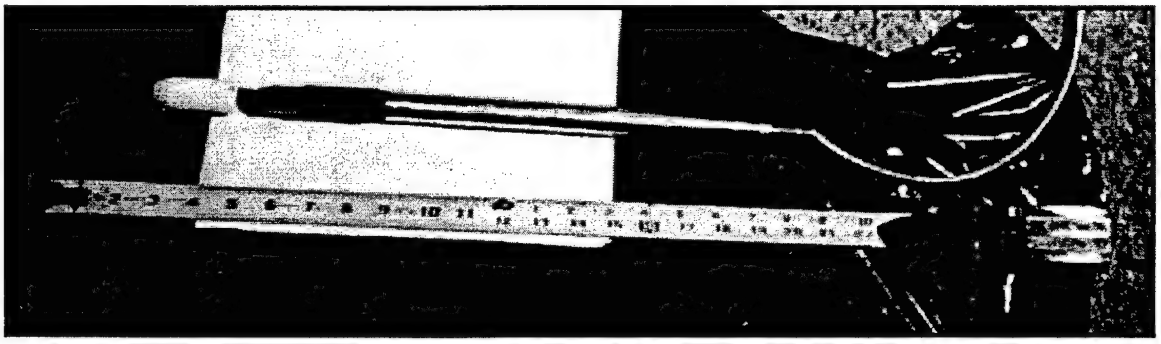

Figure 3-24. Temphion™ Submersible Water Quality Sensor

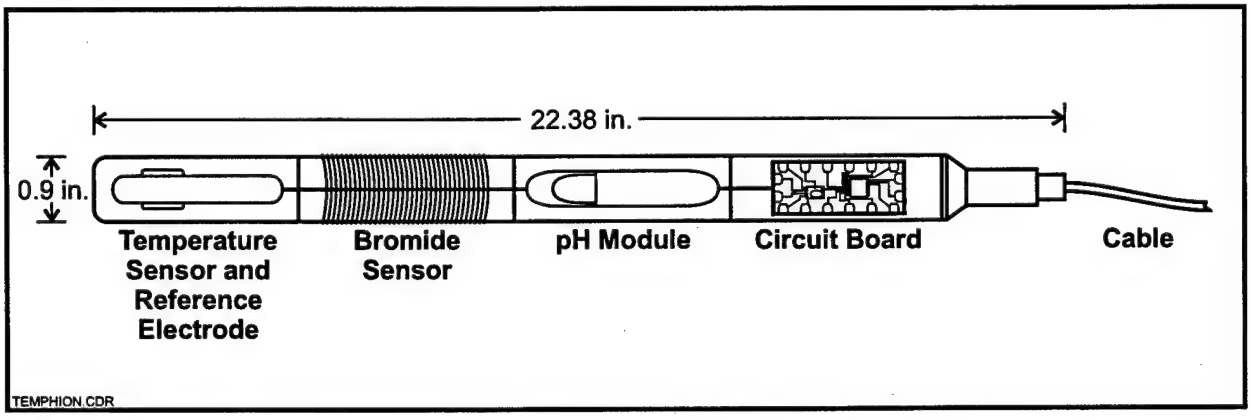

Figure 3-25. Schematic Diagram of INW Temphion™ Sensor

Two 8-channel data loggers were programmed to record sensor outputs at 5-minute intervals. The handheld meter was used to measure output from an ex-situ probe whenever water samples were pumped from additional wells for analysis above ground. Ex-situ samples were taken for bromide sensor measurements several times each day, and more frequently when the signal strength increased, indicating the presence of bromide.

The sensors were calibrated at 1, 10, 100, and 1,000 mg/L bromide. Calibration solutions were prepared using reagent grade KBr and groundwater from the reactive cell. Calibration curves were made using the three highest concentrations, because the response was nonlinear below 10 mg/L. Initial calibration curves are show in Appendix D. Calibration was performed routinely during the testing period. After the response of each sensor was checked, 15 sensors were installed down-hole and 1 sensor was used to take aboveground measurements. Due to a bend in the lower portion of the 1-inch polyvinyl chloride (PVC) casings, the probes could not be lowered to the screened sections of some of the "C" and all of the "D"-level wells. Water samples from these wells had to be pumped to the surface for sensor analysis. Water samples also were collected routinely for laboratory analysis of bromide and potassium.

Table 3-11 shows the wells that were monitored throughout the first tracer study and indicates the type of analysis method used. Some wells were monitored continuously in the vicinity of and downgradient from the injection well. Wells that are located a greater distance from the injection well or not within a suspected flowpath were monitored less frequently. A similar strategy was employed during monitoring of the second tracer injection test, although monitoring was concentrated in the upgradient pea gravel and aquifer.

3.8.7 Core Sample Collection Methods

As outlined in the performance monitoring plan, at the end of the monitoring period (approximately 20 months after installation of the barrier), a few core samples were collected from within the reactive cell to look for signs of iron encrustation, precipitate formation, and microbial growth. These conditions have the potential to reduce the efficiency of the permeable barrier by restricting flow through the gate and reducing residence time in the reactive cell. They also affect the longevity of the barrier and hence the operating costs. Cores samples were taken at several locations within the reactive cell to obtain adequate spatial information about possible changes in the granular iron medium.

Precision Sampling, Inc., of San Rafael, California, provided the equipment required to extract cores at the Moffett Field permeable barrier site. Samples from eight locations in the barrier and downgradient aquifer were extracted on December 8–9, 1997. This section describes sampling locations, sample collection methods, and procedures for storing the samples prior to analysis.

3.8.7.1 Core Sample Locations

Coring locations were chosen to provide specimens over a large area of the permeable barrier and also to include one aquifer sample downgradient of the permeable barrier. However,

Table 3-11. Types of Tracer Monitoring During the First Trace Injection Test

Type of Monitoring	Monitoring Wells Sampled				
	Upgradient A1 Aquifer Zone Wells	Upgradient Pea Gravel Wells	Reactive Cell Wells	Downgradient Pea Gravel Wells	Downgradient A1 Aquifer Zone Wells
Continuous In-Situ Monitoring	WIC-7, 8	WW-2, WW-7B,C, WW-11	WW-3(a), WW-4C, WW-5, WW-8B, C, D, WW-9C, WW-12, 14	WW-6, WW-15, WW-18D	WIC-11, 12, PIC-31
Continuous Ex-Situ Monitoring		WW-7D, WW-16D	WW-1C,D, WW-4D, WW-5, WW-8D, WW-9D, WW-12, WW-13C, D, WW-17D	WW-6, WW-10D, WW-15, WW-18D	WIC-12
Conditional Monitoring	WIC-1, 5, WIC-6, 8	WW-7C, WW-16B, D	WW-3, WW-4C, WW-8C, WW-13B, WW-14, WW-17C	WW-10B, WW-10C, WW-18C	WIC-9, 10, 11, PIC-31, 32
Laboratory Analysis		WW-2, 11, WW-16D	WW-1D, WW-3, WW-4C, D, WW-5, WW-8D, WW-9D, WW-12, WW-13C, D, WW-17D	WW-6, WW-10D	

(a) The sensor installed in this well was not responding correctly after it was installed. Therefore, data recorded do not represent true bromide concentrations.

precedence was given to the upgradient portion of the reactive cell, where four vertical cores and one angled core were taken. The vertical cores were taken slightly eastward of the centerline based on results of the April 1998 bromide tracer test, which indicated that the eastern side of the permeable barrier was hydraulically more active than the western side. Angled corings were taken to expose greater surface area and to cut across the interface of the iron and pea gravel. Table 3-12 provides the location and orientation of sample corings. This sampling strategy was expected to yield representative cores within the treatment zone. A downgradient aquifer sample was chosen to investigate whether chemical or microbiological changes in the reactive cell had become evident in the aquifer. One potential concern is that precipitate formation or microbiological growth in the reactive medium might become trapped in the aquifer due to its finer grain size.

Table 3-12. Location and Orientation of Sample Corings

Core No.	Easting[a]	Northing[a]	Angle of Penetration	Azimuth (Relative to Northing)
C-1	1548689.36	335792.96	0	–
C-2	1548689.50	335793.59	0	–
C-3	1548689.65	335794.04	0	–
C-4	1548690.72	335798.22	0	–
C-5	1548692.37	335799.76	25°	190°
C-6	1548689.30	335801.64	0	–
C-7	1548691.26	335791.23	25°	6°
C-8	1548690.00	335794.63	0	–

(a) Easting and northing coordinates correspond to the California State Plane Coordinate System for Zone 403.

Cores were taken from eight locations in the vicinity of the permeable barrier. Six of the corings were vertical and two were angled at approximately 25 degrees off normal. Figure 3-26 shows a planar view of the coring locations in relation to the groundwater monitoring wells. On this figure, square symbols represent vertical corings and triangles represent angled corings. Dashed lines indicate the approximate azimuthal orientation of the angled cores. Figure 3-27 shows a vertical profile of the permeable barrier along the northing coordinate, which coincides approximately with the regional groundwater flow direction. In this figure the filled line indicates a depth where a sample was recovered and the unfilled line indicates that no sample was recovered. Altogether, samples were obtained from 20 discrete locations and depths. The locations of these samples were chosen to provide good spatial representation and to avoid disturbing the monitoring wells. Table E-1 in Appendix E contains a summary of all the samples that were collected.

Typically, less than a full 3-foot section of core was recovered during each advancement of the sampler (see Table E-1). In some cases, no sample could be recovered, either because the coarseness of the medium (especially the pea gravel) became obstructed in the opening of the core barrel, or because the sample failed to be contained in the sleeve by the sand catcher. The minimum depth at which samples were collected was 7 feet bgs, which corresponds roughly with the upper extent of the iron. Directly above the iron zone there is a cementiceous material (flowfill) and native soil was placed above this to the ground surface. At the base of the permeable barrier (approximately 21 feet bgs) is a concrete slab, which was penetrated to 2 or 3 inches in one coring location (Core No. C-8).

3.8.7.2 Sample Collection Method

Precision Sampling uses the Enviro-Core® dual-tube sampling system to collect continuous and discrete-depth soil cores. The coring system consists of a small-diameter drive casing and an inner sample barrel that are simultaneously vibrated into the ground. Soil cores were collected in polybutyrate liners inside the sample barrel. After being advanced 3 feet, the full sample barrel

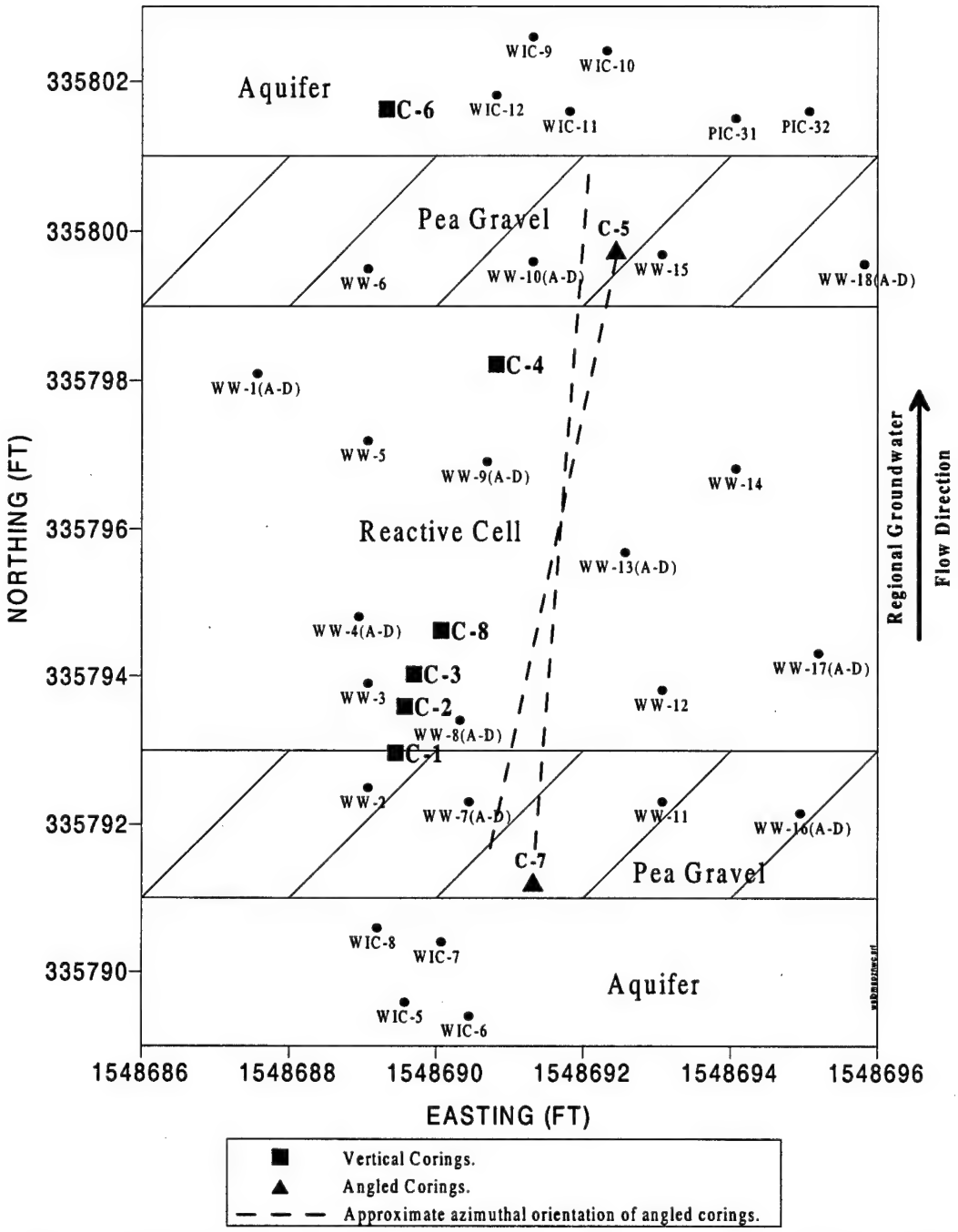

* Easting and Northing coordinates correspond to the California State Plane Coordinate System for zone 403.

Figure 3-26. Planar View of Coring Locations and Groundwater Monitoring Wells

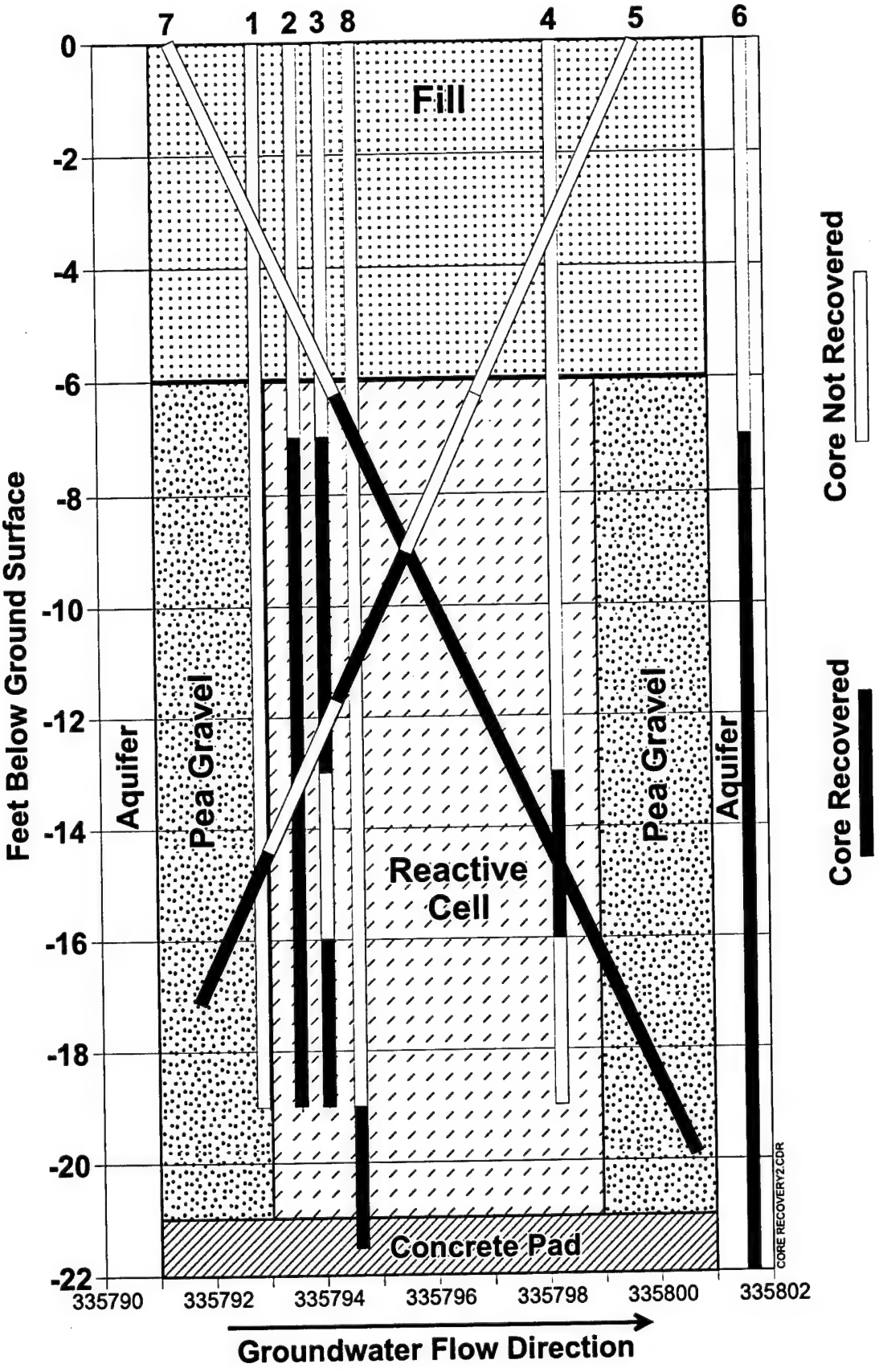

Figure 3-27. Vertical Profile of the Barrier Showing the Coring Locations

was retrieved, while the drive casing was left in place to prevent the probe hole from collapsing. The drive casing ensures that subsequent samples are collected from the targeted interval, rather than potentially contaminated slough from higher up in the probe hole. The sample sleeves measured 3 feet long and 1-¾ inches in diameter. The sampling system was mounted on an XD series all-terrain rig with a skid loader (Figure 3-28). After the sleeves were removed from the sample barrel, one end was wrapped with a sheet of Teflon™ and covered with a polyethylene cap. Water from the reactive cell was poured into the sleeve to displace air and the other end was sealed in the same fashion. Plastic tape was wrapped around the ends of the sleeves to prevent the caps from leaking or becoming loose. The boreholes were backfilled with unused granular iron or pea gravel that remained from construction of the permeable barrier, and the asphalt surface of the parking lot was patched.

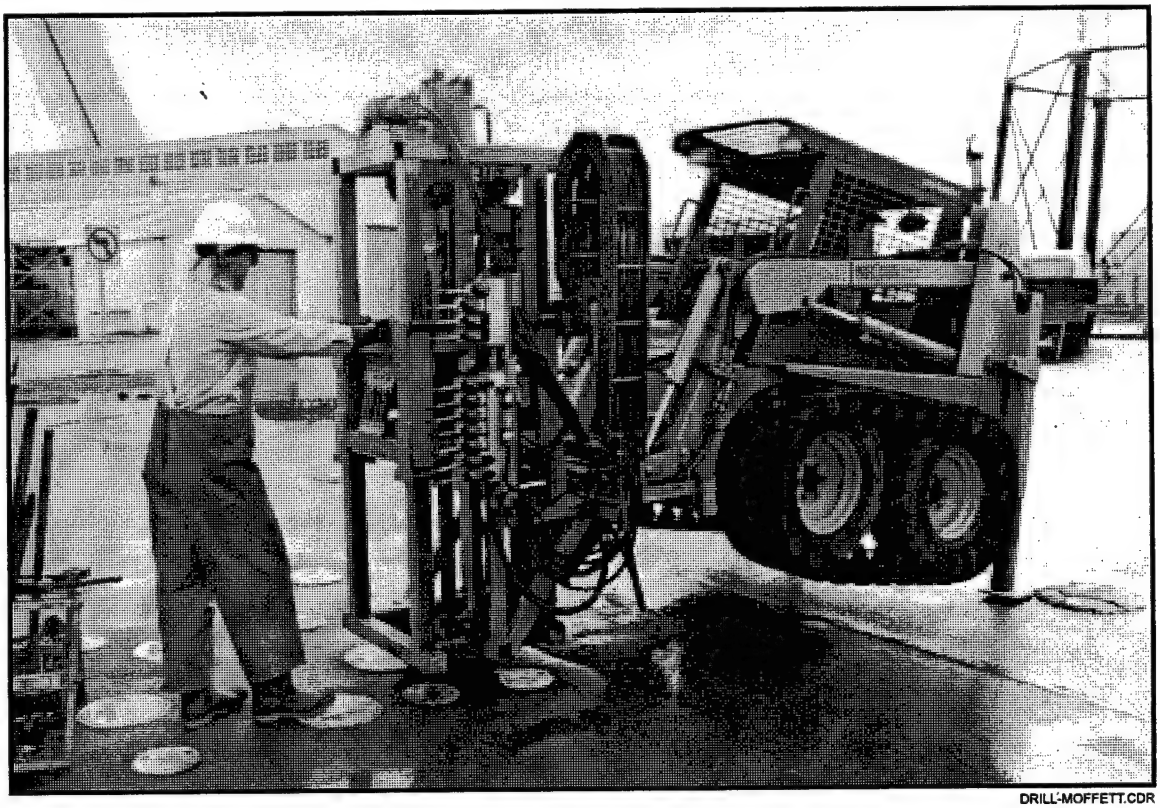

Figure 3-28. Operation of Enviro-Core® Sampler for Collection of Core Samples at Moffett Field Permeable Barrier

3.8.7.3 Core Samples Storage

The sleeves containing the core samples were refrigerated immediately after they were collected in the field and shipped on Blue Ice™ to an off-site Battelle laboratory. The laboratory transferred the samples to an anaerobic glove box that was then purged with ultrapure nitrogen. Samples for microbiological analysis were removed from the sleeves and repackaged inside the

glove box, then shipped in an airtight container to an analytical laboratory. The remaining samples were dried for inorganic analysis. Depending on the length of the core sleeves, between one and four sleeves were removed from the glove box and transferred to a heated vacuum desiccator. The tape around the sleeve end caps was removed, but it was not necessary to remove the end caps themselves to dry the core sample inside. Vacuum drying was conducted at approximately 125°F, and up to 72 hours was required to achieve complete drying. The core samples were then returned to the glove box for preparation for chemical and spectroscopic analysis.

3.8.7.4 Core Sample Preparation

In the Battelle laboratory, sleeve end caps were removed from the dried core samples inside the nitrogen-filled glove box and approximately 1 inch of material from both ends was discarded. The remainder was emptied into glass jars and mixed to homogenize the sample. There were no differences in appearance, color, or aggregation within each core section. Subsamples were prepared in small glass vials, then sealed in the nitrogen environment.

3.8.7.5 Core Analysis Methods

Samples were analyzed by Battelle and its subcontract laboratories using the methods shown in Table 3-13. Samples for wet chemical analysis were treated in the following manner. Approximately 25 grams of dry material was weighed into glass beakers and digested with 50 mL of 0.01 N acetic acid for 30 minutes with continuous stirring. The acetic acid treatment was performed to dissolve carbonates [e.g., $Ca(CO_3)$ and $Mg(CO_3)$] and soluble hydroxides [e.g., $Mg(OH)_2$]. Acid solutions were decanted and further digested with nitric acid prior to analysis for calcium and magnesium by atomic absorption spectrophotometry.

Table 3-13. Characterization Techniques for Coring Samples

Analysis Method	Description
Bulk Chemical Analysis Digestion of subsample to determine calcium and magnesium content.	Quantitative determination of bulk chemical composition. Useful for determining fraction of carbonates in core profile.
Raman Spectroscopy Confocal imaging Raman microprobe	Semiquantitative characterization of amorphous and crystalline phases. Suitable for identifying iron oxides and hydroxides.
Scanning Electron Microscopy(SEM) Secondary electron images (SEI) Backscatter electron images (BEI) Energy dispersive spectroscopy (EDS)	High-resolution visual and elemental characterization of amorphous and crystalline phases. Useful for identifying morphology and composition of precipitates and corrosion materials.
X-Ray Diffraction (XRD) Powder diffraction	Qualitative determination of crystalline phases. Suitable for identifying carbonates, magnetite, goethite, etc.
Microbiological Analysis Isolation streak Fatty acid profile (GC-FAME)	Identification of microbial population within the cored material. Relates to presence or absence of iron-oxidizing or sulfate-reducing bacteria.

Samples for Raman spectroscopy were sent to Miami University (of Ohio), Molecular Microspectroscopy Laboratory for analysis. Confocal Raman spectra were collected with a Renishaw System 2000 Raman Imaging Microscope. This system employs a 25-milliwatt HeNe laser and Peltier-cooled charged coupled device (CCD) detector for excitation and detection of Raman scattered light, respectively. The system features fast full-range scanning (100 to 4,000 wavenumbers) and direct two-dimensional (2-D) Raman imaging. Spatial resolutions of 1 micrometer and axial resolution of 2 micrometers can be achieved with the use of the confocal feature.

Samples for SEM were sent to the Battelle Microscopy Center. A JEOL 840 SEM was used to collect images. The SEM has a resolution of approximately 6 nm and magnifications ranging from 10 to 300,000X. A variety of imaging modes are possible for examination of metallic and nonmetallic samples, including secondary electron and backscattered electron imaging. An EDS permits qualitative analysis of chosen areas for elements with atomic weight equal to or greater than that of sodium. The SEM 840 is interfaced with a Tracor Northern computer for automatic stage movements and data collection.

Samples for XRD were sent to the Battelle Microscopy Center. The Center's XRD capabilities include preparation of samples, automatic, unattended acquisition of data, and computer-aided interpretation of results. A pretreatment step was performed to concentrate the corrosion compounds so that that they would not be masked by the metallic iron peaks. To separate corrosion coatings from the bulk material, the iron filings were placed in a fine sieve and brushed until a sufficient quantity of corrosion coatings was collected. A fully automated Rigaku diffractometer was used to analyze the samples.

Four samples were sent to Microbe Inotech Laboratories in St. Louis, Missouri for microbiological analysis. These samples were removed from the core sections before vacuum drying, as required by the procedure. The samples were analyzed for heterotrophic plate counts and GC-FAME (gas chromatograph-fatty acid methyl ester) of microbial strains. The laboratory procedures involved making liquid dilutions that were plated onto agar with Oxyrase enzyme in anaerobic petri plates. The plates were incubated anaerobically for 48 hours at 28°C. Following isolation, the strains were streaked onto Trypticase-soy agar (TSA), then incubated for 24 hours followed by processing by GC-FAME.

4. Performance Assessment

Following installation in April 1996, the Moffett Field barrier was monitored for six consecutive quarters. Scheduled monitoring events were conducted during the following months:

- June 1996
- September 1996
- January 1997
- April 1997
- July 1997 (partial sampling)
- October 1997

Groundwater sampling conducted in April 1997 was repeated in July 1997 because the analytical laboratory excessively diluted the April samples, resulting in unacceptably high detection limits being reported. In addition to these scheduled monitoring events, other special monitoring activities were conducted as required to meet performance objectives. These additional monitoring activities included the following:

- Thirteen periodic water level measurements over 16 months
- Two continuous water level measurement events
- One down-hole groundwater velocity measurement event
- Two tracer tests

Detailed monitoring reports for each quarterly monitoring event were prepared by Battelle and submitted to NFESC (see key references in Section 7). Summary data tables for the monitoring events are presented in Appendices D (water level data) and H (groundwater analysis data). These data are arranged by monitoring well in the same progression as the general groundwater flow (from south to north) for easier identification of concentration trends. The progression is as follows:

- Upgradient A1 and A2 aquifer zone data
- Upgradient pea gravel wells
- Reactive cell wells
- Downgradient pea gravel wells
- Downgradient A1 and A2 aquifer zone wells

The locations of the monitoring wells are mapped in Figures 3-18 and 3-19 (in Section 3). Table C-1 (in Appendix C) lists well location coordinates, top of casing elevations, casing diameters, and well screen intervals. The data from these monitoring events were used to evaluate the performance of the pilot barrier at Moffett Field in terms of its ability to accomplish the following:

- Degrade target contaminants
- Maintain downgradient water quality

- Effect hydraulic capture
- Sustain long-term performance

4.1 Degradation of Target Contaminants

Appendix H contains the results of the CVOC analyses for all five sampling events. The objectives of the contaminant data evaluation were as follows:

- To ensure that target CVOC contaminants concentrations are reduced to below their respective MCLs
- To verify the presence of byproducts expected from proposed degradation mechanisms
- To estimate the half-lives of the target contaminants in the field system and compare them to the half-lives estimated during bench-scale tests

4.1.1 Contaminant Levels in the Groundwater Influent to the Gate

Historically, TCE, *cis*-1,2-DCE, and PCE are the predominant contaminants in the groundwater underlying Site 9, the location of the permeable barrier. However, several other CVOCs are detectable in the A1 aquifer zone groundwater upgradient to the permeable barrier. Table 4-1 shows the average and range in concentrations of CVOCs in the groundwater entering the barrier gate over the five sampling events. These values are based on results of analyses from wells WIC-1, WIC-6, and WIC-7, which are located immediately upgradient of the barrier (see

Table 4-1. Concentrations of CVOCs in the Upgradient A1 Aquifer Zone Groundwater for the Five Monitoring Events

Analyte[a]	n[b]	Average (µg/L)	Minimum (µg/L)	Maximum (µg/L)
PCE	11	16	5.9	32
TCE	16	1,360	920	2,900
cis-1,2-DCE	17	230	170	310
Vinyl Chloride	2	< 0.5	< 0.5	0.4 J
1,1-DCA	12	22	18	26
1,2-DCA	0	< 0.5	< 0.5	< 0.5
1,1-DCE	12	31	18	58
trans-1,2-DCE	3	2	< 0.5	3
Carbon Tetrachloride	0	< 0.5	< 0.5	< 0.5
Chloroform	5	< 1	< 0.8	0.9
Chlorofluorocarbon (CFC)-113	10	27	13	56
Methylene Chloride	0	< 0.5	< 0.5	< 0.5
1,1,1-TCA	1	< 3	< 0.5	2.9

(a) Combined results for upgradient wells WIC-1, WIC-6, WIC-7, and WIC-8.
(b) Number of analyses above detection limit.
J Indicates that the value is qualitatively identified but is reported at an estimated quantity.

Figures 3-18 and 3-19). WIC-5, another upgradient well, was excluded from this analysis because it is a shallow well with a 1-foot screen section and generally shows anomalous water levels and much lower CVOC concentrations than the deeper wells. Concentrations of CVOCs at WIC-1 (a long-screen well) are similar to those measured at WIC-6 and WIC-7.

As shown in Table 4-1, TCE was the dominant contaminant entering the upgradient aquifer. The average concentration of TCE is 1,360 µg/L. The next most abundant analyte is *cis*-1,2-DCE, which has an average concentration of 230 µg/L. *cis*-1,2-DCE is a degradation product of TCE by the hydrogenolysis pathway and is indicative of possible natural attenuation of TCE and PCE in the plume. Similarly, vinyl chloride is also a degradation product of TCE by hydrogenolysis, but is mostly absent from the influent groundwater. Other CVOCs were detected, but at much lower concentrations; these include 1,1-DCA; 1,1-DCE; PCE; chlorofluorocarbon (CFC)-113; and 1,1,1-TCA.

The quarterly monitoring data for the six quarters summarized in Table 4-1 compares well with the historical data from well W9-35 (Table 3-3). The general agreement between the two data sets indicates that the contaminant plume composition has not changed dramatically since the site was first characterized.

Nonchlorinated VOCs were also analyzed during the five quarterly sampling events, but were generally below detection. Results of the groundwater analysis for BTEX compounds in the September 1996 sampling event are summarized in Table H-2a(2) in Appendix H. Similarly, BTEX and other nonchlorinated VOCs were either nondetectable or reported at very low concentration during other monitoring events. These results suggest that fuel-related hydrocarbons are not present in the influent groundwater.

4.1.2 Degradation of Contaminants in the Gate

Concentrations of CVOCs for the five monitoring events are presented in Appendix H. Time trends in the concentrations of TCE, *cis*-1,2-DCE, and 1,1-DCA in the permeable barrier and nearby wells over these five quarters are shown graphically for four representative wells in Figures 4-1 through 4-3. These select wells lie along the centerline through the gate in the general direction of groundwater flow.

Figure 4-1 shows that TCE concentration increased steadily in the WIC-1 aquifer well from 1,180 µg/L in June 1996 to 2,800 µg/L in October 1997. Consequently, TCE concentrations in the upgradient pea gravel well (WW-7C) showed an increasing trend from 570 to 1,000 µg/L. Concentrations of TCE are somewhat lower in the pea gravel than in the upgradient aquifer, which is thought to be due in part to horizontal and vertical mixing of the heterogeneously distributed contamination entering through the influent groundwater. Another possible explanation is that a small amount of iron may have become mixed into the pea gravel during construction, resulting in limited degradation of the contaminants there.

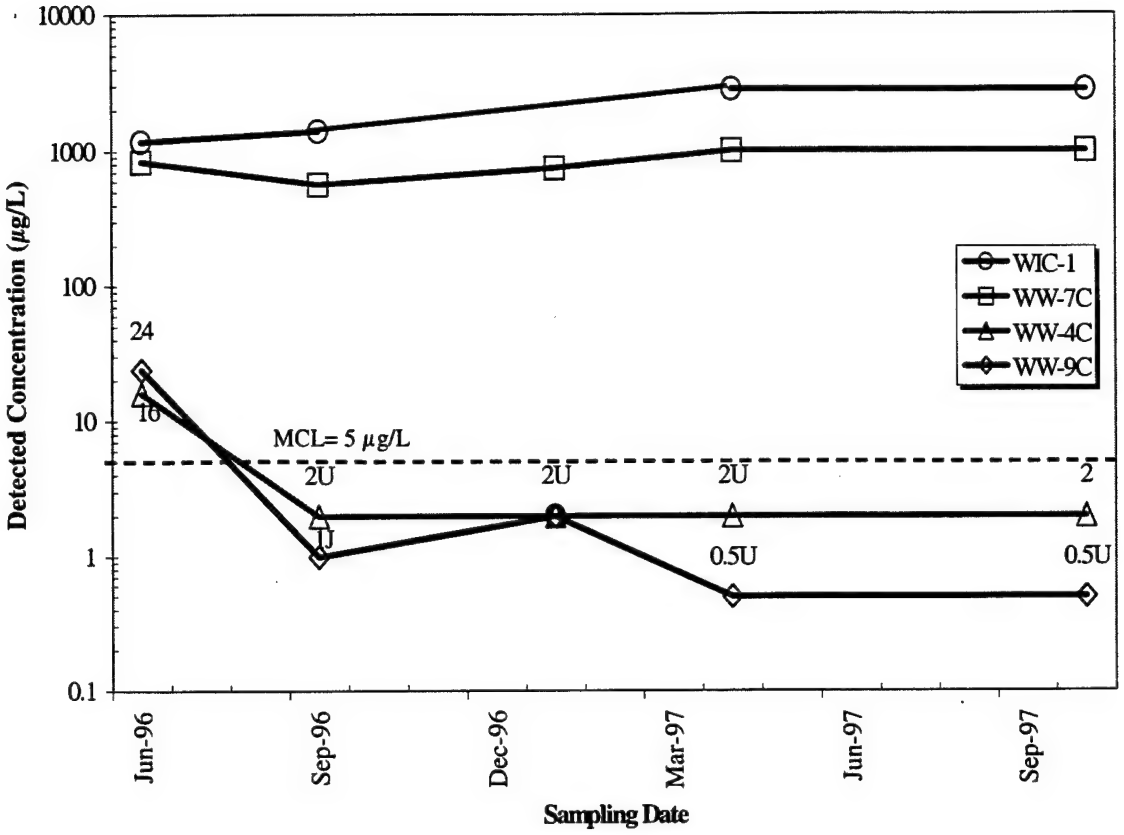

Figure 4-1. Concentrations of TCE in Four Water Samples over the Performance Monitoring Period. J indicates that the value was qualitatively identified but reported at an estimated quantity; U indicates that the analyte was not detected at the reported quantity.

In both the reactive cell wells (WW-4C and WW-9C) in Figure 4-1, TCE is below its MCL (5 µg/L) in every quarter, except June 1996. WW-4C is located approximately 2 feet into the reactive cell and WW-9C is located approximately 4 feet into the reactive cell. The relatively higher TCE concentrations in June 1996 are probably due to unsteady-state conditions within the reactive cell, which had just been constructed 2 months earlier. Factors leading to unsteady-state operation include adsorption-desorption on the iron surfaces, residual contamination in the reactive cell from construction activities, and contamination entering from the downgradient aquifer. It should be noted that the barrier was constructed within the plume boundaries. After the initial sampling event in June 1996, there were no other occurrences of such elevated TCE concentrations in the iron zone. Furthermore, the fact that TCE is reduced below detection in WW-4C indicates that more than sufficient residence time is available within the reactive cell to degrade TCE well below its MCL.

Figure 4-2 illustrates the trend in *cis*-1,2-DCE over the performance monitoring period. This figure shows that *cis*-1,2-DCE concentrations have remained fairly constant at each of the well

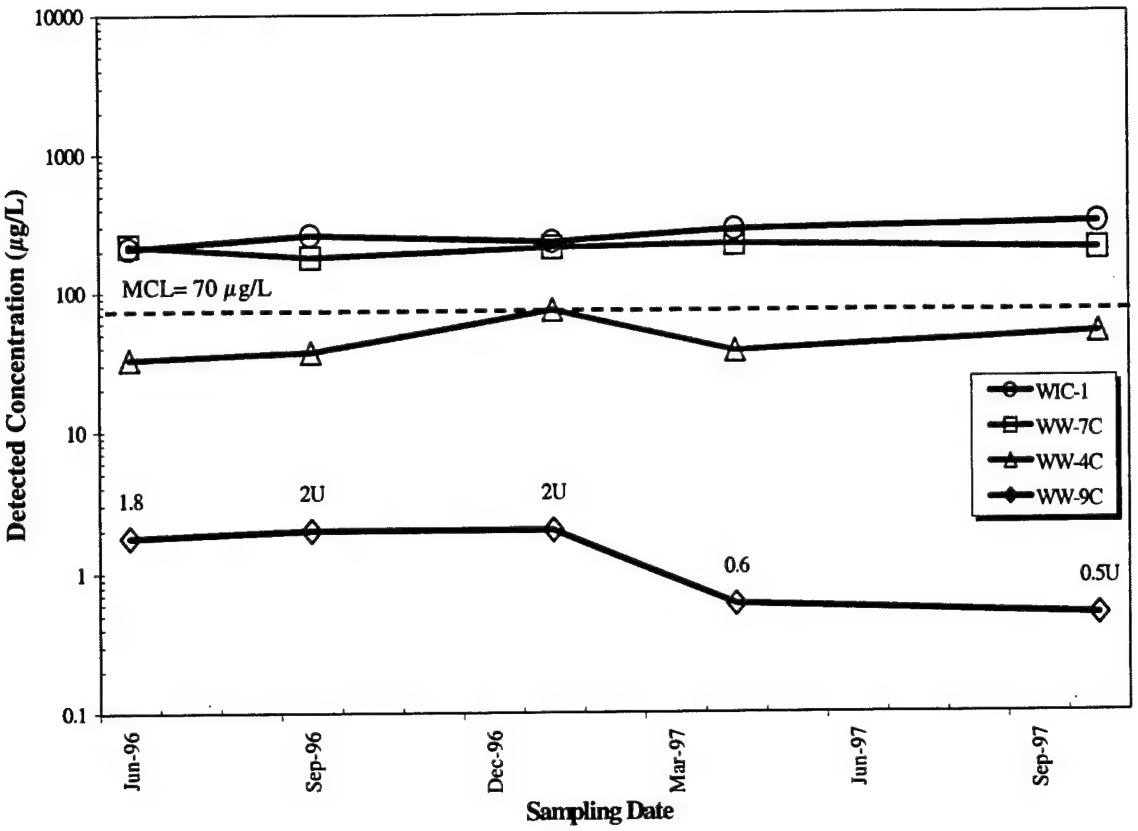

Figure 4-2. Concentrations of *cis*-1,2-DCE in Four Water Samples over the Performance Monitoring Period. U indicates that the analyte was not detected at the reported quantity.

Locations during the 16-month period. It also indicates that *cis*-1,2-DCE degrades more slowly than TCE, as there is a much wider difference between concentrations in the two reactive cell wells (WW-4C and WW-9C). However, *cis*-1,2-DCE concentrations are always below the MCL (70 µg/L) in WW-9C, which is further along the groundwater flow direction.

Figure 4-3 illustrates the trend in 1,1-DCA over the performance monitoring period. 1,1-DCA is relatively more recalcitrant and degrades more slowly than either TCE or *cis*-1,2-DCE. Also, 1,1-DCA is the only CVOC to remain at detectable levels throughout the reactive cell. However, no regulatory target (or MCL) exists for 1,1-DCA, and this compound is not an environmental concern at this site.

CVOC concentrations appear to have reached approximate steady state by the second quarterly monitoring event in September 1996. It has been reported that PCE requires more pore volumes to reach steady state than would have been achieved by the second quaterly monitoring event (Burris et al., 1995). Therefore, the data from the most recent monitoring event (October 1997) will be used as an illustration in the following discussion. The October 1997 data shown in

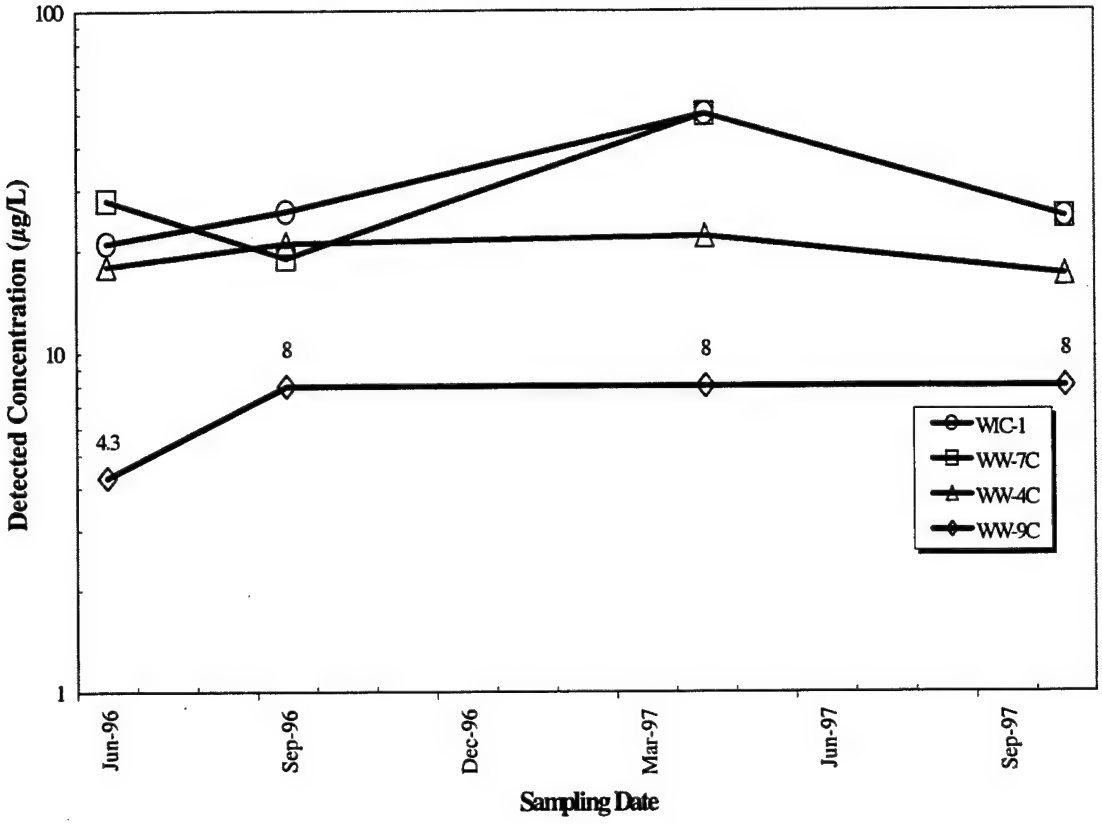

Figure 4-3. Concentrations of 1,1-DCA in Four Water Samples over the Performance Monitoring Period

Table 4-2 relate to wells along an approximate centerline through the barrier gate. Spatial concentration trends observed in the October 1997 sampling event are consistent with previous quarterly monitoring results.

4.1.2.1 TCE Degradation

In October 1997, the concentration of TCE in the upgradient aquifer wells (WIC-6 to WIC-8) was in the range of 920 to 1,300 µg/L, but homogenized to between 1,000 and 1,600 µg/L in the upgradient pea gravel (WW-7 cluster) (see Table 4-2). However, at the WW-8 well cluster, which is located less than 1 foot into the reactive cell, TCE was reduced to 1 µg/L or less, which is well below its MCL of 5 µg/L. In the WW-9 well cluster, which is located approximately 4 feet into the zero-valent iron zone, TCE is below detection (<0.5 µg/L). In fact, the majority of water samples collected elsewhere in the reactive cell are below the detection limit of 0.5 µg/L for TCE. These results demonstrate that the permeable barrier is capable of reducing influent TCE concentrations to well below the MCL.

Table 4-2. Target CVOC Concentrations in the Flow Direction Along an Approximate Centerline Through the Gate (October, 1997)

Well ID	PCE (µg/L) Result[a]	PCE (µg/L) Detection Limit	TCE (µg/L) Result[a]	TCE (µg/L) Detection Limit	*cis*-1,2-DCE (µg/L) Result[a]	*cis*-1,2-DCE (µg/L) Detection Limit	Vinyl Chloride (µg/L) Result[a]	Vinyl Chloride (µg/L) Detection Limit
Upgradient A1 Aquifer Zone Wells								
WIC-1	32	0.5	2,800 D	50	310 D	50	U	0.5
WIC-5[b]	4	2	180 D	25	320 D	25	U	2
-6	16	5	1,100 D	50	250	5	U	5
-7	17	0.5	1,300 D	25	280 D	25	U	0.5
-8	16	0.5	920 D	50	170 D	50	U	0.5
Upgradient Pea Gravel Wells								
WW-7A	14	0.5	1,100 D	25	240 D	25	U	0.5
B	13	0.5	1,200 D	25	250 D	25	U	0.5
C	12	5	1,000	50	340	5	U	5
D	16	0.5	1,600 D	25	270 D	25	U	0.5
Reactive Cell Wells								
WW-8A	U	0.5	1	0.5	200 D	5	U	0.5
B	U	0.5	1	0.5	82 D	12	1	0.5
C	U	0.5	0.9	0.5	46 D	5	U	0.5
D	U	0.5	0.8	0.5	58	5	1	0.5
WW-9A	U	0.5	U	0.5	U	0.5	U	0.5
B	U	0.5	U	0.5	U	0.5	U	0.5
C	U	0.5	U	0.5	U	0.5	U	0.5
D	U	0.5	U	0.5	0.6	0.5	U	0.5
Downgradient Pea Gravel Zone Wells								
WW-10A	U	0.5	1	0.5	U	0.5	U	0.5
B	U	0.5	4	0.5	U	0.5	U	0.5
C	U	0.5	10	0.5	1	0.5	U	0.5
D	U	0.5	5	0.5	1	0.5	U	0.5
Downgradient A1 Aquifer Zone Wells								
WIC-9	13	0.5	830 D	25	82 D	25	U	0.5
-10	5	0.5	92 D	5	8	0.5	U	0.5
-11	4	0.5	140 D	5	7	0.5	U	0.5
-12	71	25	3,400	50	360	25	U	25
W9-35	71	12	6,000 D	120	280	12	U	12
WIC-3	28	0.5	2,500 D	500	290 D	5	0.9	0.5

(a) 'D' indicates that the analysis was done at a secondary dilution factor. 'U' indicates that the analyte was below its detection limit.

(b) WIC-5 demonstrated anomalous hydraulic and chemical behavior and was excluded from most of the evaluation.

To ensure that the desired TCE degradation takes place in all parts of the reactive cell and not just along the centerline through the gate, the CVOC data were plotted in a three-dimensional (3-D) grid system using *EarthVision*™ (version 4.02) software. This software produces a 3-D grid depicting the distribution of measurements throughout a defined volume, in this case a rectangular

surface area representing the iron medium and adjacent pea gravel and containing all of the monitoring wells. To portray concentration information below the ground surface, simulated profiles were made by projecting the calculated concentration data onto a 2-D grid. Three profiles were created for the analytes discussed in this report: (1) a vertical profile through the approximate centerline of the permeable barrier; (2) a horizontal profile at Z = 3.5 feet above msl, which corresponds approximately to the Level C wells in each cluster and WIC-6 and WIC-10; and (3) a horizontal profile at Z = -1.5 feet above msl, which corresponds approximately to the Level D cluster wells and WIC-7 and WIC-11. Figures 4-4 and 4-5 show the October 1997 distribution of TCE within different profiles of the permeable barrier. These 2-D profiles show that the desired TCE degradation is being effected in all regions of the reactive cell. The 2-D concentration profiles for other target contaminants for all sampling events are presented in Appendix C.

Degradation of TCE during this demonstration can be better evaluated in terms of its concentrations in the reactive cell (as discussed above) rather than in the downgradient pea gravel or aquifer. This is because the pilot barrier was constructed within the plume and captures only part of the plume. Besides any contamination residual from construction activities, the downgradient pea gravel and aquifer are susceptible to contamination flowing around and under the barrier (in the gap between the base of the barrier and the A1/A2 aquitard). Because of the short width of the barrier in relation to the plume and the thinness of the sheet pile funnel, remixing of the treated water exiting the gate and the contaminated water flowing around and under the barrier probably takes place close to the gate. Because of the much higher conductivity of the downgradient pea gravel as compared to that of the downgradient aquifer, some of this contamination may get drawn into the pea gravel. Also, treated water emerging from the gate may be causing desorption of any TCE contamination adsorbed on the soil. Therefore, the last row of wells in the reactive cell (WW-8 cluster) is a better indicator of the degradation capability of the barrier than the downgradient pea gravel and aquifer wells.

However, over time, despite the remixing of the contaminated and treated waters downgradient, a cleaner water front appears to be emerging through the gate in the downgradient pea gravel and aquifer. Over the five quarterly events, TCE concentrations decrease progressively with time in the downgradient pea gravel wells and in the aquifer well cluster (WIC-9 to WIC-11) immediately downgradient of the reactive cell.

Contrary to the declining trend in the downgradient pea gravel and immediately downgradient aquifer well cluster (WIC-9 to WIC-11), the concentration of TCE at WIC-12 (the deepest well in the cluster at the level of the gap) is consistently higher (3,400 μg/L in October 1997). High concentrations of contaminants at the gap level may be caused by upward migration of groundwater from the more highly contaminated A2 aquifer zone. This is borne out by the water level measurements (Section 4.3.1), which show an upward hydraulic gradient present on the downgradient side of the barrier. TCE concentrations are also somewhat higher in relatively more distant downgradient A1 aquifer zone wells WIC-3 and W9-35 (2,500 and 6,000 μg/L, respectively). In the A2 aquifer zone, TCE concentrations ranged from 7,100 μg/L in WIC-4 to 9,700 μg/L in W9-20, which are greater than detected in any of the A1 aquifer zone wells.

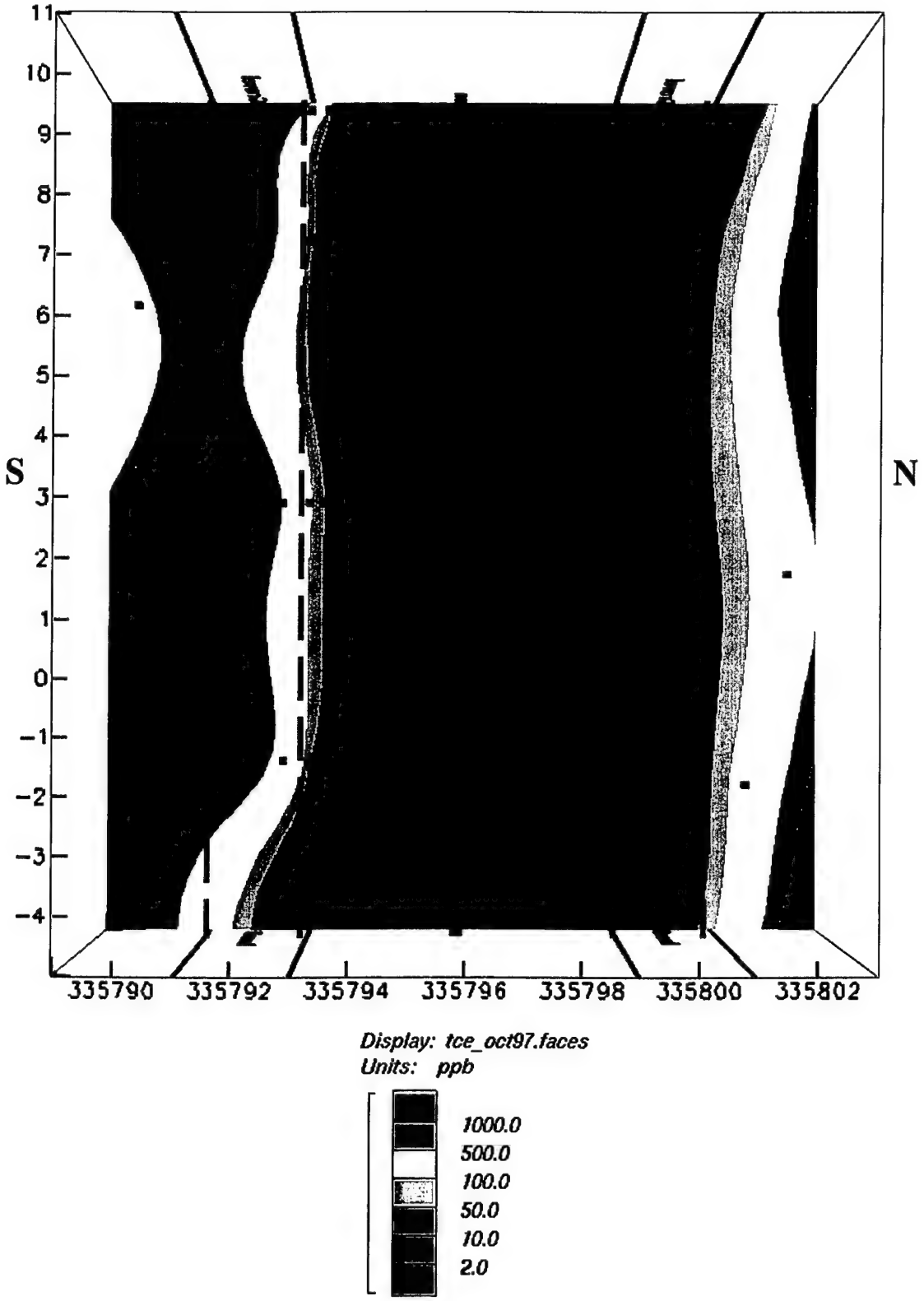

Figure 4-4. Vertical Profile Showing the Distribution of TCE in the Permeable Barrier in October 1997

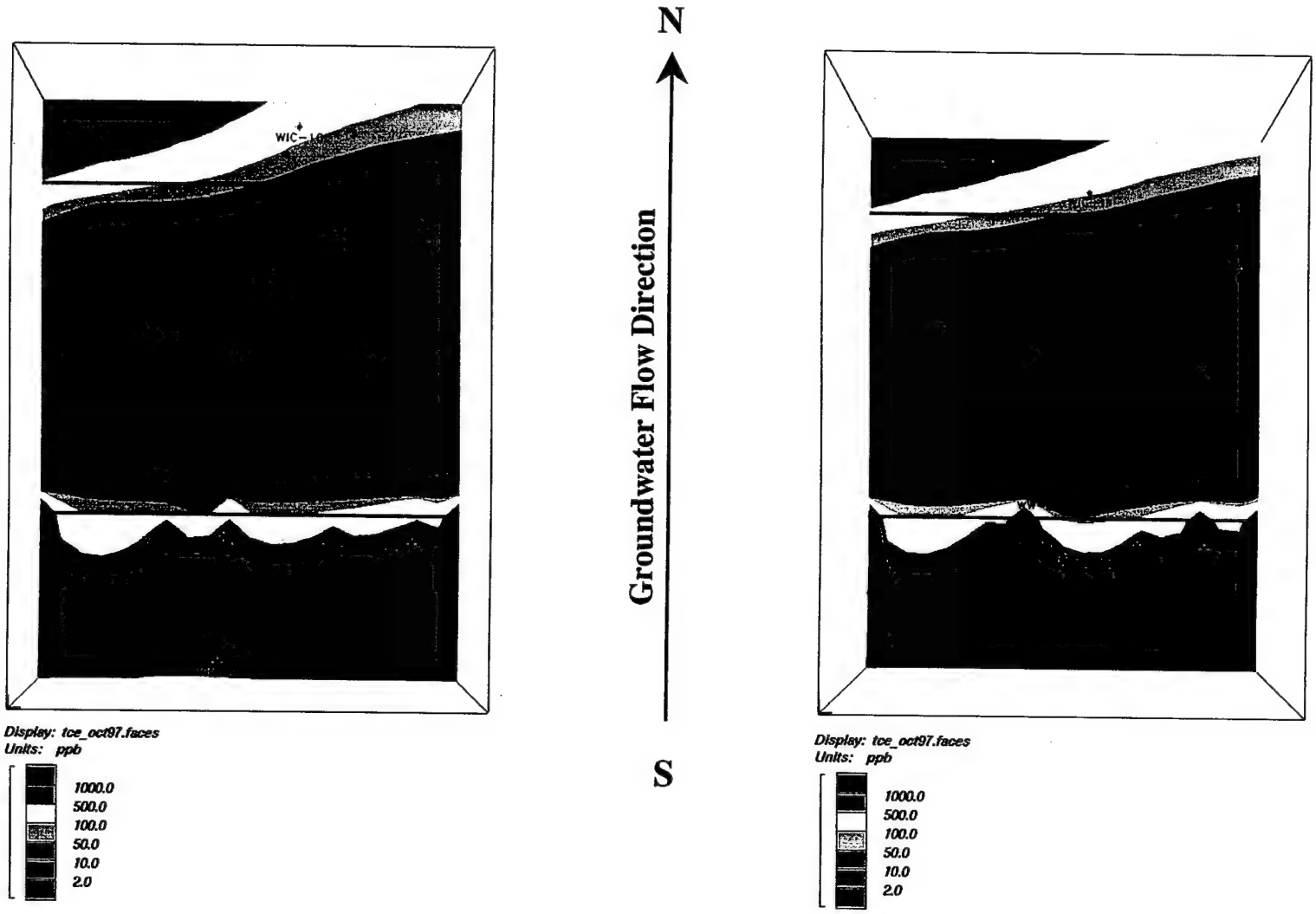

Figure 4-5. Horizontal Profiles at Z=3.5 feet (L) and Z=-1.5 feet Showing the Distribution of TCE in the Permeable Barrier in October 1997

4.1.2.2 PCE Degradation

In October 1997, PCE concentrations were relatively low (between 16 and 32 μg/L) in the upgradient A1 aquifer zone, as seen in Table 4-1. PCE concentrations in the upgradient pea gravel wells were generally very similar to those in the aquifer. In the upgradient pea gravel zone, PCE concentrations ranged between 12 to 16 μg/L. In all the reactive cell wells, PCE concentrations were uniformly below the detection limit of 0.5 μg/L, indicating that degradation took place rapidly and completely. PCE remained below detection in the downgradient pea gravel (<0.5 μg/L), but rebounded somewhat in the downgradient aquifer cluster. PCE concentrations in downgradient wells WIC-9, -10, -11, and –12 were 13, 5, 4, and 71 μg/L, respectively. This pattern parallels that for TCE and *cis*-1,2-DCE, and is consistent over the five quarters.

Further downgradient, at WIC-3 and W9-35 in the A1 aquifer zone, PCE concentrations (28 and 71 μg/L, respectively) are higher than in the upgradient A1 wells. Just as with TCE, this may indicate contaminants being drawn into the A1 aquifer zone from the A2 aquifer zone, which is more contaminated.

4.1.2.3 Degradation of *cis*-1,2-DCE

The *cis*-1,2-DCE compound is both an influent contaminant, as well as a byproduct of TCE and PCE degradation. Based on results from the October 1997 sampling round, concentrations of *cis*-1,2-DCE were approximately 170 to 340 μg/L in the upgradient A1 aquifer zone and upgradient pea gravel wells (see Table 4-2). These values are very similar to those measured in previous monitoring events. In the reactive cell, *cis*-1,2-DCE concentrations declined along the flow direction, as seen in Figures 4-6 and 4-7. The decline was slower than the declines for TCE and PCE, as evidenced by the persistence of elevated *cis*-1,2-DCE concentrations in WW-8 cluster wells in the reactive cell, because *cis*-1,2-DCE has a longer half-life. Also, there is probably some *cis*-1,2-DCE being produced as a byproduct concurrent with TCE and PCE degradation. Therefore, *cis*-1,2-DCE persists over a longer distance in the reactive cell. The *cis*-1,2-DCE concentration declined to less than 0.5 μg/L at WW-9C, which is 4 feet into the reactive cell. Thus, *cis*-1,2-DCE is reduced to well below its MCL of 70 μg/L.

In the downgradient pea gravel, October 1997 concentrations of *cis*-1,2-DCE ranged from below detection to 2 μg/L (see Appendix H). Higher concentrations have always been found at WW-18D. The reason is suspected to be an admixture of contaminated soil with the pea gravel during construction. However, *cis*-1,2-DCE concentrations at WW-18 have become progressively lower in each sampling event since September 1996, which indicates that this contamination source is diminishing as water pore volumes pass through the barrier. As with TCE, *cis*-1,2-DCE concentrations decrease over time in the downgradient aquifer cluster, except at the gap level. Further downgradient in the aquifer, *cis*-1,2-DCE concentrations were 290 and 280 μg/L at WIC-3 and W9-35, respectively. Concentrations of *cis*-1,2-DCE in the A2 aquifer zone have tended to be above 250 μg/L, as was the case in the October 1997 sampling round.

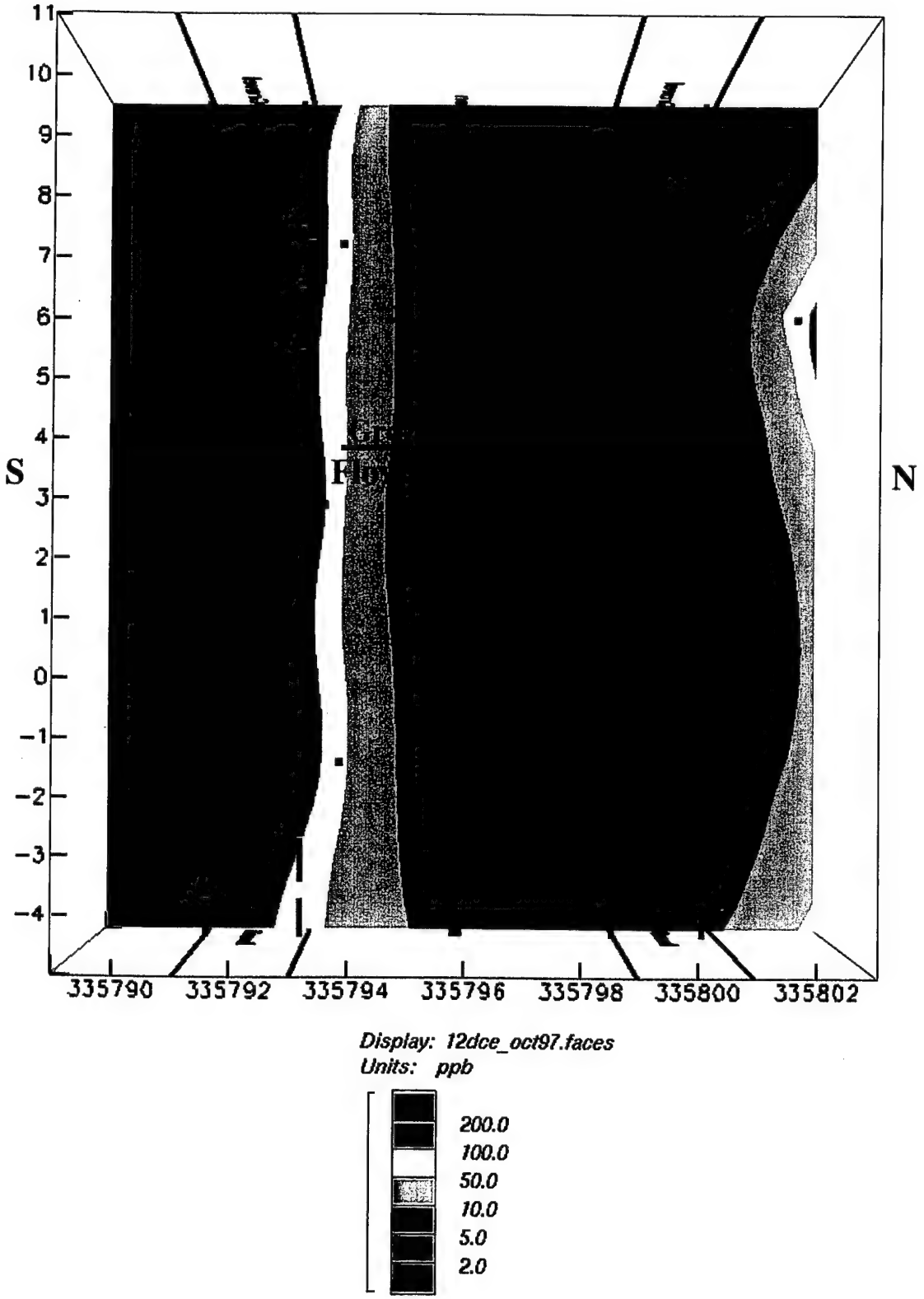

Figure 4-6. Vertical Profile Showing the Distribution of *cis*-1,2-DCE in the Permeable Barrier in October 1997

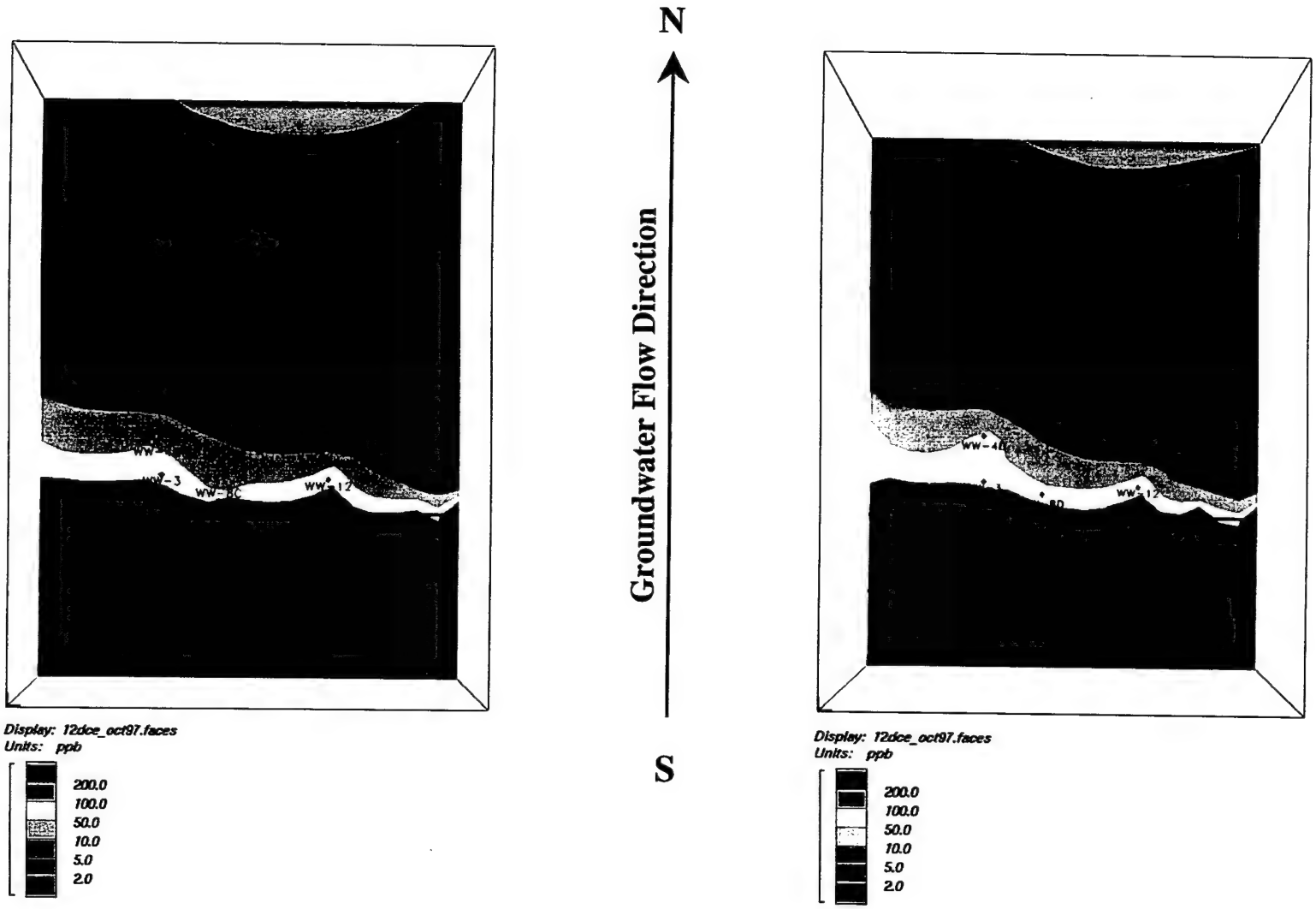

Figure 4-7. Horizontal Profile at Z=3.5 feet (L) and Z=-1.5 feet Showing the Distribution of *cis*-1,2-DCE in the Permeable Barrier in October 1997

4.1.2.4 Vinyl Chloride

As with *cis*-1,2-DCE, vinyl chloride is both an influent contaminant and a byproduct of TCE and PCE degradation. As seen in Table 4-2, vinyl chloride was below detection (0.5 µg/L) in nearly all of the reactive cell wells and does not exceed 1.0 µg/L in any well. These levels are well below its MCL of 2 µg/L. This suggests that TCE is being degraded mostly by pathways other than hydrogenolysis. An alternative pathway, described in Section 2.2, is beta-elimination, in which chlorinated ethenes are converted to ethene, ethane, and other light hydrocarbons by way of an intermediate, unstable chloroacetylene complex.

4.1.2.5 Other CVOCs

As seen in Appendix H, the concentration of CFC-113 ranges from nondetectable to around 50 µg/L in most of the upgradient A1 aquifer zone and pea gravel wells, and is below detection (2 µg/L) in the reactive cell wells. This result indicates complete destruction of CFC-113 in the reactive barrier. Similarly, 1,1-DCE is approximately 30 to 40 µg/L in the upgradient aquifer and pea gravel wells and is below detection (0.5 µg/L) in the reactive cell. However, 1,1-DCA concentrations are 20 to 30 µg/L in the upgradient aquifer and pea gravel wells and remain detectable (1 to 10 µg/L) in the downgradient portion of the reactive cell. 1,1-DCA is possibly the most resistant compound to reductive dechlorination in the treatment zone. However, 1,1-DCA has no regulatory MCL and is not perceived as an environmental concern at the site.

4.1.2.6 Light Hydrocarbons and Other VOC Byproducts

It is clear from the data presented so far that TCE and other halogenated compounds are being degraded in the reactive cell. However, there are multiple reaction pathways by which TCE is degraded. Vinyl chloride and *cis*-1,2-DCE were not major byproducts found in the reactive cell, indicating that hydrogenolysis may not be a major pathway. Therefore, water samples from a selected group of wells were analyzed for light hydrocarbons and other low molecular weight compounds. Analysis results for October 1997, which are representative of previous sampling events, are presented in Table 4-3. Appendix H contains results for light hydrocarbons and other gaseous compounds during the entire evaluation period. Within the hydrocarbon series, methane, ethane, and ethene were present in many of the groundwater samples collected in the reactive cell and downgradient pea gravel. Acetylene was measured but not detected with any certainty in the reactive cell. Acetylene and other ethynes are intermediates in the beta-elimination pathway and are potentially toxic. Fortunately, acetylene and other ethynes are believed to be short-lived and to degrade quickly to ethene and ethane, both of which were identified in the samples from the reactive cell. Ethene, ethane, and methane are benign substances at the low levels that were detected, and they are quickly lost due to degradation.

As indicated in Table 4-3, no hydrocarbon gases were detected in any of the upgradient aquifer wells. However, in the reactive cell methane concentration ranged from approximately 200 to 2,000 µg/L; ethane ranged from 8 to 38 µg/L, and ethene ranged from 3 to 52 µg/L. The few hits for propane and propene were close to detection limits and may not be significant.

Table 4-3. Selected Results for C1-C2 Hydrocarbon Compounds[a]

Well ID	Methane		Ethane		Ethene	
	Result	Detection Limit	Result	Detection Limit	Result	Detection Limit
Upgradient A1 Aquifer Zone Wells						
WIC-1	U	7.89	U	1.63	U	2.38
WIC-6	U	7.89	U	1.63	U	2.38
WIC-7	U	7.89	U	1.63	U	2.38
Upgradient Pea Gravel Wells						
WW-7C	59.9	7.89	2.74	1.63	U	2.38
WW-7D	9.44	7.89	U	1.63	U	2.38
Reactive Cell Wells						
WW-1C	204	7.89	8.08	1.63	4.35	2.38
WW-4C	1410	7.89	26.8	1.63	31.6	2.38
WW-4D	1540	7.89	37.6	1.63	43.6	2.38
WW-8C	2010	7.89	36.8	1.63	42.7	2.38
WW-8D	1190	7.89	31	1.63	52.4	2.38
WW-9C	371	7.89	13.5	1.63	13.5	2.38
WW-9D	629	7.89	33	1.63	51.9	2.38
WW-10C	1710	7.89	7.86	1.63	3.49	2.38
WW-13C	1550	7.89	18.1	1.63	23.5	2.38
WW-13D	549	7.89	18.7	1.63	24.3	2.38
Downgradient A1 Aquifer Zone Wells						
WIC-3	U	7.89	U	1.63	U	2.38
WIC-10	1080	7.89	7.25	1.63	4.23	2.38
WIC-11	945	7.89	14.4	1.63	16.9	2.38

(a) Data in this table were abstracted from the October 1997 sampling results. Only wells that are located along the centerline of the reactive barrier are shown.

In recent literature, three explanations for hydrocarbon generation by zero-valent iron have been proposed (summarized by Hardy and Gillham, 1996): (1) organic compounds in the treated water form hydrocarbon byproducts by a chemical reduction process; (2) carbon sources within the iron itself become converted to hydrocarbons as a result of corrosion reactions; and (3) hydrocarbons are formed by reduction of aqueous carbon dioxide. The second mechanism applies to commercial iron that contains carbide and graphite carbon. While Hardy and Gillham (1996) doubted this mechanism was an important pathway, Deng et al. (1997) found experimental evidence that carbide carbon in the iron is a likely carbon source for production of light hydrocarbons. Orth and Gillham (1996) and Sivavec and Horney (1995) observed that hydrocarbons were the major products of dechlorination of chlorinated ethenes. Hardy and Gillham (1996) associated an Anderson-Schulz-Flory (ASF) distribution of hydrocarbons with reduction of aqueous carbon dioxide. An ASF distribution is based on the probability of chain growth and favors the production of lighter molecular weight compounds. Therefore, methane is expected to be the dominant hydrocarbon produced by this process.

Because TCE and *cis*-1,2-DCE are the primary organic chemical constituents in the groundwater and both of these compounds are fully degraded within the reactive cell, it is possible that some fraction becomes converted to ethene and ethane. The maximum amount of ethene and ethane that can be produced by degradation of the groundwater contaminants can be determined by a mass balance calculation. Assuming that the concentration of TCE entering the reactive cell is roughly 1,000 μg/L, stoichiometric conversion of TCE to either ethene or ethane would yield about 214 μg/L ethene or 229 μg/L ethane. Actual concentrations are a minimum of five times lower than these calculated values. Because TCE and related compounds cannot be converted to methane along an energetically favorable reaction path, the high concentration of methane in the reactive cell must be a product of another process, such as processes 2 and 3 in the previous paragraph. Moreover, it is possible that some of the C2 hydrocarbons are byproducts of one of these alternative processes as well. Therefore, it is inconclusive whether the ethene and ethane detected in the reactive cell is due to degradation of chlorinated compounds.

Results are also reported for nitrogen, carbon dioxide, and hydrogen measurements (see Appendix H). These compounds were measured to provide additional information about chemical processes taking place in the reactive cell. For example, nitrogen was measured to determine whether nitrate is reduced to N_2 or if both nitrate and N_2 are reduced to ammonia. Typically, nitrate concentrations were about 3 mg/L in the untreated water (see Appendix H) and N_2 concentrations ranged from 8 to 22 mg/L in the upgradient aquifer. Nitrite also was measured, but not detected in any of the groundwater samples. In a system that is open to the atmosphere, the N_2 concentration should be approximately 16 mg/L. Therefore, the aquifer groundwater appears to be in equilibrium with the atmosphere. Because nitrate vanishes and N_2 decreases by approximately a factor of 2 in the reactive cell, it appears that nitrate and N_2 are reduced by the iron.

Carbon dioxide measurements reflect the carbonate chemistry of the groundwater and its dependence on pH. As noted earlier, production of methane may be caused by reduction of aqueous carbon dioxide. However, it should be noted that decreased levels of carbon dioxide in the reactive cell do not necessarily account for methane production because carbon dioxide concentrations are far in excess of methane. If aqueous carbon dioxide is involved in methane production it does not act as a limiting component. Hydrogen gas concentrations were measured to determine the abundance of hydrogen produced by reduction of water in the reactive cell. Appendix H shows that hydrogen was not detected in any of the water samples. While it is possible that hydrogen is produced at such a low rate that it cannot be detected, it is also quite likely that hydrogen gas was lost by diffusion through septum caps before the samples were analyzed.

4.1.3 Degradation Rate Constants and Half-Lives

The dechlorination efficiency of the barrier can be characterized by estimating the reaction rate constants and half-lives of the contaminants in the field system. Degradation rate constants were calculated for the TCE, *cis*-1,2-DCE, and 1,1-DCA as described below. Other compounds degraded too fast and rates could not be estimated for them.

Rather than relying on concentration data from individual wells, which may be subject to local flow anomalies and other uncertainties, average concentrations were estimated for five volume slices perpendicular to the groundwater flow through the gate. The volume slices were created by dividing the gate into five 2-foot-thick sections. Figure 4-8 is a diagram of these volume sections. Volumes 1 and 5 are the upgradient and downgradient pea gravel, respectively. Volumes 2 through 4 are in the reactive cell. Each volume section is 10 feet wide (same as the gate width) and extends from 11 feet above msl to 2 feet below msl. Masses of contaminants were calculated using *EarthVision*™ software by summing (integrating) isopleths (concentration ranges) over each volume section. Isopleths were chosen to provide a broad distribution of concentration contours. Average concentrations in each section were then calculated by dividing the integrated mass by the volume.

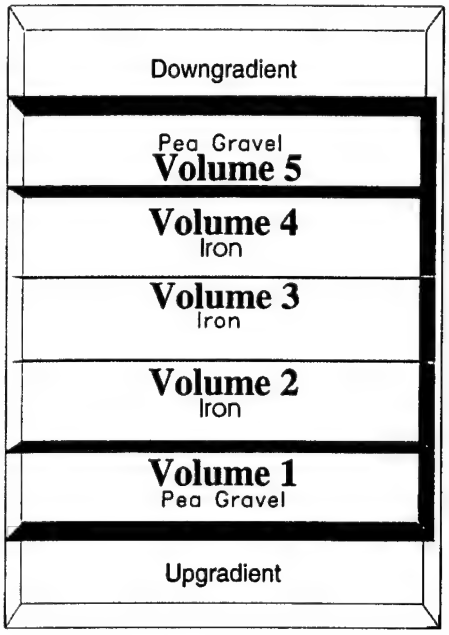

Figure 4-8. Diagram of Volume in which Average Concentrations were Calculated

Table 4-4 shows the calculated average concentration within each volume section. As expected, concentrations declined from volume 1 to volume 5 in the direction of groundwater flow through the reactive cell. Concentrations start to rebound in the downgradient pea gravel for the reasons described in Section 4.1.2. Hence, volume 5 data were ignored in the calculations.

Table 4-4 Calculation of Average Contaminant Concentrations in Volumes

Monitoring Event	Contaminant	Average Concentration (µg/L) in Volume Number[a]				
		1	2	3	4	5
January 1997	TCE	688	25.8	1.51[b]	1.51[b]	15.1[b]
	cis-1,2-DCE	257	35.1	1.88	1.50[b]	2.63[b]
	1,1-DCA	33	14.0	4.48	1.73	1.73[b]
October 1997	TCE	506	16.3	1.13[b]	1.19[b]	11.2[b]
	cis-1,2-DCE	177	43.8	2.61	1.05[b]	1.49[b]
	1,1-DCA	15.8	12.5	6.81	2.51	1.40[b]

(a) Volume 1 is at the influent end of the gate.
(b) Ignored in calculation of reaction rate constant (k), either because this average includes values below the detection limit or because it includes contamination from the downgradient aquifer.

These concentrations were then used to calculate degradation rate according to a first-order rate equation:

$$k = (1/t)\, ln(C_0/C) \qquad (5)$$

In Equation 5, C_0 and C are concentrations at initial and final points, respectively, and *ln* is the natural log function. When ln(C/Co) is plotted against time, the slope of the regression line is the reaction rate constant, k. Residence time, t, was calculated as the distance of the reactive path divided by an average flow velocity. The reactive path is normally the distance (2 feet) between the midpoints of adjoining volume sections. However, a 1-foot distance was used instead of 2 feet between volumes 1 and 2 because no degradation is expected to take place in the 1 foot of pea gravel (volume 1) before the groundwater enters the reactive cell. Ideally, concentration data should be available for at least three points along the flowpath to get a good regression line. However, TCE concentration dropped to below detection in volume 3, and hence the rate constant was calculated based on only two points. Another problem is that analysis of the hydrologic data produced a range of possible groundwater flow velocities. Therefore, no single value for residence time could be input into the rate equation. Instead, rate constants and half-lives were calculated using a range of residence times based on possible groundwater flow velocities.

Figures 4-9 through 4-11 show average concentrations in the volume sections and the regression line. It can be seen in Figure 4-9 that there are only two valid points for TCE in the reactive cell (volume 2). Valid points are characterized as being above the detection limit and are shown by filled symbols in Figure 4-9. Invalid points are characterized as being below the detection limit and are shown by open symbols in Figure 4-9. TCE concentrations in volumes 3 and 4 are below detection. Therefore, the regression line is based on concentration data in volumes 1 and 2 only. This approach may produce a slightly higher value for k_{TCE} because it ignores any degradation that may be taking place in the final few inches of the upgradient pea gravel, where some iron may have crept in during construction.

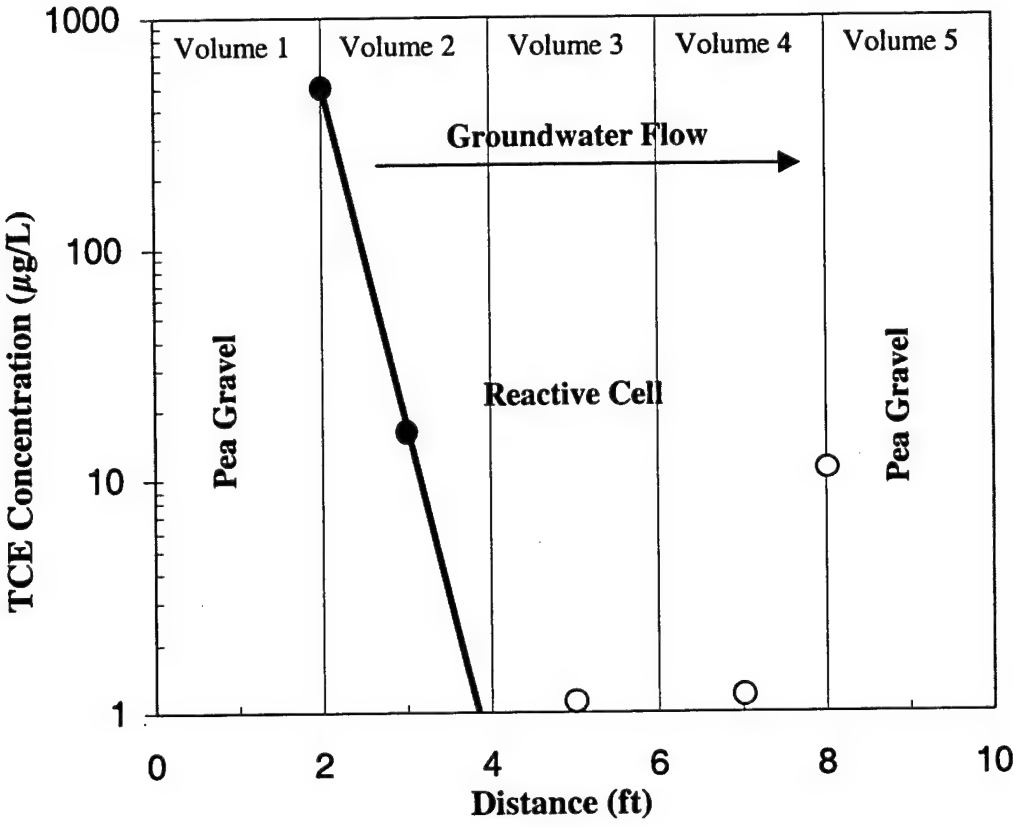

Figure 4-9. Plot of Average TCE Concentration in Five Volumes and Fitted First-Order Regression Curve

Figure 4-10 shows that there were three valid points in the reactive cell for calculating k_{DCE}. The concentration of *cis*-1,2-DCE in volume 4 was below detection and not used in the calculation. Any additional *cis*-1,2-DCE created by hydrogenolysis of TCE was assumed to be insignificant and therefore ignored in subsequent rate calculations.

Figure 4-11 shows that there were four valid points for calculating k_{DCA} in the reactive cell. It can be seen in the figure that the fit is reasonably good.

Results of the rate constant and half-life calculations are tabulated in Table 4-5. Half-lives ($t_{½}$) were calculated according to the formula,

$$t_{½} = \frac{ln\ (2)}{k} \qquad (6)$$

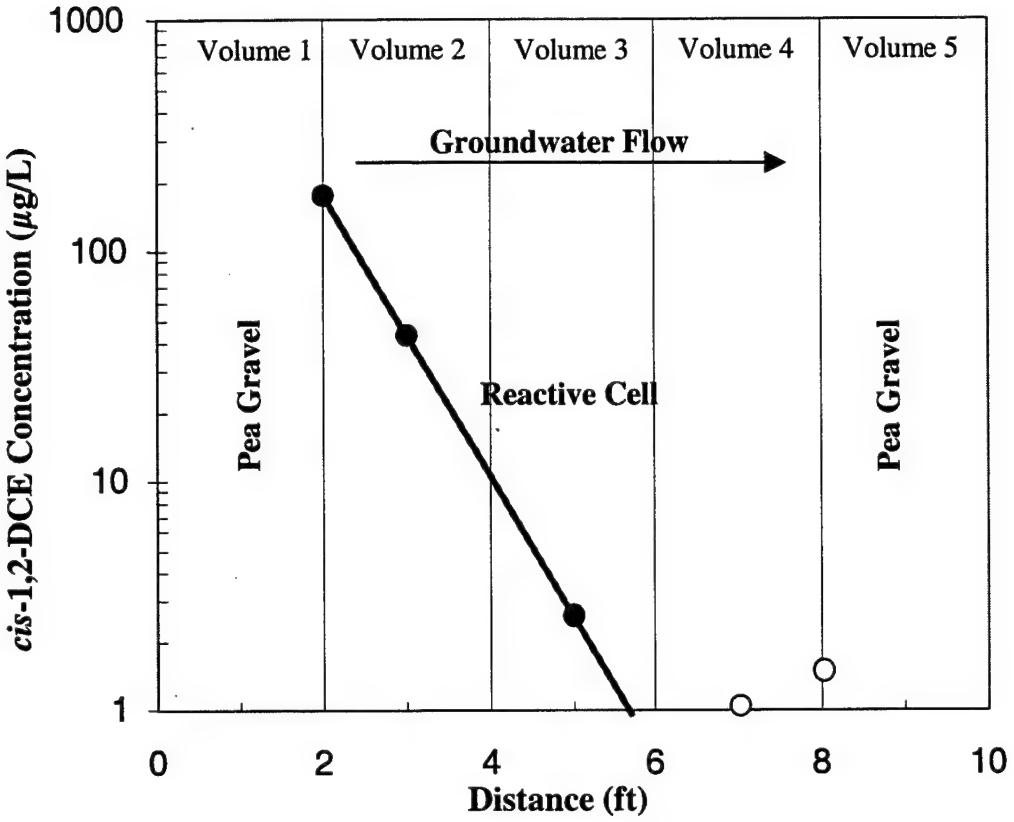

Figure 4-10. Plot of Average *cis*-1,2-DCE Concentration in Five Volumes and Fitted First-Order Regression Curve

It can be seen that as the expected flow velocity in the reactive cell increases, the estimated k increases and estimated $t_{½}$ decreases. Table 4-5 also shows the half-lives estimated during bench-scale testing (PRC, 1995); the bench-scale results were adjusted for 100% granular iron used in the field barrier as opposed to the 50:50 iron-sand mixture used in the bench tests (see footnote (b) in the table). It can be seen that for a flow velocity between 0.2 and 0.5 foot/day, there is generally good agreement between the field and bench-scale half-lives.

A number of factors affect these field degradation rate calculations. Among these are concentrations that vary by depth in the pea gravel and reactive cell; vertical mixing within the pea gravel and reactive cell; faster flow in the lower portion of the aquifer due to a higher conductivity zone; possible heterogeneities in the reactive cell that cause variability in residence times; and availability of a limited number of monitoring points. These factors impose some limitations on the field half-life estimates. However, even with these limitations, it is evident that the reactive efficiency of the barrier is within the design expectations.

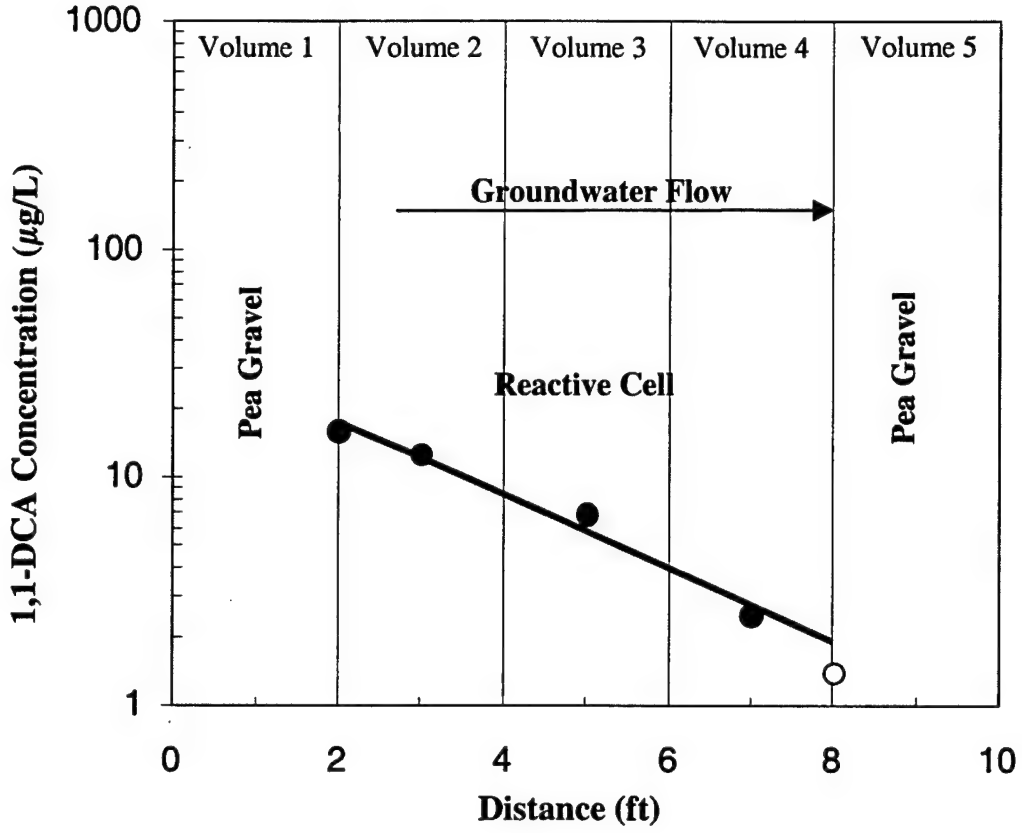

Figure 4-11. Plot of Average 1,1-DCA Concentration in Five Volumes and Fitted First-Order Regression Curve

Table 4-5. Results of Degradation Rate Calculations[a]

Monitoring Event	Flow Velocity (feet/day)	TCE		*cis*-1,2-DCE		1,1-DCA	
		k (hr^{-1})	$t_{1/2}$ (hr)	k (hr^{-1})	$t_{1/2}$ (hr)	k (hr^{-1})	$t_{1/2}$ (hr)
January 1997	**0.2**	**0.66**	**1.1**	**0.32**	**2.1**	**0.12**	**6.0**
	0.5	**1.6**	**0.42**	**0.81**	**0.86**	**0.29**	**2.4**
	1	3.3	0.21	1.6	0.43	0.58	1.2
	2	6.6	0.11	3.2	0.21	1.2	0.60
October 1997	**0.2**	**0.69**	**1.0**	**0.28**	**2.5**	**0.07**	**9.4**
	0.5	**1.7**	**0.4**	**0.70**	**0.99**	**0.20**	**3.8**
	1	3.4	0.2	1.4	0.49	0.37	1.9
	2	6.9	0.1	2.8	0.25	0.73	0.94
Bench-scale test results[b]		1.7	0.40	0.34	1.4	0.16	4.3

(a) Determination of rate constants depends on groundwater flow velocity. Velocities and rate calculations for the bolded amounts are consistent with bench-scale results in the last row of the table.

(b) Rate constants and half-lives calculated from bench-scale data (PRC, 1995). The rate constants shown in this table are 2.3 times those obtained in the column tests, where a 50:50 (by mass) mixture of iron:sand was used.

4.1.4 Contaminants Degradation Evaluation Summary

Based on the preceding evaluation of the contaminant degradation data, the following conclusions can be made regarding the reactivity performance of the Moffett Field pilot barrier:

- TCE, *cis*-1,2-DCE, and PCE were degraded to levels well below their respective MCLs.

- *cis*-1,2-DCE is present in the influent groundwater, as well as generated as a partially dechlorinated byproduct of TCE and PCE degradation. Similarly, vinyl chloride can be a byproduct by hydrogenolysis. However, the low level of vinyl chloride in the reactive cell indicates that hydrogenolysis may not be the major pathway by which TCE and PCE are degrading. This is fortunate for the technology because the hydrogenolysis byproducts (*cis*-1,2-DCE and vinyl chloride) tend to be more resistant to degradation, as evidenced by their longer half-lives.

- Intermediate products of the beta-elimination pathway were not found in the reactive cell. This is not unexpected because these intermediates (e.g., acetylene) are reported to be short lived and degrade quickly to ethene and ethane (Roberts et al., 1996). Also, the intermediates are highly volatile and may be volatilizing from the barrier.

- Hydrocarbon products, such as methane, ethene, and ethane, were detected in the reactive cell. These products have been reported as being generated from any of a variety of sources, including the contaminants, the aqueous carbon dioxide, and/or the iron itself (Gillham, 1996; Hardy and Gillham, 1996; and Burris et al., 1995).

- Concentrations of other CVOCs, such as 1,1-DCA and CFC-113, also were considerably reduced in the reactive cell.

- The half-lives of TCE, *cis*-1,2-DCE, and 1,1-DCA estimated from the field measurements were within the range of the design based on bench-scale tests. Most of the other CVOCs were degraded to below detection in the first series of wells in the reactive cell, and therefore field reaction rates and half-lives could not be determined for these compounds.

- All target CVOC contaminants were reduced to below MCLs before reaching well WW-9, which is 4 feet into the reactive cell. An additional 2-foot thickness of iron (beyond WW-9) is available to the groundwater before it exits the reactive cell, thus providing a safety factor for future increases in influent concentrations of the contaminants or for future reductions in reactivity of the iron due to precipitation.

- Evaluation of the downgradient aquifer data is difficult because of mixing of treated water from the gate and contaminated water flowing around or under the barrier, which was designed (for this pilot demonstration) to capture only a part of the plume. Other sources of contamination on the downgradient side include desorption of

contaminants from the aquifer soil (the barrier was placed inside the plume and the downgradient aquifer is already contaminated) and possible upward flow gradients from the more contaminated A2 aquifer zone below to the A1 aquifer zone. However, there are signs of a cleaner water front beginning to emerge from the downgradient side of the gate.

- Between 4 and 40 pore volumes of groundwater may have flowed through the reactive cell (at 0.2 to 2 feet/day from April to September 1996) before it reached steady-state reaction conditions.

- Between 16 and 160 pore volumes of groundwater may have flowed through the reactive cell over the 16-month period of this demonstration. The minimum residence time of the groundwater during this period was 3 days. The design was based on a residence time of at least 2 days.

4.2 Evaluation of Downgradient Aquifer Data

One of the technology performance specifications is to evaluate whether the interaction between the barrier materials and the groundwater causes environmentally deleterious materials to be released in the downgradient aquifer (Section 2.3).

Dissolved iron concentrations in the reactive cell and downgradient pea gravel are generally less than 0.02 mg/L, which is far below the secondary water quality standard of 0.3 mg/L. Iron analysis results are presented along with other inorganic constituents in Section 4.4.2. Generally, iron concentrations in the reactive cell tend to be indistinguishable from samples taken in the upgradient aquifer. These results indicate that the permeable barrier does not promote excessive levels of dissolved iron in the downgradient aquifer. Therefore, it can be concluded that the barrier does not adversely affect downgradient water quality with regard to dissolved iron content.

As discussed in Section 4.4.2, direct, down-hole measurements show that pH and Eh values are significantly altered as groundwater flows through the reactive cell. The pH rises above10 at some points in the reactive cell and Eh declines to as low as -600 mV. However, after water leaves the reactive cell, the pH and Eh begin regressing to their pretreatment values. In fact, the rebound starts in the downgradient pea gravel itself, indicating that there is some mixing between treated water exiting the reactive cell and untreated groundwater flowing around or under the barrier. Therefore, much of the groundwater's readjustment back to pretreatment geochemical conditions occurs in the pea gravel, rather than in the aquifer itself. Geochemical conditions (including parameters such as dissolved iron, DO, pH, and Eh) in the aquifer immediately downgradient of the pea gravel are similar to conditions at the upgradient end.

Another potential concern is whether creation of highly reducing conditions in the downgradient aquifer could promote microbial growth that could lead to a decrease in the hydraulic conductivity. Microbial analysis of one core sample from the downgradient aquifer resulted in the detection of one type of colony. A discussion of core sample analysis may be found in Section 4.4.6.

The match to any known species of microorganism was less than certain, but a type of *Staphylococcus* microorganism was tentatively identified. The amount of growth in the sample was not very large (50,000 colony-forming units [CFUs]/g after 48 hours incubation). The implications of the microbial analysis are unclear at this time, for these reasons: (a) the microbial buildup in the downgradient aquifer was relatively small, and (b) a sample of the upgradient aquifer could not be collected and evaluated as a reference.

4.3 Hydrogeologic Data Evaluation

The objectives of the hydrogeologic evaluation were to ensure that groundwater flows through the barrier as designed, to ensure that the targeted portion of the aquifer is being captured, and to estimate the groundwater velocity and residence time in the reactive cell. The hydraulic evaluation objectives were considered secondary at the beginning of the study. However, they assumed considerable importance midway through the demonstration when concerns of plume bypass around and over the barrier were raised at some other installations.

The hydraulic performance evaluation involved periodic and continuous water level measurements, down-hole groundwater velocity measurements, two tracer tests, and groundwater modeling. The monitoring well network (Figures 3-18 and 3-19) used for groundwater sampling was also used for water levels and other hydraulic measurements.

4.3.1 Results of Periodic Water Level Measurements

Water level measurements are available from two monitoring events performed prior to permeable barrier construction and 13 events after the construction. The objectives of the water level measurements were to determine the hydraulic capture zone width of the barrier and estimate flow volumes and groundwater flow velocity (and residence time) through the reactive cell. Other objectives included evaluation of vertical gradients and potential for flow through the gap beneath the barrier.

The complete data set of water level measurements is presented in Table D-1 (in Appendix D). The change in water level between consecutive measurements in each well is given in Table D-2. In these tables the wells have been grouped based on their distances from the permeable barrier. These groupings are shown in Figure D-1 (in Appendix D). Table D-1 also shows the average post-construction water levels and standard deviation for each group of wells. By taking average water levels for wells in close proximity to each other it is possible to minimize the effects of random water level fluctuations or measurement errors when evaluating small changes. Otherwise the random errors or fluctuations can have a significant impact on interpretations in this relatively small area of investigation.

4.3.1.1 Evaluating Flow Through the Barrier Based on Water Levels

The data in Table D-1 (in Appendix D) can be used to evaluate spatial trends in water levels across the site. In general, the water levels at the site fluctuate between about 11.5 to 13.5 feet msl over 2 years. The lowest water levels were measured during the summer months. The

highest levels were during the winter rainfall months. The data in Table D-2 can be used to evaluate overall trends in water levels over time at the site. For example, during the spring and summer of 1997 (from March 1997 to July 1997), water levels across the entire site show a declining trend. However, during the fall and winter of 1997-1998 (July 1997 to February 1998) all of the water level differences are positive, indicating an increasing water level trend due to high rainfall during this time. Further, it can be seen in Table D-2 that the increase in water level between November 1997 and February 1998 is higher in the aquifer wells than in the reactive cell wells. This trend is true in most other columns in Table D-2 and is related to the higher porosity and hydraulic conductivity in the reactive cell relative to the aquifer. Another cursory observation from Table D-1 is that except for WIC-5, the water levels in the upgradient aquifer wells (WIC-1, WIC6-8) are generally higher than in the upgradient pea gravel and the reactive cell. This indicates that there is always a hydraulic gradient from the upgradient aquifer toward the reactive cell, resulting in flow through the cell. WIC-5 has demonstrated anomalous behavior in relation to both hydraulic and groundwater chemistry measurements; therefore, data from this well have been generally excluded from the evaluation of hydraulic and geochemical trends in the system.

The water level data presented in Table D-1 were plotted on two-dimensional contour maps to evaluate spatial flow patterns and capture zone configurations. Due to the presence of multiple well clusters in the permeable cell, many different ways of presenting the maps are possible. In this case, it was decided to use the average water levels for each well cluster. The initial versions of the maps were prepared using the minimum tension gridding option of the *EarthVision*™ software. These maps were further refined by hand contouring in the vicinity of the permeable barrier. One significant feature of these maps is that the areas immediately downgradient of the two funnel walls are not included in the calculation of the grid maps. This is because the flow patterns in these areas are likely to be affected by the funnel walls, but there are no monitoring wells available in these areas to interpret the flow patterns. Finally, the flow lines were drawn on the maps to show the capture zone for the funnel-and-gate system. The final maps for each of the 13 post-construction events are shown in Appendix D (Figures D-2 to D-14).

Two of these maps for spring (May 1997) and winter (February 1998) conditions are shown in Figures 4-12 and 4-13, respectively. Examination of water level maps indicates the formation of a capture zone in front of the barrier. Although, the resolution would have been improved if more observation wells were available, in all cases the capture of groundwater by the permeable barrier can be clearly observed based on flow gradients. The capture zone appears to extend over at least half the length of the funnel wall on each side. This would indicate that the hydraulic capture zone width of the permeable barrier is about 30 feet wide, and extends across the width of the sand channel and part of the surrounding interchannel deposits.

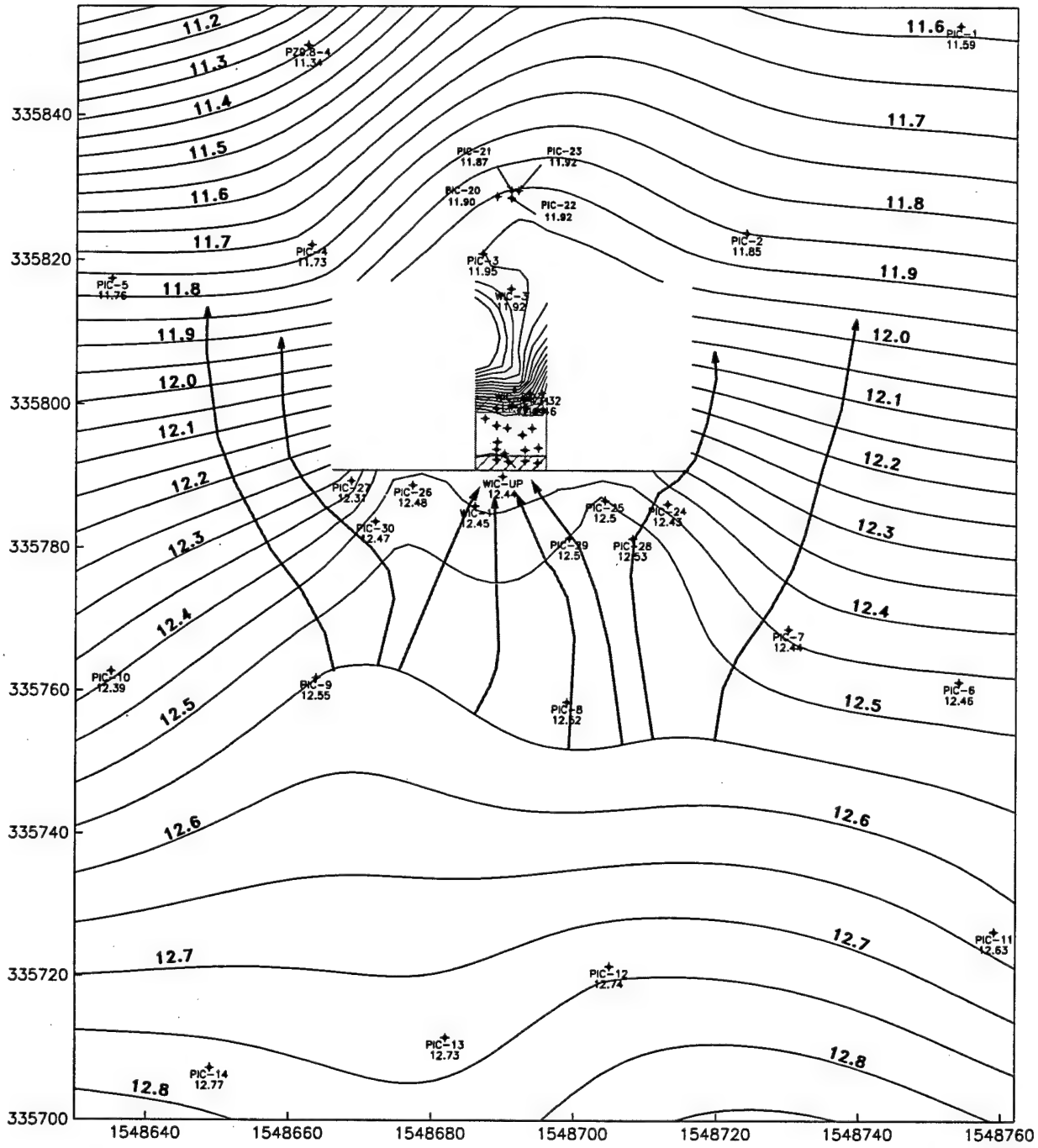

Figure 4-12. Observed Water Levels and Flow Lines in the Vicinity of the Permeable Barrier During Summer (May 1997)

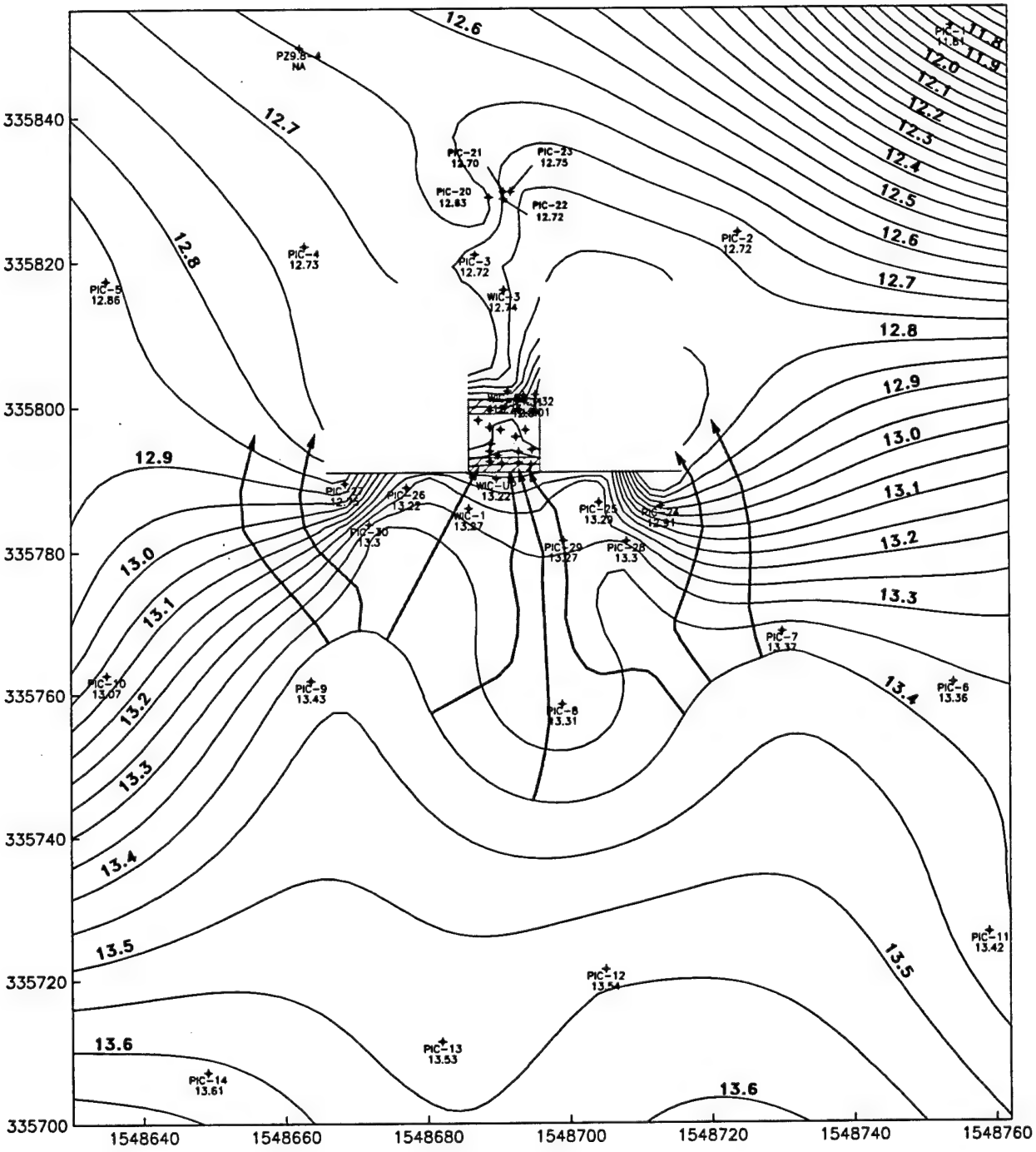

Figure 4-13. Observed Water Levels and Flow Lines in the Vicinity of the Permeable Barrier During Winter (February 1998)

The observed capture zone appears to change slightly over time (Figures D-2 to D-14); that is, the portion of the aquifer targeted for capture may not remain the same, even though the same numerical quantity of groundwater is captured. However, it is difficult to tell if this change is due to gradual evolution of the capture zone over time, to seasonal variations in groundwater flow, or simply to the addition of more monitoring wells during the later monitoring events which increased the resolution of the data. In any case, at this site, the shifts appear to be relatively small compared to the width of the capture zone and may not affect barrier performance. At other sites though, such shifts in the targeted capture zone have had greater impacts.

The water level variations in individual wells in the aquifer or reactive cell can be depicted graphically. Figure 4-14 shows water level profiles for four vertical depths in four well clusters located along the centerline of the reactive cell for several measurement rounds. These profiles can be used to determine potential for backward or stagnant flow in the reactive cell. It appears that water levels in the reactive cell either decrease slightly from upgradient pea gravel to downgradient pea gravel or are relatively flat. In these plots, based on periodic water level measurements, there is no evidence of sustained and measurable mounding of water in the upgradient pea gravel. It is obvious from these plots that the water levels in November 1997 and February 1998 were the highest observed so far. This is related to the heavy rainfall in the region during this time. The gradient between cluster WW-7 and WW-8 in February 1998 is also the steepest observed so far.

Water level profiles (hydrographs) were also prepared to depict variations in water levels over time in several wells. Figure 4-15 shows hydrographs for well clusters WW-7, WW-8, WW-9, and WW-10. In general, it appears that the water levels at the four depth levels in these clusters are almost the same and any variations are within the range of measurement error or short-term fluctuation. Overall, the water levels were the highest during the winter of 1998. Hydrographs for two upgradient wells (PIC-8 and PIC-13) are shown in Figure 4-16 and for four downgradient wells (PIC-3, PIC-21, PIC-23, and W9-35) are shown in Figure 4-17. All of these hydrographs are almost alike in shape and point to the similarity in water level variations in the A1 aquifer zone across the site. The range of variations over the 2-year period is within 2 feet.

Table D-3 (Appendix D) shows the average hydraulic gradients between various groups of wells for each monitoring event and also the overall average hydraulic gradient for all the monitoring events. These data are useful in estimating hydraulic conditions in various parts of the system. The standard deviations in Table D-3 represent the effect of seasonal water level fluctuations and other measurement uncertainties. Some key values from this table are shown in Figure 4-18. Based on this, the average gradient in the upgradient and downgradient aquifer areas is about 0.007. The gradient between upgradient pea gravel and downgradient pea gravel is 0.004 and the gradient within the reactive cell is relatively flat at 0.002. The steepest gradients occur between the downgradient pea gravel and the first group of downgradient wells. All of the gradient values in Table D-3 are positive, indicating that on an average basis, there is always flow in the expected downgradient direction (approximately south to north). The changes in the gradients are mainly a result of the hydraulic conductivity variations in the aquifer and the permeable barrier. Generally, the gradients are flatter in the higher conductivity media than in the lower conductivity media.

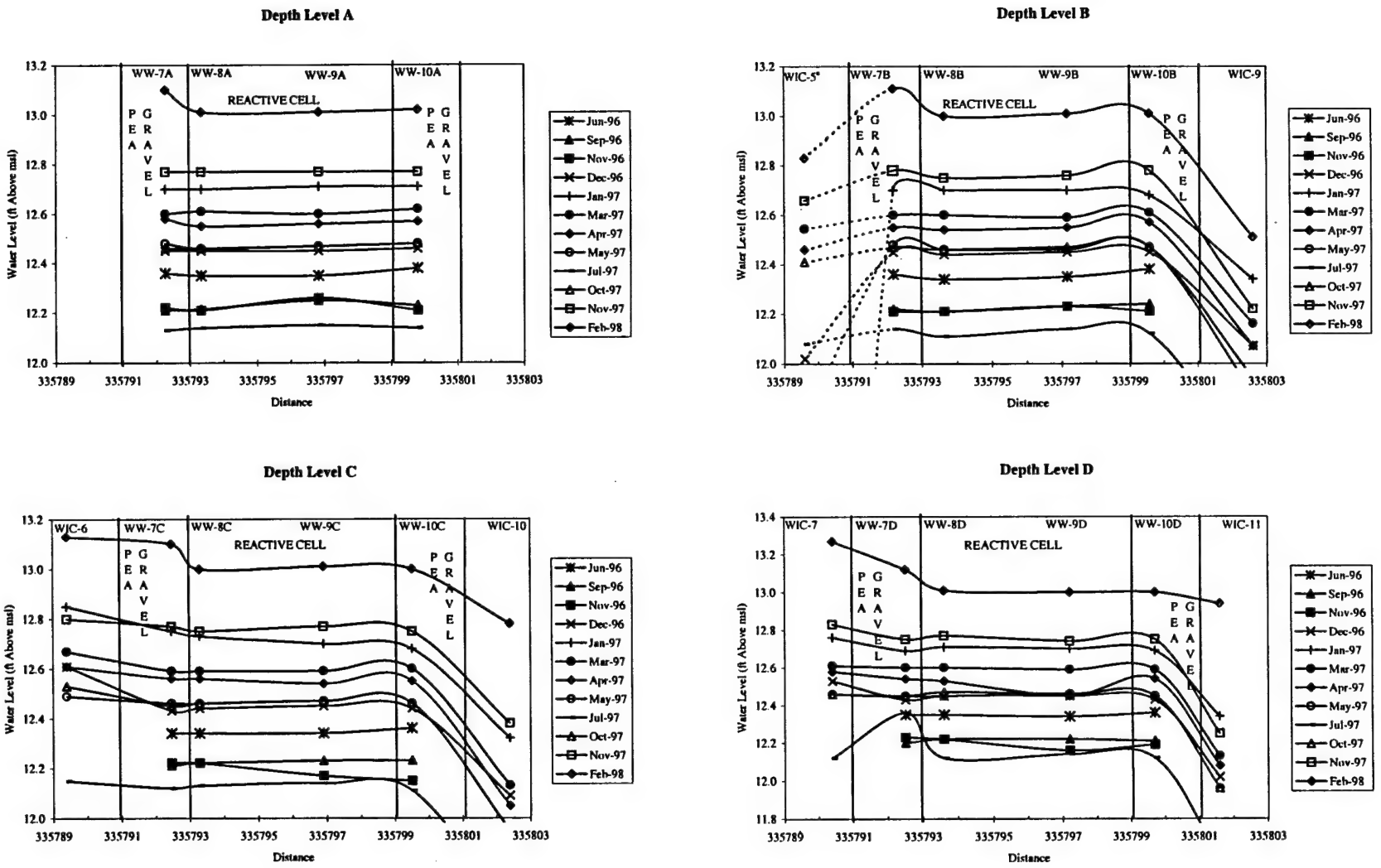

a. WIC-5 consistently shows anomalous water level and chemical concentrations probably due to a deficiency in the construction of the well.

Figure 4-14. Water Level Profiles Along the Center of the Reactive Cell

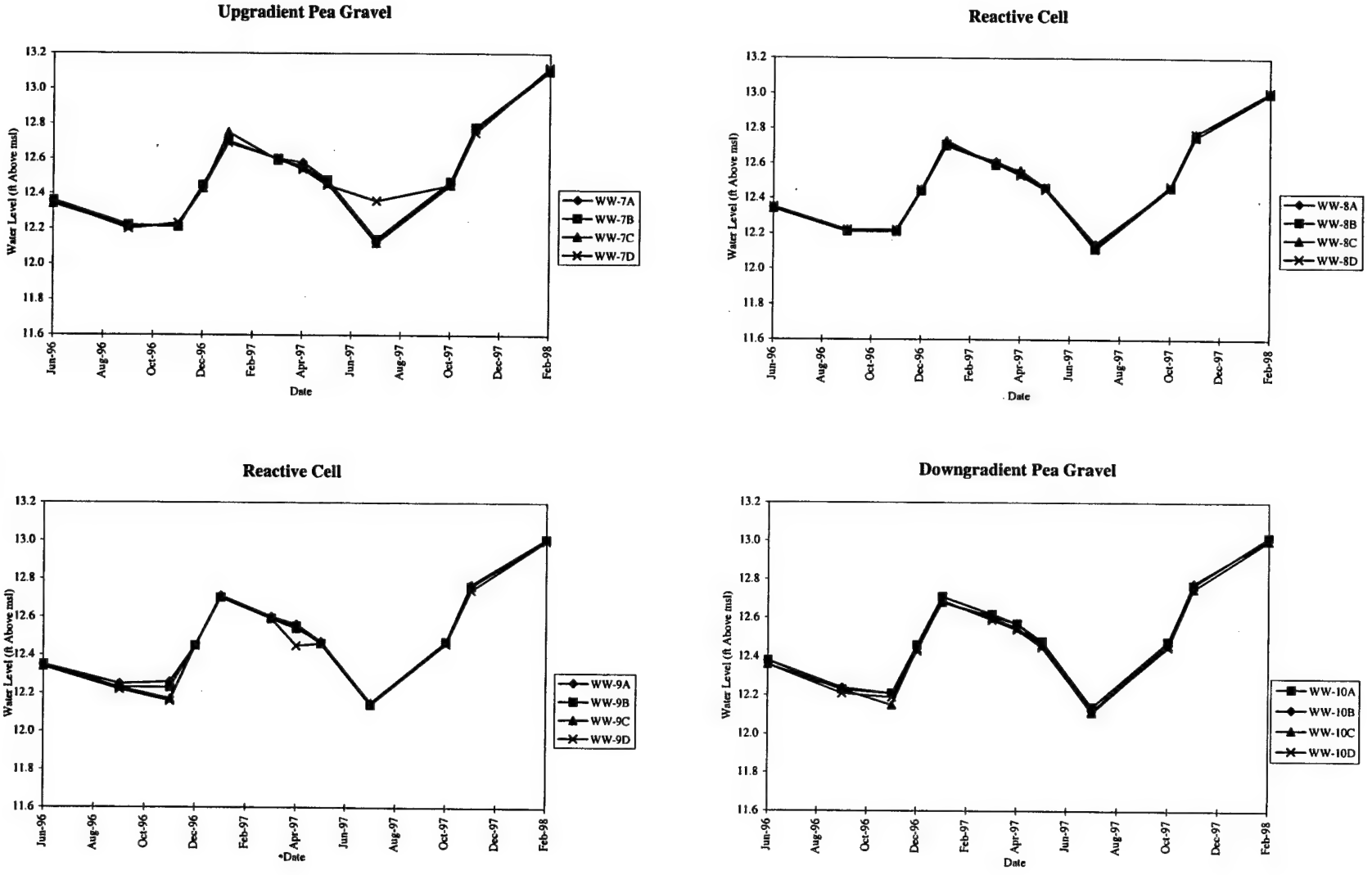

Figure 4-15. Water Level Hydrographs for Well Clusters WW-7, WW-8, WW-9, and WW-10

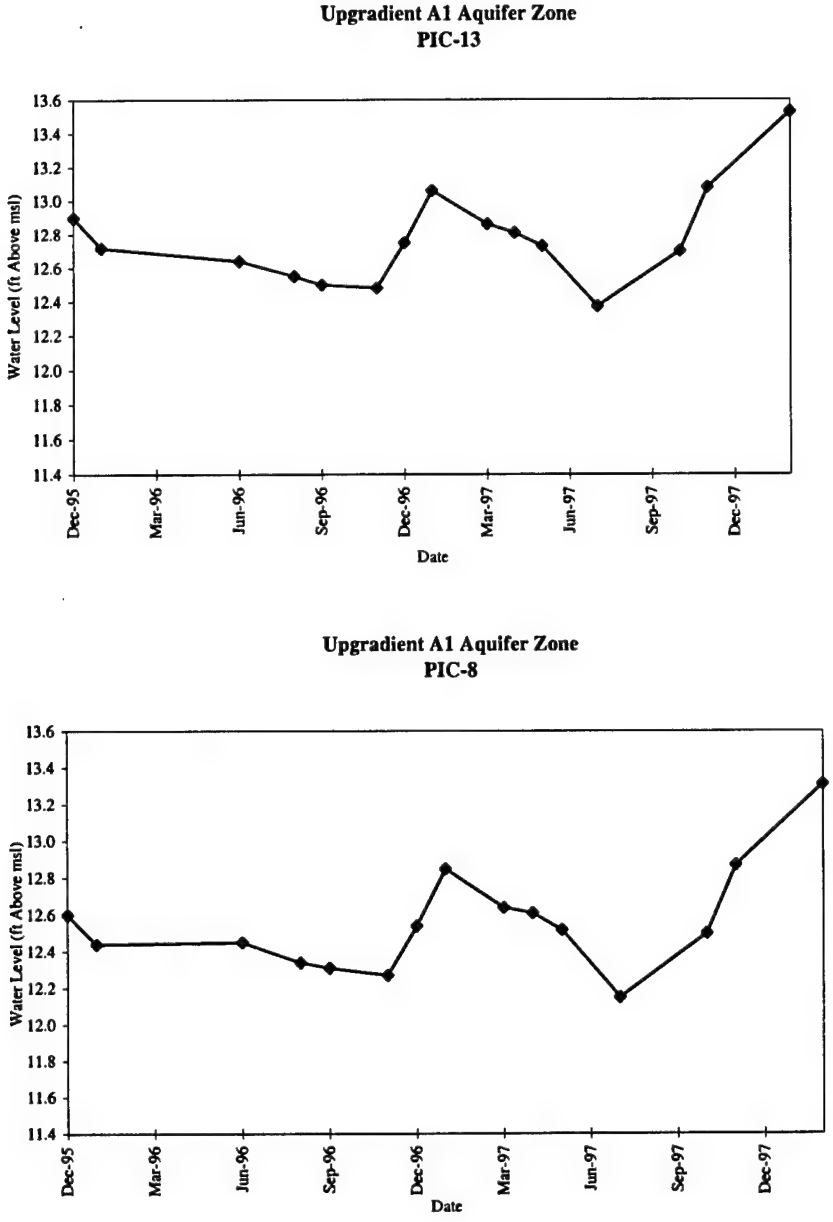

Figure 4-16. Water Level Hydrographs for Upgradient A1 Aquifer Zone Wells

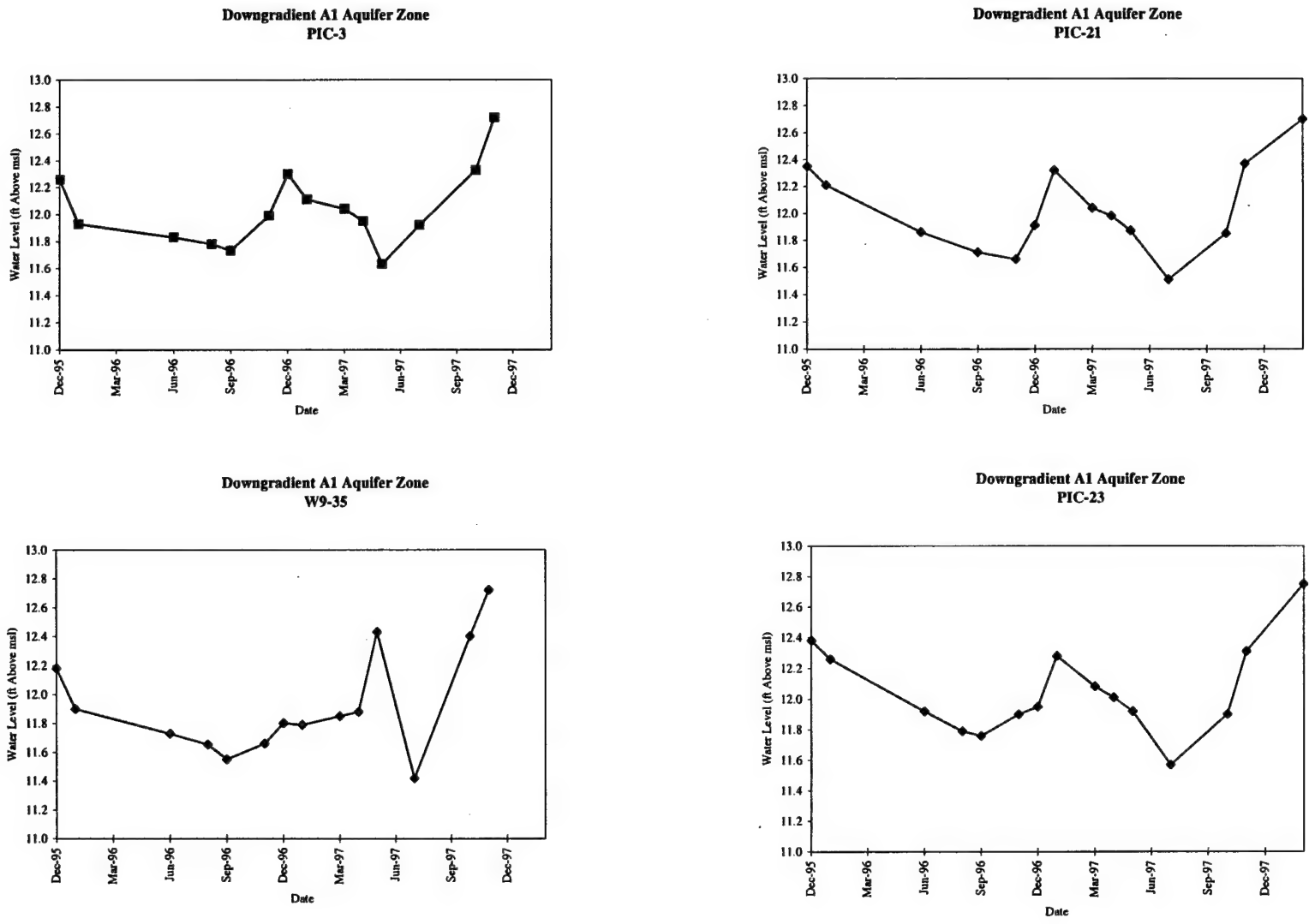

Figure 4-17. Water Level Hydrographs for Downgradient A1 Aquifer Zone Wells

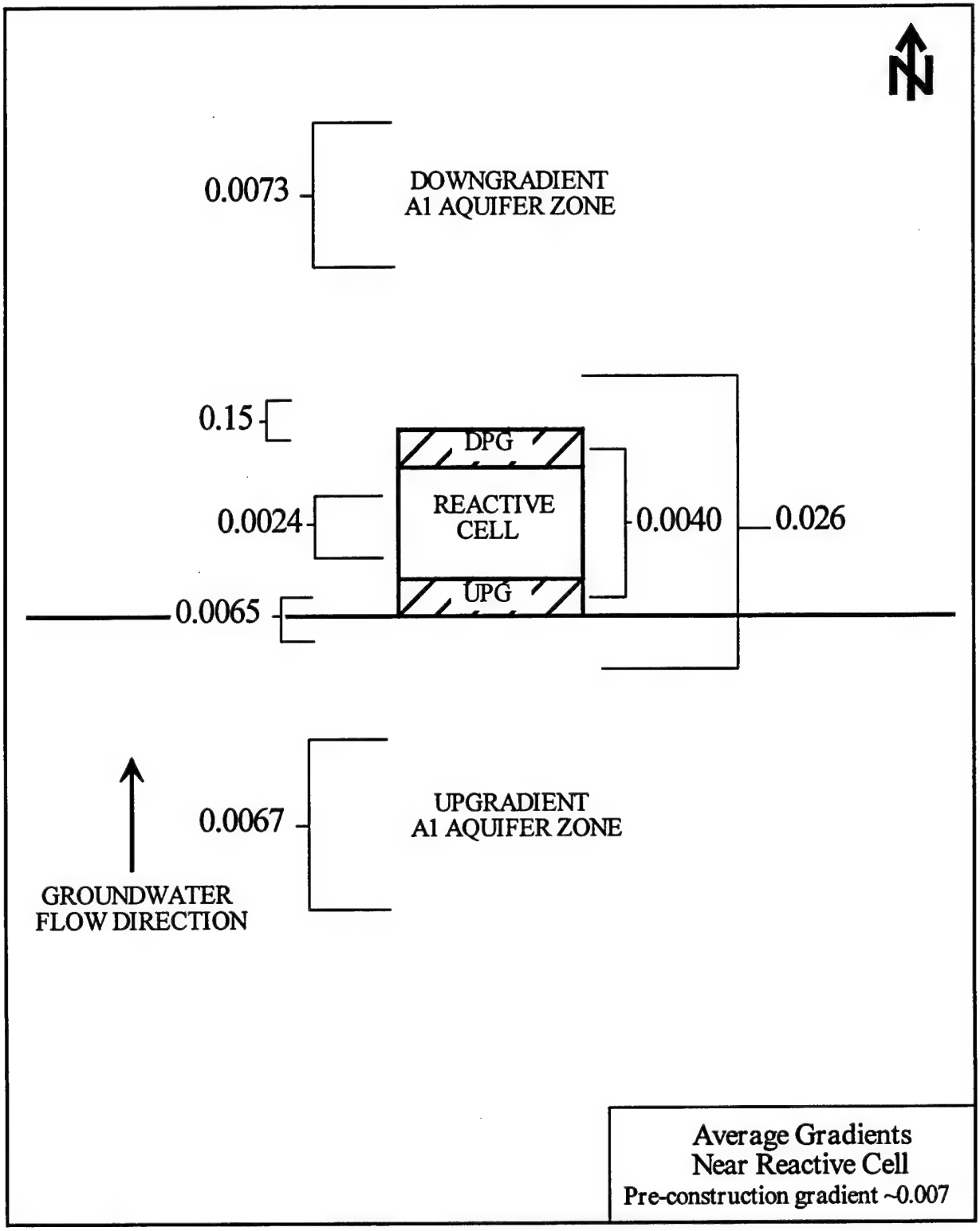

Figure 4-18. Observed Average Hydraulic Gradients Between Various Groups of Wells in the Vicinity of Permeable Barrier

4.3.1.2 Evaluating Vertical Flow Gradients Based on Water Levels

Table D-3 also shows average hydraulic gradients at the four depth levels (A, B, C, and D) in the reactive cell and the pea gravel. From upgradient pea gravel to downgradient pea gravel the gradient is about 0.004 at level A, B, and C and 0.008 at level D. Similarly, in the reactive cell, the gradient at levels A, B, C, and D is 0.0047, 0.0021, 0.0028, and 0.0199 respectively. Assuming similar hydraulic conductivity, it appears that the flowrate through the reactive cell is higher in the deeper levels than in the shallower levels. This also corresponds with the site characterization data that indicate the presence of a high conductivity sand channel at deeper levels in the aquifer. However, it should be noted that the standard deviation of the hydraulic gradient at level D is rather high.

The hydraulic gradient information in Table D-3 can be used to evaluate the potential for underflow along the gap between the bottom of the permeable cell and the base of the A1 aquifer zone. A comparison of water levels in the upgradient aquifer wells WIC-6, WIC-7, and WIC-8 shows that water levels are always highest in WIC-6, intermediate in WIC-7, and lowest in WIC-8. This indicates that there is a strong downward gradient in this well cluster. WIC-6 and WIC-7 are open at a depth similar to the lower half of the reactive cell, whereas WIC-8 is open at the same depth interval as the gap. On the downgradient side, in well cluster WIC-10, WIC-11, and WIC-12 there is an indication of upward gradient based on water levels. These patterns are not seen in the well clusters inside the barrier. The downward gradient on the upgradient side of the gap and upward gradient on the downgradient side of the gap are an indication that at least some portion of the groundwater is flowing through the gap instead of flowing through the reactive cell. A more definitive confirmation of this would require a tracer test with injection in WIC-6 or WIC-7.

The vertical hydraulic gradient information may also be used to evaluate the effect of the funnel-and-gate system on the potential for flow across the A1/A2 aquitard. Data from three pairs of wells upgradient of the permeable barrier and four pairs of downgradient wells is shown in Table D-4 (Appendix D). One well in each pair is open to the A1 aquifer zone and the other well is open to the A2 aquifer zone. Although only limited preconstruction data are available, it can be seen that prior to construction, the hydraulic gradients were generally upward. These results indicate potential for upward flow from A2 to A1. However, after construction, all the upgradient pairs changed to a downward flow potential, although the downgradient pairs showed no significant change. Even in the pair PIC-9 and PIC-17, which had downward preconstruction gradient, the extent of downward gradient increased. This switching of gradient across the aquifer zones is most likely the effect of funnel placement. In addition, in directing the groundwater flow laterally toward the reactive cell, the funnel walls also lead to a slight increase in water levels behind them, resulting in a gradient switch. At this site, the gradient switch is not a significant factor because the A2 aquifer zone is already contaminated. However, at other sites with thin lower confining zones these cross-formation gradient effects should be incorporated into the design consideration.

4.3.2 Results of Continuous Water Level Measurements

Figure 4-19 shows the results of the continuous water level data collected from three wells over 3 weeks in January 1997. Also shown are the precipitation events for this period. The December and January months usually have the highest rainfall in this area, so these data are expected to represent the high water level conditions. A strong correlation between water levels and rainfall can be seen in Figure 4-19. Results of continuous water level monitoring are consistent with the water level peak in December and January. In Figure 4-19, WIC-6 is in the upgradient aquifer approximately 1.6 feet from the pea gravel, WW-7C is in the upgradient pea gravel, and WW-8C is in the reactive cell (iron). The continuous monitoring data showed that for certain very short periods, the water level in WW-8C was higher than in WW-7C, indicating temporary incidents of mounding. Subsequent one-time water level measurements collected as part of routine quarterly monitoring events in January and March 1997 did not show mounding. In fact, the gradient across the gate appears to be relatively flat in each of the discrete water level monitoring events.

The second round of continuous water levels recorded over 4 weeks in August and September 1997 are shown in Figure 4-20. In addition to the three wells monitored in January 1997, water levels in well PZ9-8.2, located about 50 feet downgradient, are also shown. This is generally a period of low rainfall and low groundwater levels. However, there was heavy rainfall on the second day of recording. This is shown by a rapid increase of 0.1 to 0.15 foot in all four wells. The water levels in all wells show a gradual decrease following this rainfall and recharge event. The water levels in all wells are almost parallel, indicating that the wells in the aquifer and the reactive cell have a similar response to rainfall. During the period August 29 to September 5, one of the pumping wells located downgradient of the site was shut down for repairs. The effect of this is shown on Figure 4-20 by a flattening of the curves during the shutdown and a continued recession after the restart of pumping. This shows that the wells within and outside the permeable barriers respond similarly to pumping stresses on the aquifer. Finally, the water levels in the upgradient WIC-6 are always higher that those in the reactive cell. However, after the first rainfall event the water levels in the upgradient pea gravel (WW-7C) appear to be slightly lower than in the reactive cell (WW-8C). This may indicate a slight mounding in the pea gravel. Alternatively, this may be due to some movement in the water level probes during the bromide probe calibrations that were being done in the wells at the same time. Such mounding observations were not observed in the periodic water level measurements. As will be shown later in this section, the tracer tests indicated that tracer is retained in the pea gravel over an extended period of time before it starts entering the reactive cell.

In summary, the continuous water level data collected over two episodes indicates that mounding between the upgradient aquifer and the reactive cell is a transient phenomenon and confirms that, for the most part, groundwater flows from the aquifer into the reactive cell. There is some indication of a slight backup of water in the upgradient pea gravel. Whether the small amount of mounding occurred only for brief time periods following rainfall events or for extended time periods is unclear. However, it does not seem to affect the overall flow through the barrier. One factor contributing to the mounding could be the sharp (one-to-two orders of magnitude)

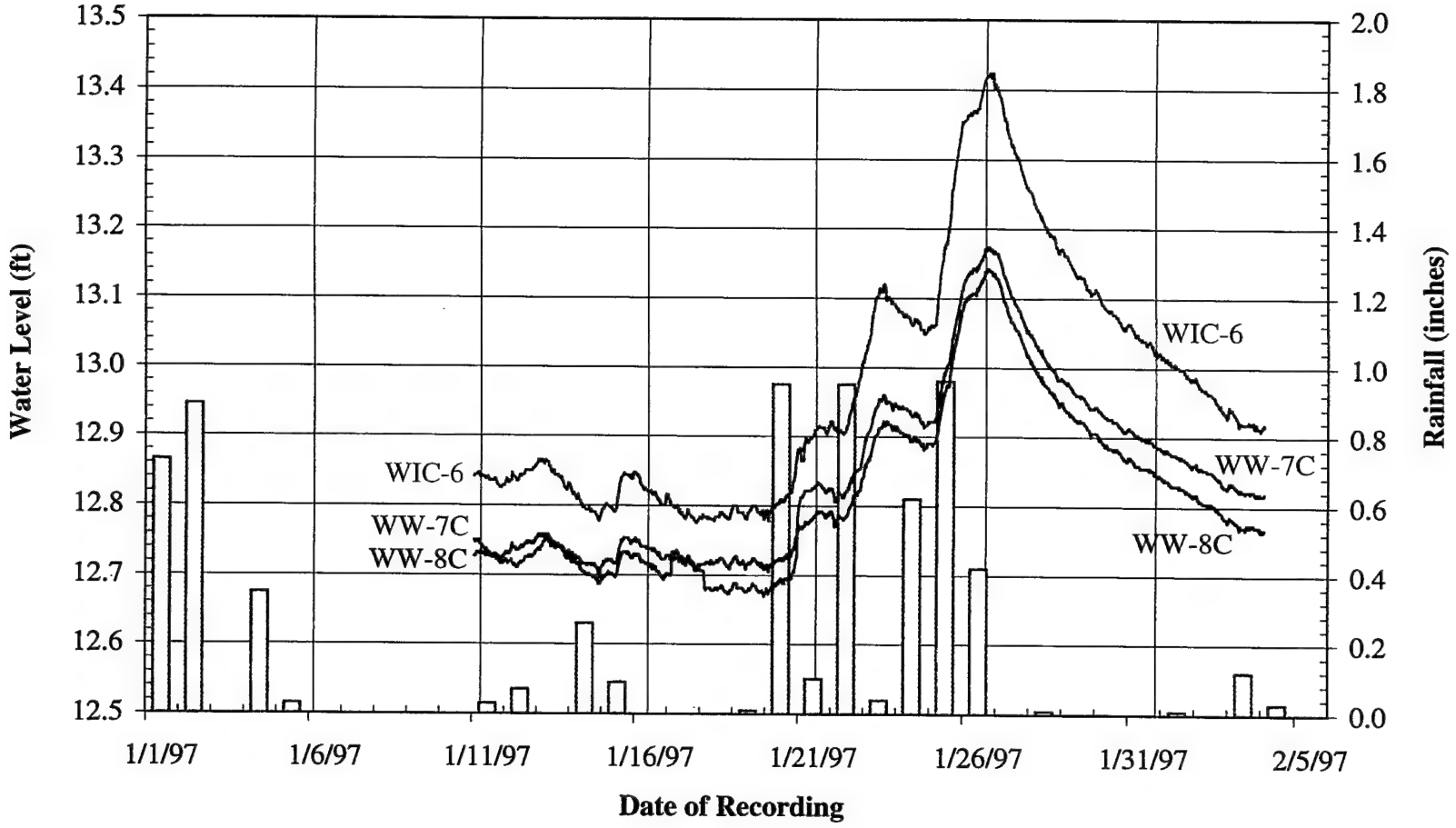

Figure 4-19. Continuous Water Level Monitoring (lines) and Rainfall Data (bars) for January 1997 Monitoring

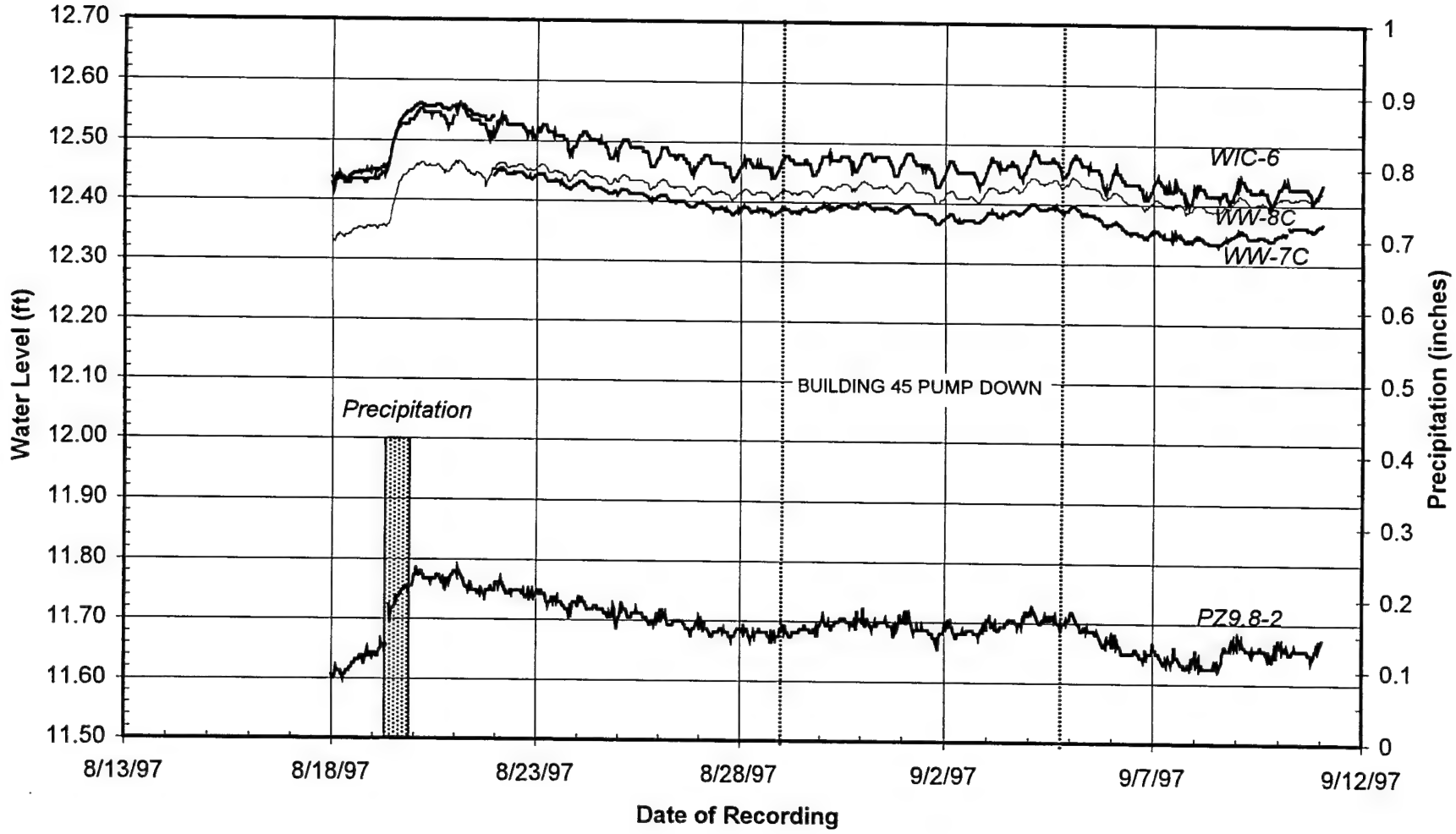

Figure 4-20. Continuous Water Level Monitoring and Rainfall Information for August-September 1997 Monitoring

conductivity contrasts at the upgradient pea gravel-reactive cell interface and at the downgradient pea gravel-aquifer interface. The net effect may be a temporary disequilibrium in the rate at which water flows from a high-conductivity zone to a low-conductivity zone. This observation of mounding and uncertainties about hydraulic capture at other permeable barrier sites, such as Denver Federal Center and Sommersworth, raised concerns about the full-scale implementation of the technology. As a result, ESTCP and the Navy requested that a tracer test (see Section 4.3.4) be conducted to confirm that hydraulic capture was indeed taking place and that groundwater was flowing through the reactive cell as designed.

4.3.3 Results of Down-Hole Groundwater Velocity Measurements

The results of the down-hole velocity measurements are summarized in Table 4-6. Figure 4-21 is a pictorial representation of the groundwater velocity vectors measured at various wells in the permeable barrier and its vicinity. Multiple arrows at a single location represent repeat measurements. The raw data, spreadsheet calculations, and the cosine test for individual measurements are presented in Battelle (1997e). Many of the velocity values measured by the velocity meter in the aquifer and pea gravel were very low (less than 1 foot/day) and below the calibration range of the instrument (2.5 to 10 feet/day). This calibration limitation makes most groundwater flow measurements suspect. Strictly speaking, we can only say that measured velocities were below 2.5 feet/day. Site characterization and modeling conducted prior to installation had indicated velocities of around 3 feet/day in the sand channel portions of the aquifer. Pump test data in the vicinity of the permeable barrier (IT, 1993) had indicated a groundwater velocity as high as 5 feet/day. Possibly as a result of the low velocities, many of the cosine test evaluations with the velocity meter had poor outcome. In particular, the slowest velocities and the poorest cosine tests were obtained in the wells located in the pea gravel. The low flow velocities in the pea gravel may be due to the relatively lower K media, granular iron or aquifer, present in front of the upgradient and downgradient pea gravel, respectively. The flow directions obtained from repeat tests in the pea gravel were also highly variable, which may be indicative of the role of pea gravel as a zone of mixing and homogenization.

Within the reactive cell (granular iron), velocities measured in WW-5 and WW-14 were mostly within the calibration range of the instrument and showed good to fair cosine tests. The velocities within the reactive cell ranged between 1.1 and 6.1 feet/day. These flow velocities are in the range expected from the design and modeling calculations. All measurements but one point to the expected flow direction toward the downgradient (northeast) end. This was a good indicator that flow was occurring through the gate at a reasonable rate and in the expected direction.

In the upgradient A1 aquifer zone, the measured velocities ranged from 0.3 to 1.8 feet/day. At WIC-1, which is located in the sand channel, the velocity meter measured a velocity of 1 foot/day. As expected, the direction of the velocity vector was to the east or northeast in wells located on the western flank of the funnel (PIC-26, PIC-27, and PIC-30). In other wells, flow directions were more variable. All of the velocity measurements in WIC-1 point to the east, rather than to the north or northeast toward the gate. It is unclear whether this unexpected flow direction reading is due to the limitations of the instrument or whether the flow direction at WIC-1

Table 4-6. Groundwater Flow Direction Test Results

Well ID	Date	Time	Measurement Depth (feet bgs)	Approximate Velocity (feet/day)	Approximate Direction	Corrected Flow Direction Angle	Cosine Test Result
Upgradient A1 Aquifer Zone Wells							
PIC-26	3/31/97	1200	16	1.1	E	96	G
PIC-26	4/4/97	1110	16	0.9	NE	73	G
PIC-27	3/31/97	1200	16	1.4	NE	66	G
PIC-28	4/4/97	1300	16	1.8	SW	215	G/F
PIC-29	3/27/97	945	16	1.3	NE	64	G
PIC-30	3/31/97	1122	16	0.3	E	93	F
WIC-1	3/27/97	1030	16	0.6	NE	73	G
WIC-1	3/31/97	1405	16	0.5	NE	63	G
WIC-1	3/31/97	1515	18	0.6	E	112	G
WIC-1	3/27/97	1105	20	0.9	NE	74	G
WIC-6	3/27/97	1215	15.25	0.6	NW	310	F
WIC-7	3/28/97	730	20.75	0.9	SW	223	G/F
Upgradient Pea Gravel Wells							
WW-2	3/28/97	845	16	1.5	NE	73	G
WW-2	3/28/97	930	20	0.4	NE	66	P
WW-11	3/26/97	1620	10	0.1	W	273	P
WW-11	3/21/97	1200	15	0.1	NW	314	P
WW-11	3/21/97	?	15	0.4	S	179	P
WW-11	3/26/97	1800	15	0	NW	338	P
WW-11	3/26/97	1715	18	0.1	N	7	P
WW-11	3/26/97	1555	19.5	0.1	NE	29	P
Reactive Cell Wells							
WW-5	3/22/97	1010	10	2.2	NW	350	G/F
WW-5	3/22/97	1045	15	1.1	N	18	G
WW-5	3/22/97	1100	20	2.4	SW	223	G/F
WW-14	3/21/97	1605	15	2.9	NE	21	F
WW-14	3/21/97	1730	15	4.3	NE	46	G
WW-14	3/22/97	900	15	2.5	N	6	P
WW-14	3/22/97	935	20	6.1	NE	59	G
Downgradient Pea Gravel Wells							
WW-6	3/22/97	1325	10	0.5	NW	324	G
WW-15	3/22/97	1135	10	0.5	NW	300	G
WW-15	3/22/97	1200	15	0.6	SE	165	G/F
WW-15	3/26/97	1120	15	0.4	SW	210	G
WW-15	3/26/97	1340	17	0.6	S	201	G
WW-15	3/26/97	1440	19	0.7	W	290	F
WW-15	3/22/97	1225	20	0.5	SE	166	F
WW-15	3/26/97	1250	20	0.5	NE	40	F/P
Downgradient A1 Aquifer Zone Well							
WIC-11	3/28/97	1110	16	2.5	SE	140	G
WIC-11	3/28/97		19.5	0.5	NE	1	P

G = good; F = fair; P = poor.

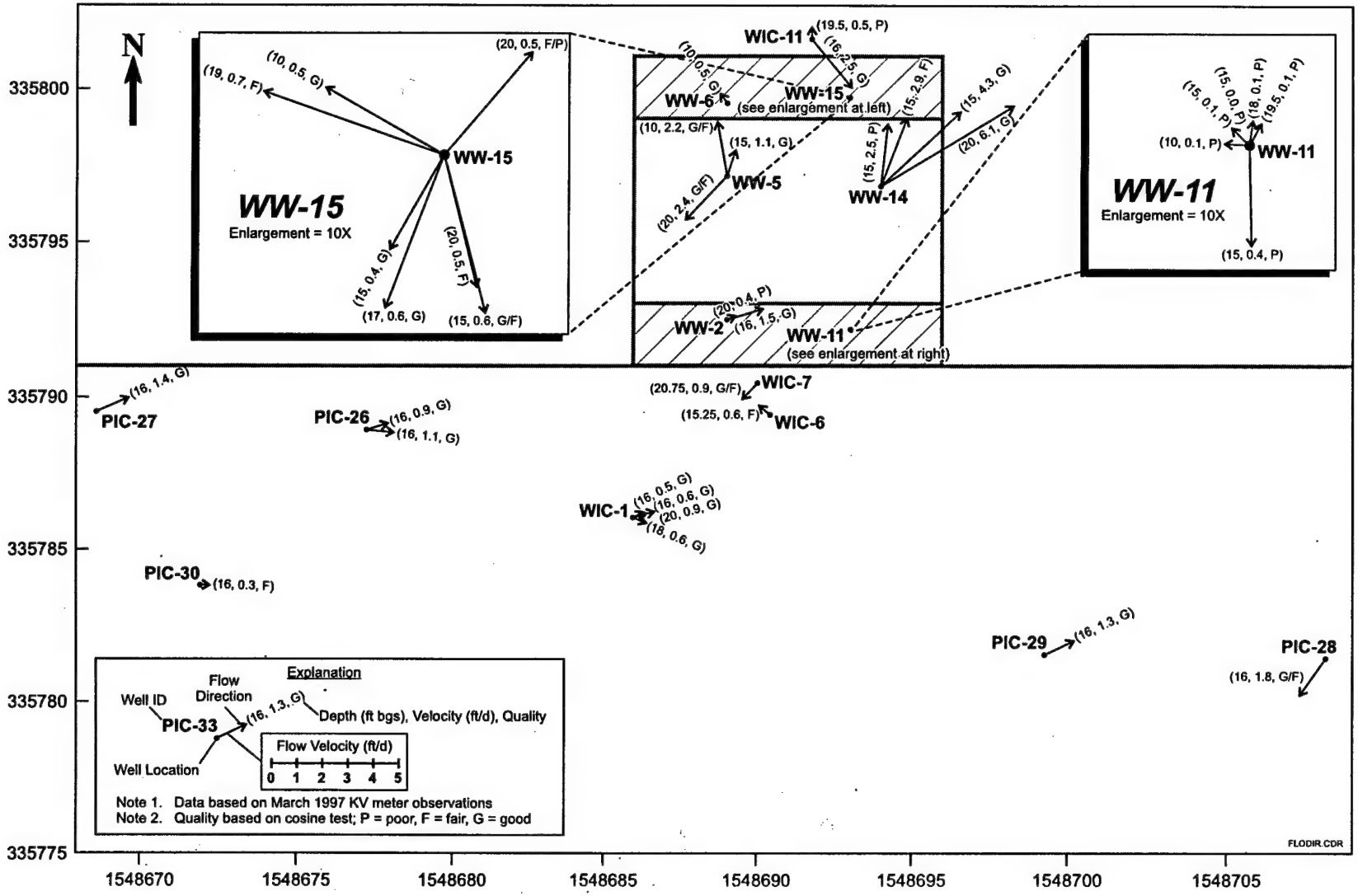

Figure 4-21. Pictorial Representation of Groundwater Velocity Vectors in the Permeable Barriers and Vicinity

actually is to the east. It is possible that the velocity meter was reading a highly localized flow path rather than the bulk groundwater flow. With the limited number of wells available and with the limitations of the velocity meter calibration, determining the location of flow divides or the capture zone upgradient of the funnel was not possible.

In summary, the magnitude of the groundwater velocity vector in the reactive cell, although somewhat on the low side, was within the range of prior expectations based on site characterization, design, and modeling. In the pea gravel, velocity magnitudes were lower than expected. The velocity in the upgradient aquifer was only slightly lower than expected from previous site characterization and pump test results (conducted before this installation of the barrier) as well as water levels and modeling (conducted after the installation).

4.3.4 Results of Tracer Tests

The main objective of the tracer tests was to test that the flow is occurring through the cell in the desired downgradient direction at a reasonable velocity. Estimating the width of the hydraulic capture zone and determining the mass balance of injected tracer compound were not objectives of this study.

The results of the two tracer tests and implications on the study objectives are discussed in the following two subsections. The first tracer test consisted of tracer injection in the upgradient pea gravel (well WW-2) and tracking the tracer in the reactive cell and the downgradient pea gravel. The second test consisted of tracer injection in the upgradient aquifer (well WIC-1) and tracking it in the upgradient aquifer and upgradient pea gravel wells. Given the logistical difficulties in conducting the tracer tests, this sequential approach offered better probability of success than a single upgradient aquifer injection.

4.3.4.1 First Tracer Test

This section presents the evaluation of the progress of tracer in groundwater through the reactive cell following injection in the upgradient pea gravel (well WW-2). The detailed data, bromide probe calibration, and time series plots for all the monitored wells are presented in Battelle (1997e).

Three of the representative time series plots, for wells WW-7B and WW-16D in the pea gravel and WW-8D in the reactive cell, are shown in Figures 4-22 through 4-24. These graphs show the injection interval (16:20 to 18:20 hours on 3/29/97), bromide concentration in the injection well (WW-2), and bromide concentration in the monitoring wells measured through continuous bromide probes, hand held probe, or laboratory analysis. Wherever confirmatory off-site laboratory analysis was done, the results are shown as triangles in the graphs. The solid lines associated with the monitoring wells are the result of smoothing the sensor data to eliminate random fluctuations and suspect readings resulting from periodic deterioration in sensor performance. Readings that showed a momentary elevation in bromide that could not be confirmed by subsequent measurements are considered suspect. A running-medium smoothing algorithm was used to smooth the data.

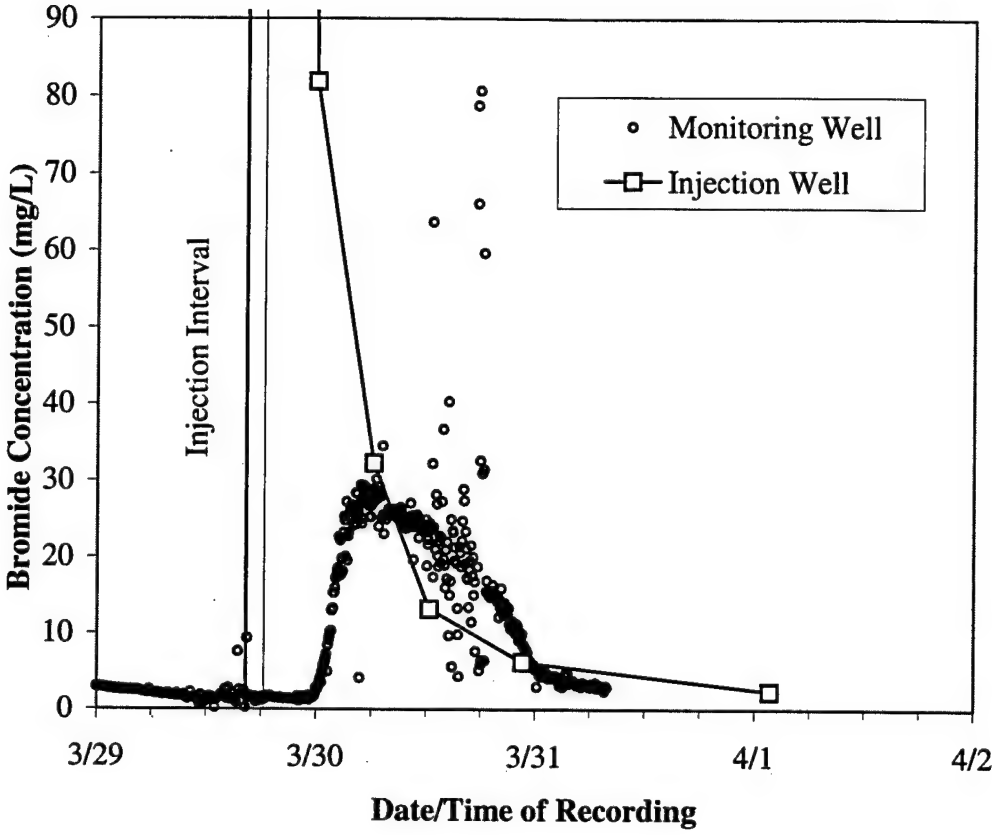

Figure 4-22. Results of Tracer Monitoring in WW-7B

Down-hole bromide sensor data collected between approximately 4/15/97 and 4/17/97 was not used in calculating the smoothed response curves, because of sensor malfunctions that occurred within these times. As understanding of the behavior of these sensors grew, and the malfunctions were corrected, the sensors were redeployed on 4/18/97. During the brief periods when the sensors malfunctioned, suspect readings of elevated bromide were recorded. These suspect measurements were recorded but disregarded in the evaluation of the tracer test data.

To help understand the movement of the tracer in the permeable barrier, information was compiled on when breakthrough of the tracer occurred at the detection points. Table 4-7 shows these data for wells that were monitored continuously. The breakthrough data reveal that tracer traveled rapidly eastward within the pea gravel during the first 2 days after injection. Bromide was first detected almost simultaneously in WW-7D and WW-11 (16.5 feet bgs) 0.21 days after injection. Based on the travel time to these two locations, groundwater velocities or mixing in the pea gravel could be as fast as 6.29 and 19.2 feet/day, respectively, directed perpendicular to the orientation of the permeable barrier. It is interesting that tracer was detected at WW-7B 0.29 day after it was detected at WW-7D, but it was not detected at WW-7C, which is at intermediate

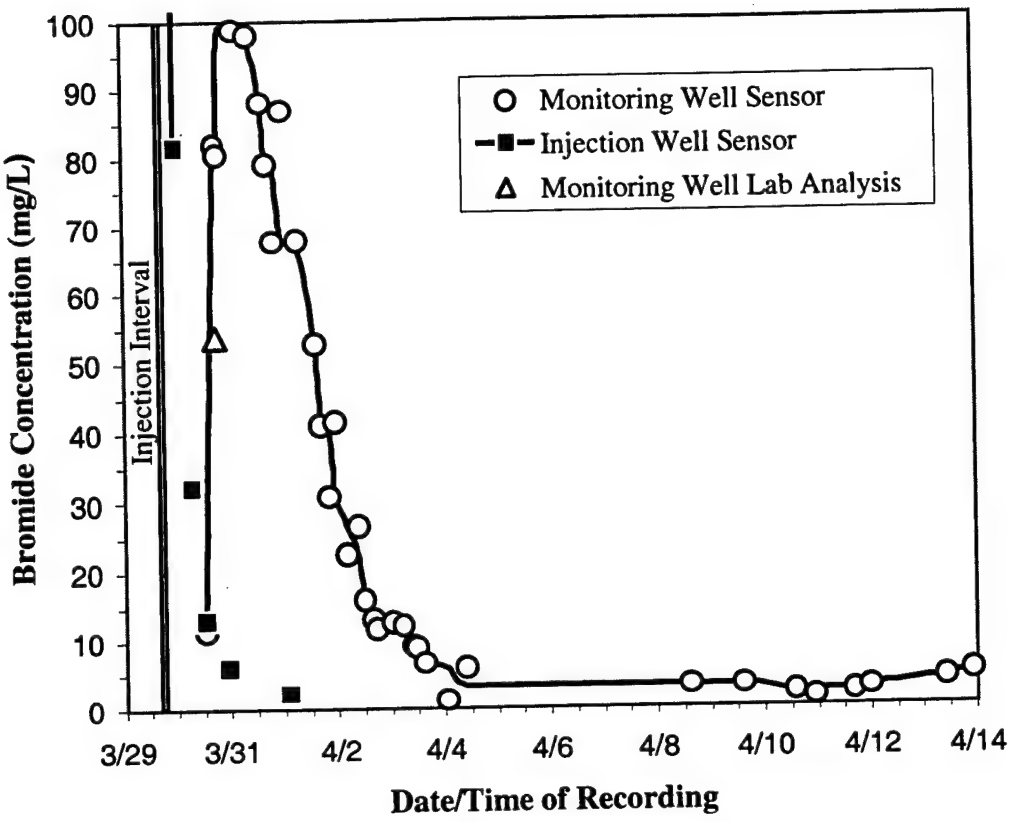

Figure 4-23. Results of Tracer Monitoring in WW-16D

depth. This may be due to the influence of local water movement and complex mixing patterns. The occurrence of tracer at WW-7B indicates that some mixing occurs in the vertical direction as well as in the horizontal direction. The rapid distribution of the tracer in the pea gravel indicates that within 5 hours after injection, the tracer was available to enter the reactive cell (granular iron) through several points along its upgradient face (vertical cross section).

Tracer movement inside the reactive cell appears to have been much slower than in the pea gravel. Tracer was first detected in the reactive cell at WW-3 after 4.29 days, based on laboratory analysis of a water sample. Unfortunately, it appears that the sensor used at this location was not responding correctly before this time and, consequently, if the tracer had reached this location prior to 4/3/97, it would not have been detected. Therefore, the breakthrough time at WW-3 may have been earlier than shown in Table 4-7.

Bromide was detected at WW-4D after 5.79 days, WW-5 after 11.35 days, and WW-1C after 15.29 days. Including WW-3, these four wells are located on the west side of the reactive cell and indicate similar reactive cell velocities, ranging from 0.33 to 0.45 foot/day, based on the

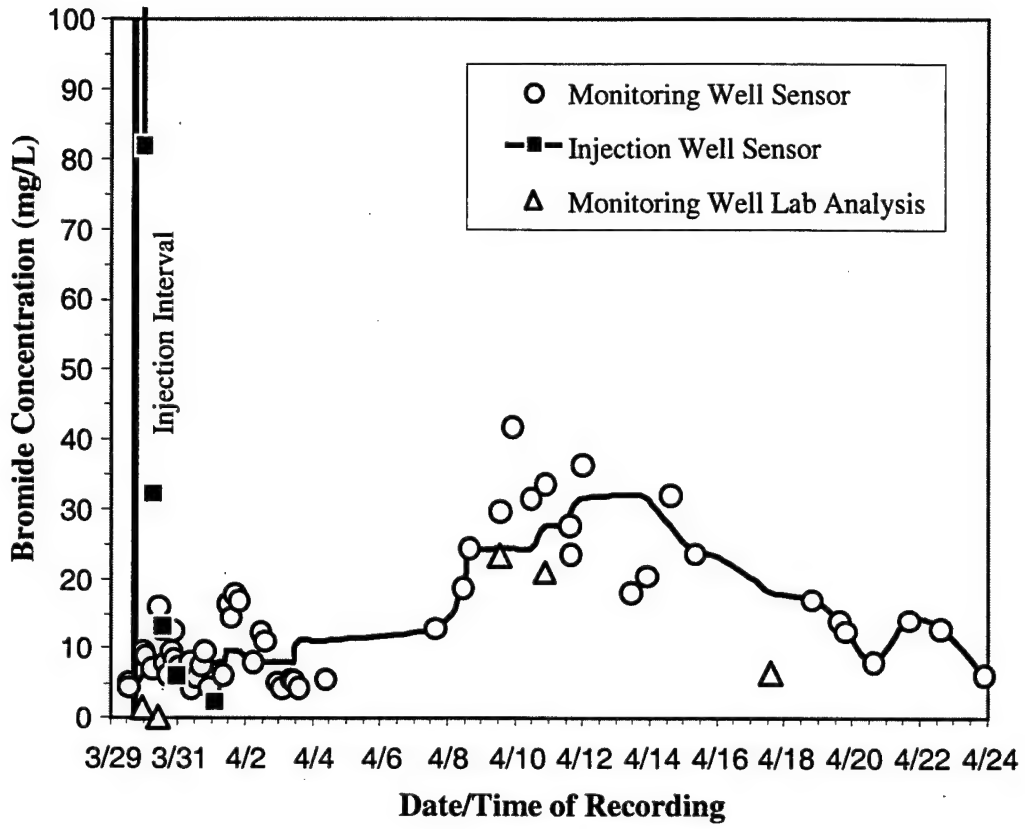

Figure 4-24. Results of Tracer Monitoring in WW-8D

distance from the injection well. Tracer was also detected at WW-8D after 9 days. WW-8D is located about 6 inches into the reactive cell and toward the centerline. The calculated velocity is 0.18 foot/day based on the distance from the injection well. Breakthrough at WW-13C and WW-12 after 13 and 16 days, respectively, is consistent with the velocity of the tracer elsewhere in the reactive cell. Figure 4-25 summarizes the sequence in which tracer was detected in the upgradient pea gravel and reactive cell.

Tracer also appeared at WW-10D after 3 days, although it was detected for little more than a day. The rapid occurrence of tracer at WW-10D would correspond to a velocity of 2.54 feet/day. This could be the result of a preferential pathway in the reactive cell, according to installation records. Along the floor of the reactive cell there is a square arrangement of welded steel pipe (closed on the ends) that was used for bracing. It is possible that this structure provides a narrow channel for water movement and is responsible for the tracer pulse. However, the pulse was small and does not agree with the lab analysis of a water sample that also was collected on 4/1/97. Other than at WW-10D, the laboratory data are in good agreement with the data collected using the bromide sensors.

Table 4-7. Tracer Breakthrough Data for Continuously Monitored Wells

Well ID	Distance from Injection Well (feet)	Sampling Depth (bgs)	Date & Time of Peak Breakthrough	Elapsed Time from Injection (days)	Peak Concentration[a] (µg/L)	Peak Horizontal[b] Velocity from Injection Point (feet/day)	Peak Horizontal Velocity[c] from Pea-Gravel Iron Interface (feet/day)
Upgradient Pea Gravel Wells							
WW-7B	1.33	11.6	3/30/97 5:00	0.50	25	2.66	NA
WW-7C	1.56	16.3	ND	NA	NA	NA	NA
WW-7D	1.31	21.0	3/29/97 22:00	0.21	800	6.29	NA
WW-11	4.00	11.5	3/30/97 5:00	0.50	80	8.01	NA
WW-11	4.00	16.5	3/29/97 22:00	0.21	30	19.2	NA
WW-16D	5.74	20.8	3/30/97 20:00	1.13	100	5.10	NA
Reactive Cells Wells							
WW-1C	5.96	16.2	4/14/97 0:00	15.29	20	0.39	0.35
WW-3	1.40	19.5	4/3/97 0:00	4.29[d]	8	0.33[d]	0.21[d]
WW-4D	2.61	21.0	4/4/97 12:00	5.79	80	0.45	0.36
WW-5	4.70	15.0	4/10/97 1:20	11.35	20	0.41	0.37
WW-8C	1.58	16.3	ND	NA	NA	NA	NA
WW-8D	1.81	21.0	4/8/97 15:00	9.92	25	0.18	0.06
WW-12	4.21	15.0	4/15/97	16.29	20	0.26	0.05
WW-13C	4.53	16.5	4/12/97	13.29	20	0.34	0.19
Downgradient Pea Gravel Well							
WW-10D	7.62	21.0	4/1/97 17:00	3.00[e]	40	2.54[e]	2.23[e]
Downgradient Aquifer Wells							
WIC-12	9.47	25.5	ND	NA	NA	NA	NA

(a) As measured by down-hole sensors.
(b) Based on the travel time of the peak concentration from the injection point to this location. This is the maximum velocity of the tracer.
(c) Based on travel time of the peak concentration from edge of pea gravel to this location. Not calculated for upgradient pea gravel wells.
(d) The sensor at this location did not respond accurately during the first 4 days. A discrete groundwater sample was analyzed for bromide in an off-site laboratory and provided the first indication of tracer appearance. The velocity component could be greater than the 0.33 foot/day maximum value estimated at this point.
(e) Based on bromide sensor readings that were not verified by laboratory analysis.
ND = not detected.
NA = not applicable.

Finally, the tracer monitoring data for all of the wells for six different times was used to produce three-dimensional plume maps showing the movement of a bromide slug through the reactive cell. The top view of these plots, based on concentration data at 0.25, 0.5, 1, 2, 6, and 12 days, is shown in Figure 4-26. These plots illustrate how the tracer first becomes mixed in the pea gravel and then migrates into the reactive cell. Because of resource limitations, the aquifer wells immediately upgradient from the gate were not monitored. Therefore it is difficult to say whether any of the tracer moved back into the upgradient aquifer.

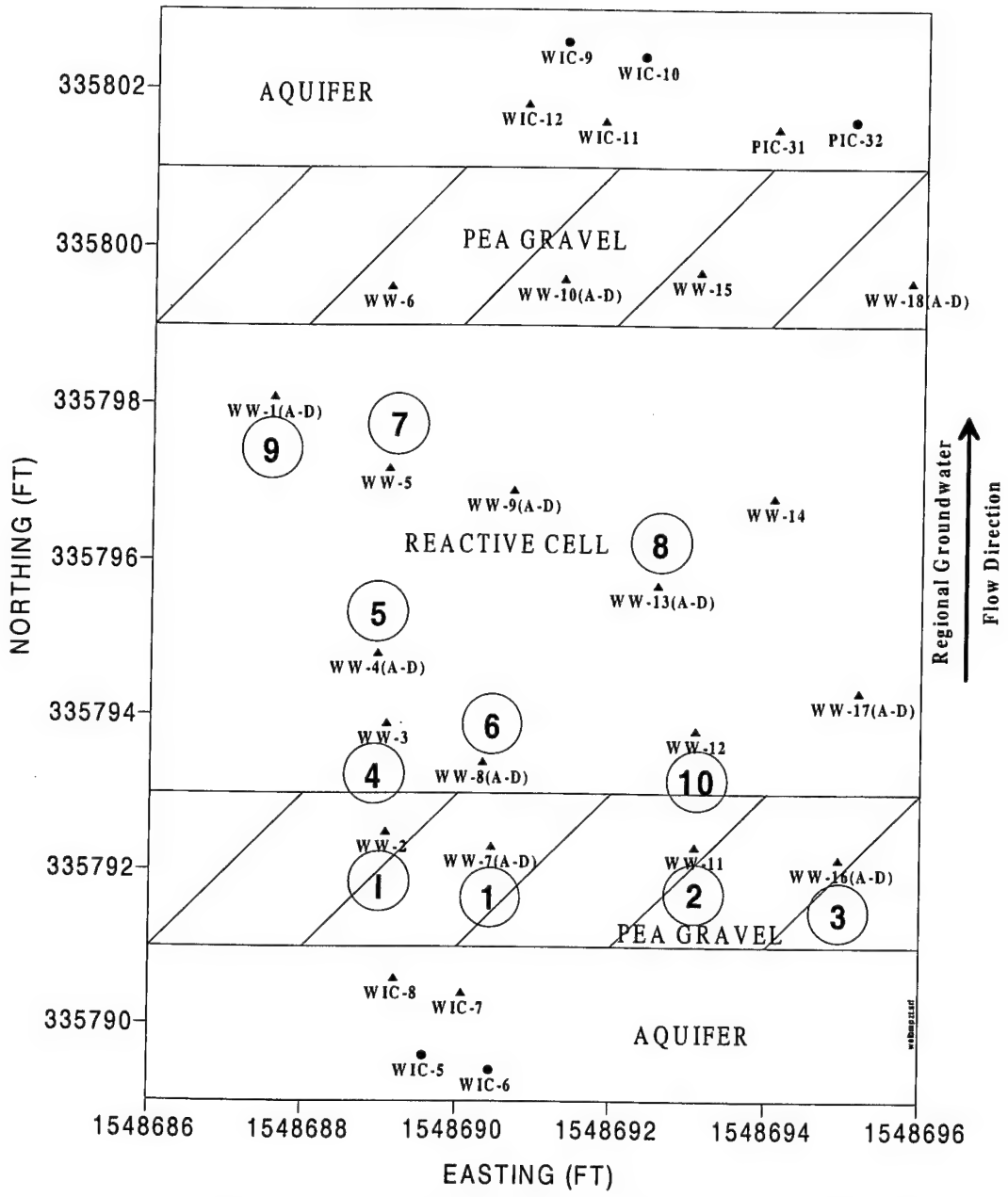

▲ Indicates that well was continuously monitored during tracer test (3/97)

* Easting and Northing coordinates correspond to the California State Plane Coordinate System for zone 403.

Figure 4-25. Sequence in which Tracer was Detected in the Upgradient Pea Gravel and Reactive Cell

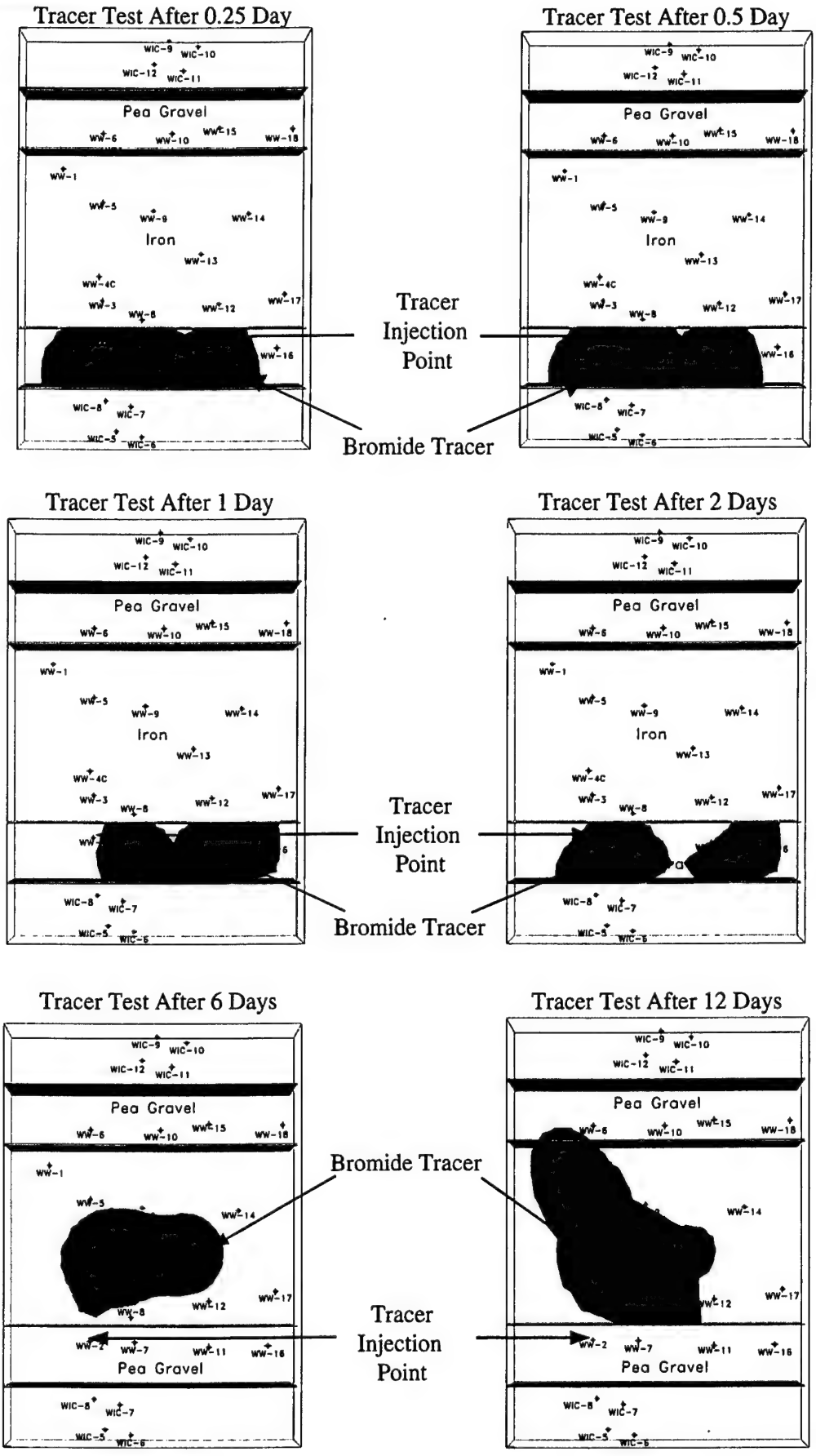

Figure 4-26. Movement of Bromide Tracer Plume Through the Reactive Cell over 12 Days Following Injection in the Upgradient Pea Gravel

In general, the tracer test was successful in its limited objectives of finding the tracer (or confirming that flow took place in the downgradient direction through the reactive cell) and estimating linear velocities or travel time (residence time) distribution in the reactive cell. The estimated linear flow velocities (and residence times) range from possibly as low as 0.2 foot/day to as high as 0.6 foot/day in the reactive cell (or residence times of 10 to 30 days) based on the tracer travel times. These flow velocities are lower than those predicted for the reactive cell by previous site characterization and modeling (approximately 3 feet/day), water level measurements (up to about 5 feet/day), and groundwater velocity meter measurements (1.1 to 6.1 feet/day). The following additional observations can be made regarding the flow through the permeable barrier gate at Moffett Field in March-April 1997:

1. The injected tracer was rapidly dispersed in the upgradient pea gravel. The 3,000-mg/L concentration of the injected bromide solution quickly dropped to about 750 mg/L (and lower) around the injection point due to dilution with native groundwater. At most other points the tracer peaked at 100 mg/L or lower. A total of 44 wells were monitored by sensor measurement or laboratory analysis during the course of the test.

2. Within 5 hours (0.21days) of injection, the tracer was available to enter the reactive cell through several points along its upgradient face. Lateral movement of the tracer continued in the pea gravel for more than 1 day as the tracer was successively discovered at new points. Some tracer persisted in the pea gravel for around 5 days. The fast mixing of the tracer in the pea gravel is in direct contrast to the slow velocities determined from the down-hole velocity measurements.

3. More horizontal than vertical mixing appears to have occurred and most of the tracer appears to have stayed in the lower levels where it was injected.

4. Flow through the reactive cell occurred in the general downgradient direction; although, based on the sequence of tracer detections at various points, flow patterns appeared to be relatively complex, possibly due to the differential compaction of the granular reactive medium in various regions of the reactive cell.

5. Based on the sensor data and laboratory analysis, it was verified that the tracer reached as far as WW-1C, which is 5 feet into the reactive cell and closest to the downgradient pea gravel. In the downgradient pea gravel itself, the tracer was detected with the down-hole sensor but its appearance could not be confirmed through laboratory analysis of discrete groundwater samples.

6. The late appearance of the tracer in WW-12, 16 days after its appearance in WW-11, indicates that flow does not always occur in straight perpendicular lines from the pea gravel interface along a horizontal plane as has been depicted in several modeling scenarios. Complex flow patterns in the permeable barrier also are predicted based on in-situ velocity measurements. Thus, the tracer test and flow velocity measurements agree qualitatively in this regard. Nondetection of the tracer could be a limitation of the sparse well density in this region.

7. Monitoring in the upgradient aquifer was accomplished only at the WIC-5 through WIC-8 wells because of the sparseness of monitoring points available in this region and the limited number of expensive probes available. No bromide tracer was detected in this well cluster. Whether any tracer flowed back from the upgradient pea gravel into the aquifer outside the range of the WIC well cluster could not be determined.

4.3.4.2 Second Tracer Test

The objective of this test was to confirm that the reactive cell is capturing the groundwater from the upgradient aquifer. A record of manual bromide sensor measurements along with calibration data for this test is presented in Battelle (1998a). Time series plots for all wells that were monitored either manually or by datalogger are also shown in that report. Battelle analyzed the time series plots for evidence that any of the sensors had detected bromide above the background concentration (approximately 0.5 mg/L). Two criteria were used to determine whether a bromide peak was detected. First, an assessment of the calibration data indicated that sensor output was linear with respect to bromide concentrations above 10 mg/L. Below 10 mg/L the response was nonlinear. Output varied somewhat between probes, but typically the response was between −90 to −70 mV for a 10 mg/L calibration standard. The signal became more negative as the concentration of bromide increased. Thus, the first search criterion was to identify signals that were more negative than −70 mV. The second criterion was to identify possible peaks based on the shape of the response data. If both of these criteria were met for a particular sensor, the calibration data were converted to concentration units.

Based on these criteria, only two sensors were suspected to have detected bromide concentrations in excess of background levels: the injection well (WIC-1) and WIC-5. WIC-5 is a 2-inch monitoring well and is located approximately 5 feet northeast of WIC-1. WIC-5 is the shallowest well in the upgradient aquifer well cluster and is screened from 11 to 12 feet bgs. The concentration profiles for WIC-1 and WIC-5 are shown in Figure 4-27. Altogether, 17 wells outside the reactive cell and 14 wells inside the reactive cell were monitored for bromide during the course of the second tracer test.

Figure 4-27 shows that the bromide concentration in WIC-1 is greatest following tracer injection and decreases rapidly thereafter. The tracer was no longer measurable 3 days after injection had stopped, indicating that the injection solution had rapidly mixed with aquifer water inside the PVC column and had become diluted to background concentration. Two measurements on August 19 (not shown) confirmed that the bromide concentration in the injection well was still at background.

At WIC-5 the bromide concentration began to increase on August 7 (8 days after injection) and decreased to background on August 12 (Figure 4-27). During a 5-day period the bromide concentration reached a maximum of approximately 11 mg/L. Note that some of the scatter in the points is due to the probe having been removed from the monitoring well on several occasions and inserted into calibration solutions. Assuming that the concentration maximum at approximately 10 days after injection represents the average travel time, then the average horizontal

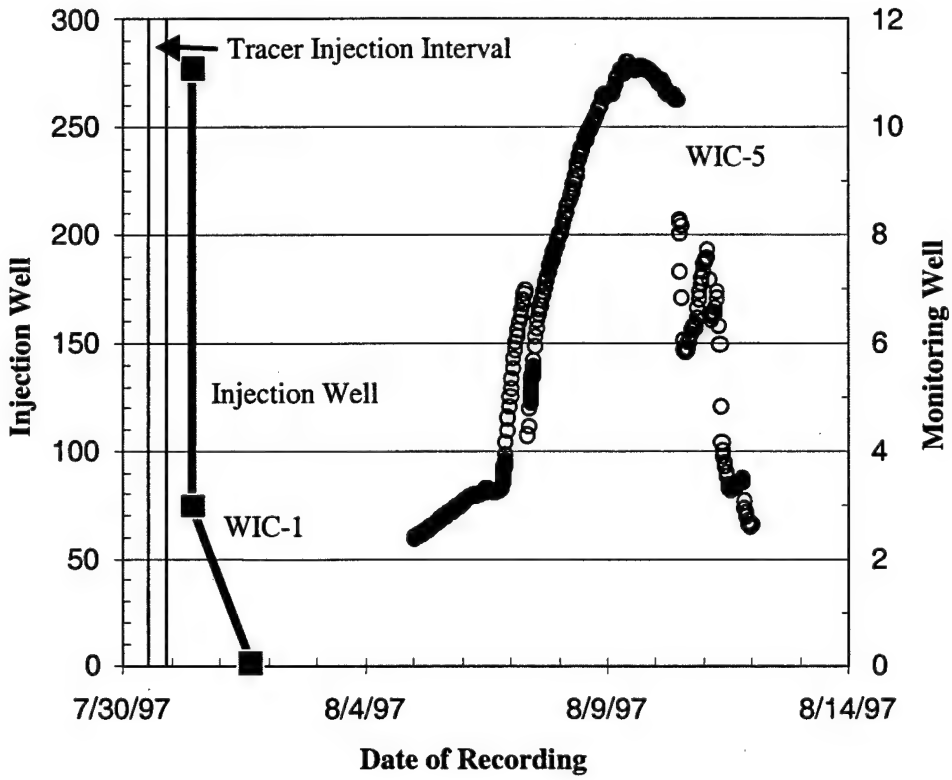

Figure 4-27. Concentration Profile of Tracer in WIC-1 and WIC-5 for Second Tracer Test

velocity component between WIC-1 and WIC-5 is about 0.5 foot/day. This value is in close agreement with aquifer velocities obtained by down-hole velocity meter measurements at that depth. The observation of tracer in WIC-5 confirms that a component of the groundwater from WIC-1 is flowing toward the reactive cell.

In summary, the second tracer test was partially successful in its objectives of finding the tracer in nearby monitoring wells and estimating linear velocities. No tracer was detected in any of the pea gravel or reactive cell wells. Possible reasons for not detecting tracer include migration into the pea gravel followed by quick dilution, insufficient number of upgradient aquifer monitoring wells and sensors, and presence of preferential pathways due to heterogeneities.

4.3.5 Groundwater Model Evaluation

The field barrier hydraulic monitoring results can be compared with the predictions of the groundwater flow model developed for the design of the permeable barrier and mapping of the monitoring well network. This comparison includes capture zone and flow paths, the discharge through the cell, and velocity and residence times in the reactive cell. Table 4-8 shows the model-simulated and field-observed hydraulic parameters. Each field evaluation method (water

Table 4-8. Hydraulic Parameter Comparison (Independent Parameter Shaded)

Scenario	Geometric Mean K (feet/day)	Gradient Through Cell	Average Linear Velocity (feet/day)	Residence Time in Cell (days)	Discharge (gpm)
MODFLOW Simulations					
Preconstruction Model[a]	N/A	N/A	1.18	5.08	0.81
Post-Construction Model[a]	1,302	N/A	1.50	3.99	1.0
Post-Construction Model (Low iron K)[a]	1,134	N/A	0.76	7.91	0.52
Post-Construction Model (High iron K)[a]	1,732	N/A	2.48	2.42	1.7
Field Observations					
Observed Hydraulic Gradients in Reactive Cell[b]	503	0.002	1.5	3.94	1.0
Observed Hydraulic Gradients in Entire Gate[b]	283	0.004	1.7	3.50	1.2
Tracer Test 1[c]	N/A	N/A	0.2 to 0.6	30 to 10	0.1 to 0.4
Velocity Meters in Reactive Cell Wells[c]	N/A	N/A	1.1 to 6.1	5.4 to 0.98	0.75 to 4.2
Velocity Meters in Pea Gravel Wells[c]	N/A	N/A	0.1 to 1.5	60 to 4.0	0.07 to 1.0

(a) Discharge calculated from modeled zone budgets, v = Q/nA.
(b) Based on average pea gravel to pea gravel gradients using Q = KA dH/dL.
(c) Q = nvA.
N/A = not applicable.
Shaded cells indicate field-observed values that were used to calculate other hydraulic parameters in the table.

levels, down-hole velocity measurements, or tracer tests) has its own limitations. A comparison of the range of discharge through the cell obtained from these different methods is shown in Figure 4-28. The significant implications of this comparison are discussed below. All the calculations here are based on a reactive cell porosity of 0.66, a value commonly reported from field barriers.

4.3.5.1 Simulated Versus Observed Discharge

The amount of groundwater flowing through the gate is a direct measure of the treatment effectiveness of the permeable barrier. Ideally, the permeable barrier should allow more discharge through the portion of the aquifer replaced by the gate after installation of the barrier (post-construction scenario) than before its installation (preconstruction scenario). The field-observed discharge through the gate was calculated from the various field measurements (water levels, velocity, tracer tests). The model-simulated discharge was calculated with the utility ZONEBUD in MODFLOW, which uses simulated cell-by-cell flow information to determine water budget for a user-specified group of cells.

Simulated preconstruction flow through the reactive cell area is 0.81 gpm. Post-construction flow through the gate for K_{cell} of 283 feet/day is 1.0 gpm, indicating that the volume of flow through the gate increased after the barrier was installed (Table 4-8). This is probably the best possible estimate for simulated discharge based on current conditions. For the scenario with reactive cell being 100 times less permeable (to represent any effects of future precipitation or clogging), discharge through the cell dropped to 0.5 gpm. This is a long-term scenario that is

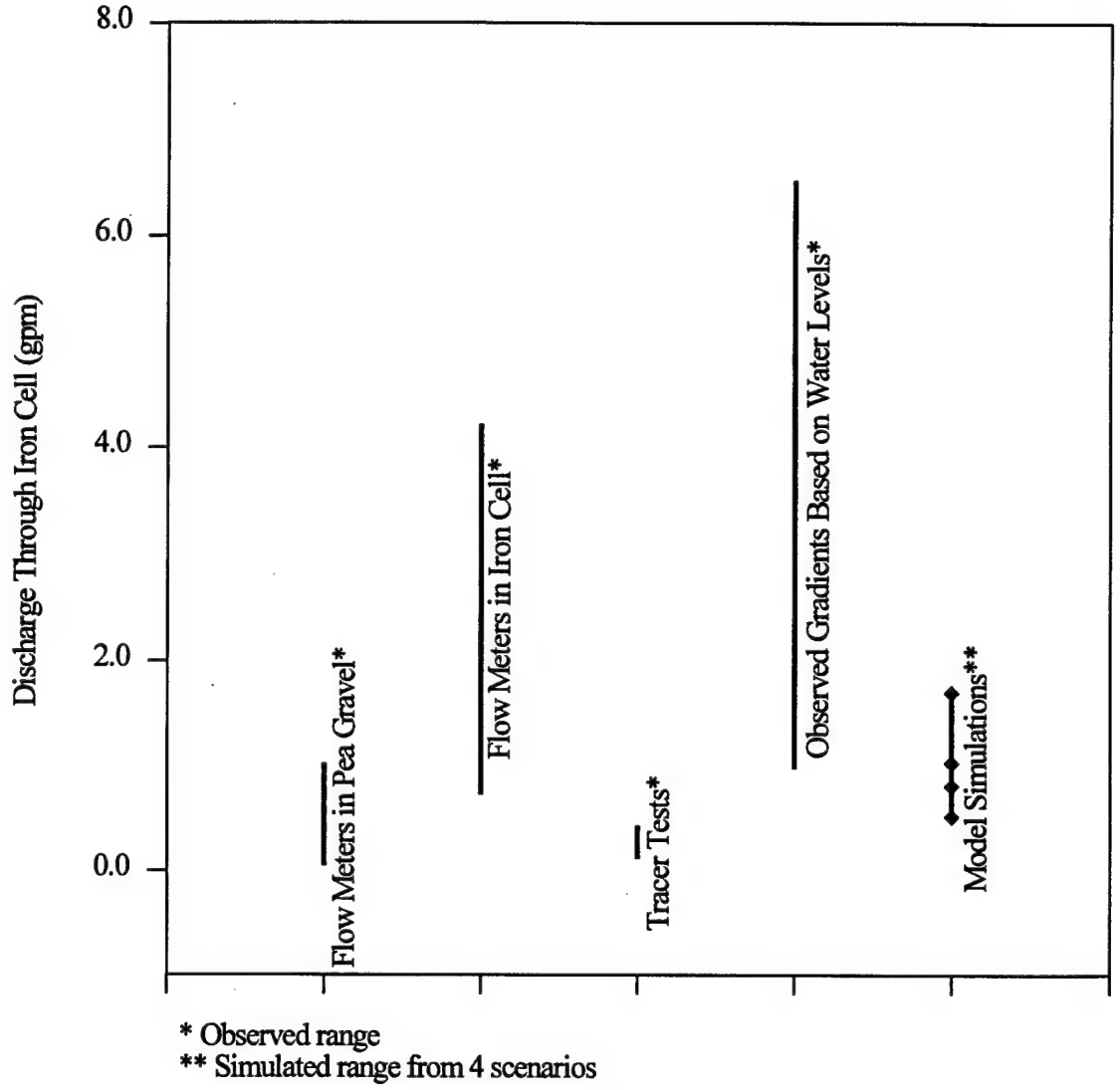

Figure 4-28. Range of Discharge Through the Gate

unlikely to occur for many years, based on the geochemical evaluation and core sampling results at Moffett Field (Section 4.4.6) and other permeable barrier sites. To evaluate the effect of K_{cell} being higher than estimated, a revised model with a K_{cell} of 1,000 feet/day was run. This revised higher conductivity model showed a discharge of 1.7 gpm through the cell.

The observed discharge based on the average hydraulic gradient of 0.004 through the reactive cell (based on water level measurements) and a K_{cell} of 283 feet/day is 1.2 gpm. If only the observed average gradient in the reactive cell (0.002) is considered, the discharge is 1.0 gpm. Both of these observed numbers are very close to the simulated discharge value of 1.7 gpm.

Based on tracer tests, the discharge is in the range of 0.1 to 0.4 gpm. The discharge values based on the velocity meter measurements range from 0.1 to 4 gpm. The discharge values based on the average hydraulic gradients are considered to be more representative of site conditions than the tracer test or velocity meter data. This is because the hydraulic gradients are based on water levels collected over 2 years in wells scattered throughout the study area, whereas tracer tests and velocity meter data apply to only a short period of time and are limited in spatial coverage.

4.3.5.2 Groundwater Flow Velocities and Residence Times

Simulated groundwater flow velocities in the reactive cell were determined by using a particle tracking code with the flow model. In particle tracking, particles are placed at appropriate starting positions within a specified area of the simulated flow field. The movement of the particles is then traced over time. Due to the heterogeneities incorporated into the model (based on site characterization results), particle velocities will vary depending on their starting location in the flow field. Thus, several particles are often simulated and the average of the velocities is calculated. Based on the modeling scenarios, average velocity through the reactive cell was predicted to be in the range of 0.76 to 2.5 feet/day, with 1.5 feet/day being the most likely estimate. Based on a reactive cell thickness of 6 feet, these velocities correspond to residence times of 2.4 to 7.9 days in the reactive cell, with 4 days being the most likely estimate. All of these residence times are higher than the design residence time of approximately 2 days (based on the bench-scale half-life data) and are sufficient for degradation of the CVOCs to their MCLs.

The observed groundwater flow velocities were determined from the hydraulic gradient data, velocity meter measurements, and tracer tests. Field observations based on water levels and average hydraulic gradients suggest that the reactive cell velocities are about 1.5 to 1.7 feet/day. This is a very good match with the simulated velocities. The velocities from the tracer tests (0.2 to 0.6 foot/day) are somewhat lower than the estimates from the hydraulic gradients. Tracer tests represent the average linear velocity through the media between injection and monitoring points. The velocity meter measurements (1.1 to 6.1 feet/day) within the reactive cell show a much wider range and higher velocity numbers. The observed groundwater flow velocities from velocity meters represent only one point in space and may indicate highly localized pore-level flow rather than bulk flow. A possible range of groundwater velocities in the reactive cell, after taking into account the limitations of various field measurement methods, may be estimated as 0.2 to 2.0 feet/day. These velocities correspond to residence times of from 12 to 3 days. Therefore, the field estimates of velocity are in fair agreement with the modeling estimates, and both provide enough residence time to achieve the desired degradation.

4.3.5.3 Simulated Versus Observed Capture Zones

The simulated capture zones, including the effects of heterogeneities, are presented in Figures 3-11 and 3-12. In these figures, the simulated capture zone is highly asymmetrical and somewhat larger than half the funnel length on the west funnel wall. The capture zone shapes also differ with depth. Because only a small number of monitoring wells were available for capture zone delineation, it is not possible to realize all of the detailed features of the simulated

capture zones in the observed water levels. However, the available observed water levels still show a substantial similarity to model results. The capture zones based on observed water levels for two of the monitoring events are presented in Figures 4-12 and 4-13. These observed water level and flow line maps show that the capture zones of the permeable barrier extends to at least halfway across the funnel on each side. That is, the capture zone is at least 30 feet wide (which makes it wider than the 10-foot gate) and straddles most of the sand channel. This observed capture zone is similar to the capture zone for the simulated system. The general capture pattern of the simulated and observed water levels is also comparable, with a flow divide upgradient of the sheet pile wings. In several monitoring events (Figures D-2 through D-14 in Appendix D), the observed flow divides are actually more pronounced than the simulated flow divides. The extent of change in water levels due to placement of the permeable barrier is similar for both simulated and observed water levels. Both show that the construction of the barrier affects water levels in a region that extends about 20 feet upgradient from the barrier.

4.3.6 Hydraulic Performance Summary

The hydraulic evaluation indicates that the permeable barrier is achieving the major objectives of maintaining sufficient flow through the gate, capturing the desired portions of the contaminant plume, and providing sufficient residence time in the reactive cell. The periodic water level data collected over 2 years appears to be the most representative of the spatial and temporal variations in hydraulic conditions within the barrier and in its vicinity. The observed water levels show that both the gate and the funnel contributed to the hydraulic capture. This indicates that in the heterogeneous aquifer at Moffett Field, a viable permeable barrier configuration may be one in which the gates are placed in the high-conductivity sand channels and the funnels are placed in the surrounding low-conductivity interchannel deposits for efficient capture of the plume. Such a scenario is desirable because the reactive medium, which is much more costly than impermeable walls, need only be placed in optimum locations across the site.

In general, the hydraulic gradients measured were relatively flat within the reactive cell. This may be due to the fact that the reactive cell has a much higher porosity and hydraulic conductivity compared to the aquifer, and is therefore able to accommodate a much higher volume of water without raising the gradient.

The groundwater flow velocities in the reactive cell determined from the observed water levels show a good match with the simulated flowrates. However, the tracer-determined flow velocities appear to be slower than expected.

There was no sustained and significant evidence of mounding or backflow in the cell despite occasional reversals of water levels observed during continuous water level monitoring. The flow patterns in the reactive cell are complex, both as a result of aquifer heterogeneities and possible differential compaction. This complexity is seen in all the evaluation methods—water levels, tracer tests, velocity measurements, and modeling. There appears to be more flow moving through the lower half of the gate than through the upper half. In addition, there is most likely some underflow through the gap beneath the cell.

In light of the tracer test and water level measurement results, it is unclear how accurately the down-hole groundwater velocity meter was able to predict flow magnitude and direction under these site conditions. Two possible limitations of using these meters could be the localized nature of the measurement (where the instrument measures pore level flow instead of bulk flow) and the lower-than-anticipated velocities in the aquifer that could be below the practical calibration level of the meters.

In summary, the hydraulic evaluation at Moffett Field showed the following:

- The targeted groundwater is being captured and is flowing through the gate as expected. The estimated capture zone is approximately 30 feet wide. Both the gate and the funnel contribute to this capture.

- The average linear groundwater flow velocity through the reactive cell may be lower than expected from site characterization and modeling results. Consequently, the actual residence time may be higher than designed. The estimated range of velocities through the reactive cell is 0.2 to 2 feet/day, which implies a residence time of at least 3 days; the design requirement was at least 2 days.

- Within the uncertainties of each type of measurement—water levels, groundwater velocity meter measurements, and tracer testing—the flow system in the reactive cell did appear to be within the range of the design.

4.4 Evaluation of Geochemical Data

The purpose of collecting geochemical data is to determine to what extent inorganic chemical reactions affect both the short-term and long-term performance of the permeable barrier. The native inorganic content of the groundwater, such as DO, calcium, magnesium, alkalinity, and sulfate, can be induced to cause precipitation within the reactive cell, which may affect both the surface reactivity of the iron and the hydraulic conductivity of the cell. This section of the report discusses the results of field parameter, groundwater, and core sample analyses that were conducted to address the issue of precipitation. Field parameters and groundwater sampling were conducted during each of the five quarterly monitoring events. Core samples of iron from the reactive cell and aquifer were collected at the end of the monitoring program.

4.4.1 Results of Field Parameter Measurements

Field parameter measurements included pH, oxidation-reduction potential (ORP), temperature, and DO. Summary tables for all five quarterly monitoring events may be found in Appendix H of this report. Table 4-9 lists selected results of field parameter measurements taken during the April 1997 monitoring event, which was the most recent event from which a complete set of groundwater samples was analyzed. In October 1997, less than half of the wells were sampled for inorganic constituents, so that resources could be used for coring activities. The results in Table 4-9 are representative of these parameters during other monitoring events.

Table 4-9. Selected Results of Field Parameter Measurements for April 1997

Well ID	pH	Temp (°C)	ORP (mV)[a]	Eh (mV)[b]	Deep DO (mg/L)[c]	Shallow DO (mg/L)[d]
Upgradient A1 Aquifer Zone Wells						
WIC-1	6.8	19.9	177.2	374.2	< 0.1	< 0.1
5	7.1	20.2	144.3	341.3	< 0.1	8.8
6	8.8	20.2	92.2	289.2	< 0.1	4.3
7	7.0	20.1	155.5	352.5	< 0.1	0.5
8	7.1	20.1	157.8	354.8	< 0.1	0.7
Upgradient Pea Gravel Wells						
WW-7A	7.1	20.6	101.6	298.6	0.3	2.2
7B	7.1	20.7	122.5	319.5	< 0.1	0.7
7C	7.1	20.5	117.1	314.1	< 0.1	1.8
7D	7.4	20.3	110.4	307.4	< 0.1	1.1
Reactive Cell Wells						
WW-8A	10.2	20.8	-343.4	-146.4	< 0.1	0.3
8B	10.2	20.9	-327.5	-130.5	< 0.1	0.3
8C	9.9	20.4	-309.0	-112.0	< 0.1	0.8
8D	11.2	20.4	-359.3	-162.3	< 0.1	0.7
WW-9A	10.4	20.9	-626.2	-429.2	< 0.1	0.2
9B	10.4	21.1	-634.8	-437.8	< 0.1	0.3
9C	10.3	21.1	-507.6	-310.6	< 0.1	0.2
9D	11.3	20.8	-665.6	-468.6	< 0.1	0.3
Downgradient Pea Gravel Wells						
WW-10A	9.9	20.9	-554.6	-357.6	< 0.1	< 0.1
10B	9.0	20.8	-433.8	-236.8	< 0.1	0.3
10C	9.0	20.6	-351.9	-154.9	< 0.1	0.3
10D	10.5	20.7	-364.5	-167.5	< 0.1	1.0
Downgradient A1 Aquifer Zone Wells						
WIC-3	6.9	20.1	62.1	259.1	< 0.1	1.8
9	7.1	20.4	-16.4	180.6	0.2	8.6
10	8.4	20.4	-149.7	47.3	< 0.1	0.1
11	12.0	20.3	-245.0	-48.0	< 0.1	4.5
12	7.0	20.2	9.6	206.6	< 0.1	1.0
Downgradient A2 Aquifer Zone Well						
WIC-4	7.1	19.9	85.1	282.1	< 0.1	4.6

(a) In-situ ORP measured against Ag/AgCl reference electrode.
(b) Eh calculated by adding 197 mV to the ORP measurement.
(c) DO measurement at mid-screen or 15 feet bgs.
(d) DO measurement just below water level (~6 feet bgs).

Measurements of pH, ORP, and temperature were taken in-situ, either at mid-screen level, in the case of short-screen wells, or 15 feet bgs in the case of long-screen wells. Eh was calculated by adding 197 mV to the ORP measurement to account for the potential of the Ag/AgCl reference electrode. DO measurements were taken in-situ at two depths: (1) just below the water level (approximately 6 feet bgs) in an unscreened portion of the well casing, and (2) either at mid-screen level, in the case of short-screen wells, or 15 feet bgs in the case of long-screen wells.

The measurements at greater depth are believed to be more representative of groundwater conditions.

4.4.1.1 Eh and pH Measurements

Results of Eh measurements indicate that values are generally positive in the A1 and A2 aquifer zone wells and generally negative within the reactive cell, indicating strong reducing conditions created by the iron. Similarly, pH values are close to neutral in the A1 and A2 aquifer zone wells and become somewhat alkaline (pH ~ 9 to 11) within the reactive cell. A decrease in Eh and an increase in pH are expected trends in the reactive cell, due to chemical reactions involving the strongly reducing zero-valent iron (Section 2.2). In the downgradient pea gravel and aquifer, Eh values increase somewhat and pH values decrease. As with the measured VOCs, this behavior seems to signify some mixing of treated effluent from the reactive cell with untreated groundwater flowing around or under the barrier.

Trends in Eh and pH throughout this entire investigation are shown in Figures 4-29 and 4-30 for four selected wells. It can be seen in Figure 4-29 that the Eh of the upgradient aquifer well WIC-1 and upgradient pea gravel well WW-7C generally remain positive, between 200 and 400 mV. A low Eh reading of 58 mV at WW-7C in September 1996 is characteristic of the upgradient pea gravel wells during that sampling period. Reactive cell wells are highly reducing and vary between approximately −100 and −400 mV in Eh. Results from October 1997 are not considered valid because the redox probe failed calibration requirements.

Figure 4-30 shows that pH values range from approximately 6.1 to 7.3 in the two upgradient aquifer and upgradient pea gravel wells. Native groundwater is slightly more acidic than pore water in the pea gravel zone, which remains close to neutral throughout the monitoring period. Higher pH in the upgradient pea gravel may be caused by a small admixture of iron during construction of the barrier. In the two reactive cell wells, pH ranges from approximately 8.3 to 10.7. Somewhat more variability can be seen in WW-4C, perhaps because it lies only about a foot away from the pea gravel zone.

4.4.1.2 Dissolved Oxygen Measurements

DO concentrations at the top of the water table typically range from below detection to 9 mg/L in the aquifer and pea gravel wells (Table 4-9), which are consistent with partitioning of atmospheric levels of O_2 in the groundwater. Shallow DO measurements in the reactive cell are typically less than 1 mg/L, indicating that DO is quickly consumed by the iron. DO measurements at deeper levels (mid-screen or 15 feet bgs) are generally much less than 1 mg/L and often are below the detection limit (0.1 mg/L) within the reactive cell, pea gravel, and the aquifer. This is indicative of naturally anaerobic conditions in the deeper aquifer. The field DO readings are not sufficiently sensitive to appraise the reducing environment within the reactive cell and deep aquifer. Redox measurement is more meaningful under low DO conditions, because the Eh range is sufficiently broad to discern differences in reducing conditions within the reactive cell.

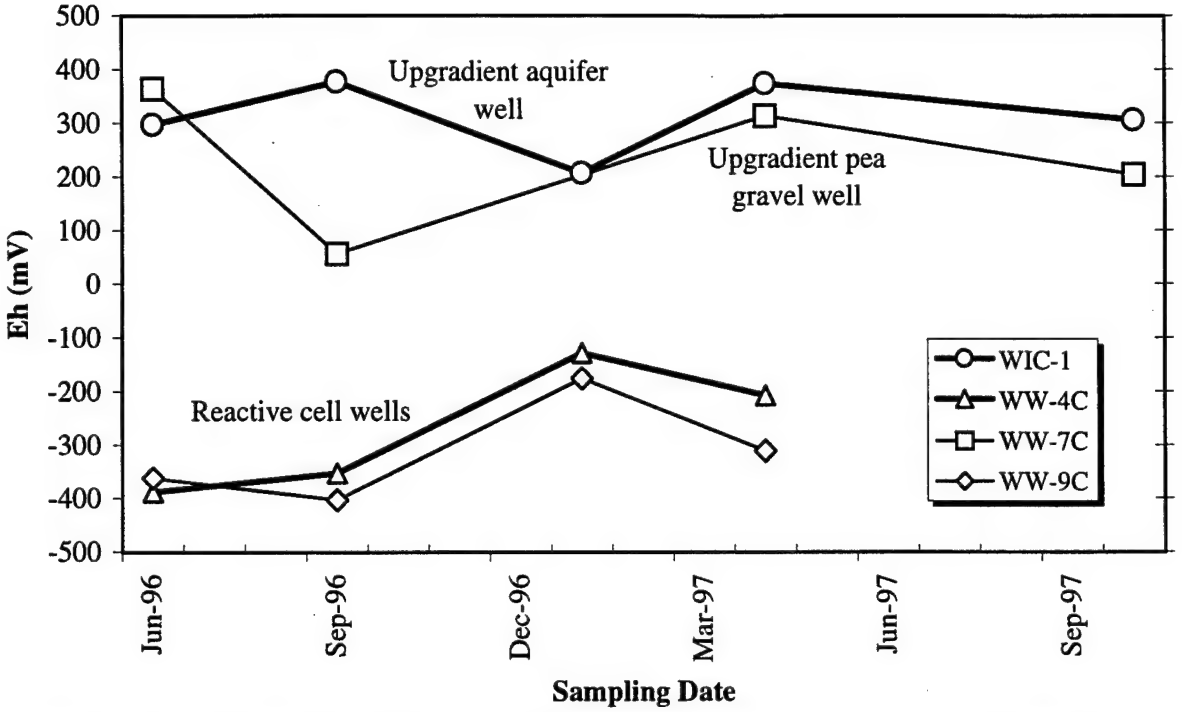

Figure 4-29. In-Situ Eh Measurements of Four Water Samples over the Performance Monitoring Period

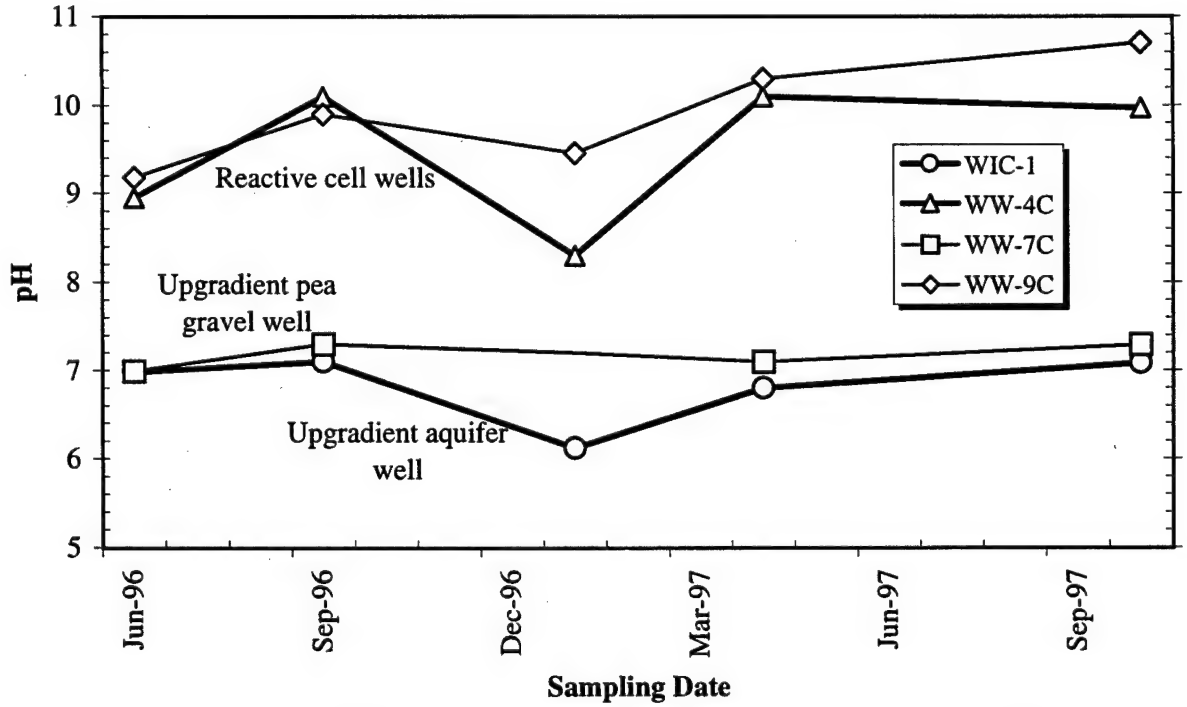

Figure 4-30. In-Situ pH Measurements of Four Water Samples over the Performance Monitoring Period

Vertical and horizontal profiles for Eh measurements taken during the quarterly monitoring events are shown in Appendix E.

4.4.1.3 Temperature

Temperatures within the permeable barrier range from to 19 to 23°C throughout the monitoring period (see Tables H-1b through H-5b in Appendix H). The highest average temperatures were recorded in October and the lowest temperatures were recorded in January.

4.4.2 Results of Inorganic Chemical Measurements

Appendix H contains summary tables of inorganic analytical data for the groundwater samples collected during the five quarterly monitoring events. Data are reported in units of mg/L and millimoles/L (mmol/L) in separate tables. Millimolar data are used to calculate charge equivalents, which is an additional indicator of data quality. The predominant ions in the A1 aquifer zone groundwater are sodium, potassium, magnesium, calcium, sulfate, bicarbonate (alkalinity), and chloride. On a molar basis, calcium is the dominant cation, followed by Mg ~ Na >K. Sulfate and bicarbonate are the dominant anions, followed by Cl. Nitrate is a minor constituent in the A1 aquifer zone (~1 to 3 mg/L). Other minor constituents include bromide, which is close to 0.5 mg/L in all groundwater samples, and fluoride and phosphate, at average concentrations of 0.15 and 0.1 mg/L, respectively (see Tables H-1d through H-5d in Appendix H). Table 4-10 lists selected results of inorganic chemical measurements for wells from the April 1997 sampling event. These results are representative of results obtained during other sampling events.

Samples for metals analysis (Na, K, Mg, Ca, Fe) were filtered in the field using 0.45-μm pore-size membranes. This procedure was intended to prevent colloidal material and suspended iron fines from being collected with the water sample and subsequently acid-digested and analyzed. Iron is perhaps the most problematic metal to analyze accurately, due to the difficulty in separating colloidal material from the dissolved phase. Table 4-10 shows that iron concentrations in the filtered samples were generally below 0.02 mg/L. Most importantly, iron concentrations in the reactive cell tend to be indistinguishable from samples taken elsewhere in the permeable barrier and surrounding aquifer. These results indicate that the permeable barrier does not promote excessive levels of dissolved iron in the downgradient aquifer. Thus, the barrier does not adversely affect water quality in regard to dissolved iron content.

The charge balance was calculated to provide a measure of inorganic data quality. Charge balance is calculated as the percent difference in cation and anion milliequivalencies (meq), as shown in the following equation:

$$\text{Charge Balance} = 100 \times \frac{\text{meq cations} - \text{meq anions}}{\text{meq cations} + \text{meq anions}} \qquad (7)$$

Table 4-10. Selected Results of Inorganic Chemical Measurements for April 1997

Well ID	Calcium (mg/L)		Magnesium (mg/L)		Sodium (mg/L)		Iron (mg/L)	
	Result	Detection Limit	Result	Detection Limit	Result	Detection Limit	Result	Detection Limit
Upgradient A1 Aquifer Zone Wells								
WIC-1	158	0.04	58.3	0.04	30.3	0.09	U	0.02
WIC-5	137	0.04	49.9	0.04	37.8	0.09	U	0.02
WIC-6	134	0.04	63.6	0.04	30.7	0.09	U	0.02
WIC-7	159	0.04	61.2	0.04	33.8	0.09	U	0.02
WIC-8	158	0.04	59.3	0.04	33.2	0.09	U	0.02
Upgradient Pea Gravel Wells								
WW-7A	164 E	0.04	65.7 E	0.04	33.6 E	0.09	U	0.02
WW-7B	163 E	0.04	63.7 E	0.04	31.9 E	0.09	U	0.02
WW-7C	177	0.04	72.8	0.04	38.5	0.09	U	0.02
WW-7D	164	0.04	63.9	0.04	35	0.09	0.118	0.02
Reactive Cell Wells								
WW-8A	2.02 B	0.04	30.4	0.04	36.1	0.09	U	0.02
WW-8B	2.25 B	0.04	17.5	0.04	34.3	0.09	U	0.02
WW-8C	3.49 B	0.04	32.8	0.04	32.6	0.09	U	0.02
WW-8D	8.27	0.04	16.3	0.04	33	0.09	U	0.02
WW-9A	0.921 B	0.04	0.349 B	0.04	36	0.09	0.029 B	0.02
WW-9B	1.48 B	0.04	0.488 B	0.04	35.7	0.09	0.044 B	0.02
WW-9C	0.486 B	0.04	0.852 B	0.04	34.7	0.09	U	0.02
WW-9D	87.8 E	0.04	1.16 EB	0.04	41.6 E	0.09	0.035 B	0.02
Downgradient Pea Gravel Zone Wells								
WW-10A	1.41 EB	0.04	0.593 EB	0.04	26 E	0.09	0.347	0.02
WW-10B	5.21	0.04	1.13 B	0.04	27.1	0.09	0.326	0.02
WW-10C	7.51	0.04	2.31 B	0.04	28.5	0.09	0.053 B	0.02
WW-10D	13.2	0.04	0.327 B	0.04	32.1	0.09	U	0.02
Downgradient A1 Aquifer Zone Wells								
W9-35	156	0.04	53.7	0.04	35	0.09	0.027 B	0.02
WIC-3	162	0.04	57.9	0.04	29.2	0.09	U	0.02
WIC-9	58	0.04	20.9	0.04	29.3	0.09	U	0.02
WIC-10	12.7	0.04	1.52 B	0.04	24.7	0.09	U	0.02
WIC-11	ND		ND		ND		ND	
WIC-12	132	0.04	44.1	0.04	40.5	0.09	U	0.02

Table 4-10. Selected Results of Inorganic Chemical Measurements for April 1997 (Continued)

Well ID	Alkalinity[a] (mg/L)		Chloride (mg/L)		Nitrate (mg/L)		Sulfate (mg/L)	
	Result	Detection Limit	Result	Detection Limit	Result	Detection Limit	Result	Detection Limit
Upgradient A1 Aquifer Zone Wells								
WIC-1	314	50	45.1	12.5	3.2	0.05	349	12.5
WIC-5	250	10	43	12.5	U	0.05	322	12.5
WIC-6	288	10	39.7	12.5	2.4	0.05	352	12.5
WIC-7	330	50	40.9	12.5	2.3	1	350	12.5
WIC-8	273	50	40.6	12.5	2.6	0.05	362	12.5
Upgradient Pea Gravel Wells								
WW-7A	215	50	45.2	12.5	1.5	0.05	329	12.5
WW-7B	289	10	45.7	12.5	U	0.05	335	12.5
WW-7C	276	50	31.3	2.5	1.8	0.05	264	12.5
WW-7D	310	10	46.1	12.5	2.8	0.05	342	12.5
Reactive Cell Wells								
WW-8A	U	1,000	38.3	5	U	0.5	56.7	5
WW-8B	89.2	10	37.8	2.5	U	0.05	21.8	0.5
WW-8C	70.8	10	39.5	5	U	0.05	94.4	5
WW-8D	62.2	10	39	5	U	0.05	51	5
WW-9A	14.3	10	42.4	2.5	U	0.05	1	0.5
WW-9B	14.1	10	43.3	2.5	U	0.05	1.1	0.5
WW-9C	16.6	10	41.2	2.5	U	0.05	4.2	0.5
WW-9D	134	10	39	5	U	0.05	111	5
Downgradient Pea Gravel Wells								
WW-10A	12.4	10	41.7	2.5	U	0.05	1	0.5
WW-10B	U	10	39.1	5	U	0.05	4.6	0.5
WW-10C	13.6	10	37.1	2.5	U	0.05	11	0.5
WW-10D	19.4	10	36.5	2.5	U	0.05	29	2.5
Downgradient A1 Aquifer Zone Wells								
W9-35	261	50	43.5	12.5	2.1	0.05	320	12.5
WIC-3	209	50	45	12.5	3	0.05	347	12.5
WIC-9	U	1,000	42.2	5	U	0.5	121	5
WIC-10	18.3	10	39.8	2.5	U	0.05	19	0.5
WIC-11	ND		ND		ND		ND	
WIC-12	270	10	40.7	12.5	1.8	0.05	308	12.5

(a) Alkalinity as $CaCO_3$.
ND: No data available.
U: The compound was analyzed but not detected at or above the specified reporting limit.
B: The compound was detected in the associated method blank.
E: The amount reported exceeded the linear range of the instrumentation calibration.

Electrolyte solutions such as groundwater are neutral by nature, therefore any deficiencies reflect cumulative errors in analysis of the ionic species. Solutions that are within 10% cation-anion balance may be considered adequately balanced for subsequent uses such as geochemical modeling. The majority of data collected in the five sampling rounds are within 10% of charge balance. Figure 4-31 shows the charge balance calculations for January 1997. In this figure, the data are distributed near the charge balance line (heavy line) and most points fall within the ±10% envelope.

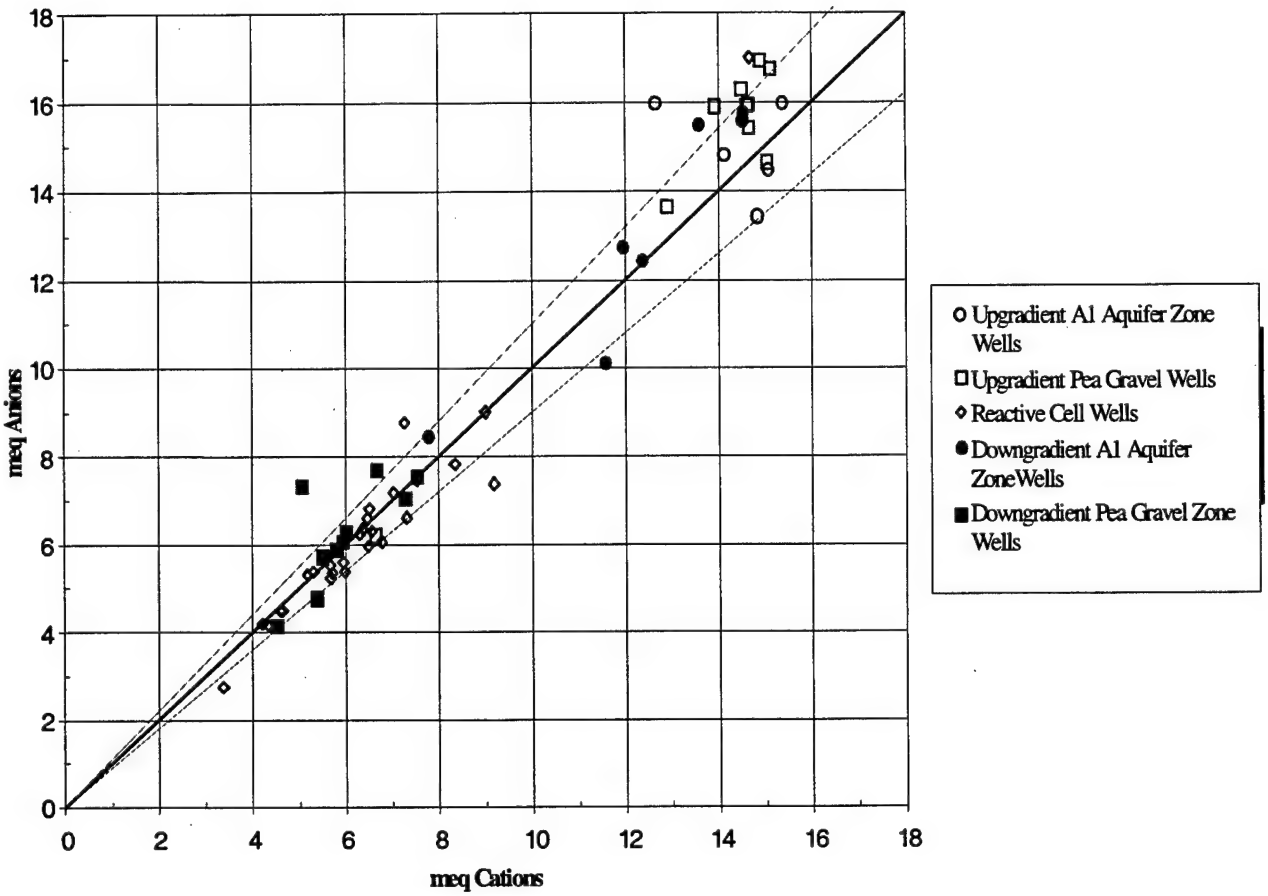

Figure 4-31. Charges of Anions and Cations in January 1997 Groundwater Samples. Heavy line represents charge balance; light lines represent deficiencies of ±10%

4.4.3 Time Series Evaluation

To determine whether the groundwater composition has changed systematically during the 16-month-long evaluation period, the concentrations of sodium and chloride were evaluated over each of the five sampling events. Sodium and chloride were chosen because they behave

conservatively in the groundwater system, i.e., these ions do not take part in mineral-phase equilibrium reactions. However, sodium may equilibrate with clay minerals via ion exchange. The data suggest that no significant changes have taken place. Figure 4-32 shows plots of sodium and chloride concentrations in the following well locations: upgradient aquifer (WIC-1); upgradient pea gravel (WW-7C); upgradient reactive cell (WW-4C); and downgradient reactive cell (WW-9C). While the data vary somewhat in both time and location, these variations do not point to any discernable trends for the reactive cell as a whole. Therefore, there do not seem to have been any large changes in the groundwater inorganic composition over time. Effects of dilution by greater-than-normal rainwater infiltration or concentration by evaporation were largely absent.

4.4.4 Inorganic Chemical Reactions in the Reactive Cell

In addition to degradation of CVOCs, there are indications that chemical reactions involving inorganic ions are taking place within the reactive cell. Table 4-10 shows that concentrations of alkalinity, calcium, magnesium, nitrate, and sulfate are significantly lower in the reactive cell than either the upgradient aquifer or pea gravel. Table 4-10 shows alkalinity values are generally about 215 to 330 mg/L upgradient of the reactive cell and fall below 100 mg/L in the WW-8 and WW-9 well clusters in the reactive cell. Calcium concentrations are approximately 160 mg/L in the aquifer and typically less than 10 in the reactive cell. Changes in magnesium are less pronounced but are also apparent. The magnesium concentration in the aquifer is about 50 to 73 mg/L and decreases below 40 mg/L in the WW-8 well cluster to approximately 1 mg/L in the WW-9 well cluster. Nitrate levels are about 1 to 3 mg/L in the aquifer and below detection (0.05 mg/L) in the reactive cell. Sulfate ranges from about 250 to 360 mg/L in the aquifer and pea gravel and decreases to less than 100 mg/L in most reactive cell wells.

The decrease in calcium, nitrate, and sulfate concentrations appears to take place quickly in the iron. Concentrations of these ions decrease sharply (relative to the aquifer) as the water enters the reactive cell. However, following this initial decline, the concentrations of these ions remain stationary as the water moves through the rest of the reactive cell. This suggests that the kinetics of the controlling reactions for these ions are fast, relative to the residence time within the reactive cell. The converse seems to be true for alkalinity and magnesium, which appear to decrease gradually in the downgradient direction in the reactive cell. The behavior of these ions suggests that reaction kinetics for controlling reactions are such that the chemistry of these ions is continuously changing throughout the reactive cell.

The above changes in inorganic constituents suggest that inorganic compounds are precipitating within the reactive cell due to changes in pH and Eh. For example, reductions in the concentrations of alkalinity, calcium, and magnesium are believed to be caused by precipitation of calcite ($CaCO_3$) and magnesite ($MgCO_3$). The magnesium concentration may also be affected by precipitation of magnesium hydroxide (brucite). Sulfate concentrations are not sufficiently high to cause precipitation of minerals, such as gypsum ($CaSO_4 \cdot 2H_2O$). It is more likely that reducing conditions lead to abiotic reduction of sulfate to a lower oxidation state. Water samples were analyzed for sulfide in the October 1997 sampling event, but concentrations were generally at or

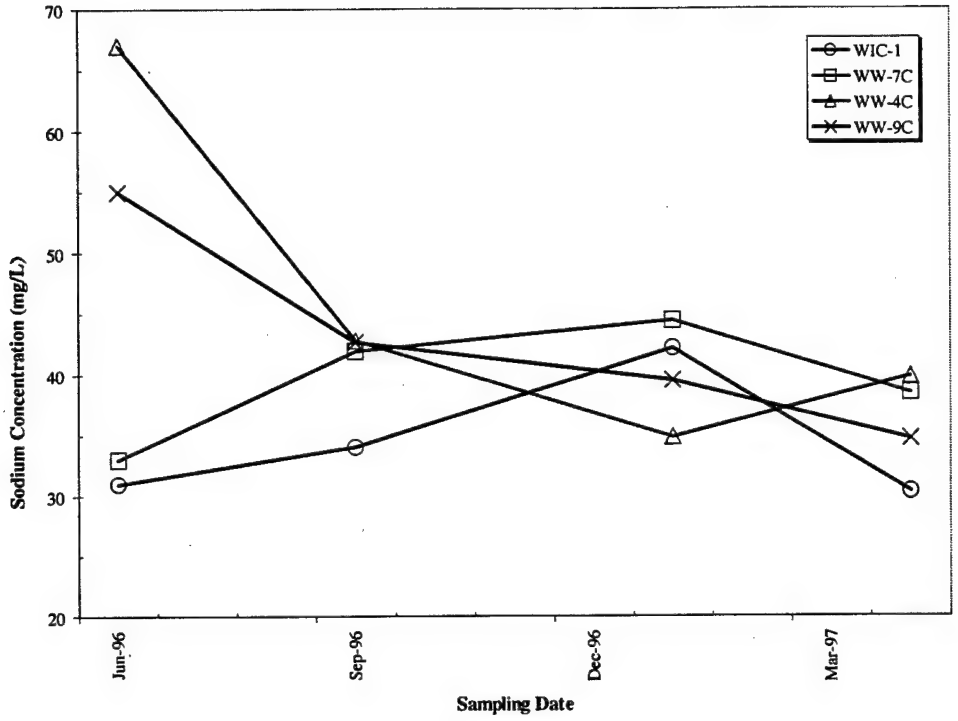

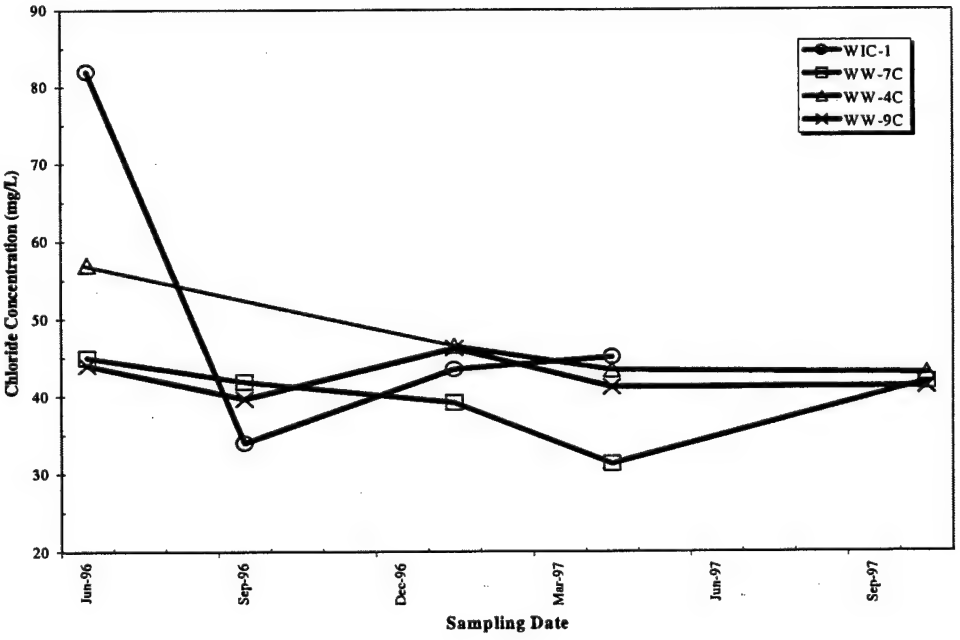

Figure 4-32. Sodium and Chloride Concentration Changes

below the detection limit (2.5 mg/L). One explanation is that sulfate is reduced to an aqueous species that quickly precipitates as an insoluble compound, such as ferrous sulfide (FeS or FeS_2).

4.4.5 Geochemical Modeling

Geochemical modeling was conducted to further investigate changes in inorganic groundwater chemistry using PHREEQC (Parkhurst, 1995). Table 4-11 contains results of calculations of mineral saturation indices using monitoring data from January 1997. The mineral saturation index (SI) is defined by SI = log (IAP/K), where IAP is ion activity product and K is the thermodynamic equilibrium constant for a particular mineralogical reaction. When SI = 0, the mineral and groundwater are considered to be in equilibrium; negative values imply undersaturation of the mineral phase and positive values imply oversaturation. The positive values in Table 4-11 are bolded, indicating saturation or oversaturation with respect to the mineral phase. In practice, mineral equilibrium may be assumed when SI = ±0.20. The minerals listed in Table 4-11 are those whose composition lies in the groundwater chemical system (H_2O-Na-Mg-Ca-Fe-Cl-SO_4-CO_2).

The data in Table 4-11 indicate that saturation indices vary spatially for most minerals within the permeable barrier. One exception is the carbonate mineral, calcite ($CaCO_3$), which is close to equilibrium at all locations. Because calcium and alkalinity levels in the groundwater decline during flow through the reactive cell, the relatively constant SI for calcite is evidence of precipitation in the reactive cell. Dolomite [$MgCa(CO_3)_2$] behaves differently due to slow precipitation kinetics. If the pore water chemistry is close to equilibrium with respect to dolomite in the upgradient pea gravel, then it becomes oversaturated in the reactive cell, and undersaturated in the downgradient pea gravel.

Aragonite is metastable with respect to calcite in groundwater environments, but has been found to precipitate in column tests during prior research. Siderite ($FeCO_3$), a ferrous carbonate mineral, is below saturation throughout most of the permeable barrier, but its SI is close to zero in the reactive cell. The other ferrous mineral considered, melanterite ($FeSO_4 \cdot 7H_2O$), is undersaturated at all locations in the permeable barrier. Based on these data, the model predicts that siderite is controlling ferrous ion concentration in the reactive cell.

The stabilities of two ferric minerals were evaluated. Goethite (FeOOH) tends to be oversaturated throughout the permeable barrier and amorphous ferric hydroxide [$Fe(OH)_3$] is mostly undersaturated. However, because thermodynamic data for amorphous compounds vary considerably, precipitation of $Fe(OH)_3$ is a strong possibility.

Gypsum ($CaSO_4 \cdot 2H_2O$) and anhydrite ($CaSO_4$) are undersaturated at all locations, as is melanterite ($FeSO_4 \cdot 7H_2O$). This suggests that the decline in sulfate levels in the reactive cell is not due to precipitation of sulfate minerals. A more likely explanation is that sulfate is reduced to sulfide due to low Eh. Additional calculations show that water in the reactive cell could be in equilibrium with marcasite (FeS_2) or mackinawite (FeS).

Table 4-11. Results of PHREEQC Calculation of Groundwater Saturation Indices[a]

Well ID	Anhydrite	Aragonite	Brucite	Calcite	Dolomite	$Fe(OH)_3$	Goethite	Gypsum	Melanterite	Portlandite	Siderite
Upgradient A1 Aquifer Zone Wells											
WIC-1	-1.17	-1.14	-7.85	-1.00	-2.13	-5.83	**0.01**	-0.93	-6.86	-13.67	-2.22
WIC-5	-1.13	-3.06	-11.33	-2.91	-6.00	-10.07	-4.21	-0.90	-7.22	-17.08	-4.50
WIC-6	-1.29	**1.88**	**0.02**	**2.03**	**4.06**	**0.92**	**6.78**	-1.06	-16.65	-5.87	-8.82
WIC-8	-1.21	-2.39	-10.24	-2.25	-4.62	-8.72	-2.86	-0.97	-7.43	-16.04	-3.98
Upgradient A2 Aquifer Zone Well											
WIC-2	-1.24	-0.61	-6.54	-0.46	-1.12	-3.27	**2.58**	-1.01	-6.61	-12.29	-1.35
Upgradient Pea Gravel Wells											
WW-2	-1.16	-0.21	-5.98	-0.06	-0.24	-5.49	**0.36**	-0.92	-7.44	-11.80	-1.85
WW-7A	-1.19	-0.03	-5.57	**0.12**	**0.14**	-2.64	**3.21**	-0.95	-7.02	-11.42	-1.23
WW-7B	-1.17	-0.32	-6.17	-0.17	-0.44	-4.52	**1.33**	-0.94	-7.41	-11.98	-1.91
WW-7C	-1.19	-0.31	-5.93	-0.16	-0.41	**1.23**	**7.10**	-0.96	-7.37	-11.74	-1.83
WW-7D	-2.70	-1.55	-5.00	-1.41	-1.66	-3.76	**2.10**	-2.47	-7.82	-12.06	-2.03
WW-11	-1.20	-0.21	-5.92	-0.06	-0.22	-3.30	**2.56**	-0.96	-6.65	-11.73	-1.01
WW-16A	-1.31	-0.58	-6.28	-0.43	-0.88	-3.39	**2.46**	-1.07	-6.79	-12.20	-1.43
WW-16B	-1.23	-0.40	-6.29	-0.25	-0.59	-3.27	**2.58**	-0.99	-6.66	-12.14	-1.20
WW-16C	-1.20	-0.08	-5.69	**0.07**	**0.02**	-2.35	**3.51**	-0.96	-6.42	-11.51	-0.67
WW-16D	-1.18	**0.39**	-4.68	**0.54**	**0.98**	-2.10	**3.76**	-0.95	-6.79	-10.50	-0.57
Reactive Cell Wells											
WW-1B	-1.62	-0.45	-0.57	-0.31	-0.65	-2.99	**2.85**	-1.38	-7.56	-6.49	-1.77
WW-1C	-2.49	-0.94	-0.72	-0.80	-0.63	-2.14	**3.71**	-2.25	-7.54	-7.62	-1.36
WW-3	-2.68	-0.17	-1.09	-0.02	**1.23**	-0.85	**5.01**	-2.44	-6.74	-8.29	**0.41**
WW-4A	-2.12	-0.94	-3.26	-0.79	-0.93	-4.54	**1.31**	-1.88	-7.15	-9.87	-1.35
WW-4B	-2.46	-0.53	-2.37	-0.38	**0.16**	-2.77	**3.08**	-2.22	-7.45	-9.22	-0.89
WW-4C	-2.94	-1.15	-3.47	-1.01	-0.69	-5.25	**0.61**	-2.70	-7.46	-10.71	-1.04
WW-4D	-1.18	**1.17**	-3.08	**1.31**	**2.53**	-5.23	**0.63**	-0.94	-7.72	-8.90	-0.73
WW-5	-2.57	-1.05	-3.11	-0.90	-1.02	-4.49	**1.37**	-2.33	-7.81	-9.81	-1.65
WW-8A	-2.12	-0.31	-2.54	-0.16	**0.49**	-2.85	**3.00**	-1.89	-6.81	-9.28	-0.36
WW-8B	-2.48	**0.05**	-1.24	**0.20**	**1.51**	-1.28	**4.57**	-2.24	-7.10	-8.28	**0.06**
WW-8C	-2.75	-0.37	-1.94	-0.22	**0.86**	-0.66	**5.21**	-2.52	-7.03	-9.14	**0.01**
WW-8D	-2.28	**0.29**	**0.61**	0.43	**1.41**	-0.38	**5.48**	-2.04	-8.28	-5.85	-1.08
WW-9A	-1.91	-0.84	-2.64	-0.69	-0.93	-4.56	**1.29**	-1.68	-7.02	-9.02	-1.32
WW-9B	-2.78	-0.94	-2.14	-0.79	-1.00	-4.09	**1.76**	-2.54	-6.88	-8.69	-0.43

Table 4-11. Results of PHREEQC Calculation of Groundwater Saturation Indices[a] (Continued)

Well ID	Anhydrite	Aragonite	Brucite	Calcite	Dolomite	$Fe(OH)_3$	Goethite	Gypsum	Melanterite	Portlandite	Siderite
Reactive Cell Wells (cont'd)											
WW-9C	-2.71	-1.02	-1.37	-0.87	-0.73	-2.71	**3.14**	-2.47	-7.48	-8.33	-1.16
WW-9D	-1.31	**1.02**	-2.88	**1.17**	**1.26**	-5.27	**0.59**	-1.07	-7.95	-7.72	-0.98
WW-12	-2.15	-1.71	-6.06	-1.57	-2.30	-2.14	**3.71**	-1.92	-5.81	-12.83	-0.75
WW-13A	-2.11	-2.56	-6.12	-2.42	-4.14	-3.29	**2.56**	-1.87	-6.86	-12.76	-2.69
WW-13B	-2.25	-0.60	-1.83	-0.45	-0.09	-4.71	**1.13**	-2.01	-7.52	-8.60	-1.25
WW-13C	-2.95	-0.97	-1.37	-0.82	-0.48	-3.53	**2.32**	-2.72	-7.59	-8.45	-0.96
WW-14	-2.05	-0.49	-1.12	-0.34	-0.21	-1.98	**3.87**	-1.81	-6.62	-7.52	-0.42
WW-17A	-2.21	-0.19	-1.60	-0.05	**0.76**	-3.75	**2.10**	-1.98	-7.83	-8.39	-1.18
WW-17B	-2.42	-2.28	-6.18	-2.13	-3.40	-3.36	**2.48**	-2.18	-7.03	-12.99	-2.27
WW-17C	-2.84	-0.56	-0.78	-0.41	**0.20**	-2.62	**3.24**	-2.60	-7.74	-7.72	-0.82
WW-17D	-1.94	-1.96	-6.55	-1.81	-3.61	-3.54	**2.31**	-1.70	-7.19	-12.50	-2.59
Downgradient Pea Gravel Zone Wells											
WW-10A	-1.57	-0.39	-2.37	-0.25	-0.47	**1.50**	**7.34**	-1.33	-7.97	-8.34	-2.18
WW-10B	-1.71	-1.45	-5.22	-1.30	-3.03	-6.39	-0.54	-1.47	-7.54	-10.74	-2.66
WW-10C	-1.64	-1.96	-6.23	-1.82	-4.04	-2.79	**3.05**	-1.41	-7.00	-11.77	-2.70
WW-10D	-1.63	-1.83	-5.86	-1.69	-3.71	-7.23	-1.37	-1.40	-7.61	-11.44	-3.16
WW-15	-1.98	-2.41	-6.66	-2.27	-4.68	-8.21	-2.35	-1.74	-7.77	-12.42	-3.56
WW-18A	-1.66	-0.77	-3.31	-0.62	-1.29	-4.53	**1.32**	-1.43	-6.67	-9.21	-1.15
WW-18B	-1.55	-0.07	-2.11	**0.08**	-0.45	-2.97	**2.88**	-1.31	-6.99	-7.43	-0.87
WW-18C	-1.95	**1.49**	**0.29**	**1.64**	**1.68**	-0.65	**5.21**	-1.72	-12.05	-4.03	-3.96
WW-18D	-1.43	**0.92**	-1.40	**1.06**	-1.15	-1.13	**4.73**	-1.19	-9.04	-4.05	-2.05
Downgradient A1 Aquifer Zone Wells											
WIC-3	-1.17	-0.31	-6.12	-0.16	-0.47	-2.81	**3.04**	-0.94	-6.83	-11.91	-1.33
WIC-9	-1.62	-0.87	-6.42	-0.72	-1.64	-3.99	**1.86**	-1.38	-7.84	-12.16	-2.46
WIC-10	-1.63	-1.02	-4.80	-0.88	-2.39	**0.68**	**6.53**	-1.40	-8.03	-10.11	-2.80
WIC-12	-1.26	-0.40	-5.90	-0.25	-0.68	-3.58	**2.28**	-1.02	-7.48	-11.64	-1.98
Downgradient A2 Aquifer Zone Well											
WIC-4	-1.27	-0.32	-5.92	-0.17	-0.54	-2.39	**3.45**	-1.03	-6.76	-11.67	-1.19

(a) Bold values are nonnegative, indicating saturation or oversaturation with respect to the referenced mineral phase.

Other hydroxides, brucite [$Mg(OH)_2$] and portlandite [$Ca(OH)_2$], are undersaturated throughout most of the permeable barrier. While brucite achieves saturation in a few wells, neither brucite nor portlandite seems to control equilibrium in any particular portion of the permeable barrier.

4.4.6 Evaluation of Core Samples

This section describes the analytical results from the core samples that were collected as described in Section 3. A detailed report on core sample evaluation was prepared by Battelle and submitted to NFESC (Battelle, 1998b). Cores were collected from the permeable barrier so the iron could be examined for signs of the corrosion and precipitation predicted by the groundwater analysis and geochemical modeling. Possible changes in the iron near the interfaces with the adjoining pea gravel sections were of particular interest. The upgradient interface is very important because this is where the most sudden change in chemical environments occurs. To examine these interfaces, vertical core samples of iron were taken as close as possible to the upgradient pea gravel (see Core No. 2 in Figure 3-26) and angled cores were taken in both upgradient and downgradient directions (see Core Nos. 5 and 7 in Figure 3-26). However, the actual interfaces between iron and pea gravel were not easily distinguished in the recovered core samples, due to clogging of the sampling system when pea gravel was encountered. Nevertheless, it is believed that core samples collected near the interfaces are as representative as possible of material present at those locations.

4.4.6.1 Bulk Chemical Analysis

Bulk chemical analysis involves digesting the iron in the core samples with an acid and analyzing the digestate for calcium and magnesium. Results of the bulk chemical analysis of the Moffett Field Barrier cores are shown in Table 4-12. The corresponding laboratory

Table 4-12. Results of Bulk Chemical Analysis

Core No.	Location[a]	Matrix	Sample Depth Interval (feet bgs)	Calcium Concentration (mg/kg)	Magnesium Concentration (mg/kg)
C-2	Upgradient iron	Iron	7 to 10	85	25
C-2	Upgradient iron	Iron	10 to 13	82	70
C-2	Upgradient iron	Iron	13 to 16	34	75
C-2	Upgradient iron	Iron	16 to 19	72	57
C-3	Upgradient iron	Iron	16 to 19	116	53
C-4	Downgradient iron	Iron	13 to 16	6.6	190
C-5	Mid-iron	Iron	10 to 13	5.7	250
C-5	Upgradient iron	Iron	16 to 19	63	37
C-6	Downgradient aquifer	Soil	16 to 19	930	1,260
C-7	Mid-iron	Iron	13 to 16	96	88
C-7	Downgradient iron	Iron	19 to 22	102	168
C-8	Upgradient iron	Iron	19 to 21.5	260	33
Unused Fe	Lab sample	Iron	NA	2.9	0.6

(a) See diagrams of core sample locations in Figures 3-26 and 3-27.

Measurements and raw analytical data are provided in Appendix C. The data in Table 4-12 show that calcium concentrations on the granular iron range from approximately 6 to 260 mg/kg of iron and magnesium concentrations range from approximately 25 to 250 mg/kg of the reactive cell iron. As a comparison, analysis of the unused iron showed that calcium and magnesium concentrations were much lower to start with (2.9 and 0.6 mg/kg, respectively).

These results suggest that calcium and magnesium compounds precipitated in the reactive cell as a result of 16 months exposure to the native groundwater. However, the concentrations are relatively small and therefore do not indicate that precipitation of carbonate and hydroxide compounds has occurred to a significant extent. Furthermore, the distribution of calcium and magnesium concentrations is not highly correlated with the locations where the samples were taken (see Figure 4-33). In general, calcium and magnesium concentrations increase somewhat along the direction of groundwater flow, suggesting that precipitated materials may be migrating downgradient, where they tend to accumulate. However, the concentrations of calcium and magnesium precipitates on the iron were relatively low at the time the core samples were collected. For example, in the following calculation a "worst case" result of 500 mg calcium per kilogram of iron was considered. Assuming that the calcium is indicative of aragonite (3.0 g/cm^3), the concentration of precipitate in the iron is 1.25 grams $CaCO_3$/kg iron. The porosity and bulk density of iron are about 0.6 and

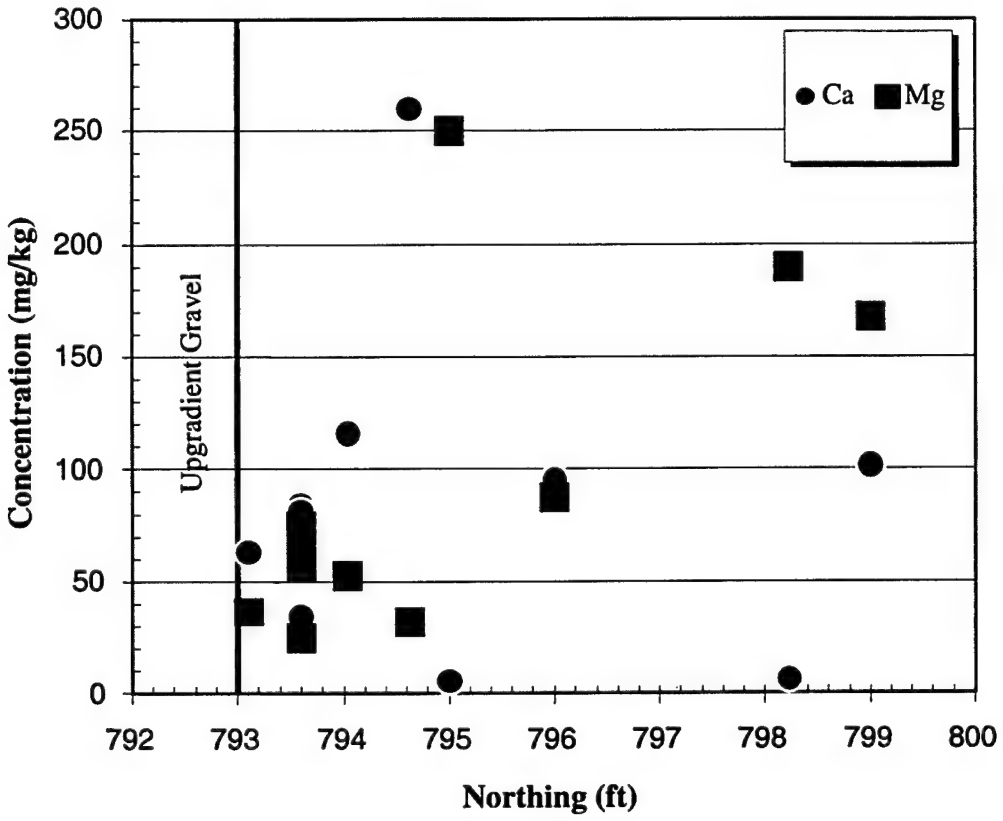

Figure 4-33. Concentrations of Ca and Mg Along Northing Direction

3 g/cm^3, respectively. By a calculation, the volume fraction of precipitate in the pore space is about 0.2%. This level is probably too low to significantly reduce porosity; percent level amounts of precipitate probably would be required to have a measurable impact. However, if the rate of precipitate buildup is constant (0.2% every 16 months), then the accumulation could reach 3% after 20 years. At this level of fouling, the effect on hydraulic conductivity could be measurable. Hydrologic modeling has shown that hydraulic conductivity of the reactive cell has to reduce by more than half (or the ratio of K_{cell}:$K_{aquifer}$ has to drop to about 5 from 10 initially) before any significant hydrologic change occurs (Gavaskar et al., 1998b).

It is useful to compare the measured level of precipitate formation to a calculation based on changes in groundwater chemistry. To estimate the potential for calcium carbonate buildup, one can consider the decline in calcium as water passes from the pea gravel into the reactive cell. Using values from Table 4-10, the concentration of calcium decreases from approximately 160 mg/L in the pea gravel to about 15 mg/L within the first 1 foot of the reactive cell. The change of 145 mg/L calcium is equivalent to 362 mg/L $CaCO_3$. Using a porosity factor of 0.6, 1 liter of water contacts 5.27 kg iron (density = 7.9 g/cm^3). Thus, with each pore volume of water passing through the iron, approximately 69 mg $CaCO_3$/kg iron precipitates. Calculations show that 96 pore volumes have passed through 1 foot of the reactive cell in 16 months (480 days) if the flowrate is assumed to be 0.2 foot/day. This would give a total calcium carbonate mass fraction of 6,600 mg/kg Fe (or 0.66% by mass of iron). If the flowrate were 2 feet/day instead of 0.2 foot/day, then the precipitate buildup would be 6.6% by mass of the iron. Both numbers are considerably higher than were measured in the core samples (Table 4-12). The corresponding volume fraction of precipitate in the pore space is 1.2% for 0.2 foot/day flow and 12% for 2 feet/day flow. Again, these calculations show there is a large disparity with the measured rate of precipitate formation. Because mineral matter does not seem to be accumulating in the iron, it is plausible that precipitates are migrating downgradient, possibly as colloidal-size material.

As a comparison, Table 4-12 also includes data for the aquifer sample, Core No. 6. The depth interval chosen for investigation (16 to 19 feet bgs) contained coarse sand, which is believed to be part of the sand channel that affords high permeability in the vicinity of the barrier. According to Table 4-12, calcium and magnesium concentrations in the aquifer sand are 930 and 1,260 mg/kg, respectively. Concentrations of calcium and magnesium are much higher in the aquifer than in the iron due to the abundance of native carbonate minerals that may include calcite, dolomite, and magnesite.

4.4.6.2 Raman Spectroscopy

Raman spectroscopy enables semiquantitative characterization of amorphous and crystalline deposits on the iron. This method is suitable for identifying iron oxides and hydroxides. Raman spectra were recorded at three different grain locations for each sample. Multiple locations were chosen because the material was found to be heterogeneous in appearance. For this reason, each spectrum was recorded separately rather than averaging them together.

In all of the iron samples the strongest Raman bands appeared near the 1,350 and 1,600 cm^{-1} (wavenumber) shift. These bands do not correspond with any iron oxide or carbonate species,

but are suspected to originate from reduced carbon. The 1,600 cm^{-1} shift corresponds to graphite-carbon and the 1,350 cm^{-1} shift corresponds to finely ground graphite. One explanation for the presence of carbon is that cutting oils used in grinding were baked onto the filings during processing. Carbonate, which would be identified by a sharp 1,080 cm^{-1} shift, was not observed, indicating that the carbonate content was below detection for these samples.

Results of Raman spectroscopy are shown in Table 4-13. The predominant iron species are α-Fe_2O_3 (hematite) and Fe_3O_4 (magnetite). These species were present in all samples, including the unused iron. There is some evidence for γ-FeOOH (lepidocrocite) in seven samples and $Fe(OH)_3$ (amorphous ferric hydroxide) in two samples, also including the unused iron. Thus, according to Raman spectroscopy, the differences in iron oxide content among these samples are relatively minor. Analysis of the spectra also shows a shoulder that could be due to marcasite (FeS_2).

Table 4-13. Results of Raman Spectra[(a)]

Core No.	Location	Sample Depth (feet)	α-Fe_2O_3 Hematite	Fe_3O_4 Magnetite	γ-FeOOH Lepidocrocite	$Fe(OH)_3$ Ferric Hydroxide
Unused Fe	NA	NA	S	S	W	W
C-2	Upgradient iron	7 to 10	S	S	W	–
	Upgradient iron	10 to 13	S	S	W	–
	Upgradient iron	13 to 16	S	S	W	W
	Upgradient iron	16 to 19	S	S	–	–
C-3	Downgradient iron	16 to 19	S	S	–	–
C-4	Mid-iron	13 to 16	S	S	W	–
C-5	Upgradient iron	10 to 13	S	S	–	–
	Downgradient iron	16 to 19	S	S	–	–
C-6	Mid-iron	16 to 19	–	–	–	–
C-7	Downgradient iron	13 to 16	S	S	W	–
	Upgradient iron	19 to 22	S	S	–	–
C-8	Upgradient iron	19 to 21.5	S	S	W	–

(a) S = strong line; W = weak line; – = not observed.

4.4.6.3 Scanning Electron Microscopy

SEM provides high-resolution visual and elemental characterization of amorphous and crystalline phases. This method is suitable for identifying precipitates. SEM results indicate that the surfaces of the iron particles are coated with iron oxides and that the abundance of these oxides is strong on all samples, including the unused iron. Figure 4-34 shows the surface of a typical grain of iron, which is coated with small particles of corrosion products. Figure 4-35 shows the surface of an iron particle under greater magnification (see scale bar on photograph). It can be seen that the particle's surface is comprised of small (<5 μm), irregular particles (possibly iron oxides) and filamentous material (possibly iron hydroxide). Based on these results, it would appear that the extent of corrosion on individual iron particles does not vary significantly with location in the Moffett Field permeable barrier.

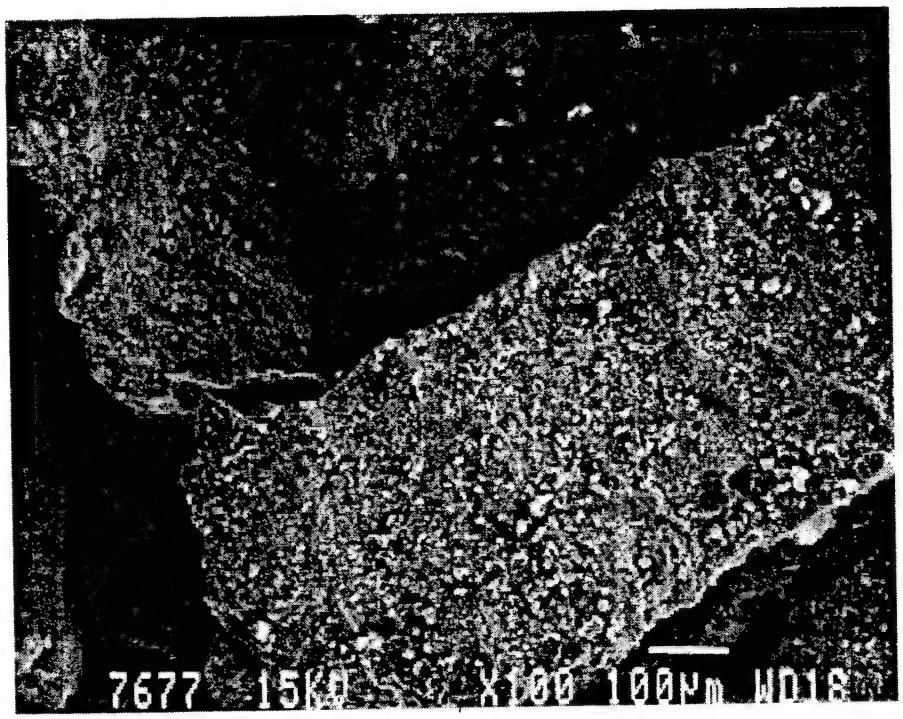

Figure 4-34. SEM Micrograph of Sample C-5 (16 to 19 feet) at 100X Magnification

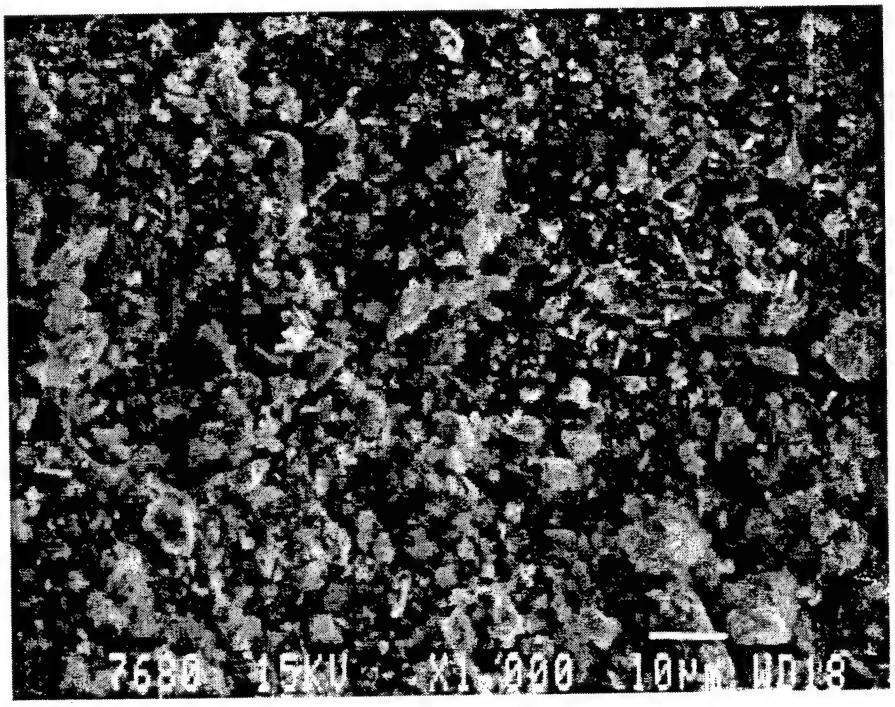

Figure 4-35. SEM Micrograph of Sample C-5 (16 to 19 feet) at 1,000X Magnification

4.4.6.4 Energy Dispersive Spectroscopy

As with SEM, EDS is helpful in identifying precipitates on the iron. Results of EDS measurements are given in Table 4-14. These data show in atom percent units the concentrations of various elements in the analysis beam. Because the EDS instrument was not calibrated to known standards, the results should be considered relative values, rather than absolute. For this reason, it is more useful to consider ratios instead of individual measurements. In Figure 4-36, the ratio of sulfur to oxygen (S/O) is shown at different spatial points in the permeable barrier. This plot indicates a higher proportion of sulfur in the upgradient iron samples than in the downgradient samples. Also, the S/O ratio of the downgradient samples is approximately the same as in the unused iron. This suggests that conversion of sulfate to sulfide and concomitant precipitation take place primarily in the upgradient portion of the reactive cell.

Table 4-14. Results of EDS Measurements

Core No.	Sample Depth (feet)	Concentration (atom percent)					
		Ca	Mg	Fe	S	O	S/O
C-2	7 to 10	0.5	0.9	61.6	2.3	29.1	0.080
	10 to 13	1.0	4.7	55.1	2.8	31.7	0.089
	13 to 16	0.9	3.4	50.2	2.2	32.6	0.068
	16 to 19	1.3	2.7	56.3	0.8	34.0	0.023
C-3	16 to 19	1.5	2.4	62.7	1.5	26.2	0.058
C-4	13 to 16	0.3	0.9	57.4	0.7	26.8	0.026
C-5	10 to 13	0.1	2.1	62.8	2.5	28.8	0.087
	16 to 19	1.1	2.4	56.0	3.4	29.3	0.117
C-6	16 to 19	2.0	2.2	6.3	< 0.1	48.0	<0.002
C-7	13 to 16	1.9	2.0	33.1	< 0.1	35.3	<0.003
	19 to 22	1.6	1.8	23.9	0.2	36.2	0.005
C-8	19 to 21.5	7.7	2.1	53.3	1.5	24.4	0.063
Unused Fe	NA	< 0.1	< 0.1	67.4	0.3	29.7	0.010

4.4.6.5 X-Ray Diffraction

XRD provides a qualitative determination of crystalline phases. It is suitable for identifying carbonates, magnetite, goethite, etc. XRD results indicated that the crystalline material contained in the corrosion coatings on the iron is composed principally of magnetite and contains minor amounts of hematite (α–Fe_2O_3) or maghemite (γ–Fe_2O_3). Samples from the reactive cell also contain minor amounts of aragonite ($CaCO_3$) and marcasite (FeS_2). Based on these results, it would appear that the nature of the corrosion process does not vary significantly with location in the Moffett Field reactive cell. Also, detection of marcasite shows agreement with the Raman analysis and is consistent with sulfur detection by EDS. However, detection of aragonite is inconsistent with Raman results.

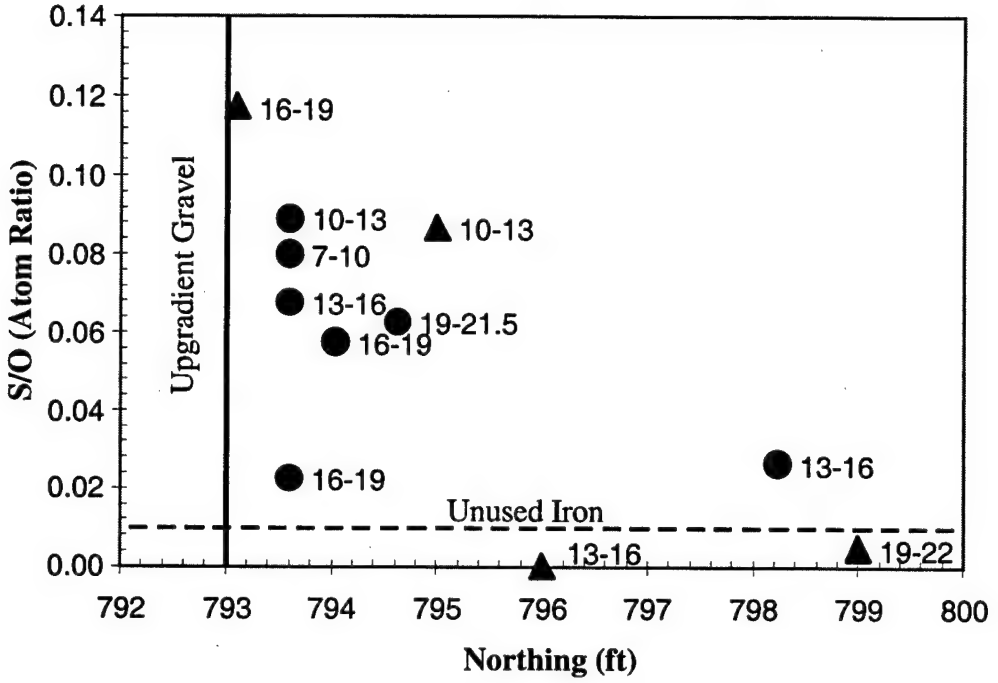

Figure 4-36. Plot of S/O Along the Northing Direction of the Reactive Cell. Circles indicate vertical borings and triangles indicate angled borings.

4.4.6.6 Microbiological Analysis

The microbiological results indicate that none of the three iron core samples (C-3, C-4, and C-7) showed measurable CFUs after 48 hours of incubation. Only one type of colony was detected in the downgradient aquifer core sample (C-6). The match to any known species of microorganism was not certain, but the analytical laboratory that performed the analysis (Microbe Inotech Laboratories, St. Louis, Missouri) identified two possibilities: *Staphylococcus warneri* (an anaerobic microorganism) and *Staphylococcus cohnii* (a facultative anaerobic microorganism). The amount of growth in C-6 was not very large; 50,000 CFU/g after 48 hours. The implications of the biological results are unclear because the comparative samples of the upgradient aquifer needed to put these numbers in perspective could not be collected due to time and resource constraints.

4.4.7 Summary of Geochemical Evaluation

- Groundwater near the Moffett Field permeable barrier is moderately high in dissolved solids; TDS is estimated at approximately 1,000 mg/L, based on a summation of ionic concentrations and on direct measurements (see Appendix H). A high level of TDS is perhaps the most important factor affecting the longevity of the permeable barrier, because of the potential impact on mineral precipitation and subsequent impact on hydraulic conductivity.

- Field parameters indicate that electrochemical conditions in the reactive cell are favorable for abiotic reduction. DO is effectively scrubbed from the groundwater quickly after it enters the reactive cell. Low Eh readings indicate that the environment within

the reactive cell is highly reducing and, therefore, conducive to reductive dehalogenation of CVOCs. The pH within the reactive cell increased to approximately 11, at which level it is not expected to induce passivation of iron surfaces and loss of reactivity.

- Charge balance calculations performed on the inorganic chemical data show good data quality. This indicates that sampling and analysis for major ions was performed appropriately and that no major ions have been neglected in the analysis protocol.

- Iron concentrations in the reactive cell tend to be indistinguishable from samples taken elsewhere in the permeable barrier and surrounding aquifer. This indicates that the permeable barrier does not promote excessive levels of dissolved iron in the downgradient aquifer. Thus, the barrier does not adversely affect water quality in regard to dissolved iron content. Iron concentrations in the reactive cell were below the 0.3 mg/L secondary drinking water standard.

- Groundwater concentrations of inorganic parameters change as the groundwater flows through the reactive cell. Calcium and sulfate sharply decrease in the upgradient end of the reactive cell. Magnesium and alkalinity decrease gradually through the reactive cell. These changes in groundwater chemistry are believed to be caused by precipitation of aragonite (calcium carbonate), magnesite (magnesium carbonate), and siderite (iron carbonate). Geochemical modeling shows that formation of siderite is the most important precipitation reaction for controlling the concentration of dissolved (ferrous) iron in the reactive cell. Because sulfate minerals are unstable under the geochemical conditions present within the barrier, a probable explanation for the loss of sulfate is abiotic reduction and subsequent precipitation as an iron sulfide compound.

- Acid digestion of core samples revealed increased levels of calcium and magnesium, compared to unused granular iron. The presence of aragonite (calcium carbonate) was confirmed by XRD analysis. However, the amount of carbonate present in the samples was far less than predicted, based on geochemical modeling. The discrepancy suggests that the majority of the material precipitated does not remain in the pore spaces of the reactive cell. Rather, colloidal-size carbonate precipitates may be flushed through the barrier with the flow or settle within it. In either case, not enough carbonate appears to have precipitated out to have had a major effect on the porosity and permeability of the barrier. Although the hydraulic efficiency of the barrier may be maintained over the long term, it is not clear how or when its reactivity will be affected significantly enough to decrease the degradation rate of CVOCs in the groundwater.

- Sulfide minerals on iron surfaces were investigated using Raman spectroscopy and SEM with EDS. Results indicate that sulfide precipitate levels are elevated in the upgradient portion of the iron. This indicates that sulfides have a tendency to remain attached to granular iron surfaces. Thus, sulfide precipitation could have important consequences on the long-term reactivity and/or hydraulic performance of the permeable barrier.

- Corrosion compounds on granular iron surfaces were investigated using Raman spectroscopy and SEM with EDS. The predominant iron species were found to be α-Fe_2O_3 (hematite) and Fe_3O_4 (magnetite). These species were present in all samples, including the unused iron. Therefore, it was concluded that differences in iron oxide composition among all the samples analyzed were relatively small. There was some evidence for γ-FeOOH (lepidocrocite) in seven samples and $Fe(OH)_3$ (amorphous ferric hydroxide) in two samples, including the unused iron.

4.5 Data Quality Assessment

Sampling and analysis were conducted under the quality assurance (QA) procedures described in the Performance Monitoring Plan (Battelle, 1997a). Appendix F contains the QA data related to the evaluation of the Moffett Field permeable barrier.

4.5.1 Completeness

Between 90 and 100% valid measurements were obtained in all five sampling events for all organic and inorganic analytes. This completeness indicator exceeded the 90% amount specified in the Performance Monitoring Plan (Battelle 1997a). In addition, greater than 5% field duplicates, equipment rinsate blanks, and trip blanks (one per cooler) were collected during each sampling event.

4.5.2 Field Sample Collection and Analysis

Field QA consisted of trip blanks, equipment rinsate blanks, and field duplicates. The results of the analysis of field QA samples are described in this section.

4.5.2.1 Trip Blanks

Four trip blanks were processed during the June 1996 sampling event and were analyzed for the same volatile organic analytes as the associated investigative samples. Results presented in Table F-1a show that none of the trip blanks were found to have detectable concentrations of the target analytes. Similarly, no contaminants were detected in any of the trip blanks for subsequent sampling events, including four trip blanks that were collected in September 1996 (Table F-2a), six trip blanks that were collected in January 1997 (Table F-3a), seven trip blanks that were collected in April 1997 (Table F-4a), and five trip blanks that were collected in October 1997 (Table F-5a). These results demonstrate that sample containers provided an effective barrier during shipment against transfer of contamination that might have led to invalidation of the investigative samples.

4.5.2.2 Equipment Rinsate Blanks

Two equipment rinsate blanks were collected during the June sampling event and were analyzed for the same volatile organic analytes as the associated investigative samples. Four organic compounds were detected in rinsate blank WW-102, including 240 µg/L TCE, as shown in Table F-1b in Appendix F. Chloroform was detected in WW-101 at 61 µg/L, which is much higher than was found in any investigative sample. Results of these two rinsate blanks prompted a review of decontamination procedures that led to improvements in subsequent sampling events.

Six equipment rinsate blanks were collected during the September 1996 sampling event. Results given in Table F-2b (in Appendix F) show that VOC concentrations were lower than laboratory detection limits in five of these blanks, while measurable levels of TCE (74 µg/L), PCE (2 µg/L), and *cis*-1,2-DCE (2 µg/L) were found in one equipment rinsate blank. These results demonstrate that, in general, decontamination procedures between collection of different samples were adequate. The one case where VOCs were detected (WW-102) followed sample collection at WW-7D, where groundwater concentrations were at their highest levels inside the permeable barrier.

Results of five equipment rinsate blanks for the January 1997 sampling event are given in Table F-3b (in Appendix F). In all but five analyses the results were below detection. In WW-101 (equipment blank following collection of WW-18C) TCE was detected at 9 µg/L, *cis*-1,2-DCE was detected at 3 µg/L, and chloroform was detected at 5 µg/L. Chloroform was detected in two other equipment blanks; however, because chloroform was not present in the investigative samples, its occurrence in the equipment blanks does not have much significance.

Eight equipment rinsate blanks were collected during the April 1997 sampling event. Results are given in Table F-4b (in Appendix F). In three of the rinsate blanks TCE concentrations were above detection. In WW-103 (equipment blank following collection of WW-2) TCE was detected at 41 µg/L; in WW-107 (equipment blank following collection of WW-13D) TCE was detected at 3 µg/L; and in WW-108 (equipment blank following collection of WIC-8) TCE was detected at 10 µg/L. No other contaminants of significance were noted. Overall, these results indicate that equipment decontamination procedures were adequate during the April 1997 sampling event.

Results of five equipment rinsate blanks are given for October 1997 in Table F-5b (in Appendix F). In two of the rinsate blanks TCE concentrations were above detection. In WW-101 (equipment blank following collection of WW-16A) TCE was detected at 11 µg/L; in WW-102 (equipment blank following collection of WIC-10) TCE was detected at 16 µg/L. No other contaminants of significance were noted.

4.5.2.3 Field Duplicates

In June 1996, duplicate groundwater samples were collected from three wells by means of a bailer (WW-2, -11, and –12) and one sample was collected using a dedicated down-hole pump (W9-35). Primary samples were collected by the standard (peristaltic pump) procedure. Results are shown in Table F-1c (in Appendix F). In general, results of analyses based on alternative collection procedures compared favorably with those collected by the standard procedure. However, analytical data for WW-11 show significantly higher concentrations of VOCs in the bailer-collected sample. The reason for the difference between the pumped sample and bailer sample may have had to do with depth of collection.

Six field duplicates were collected during the September 1996 sampling event and were analyzed for the same volatile organic analytes as the associated investigative samples. Results, shown in

Table F-2c, show that reproducibility is high in cases where statistical calculations can be made. In other cases, concentrations were close to detection limits or the analyte was not analyzed in the replicate sample, so no conclusion can be made about reproducibility. Table F-2c contains results of duplicate analyses from a uni-level well (WIC-1) and one level of a cluster well (WW-7D). Relative percent difference (RPD) calculations are within ±25% for TCE, PCE, and *cis*-1,2-DCE. RPD is greatest for TCE, where it was noted that the amounts reported exceeded the linear range of instrument calibration (see Appendix F). The RPD is smaller for PCE and *cis*-1,2-DCE, where the amounts detected are within the linear range of instrument calibration.

Results of six field duplicates are given in Table F-3c for January 1997. RPDs are less than or equal to 15% for TCE and *cis*-1,2-DCE. RPDs could not be calculated for most other analytes due to detection limitations.

Results of seven field duplicates are given in Table F-4c for April 1997. In two samples, WW-2 and WIC-8, duplicate TCE measurements were in apparent poor agreement with those of the primary samples. However, the representativeness of the duplicate for WW-2 (WW-99-2) is in doubt due to the reported high level of methylene chloride in the duplicate and its presence in the associated laboratory blank. It also appears that high detection limits were the major cause of poor reproducibility in a few cases. These results suggest that field duplicates were sufficiently representative, in general.

Results of six field duplicates are given in Table F-5c for October 1997. Only in three samples were concentrations sufficiently above detection limits to make valid assessments of the duplicate measurements. In WW-10C the RPD for two TCE measurements was 0%. In WW-8D the RPD for two *cis*-1,2-DCE measurements was 28%. In WIC-8 RPDs for 1,1-DCA, 1,1-DCE, *cis*-1,2-DCE, PCE, and TCE were 19%, 19%, 52%, 13%, and 7%, respectively. Overall, the results of the field duplicate measurements indicate that samples were collected in such a manner that the samples are representative of the site groundwater and that the data are reproducible.

4.5.3 Laboratory Sample Analysis

Accuracy for VOCs and inorganic analytes was determined by matrix spike (MS) recovery. Precision for VOCs and inorganic analytes was to be determined by duplicate (MSD) analysis. Matrix spikes were analyzed with a minimum frequency of 5% (one for each batch of 20 samples). Laboratory QC was evaluated by means of method blanks.

4.5.3.1 Laboratory Accuracy and Precision

Results of the surrogate recovery test for June 1996 are provided in Table F-1d (in Appendix F). Four surrogate spikes were used: dibromofluoromethane (DBFM), 1,2-DCA, toluene-d8, and 4-bromofluorobenzene (4-BFM). Laboratory QC limits are 86 to 118%, 80 to 120%, 88 to 110%, and 86 to 115%, respectively. Out of 516 determinations (129 samples), 53 (10%) were outside QC limits for accuracy.

Results of MS/MSD tests for June 1996 are also included in Table F-1d. Seven MS/MSD pairs were analyzed. Results summarized show that laboratory QC limits for precision were within acceptable bounds.

Results of MS/MSD analysis for October 1997 are shown in Table F-5d. RPDs that are outside of QC limits (± 25%) are flagged. Among the target analytes, the RPD for *cis*-1,2-DCE exceeded the QC limit for one sample (WW-3). Matrix spike recoveries were mostly within the targeted range of 75% to 125%, as shown in Table F-5e. One of the matrix spike recoveries (*cis*-1,2-DCE for WW-3) was significantly higher than targeted. Over-recovery of *cis*-1,2-DCE indicates a problem with instrument calibration or a standard being out of specifications on the day the analysis was done. No such problems exist for sample WW-1D for any of the target or other chlorinated compounds.

4.5.3.2 Laboratory Quality Control Checks

Results of method blanks for June 1996 are included in Table F-1e (in Appendix F). No hits above the laboratory detection limits were reported for 15 sets of method blanks. Results of method blanks for October 1997 are shown in Table F-5f. No hits above the laboratory detection limits were reported for 18 sets of method blanks.

4.6 Significant Deviations from Performance Monitoring Plan

There were no significant deviations from the general methodology outlined in the Performance Monitoring Plan (Battelle, 1997a) for the Moffett Field pilot barrier demonstration.

4.7 Comparison to Technology Claims

In general, as demonstrated in Table 4-15, the performance of the pilot barrier at Moffett Field was able to meet the claims made for the technology.

4.8 Overall Conclusions

In general, the barrier performance was within the expectations of the technology and the design for this site. Although the precipitation caused by inorganic reactions in the reactive cell is a long-term concern, there was no evidence that the hydraulic performance of the barrier would be affected in the next several years. It is unclear when the precipitation may cause the reactivity of the iron medium to decline, but there were no signs during the 20-month period of the demonstration that such a decline had begun.

Specific conclusions from the demonstration regarding the performance of the pilot permeable barrier at Moffett Field are listed below.

Table 4-15. Verification of Technology Claims

Evaluation Criteria	Technology Claim	Observed Performance During Moffett Field Demonstration
Contaminant degradation	Reduces dissolved CVOCs to their MCLs	TCE, PCE, *cis*-1,2-DCE, and vinyl chloride reduced to MCLs
	Hydrogenolysis and beta-elimination are the reaction pathways, with beta-elimination being dominant	Byproducts of hydrogenolysis (*cis*-1,2-DCE and vinyl chloride) were identified but in minimal quantities. Ethene and ethane, the products of both mechanisms, were identified.
	Half-lives based on bench-scale predictions for TCE, *cis*-1,2-DCE, and 1,1-DCA were 0.4, 1.4, and 4.3 hours, respectively	Half-life ranges of TCE (0.1 to 1.0 hour), *cis*-1,2-DCE (0.2 to 2.5 hours), and 1,1-DCA (0.6 to 9.4 hours) include predicted values.
Downgradient water quality	Barrier does not contribute significantly to dissolved iron levels in the effluent groundwater. Iron levels preferably below 0.3 mg/L.	No significant changes in dissolved iron concentrations as the groundwater flows through the reactive cell. Iron levels below 0.3 mg/L.
Hydraulic performance	Barrier captures the targeted volume of groundwater	Barrier captured a 30-foot-wide volume of groundwater encompassing the sand channel and part of the interchannel deposits.
	Barrier provides sufficient residence time for CVOC degradation to MCLs. Residence time requirement of 2 days (including safety factors) based on bench-scale tests.	Taking into account the limitations of field methods and complexity of flow system, estimates indicate a minimum of 3 days residence time was achieved.
	Seasonal variations in groundwater flow volume and/or direction can be handled	Seasonal variations did not cause any flow problems at this site. Appropriate safety factors should be applied in the design to account for such variations.
Geochemical performance	Level of precipitation on iron surfaces caused by inorganic reactions is not high enough to affect reactivity and hydraulic performance of the barrier over the next several years.	Level of precipitation appears to be relatively low. No indication that hydraulic performance will be affected over the next several years. It is unclear when reactivity may start being affected.
	Native alkalinity controls pH and keeps it from rising too high	The pH in the reactive cell was generally below 11, which is an expected outcome.
Personnel/ training	General construction training and HAZWOPER	General construction training and HAZWOPER
Health and safety	Level D personal protective equipment (PPE) Hearing protection during sheet pile driving	Level D PPE Hearing protection during sheet pile driving
Ease of operation	Operation restricted to quarterly or annual monitoring Maintenance not required for several years	Operation restricted to quarterly or annual monitoring No indication that maintenance will be required in the next several years.
Limitations	Some CVOCs may have relatively long half-lives, thus requiring higher reactive cell thickness	1,1-DCA has a relatively long half-life, but because it is not regulated at this site, reactive cell thickness was not an issue.

4.8.1 Reactivity Performance

The following conclusions were drawn about the reactivity performance of the pilot permeable reactive barrier:

- Strongly reducing (low Eh) conditions conducive to abiotic reduction of CVOCs were generated in the reactive cell by the iron medium.

- Concentrations of dissolved TCE, PCE, *cis*-1,2-DCE, and vinyl chloride (which may have formed in the reactive cell as a byproduct of higher-chlorinated species) were abiotically reduced in the reactive cell to well below their respective MCLs.

- Other CVOCs, such as 1,1-DCA and CFC-113, were also significantly reduced by the iron medium.

- *cis*-1,2-DCE and vinyl chloride, the byproducts from the hydrogenolysis pathway of TCE and PCE degradation, were present in the reactive cell at minimal levels. This indicated that TCE and PCE were being reduced to ethene and ethane mostly through another pathway. Beta-elimination, an alternative pathway (Roberts et al., 1996) that generates ethene and ethane without forming *cis*-1,2-DCE and vinyl chloride, appears to be the dominant pathway. This is fortunate for the technology because *cis*-1,2-DCE and vinyl chloride have longer half-lives (and are therefore harder to degrade) than the short-lived intermediates (such as acetylene) formed by beta-elimination.

4.8.2 Downgradient Groundwater Quality

The following conclusions were drawn about water quality downgradient of the pilot permeable reactive barrier:

- Organic byproducts, primarily ethene and ethane, were found to be present in low concentrations (typically less than 1 mg/L) in the reactive cell. The presence of these dissolved gases does not adversely affect downgradient groundwater quality because they are benign at such low levels and should be quickly degraded in the aquifer.

- The concentrations of dissolved iron did not increase as groundwater flowed through the reactive cell. The potential for an increase in the level of dissolved iron in the downgradient water was a minor concern because iron is subject to a secondary drinking water standard of 0.3 mg/L. In the five quarterly monitoring events, dissolved iron levels in the water exiting the reactive cell were below 0.3 mg/L.

- Other inorganic parameters in the groundwater that underwent a change in the reactive cell included DO (decreased), pH (increased), and Eh (decreased). However, these parameters started rebounding to their original values as the water flowed into the downgradient pea gravel and into the downgradient aquifer. This rebound was due to mixing of treated water exiting the reactive cell and untreated water flowing around or under the pilot barrier. Similarly, in a full-scale barrier that targets the entire plume, it is expected that the groundwater flowing around the barrier will be uncontaminated (i.e., not part of the plume) and will help restore the geochemical character of the treated water within a short distance downgradient of the barrier. At Moffett Field, mixing of treated and untreated groundwater appeared to be taking place immmediately downgradient of the barrier, and to some extent in the downgradient pea gravel itself.

4.8.3 Hydraulic Performance

The following conclusions were drawn about the hydraulic performance of the pilot permeable barrier:

- The barrier captured groundwater from an estimated 30-foot-wide region of the upgradient aquifer. This encompasses most of the sand channel and a portion of the interchannel deposits. The capture zone met the design expectations based on the groundwater flow model and site characterization.

- Both gate and funnel contributed to the groundwater capture. A viable configuration for a full-scale barrier at Moffett Field would be a combination of multiple gates placed in high-conductivity sand channels and funnels placed in the surrounding low-conductivity interchannel deposits.

- Seasonal variations in flow magnitude and direction did not significantly affect the capture zone at this site, probably because most of the water still flowed through the sand channel. Although water levels rose or fell seasonally, the barrier did not exhibit flow over the barrier, as was encountered at another site. This indicates that the height of the gate was sufficient to handle seasonal high-water table conditions. Flow under the pilot barrier was an anticipated problem because the barrier was not keyed into the aquitard.

- Water level, velocity meter, and tracer test measurements gave somewhat differing estimates of groundwater velocity (and residence time), but all estimates were within an order of magnitude. The estimated groundwater velocity range of 0.2 to 2 feet/day provides a minimum residence time of 3 days in the reactive cell; the design requirement was projected to be 2 days.

- The relatively wide range of velocity estimates reflects the limitations of the monitoring methods as well as the extremely heterogeneous nature of the aquifer sediments. The water level measurements agreed most closely with the design model predictions (which were based on heterogeneities modeled on the basis of fairly detailed site chararacterization), although considerable care was required to collect and interpret very small differences in water levels over the small region affected by the barrier. Velocities estimated with the tracer test were below the model predictions. This may indicate either that flow is indeed slower than expected, or that the single injection tracer test in the gate was limited in its ability to account for all the complexities of flow (such as heterogenously distributed flow input to the gate, mixing in the pea gravel, and differential compaction of iron).

- The down-hole velocity meter estimates had the widest range and there is some uncertainty about these measurements, especially with respect to measurements in the lower part of the range. Also, the variability in the velocity vector for readings taken

in the same well may indicate that these meters are reading very localized (pore level) flows, rather than the bulk flow through the medium.

4.8.4 Long-Term Implications of Geochemical Interactions

- Native groundwater parameters, such as DO, alkalinity, calcium, and magnesium, contribute to precipitation in the reactive cell. Some fraction of these precipitates deposit on the iron surfaces, as evidenced by the minerals found on the core samples of the iron from the reactive cell after about 1.5 years of operation.

- The amount of precipitates deposited on the iron did not appear to be high enough to indicate that the hydraulic performance of the barrier would be affected in the next several years, assuming that the hydraulic conductivity of the reactive cell would have to decline by a factor of 2 before any adverse effects become noticeable.

- It is harder to predict how this precipitation will affect the reactivity of the medium. Although the precipitates formed in the 1.5 years of study occupy a small enough proportion of the pore volume in the reactive cell that the hydraulic properties are not significantly affected, coating of reactive sites could inhibit reactivity. However, there was no indication during this demonstration of any approaching decline in the barrier's reactivity performance.

5. Cost Assessment

This section discusses the cost considerations involved in the application of the permeable barrier technology.

5.1 Summary of Treatment Costs for the Demonstration

The groundwater treatment and monitoring costs incurred during the demonstration are shown in Table 5-1. Only the costs associated with the treatment of the groundwater are included; costs associated with the entire validation effort are not included. The cost of purchasing the iron medium ($39,375) and the construction cost ($323,000) were based on actual vendor bids. The other costs were based on the best available estimates. Spoils generated during trenching were reused at another site at Moffett Field because they were found to be mostly uncontaminated.

Table 5-1. Groundwater Treatment and Monitoring Costs for the Demonstration

Item	Sub-Total ($)	Total Cost ($)
Capital Cost Items		
Site characterization		100,000
Bench-scale tests		75,000
Engineering design, modeling, and planning		100,000
Iron Medium		39,375
—75 tons @ $450/ton	33,750	
—Transportation to site (75 tons @ $75/ton)	5,625	
Construction of Barrier		323,000
—Site preparation/restoration	133,000	
—Sheet pile funnel	60,000	
—Trench gate (with backhoe)	100,000	
—Monitoring wells within gate	30,000	
Monitoring wells in the aquifer vicinity (10 wells @ $1,500/well)		15,000
Disposal of trench spoils (as nonhazardous waste)		0
Total Capital Cost		**652,375**
Annual O&M Cost Items		
Maintenance (over the 20 months of operation)		0
Monitoring (five full events @ $30K each)		150,000
Total O&M Cost		**150,000**
Total Demonstration Cost		**802,375**

The primary advantage of the permeable barrier is immediately apparent. Once installed, there are no O&M costs involved (other than monitoring), at least in the first few (or several) years of operation. At some point in time, it is anticipated that there will be maintenance costs for regenerating the iron reactive medium.

Because this was a demonstration, the technology licensing fee was waived by ETI, the license-holder for in-situ use of zero-valent iron. For full-scale implementation, licensing costs are largely unknown at this time. However, a licensing fee of up to 12% of materials (iron) and construction costs may be imposed, depending on the outcome of contract negotiations.

5.2 Scale-Up Recommendations

The conclusions from the Moffett Field demonstration (Section 4.8) and the performance observations and lessons learned (Section 6.2) were used as the basis for examining the viability of a full-scale barrier for the West Side Plume at Moffett Field. Unlike an aboveground treatment system, where scaling up involves increasing the size of the equipment to handle larger volumes of feed, an in-situ treatment system has to be scaled up by taking into account the subsurface characteristics of the aquifer region that will be affected. This is especially true if, as has been proposed at Moffett Field by site representatives, the probable full-scale system will be installed at locations different from the location of the pilot barrier. The need for a different location for the full-scale system derives from differences in the objectives of the pilot- and full-scale reactive barriers. For the pilot system, it was important to be within the plume so that the barrier would have immediate access to the contaminants. Aside from that consideration, the location of the pilot barrier was determined primarily by considerations of ease of access and maximization of benefits from limited resources. If, on the other hand, the objective of the full-scale system is to prevent the plume from migrating any further, the barrier will have to be placed downgradient of the leading edge of the plume.

The Navy currently is negotiating the areas of responsibility for cleanup of the regional plume. This will have a major effect on the actual placement of the permeable wall. The wall locations chosen for this exercise are for costing purposes only. One possible scenario is schematically depicted in Figure 5-1 and is discussed further in Section 5.2.2. Considerable study of the aboveground features of the site (buildings, roads, etc,), subsurface features (utilities, exact location of sand channels, etc.), contaminants distribution, and groundwater movement is required to select an optimal scenario. Of these site features, probably the most important scale-up consideration at Moffett Field is the exact location, extent, and flow characteristics of the various sand channels interspersed through the plume region. The location, configuration, and dimensions of the full-scale barrier would be determined primarily by the vertical and horizontal extent of each sand channel in the plume region, the distribution of contaminants in the various channels, and the groundwater flow velocities in the channels.

If the full-scale barrier is to extend into the A2 aquifer zone as well as the A1 aquifer zone, then the effect of the A1/A2 aquitard on the flow system will have to be modeled. Because the pilot barrier extended only into the A1 aquifer zone, further site characterization and modeling are needed to assess the impact of the A1/A2 aquitard on the flow system and the hydrologic characteristics of the A2 aquifer zone.

5.2.1 Design of a Full-Scale Barrier at Moffett Field

Figure 5-2 (also presented in Section 2.4) shows the methodology recommended for permeable barrier design (Gavaskar et al., 1998a). The bench-scale column testing and geochemical evaluation conducted during the pilot barrier design should be sufficient, and these two steps need not be repeated. But the remaining steps will have to be implemented to design the full-scale application.

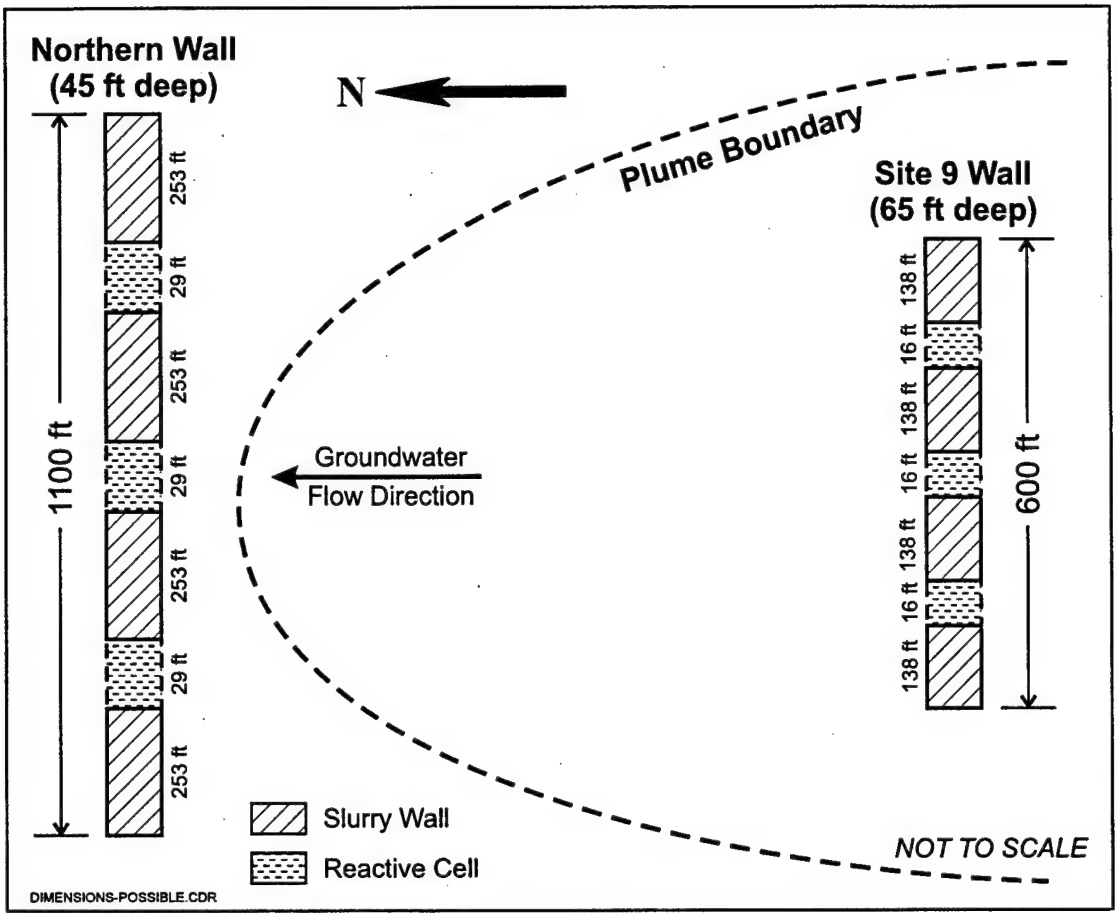

Figure 5-1. Configuration and Dimensions of Possible Full-Scale Barrier at Moffett Field

5.2.1.1 Additional Site Characterization

As mentioned earlier, the most important feature of the Moffett Field site affecting the full-scale barrier design are the sand channels present in the plume region. These channels carry most of the contamination and will have to be characterized well. Existing site maps showing the sand channels (Figures G-1 to G-4 in Appendix G) cover a wide region. A sand channel map for the shallow regions of the West Side Plume is shown in Figure 5-3 as an example. The dashed-line boundaries of the channels indicate extrapolation in the absence of sufficient data. In addition, the distribution of the channels varies by depth, as evidenced by the fact that the four maps in Appendix G (representing different depth profiles) do not match. For the more localized setting of the permeable barrier, more resolution of these channels at prospective barrier locations is needed.

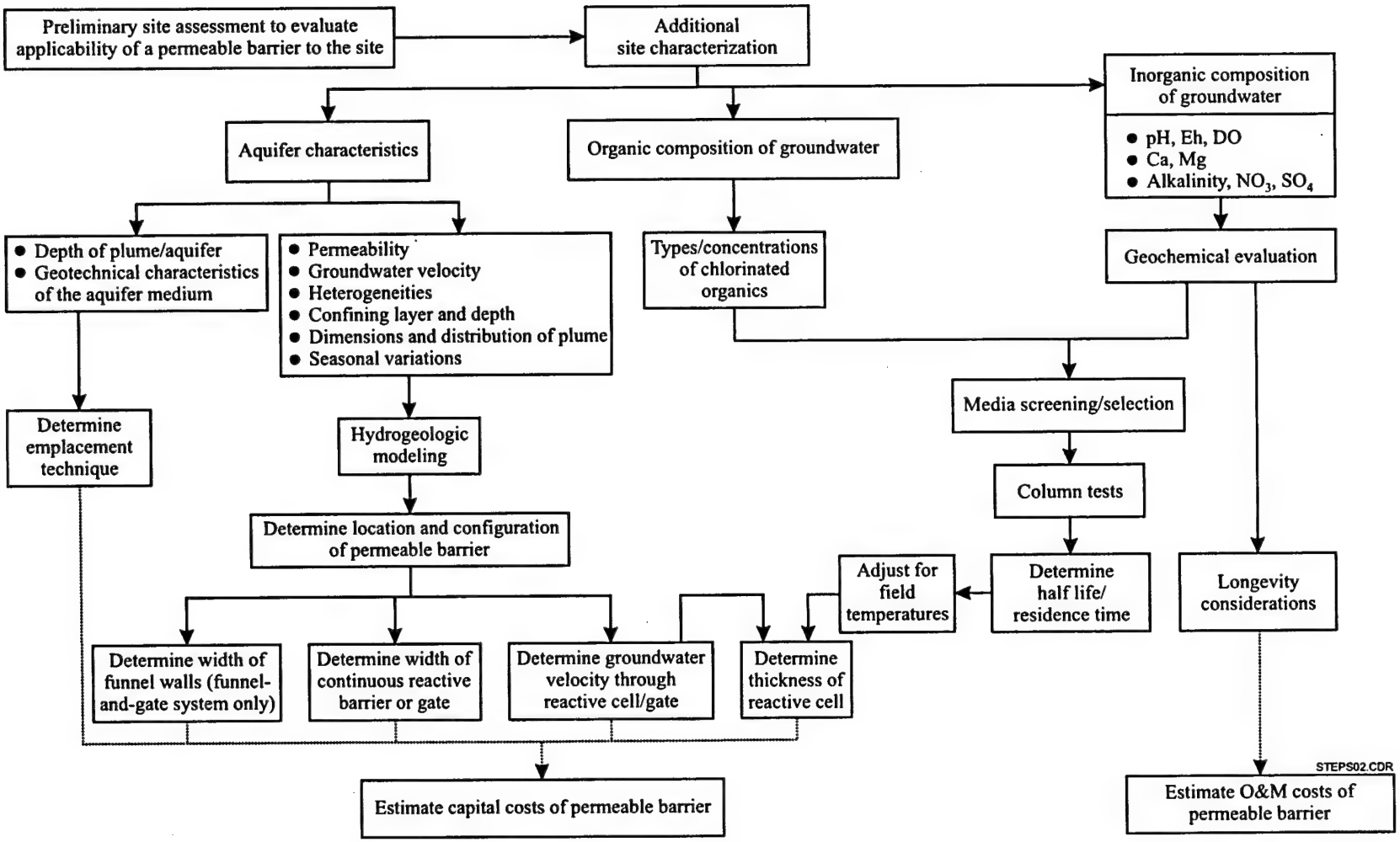

Figure 5-2. Design Methodology

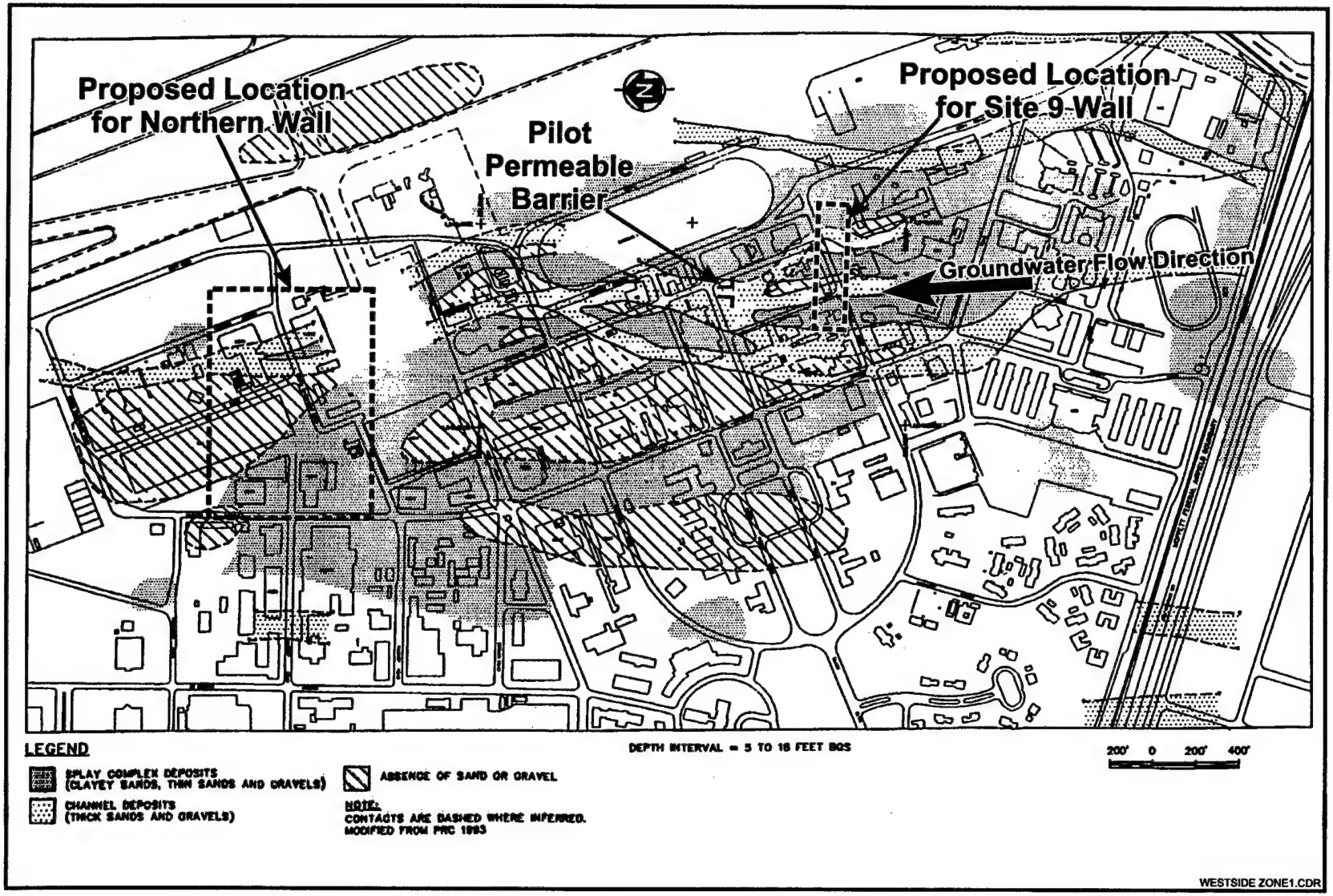

Figure 5-3. Example Map of Sand Channels at Moffett Field (Source: NFESC, 1998)

To avoid having to characterize large regions of the subsurface covered by the plume, the following procedure is recommended:

- Based on the regional plume maps (Figure 5-4 a and b), identify prospective locations for the full-scale barrier. If the objective is to capture the more contaminated portions of the plume, the barrier would probably be located within the plume in the more upgradient portion. This location would make sense if it is judged that treatment of the highly contaminated portion of the plume would allow the rest of the plume to attenuate naturally. If the objective is to prevent further migration of the plume, the barrier could be placed on the downgradient edge of the plume. These determinations should be made based on the most current plume map available, because the plume could have redistributed since the 1993 plume maps in Figure 5-4.

- Once prospective locations have been identified on the basis of contaminant distribution, it may be possible to narrow the search down to one or two locations based on geotechnical considerations. If some of the prospective locations are overlain by buildings or underlain by utilities, such locations could be ranked lower. Utilities can sometimes be cut and reconnected after installation of the barrier, but buildings or roads that need to stay open during construction may pose a greater challenge.

- Once the search is narrowed down to one or two locations, these locations could be characterized in more detail. An efficient way of characterizing such locations would be to trace a line on the surface for the proposed barrier orientation, making sure to avoid, as much as possible, any aboveground obstacles or underground utilities. A cone penetrometer test (CPT) rig or GeoProbe™ can be used to perform multilevel characterization along this line and along a few more cross sections parallel to it on either side. In addition to characterizing the hydrogeology, temporary wells can be placed by these techniques and the groundwater sampled to further delineate the concentrations of the contaminants at that location. Other techniques discussed in Section 3, such as slug tests or water levels, could be used to evaluate the flow system and determine the groundwater velocity range at this location.

5.2.1.2 Configuration and Dimensions of the Barrier

Based on the bench-scale and field half-lives described in Section 4.3, and the groundwater velocity range determined at the prospective location, the residence time requirement and reactive cell thickness can be determined.

Hydrogeologic modeling should then be conducted to determine the width of the reactive cell (or gate) and an optimum configuration of gates and funnel and orientation. Because of interbraided high and low conductivity deposits at the site, a funnel-and-gate system with multiple gates may turn out to be a good configuration scenario. The gates capture the bulk of the contamination in the sand channels while the funnel walls divert additional flow from the low-conductivity interchannel deposits toward the gates. Once an initial flow model is set up, multiple scenarios can be modeled. The pea gravel sections of the gate can be eliminated for the full-scale barrier as

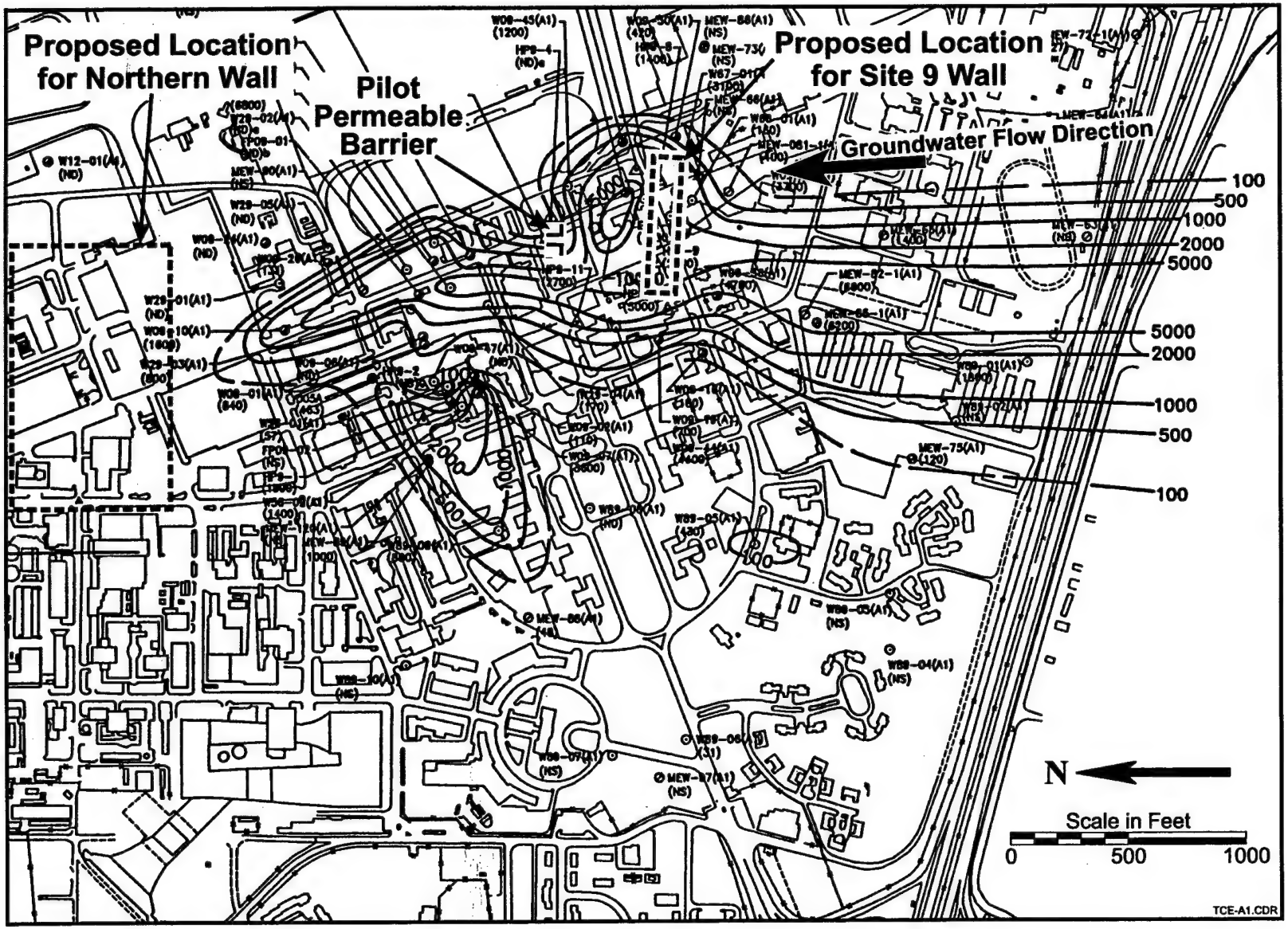

Figure 5-4a. West Side Plume Map for A1 Aquifer Zone at Moffett Field (Source: IT Corp., 1991)

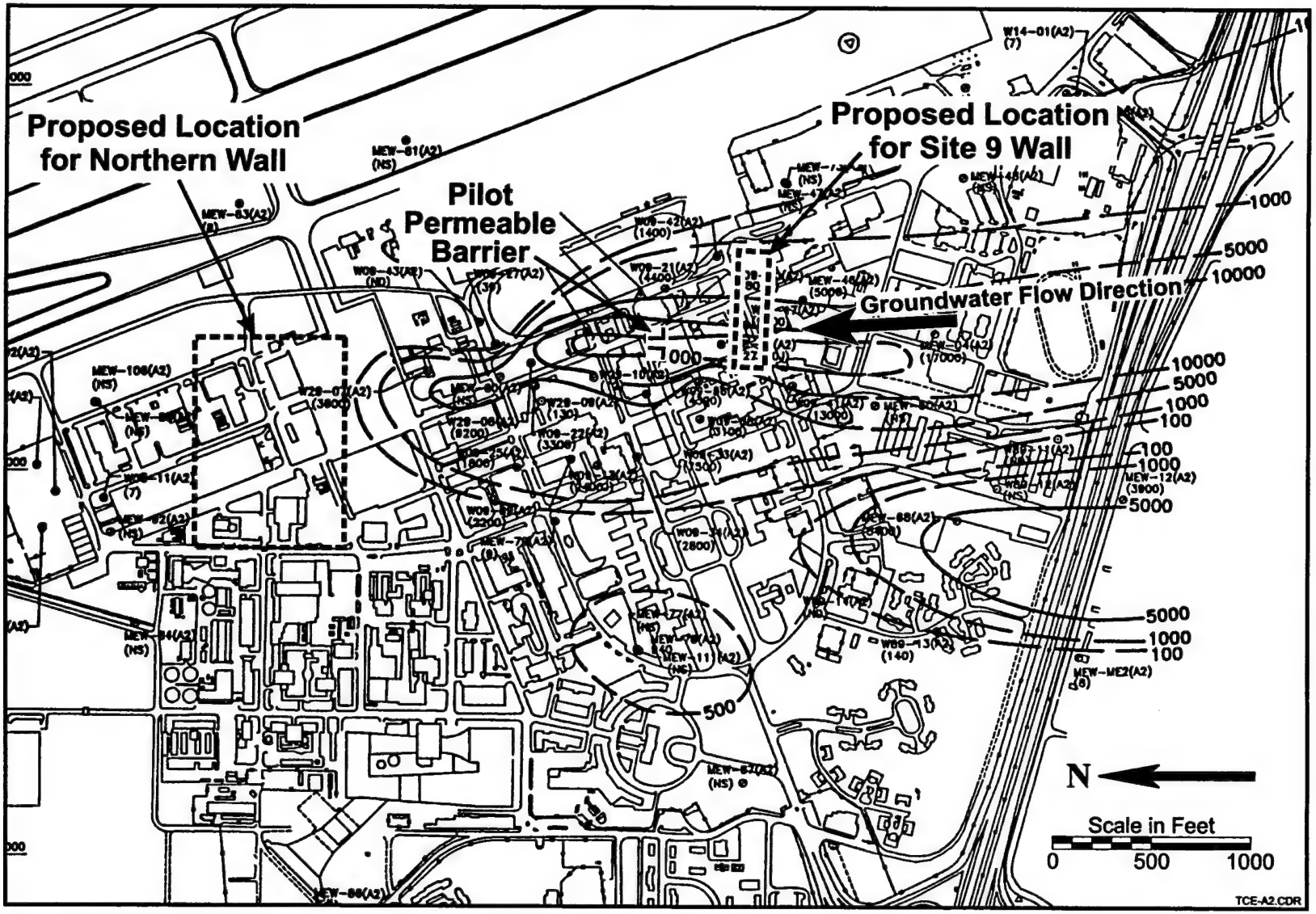

Figure 5-4b. West Side Plume Map for A2 Aquifer at Moffett Field (Source: IT Corp., 1991)

discussed in Section 6.2. Alternatively, coarse sand can be added along the upgradient edge of each gate to homogenize flow and contaminant loading.

5.2.1.3 Construction of the Barrier

Construction techniques selected will be determined mainly by the depth of the barrier. Assuming that the barrier will be around 65 feet deep and keyed into the aquitard below the A2 aquifer zone, a standard backhoe (used in the pilot barrier construction) will be inadequate for excavating the trenches. A clamshell or long-stick backhoe will be required, and this will involve higher cost. More cost-effective caisson-based installation of the gates has been tried at Somersworth and Dover Air Force Base (AFB) sites and appears promising.

Construction of the funnel will involve sheet piles (used in the pilot barrier) or slurry wall. The integrity of sheet pile joints at depths below 50 feet is somewhat uncertain. Also for a 65-foot depth, the sheet piles will most probably have to be transported in sections and welded on site. A slurry wall may be more cost-effective for the full-scale funnel.

5.2.1.4 Monitoring

The monitoring network for the full-scale barrier need not be extensive. Based on the guidelines for monitoring in this report and in other references (Gavaskar et al., 1998a; ITRC, 1997), an appropriate monitoring system for this width of plume at Moffett Field need involve only about 30 wells. Based on the illustration in Figure 5-5, the monitoring wells would be located as follows:

- Aquifer wells upgradient and downgradient of each gate (for evaluating water levels and water quality of the influent and effluent water)
- Wells at the tip of the outer wing walls (to evaluate flow bypass)
- Wells within the last 6 inches of the iron (for evaluating contaminant breakthrough from the reactive cell, if the barrier is placed within the plume)
- Wells upgradient and downgradient of the funnel walls (to evaluate contaminant breakthrough from the funnel).

Based on the trends observed during the demonstration, the frequency of monitoring should probably be once a year for all parameters. Target contaminants (TCE, PCE, *cis*-1,2-DCE, and vinyl chloride) could be monitored on a quarterly basis if required by the established basewide monitoring schedule. Water levels may be monitored more frequently in the first quarter if necessary to determine that the required flow pattern has been established. Once-a-year monitoring should be more than sufficient for inorganic parameters. These recommendations are expected to be consistent with the flexibility provided by recent regulatory guidance (ITRC, 1997).

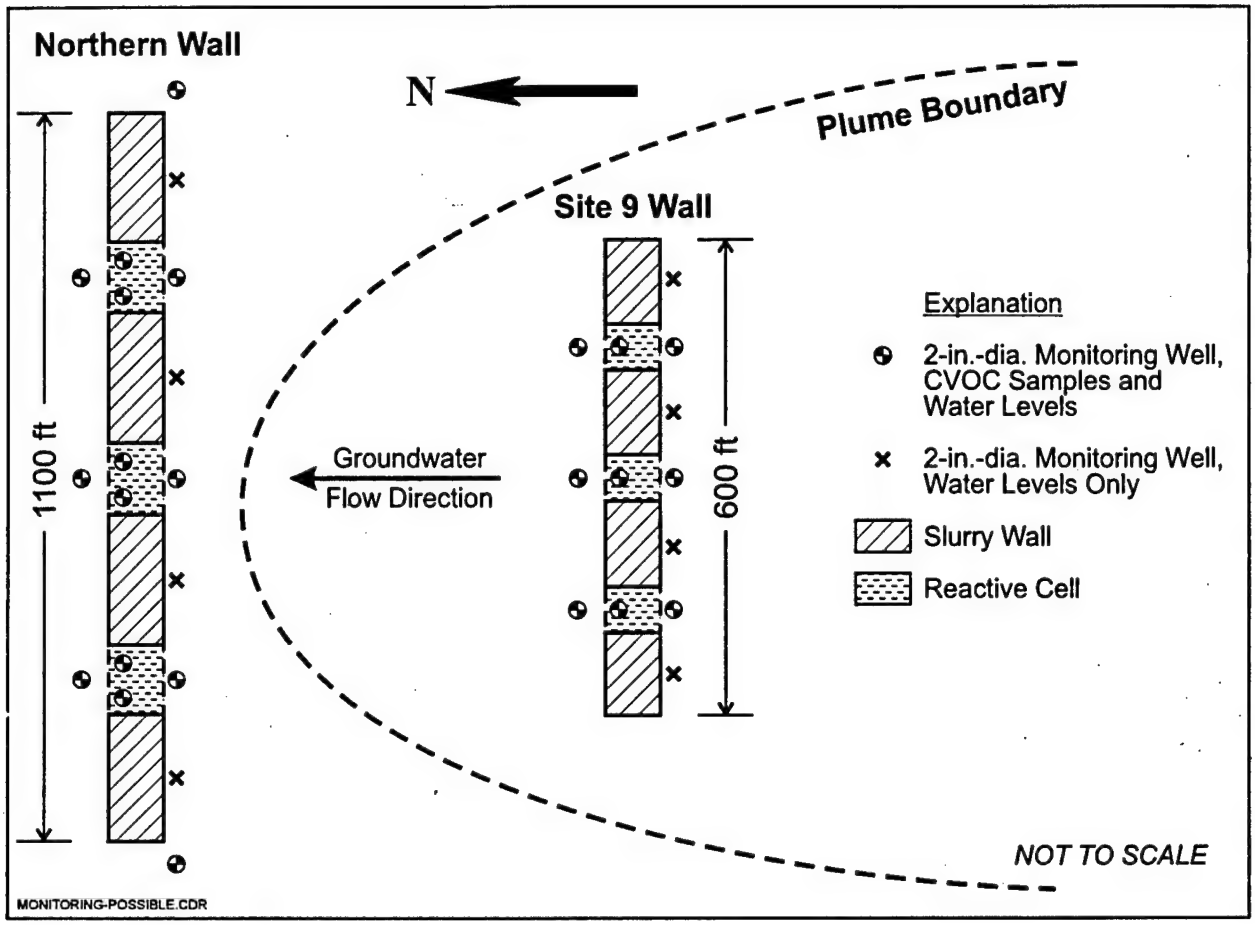

Figure 5-5. Schematic of a Possible Monitoring Well Network for Full-Scale Barrier

5.2.2 Cost Projections for Full-Scale Barrier at Moffett Field

One of the scenarios proposed by site representatives is used here, with some modifications, for presenting the scale-up guidance. In this scenario (Figure 5-1), the full-scale permeable barrier for the West Side plume at Moffett Field would be constructed in two sections. One section, called the Site 9 Wall, would be constructed just south of Building 88, and would capture and treat the highly concentrated portion of the contamination moving through a key sand channel. The other section, called the Northern Wall, would be constructed downgradient from the leading edge of the plume, and would control further migration of the plume. In all the scenarios, a barrier that extends down to the base of the A2 aquifer zone is envisioned. The aquitard in some locations can be up to 65 feet deep, making this barrier deeper than any full-scale barrier installed so far. This depth consideration increases the construction cost compared to other sites.

The dimensions of the barrier in this scenario are shown in Table 5-2 and Figure 5-1. The Site 9 Wall has three gates, each being 4 feet thick and 16 feet wide (48 feet total width). A 4-foot-thick slurry wall is used to form the funnel and the sides of the gates. Sheet piles will be used as

Table 5-2. Barrier Dimensions in a Proposed Full-Scale Permeable Barrier Scenario

Barrier/Section	Thickness (feet)	Total Width (feet)	Total Depth (feet)	Excavation Volume ($feet^3$)
Site 9 Wall				
▪ Reactive cells (3)	4	48	65	12,480
▪ Slurry wall (funnel and sides of gates)	4	552	65	71,760
Northern Wall				
▪ Reactive cells (3)	4	88	45	15,840
▪ Surry wall (funnel and sides of gates)	4	1,012	45	91,080
Total				
▪ **Reactive cells (6)**	4	136	65/45	28,320
▪ **Slurry wall**	4	1,564	65/45	162,840

temporary dividers at the transitions between each gate and funnel wall to retain the iron medium. The slurry wall width (in Table 5-2) includes the portions forming the funnel (516 feet) and portions forming the sides of the reactive cells or gates (36 feet). The 48 feet of gate and 516 feet of funnel provide a funnel-to-gate ratio of around 11:1. This ratio is higher than normal (6:1 being the maximum recommended at most sites). A high funnel-to-gate ratio could cause mounding of water on the upgradient side of the barrier and potential flow over the barrier (as at the Denver Federal Center site). However, at Moffett Field, because the funnels are placed in the low-conductivity interchannel deposits, in which the flows are low, a higher funnel:gate ratio may be justifiable. Hydrologic modeling and site characterization for the proposed location should assist in evaluating the feasibility of this design.

The Northern Wall is longer, but has similar features as the Site 9 Wall. Because the Northern Wall is at the edge of the plume and likely to encounter lower concentrations, the 4-foot thickness of iron may be sufficient. For the Site 9 Wall, which encounters higher concentrations within the plume, the proposed 4-foot thickness of iron should be reevaluated in light of the estimated required groundwater flow velocities. Final thicknesses of these two barrier sections will have to be determined based on the groundwater velocity estimates at these locations.

Table 5-3 summarizes the costs of this full-scale barrier illustration. Details for individual cost items are provided in Appendix G and were developed by NFESC based on preliminary projections by site representatives for the application (TetraTech EMI, personal communication). Technology licensing issues are being negotiated with ETI.

The present value method is used to account for the time value of money, at a real rate of return of 8%. This method accounts for the fact that, whereas capital costs are incurred immediately (and the money is lost for other uses), O&M costs are postponed to later years. The further down in time these cost items are incurred, the lower the present value of these costs because a lower amount of money has to be set aside today to meet future O&M obligations, if the interest earned during this period is taken into account. Therefore, the longer the barrier retains its performance, the lower will be the cost impact of the maintenance required.

Table 5-3. Projected Cost of A Full-Scale Permeable Barrier at Moffett Field[a]

Item	Sub-Total ($)	Total ($)
Capital Costs:		
Bench-scale tests		75,000[b]
Site characterization —Site characterization (hydrogeologic/chemical) —Other testing and welding	 100,000 17,820	117,820
Engineering Design, Modeling		100,000
Site Preparation		115,258
Construction —Mobilization —Trench installation —Gates completion (including iron medium) —Funnel completion —Demobilization —Surface restoration	 39,693 557,812 1,847,910 1,156,164 39,693 18,133	3,659,405
Monitoring wells installation		46,000
Spoils disposal on-site (trench soils)		16,370
Spoils disposal off-site (removed asphalt)		387,989
Site Restoration and Post-Construction Reports —Site cleanup —Removal of temporary utilities/facilities —Post-construction submittals	 6,032 81,021 35,000	122,053
Distributive costs (administrative, health & safety)		271,047[c]
Total Capital Cost		**4,910,942**
O&M Costs:		
Annual operations (monitoring cost incurred every year)		72,278
Maintenance (incurred every 10 years)		267,538 [d]

(a) Details of individual cost items are provided in Appendix G (Table G-1).
(b) Bench-scale testing for the pilot permeable barrier should be sufficient for implementing the full-scale barrier. However, the costs of additional bench-scale tests are included in this cost estimate, in the event they are needed.
(c) Distributive cost estimate does not include overhead costs and profit.
(d) Rule-of-thumb estimate of 25% of iron medium cost every 10 years.

To obtain some perspective on the economic benefits of the permeable barrier, the total cost of the permeable barrier was compared with the total cost of the pump-and-treat option. The cost of the pump-and-treat system for the West Side plume was estimated by NFESC, based on projections made in a long-term action plan by site representatives (PRC, 1996b). Table 5-4 summarizes the comparison of permeable barrier and pump-and-treat options. As seen in this table, the permeable barrier requires a higher initial capital investment. However, over time, the O&M savings keep accruing and the permeable barrier breaks even in approximately the eighth year, based on these calculations.

While the present value method is a useful way for analyzing cost differences over an extended period of time, it may not be appropriate in some instances. For example, when the operation is financed by the government, it is not feasible to consider that a portion of the capital budget can be invested for future profit. Therefore, it is worthwhile to compare total costs of a permeable

Table 5-4. Present Value Cost Comparison of Permeable Barrier and Pump-and-Treat Options at Moffett Field[a]

Years of Operation	Item	Permeable Barrier	Pump & Treat System
0	Capital cost	$4,910,943[b]	$1,412,086[c]
Today's estimate	Annual O&M cost	$72,278	$694,746
Today's estimate	Barrier maintenance every 10years	$267,538	Not applicable
Expected	Real discount factor	8%	8%
5	PV of capital and O&M cost	$5,199,528	$4,186,005
8	PV of capital and O&M cost	$5,326,299	$5,404,540
10	PV of capital and O&M cost	$5,519,856	$6,073,888
20	PV of capital and O&M cost	$5,801,901	$8,233,205
30	PV of capital and O&M cost	$5,932,542	$9,233,386
40	PV of capital and O&M cost	$5,993,054	$9,696,663
50	PV of capital and O&M cost	$6,021,083	$9,911,251

(a) Details of present value calculations provided in Table G-2 in Appendix G.
(b) Construction cost is higher at Moffett Field compared to other sites because of the greater depth involved.
(c) Based on modified estimates prepared by NFESC and site representatives for an example scenario.

barrier with a pump & treat system in a direct manner. Table 5-5 summarizes total costs for these operations, wherein the respective O&M costs are factored in annually and barrier maintenance cost is factored in every 10 years; calculations of cost savings (or additional costs) for the permeable barrier are shown in the last column. Initial costs are same as shown in Table 5-4 (note the additional startup cost of $3.5 M). However, using the total cost calculation

Table 5-5. Total Cost Comparison of Permeable Barrier and Pump-and-Treat Options at Moffett Field[a]

Years of Operation	Item	Permeable Barrier	Pump & Treat System	Cost Savings for Permeable Barrier
0	Capital ~~Cost~~ Investment	$4.9 M	$1.4 M	-$3.5 M
Today's estimate	Annual O&M cost	$72 K	$695 K	Not applicable
Today's estimate	Barrier maintenance cost every 10 years	$268 K	Not applicable	Not applicable
6	Capital and O&M cost	$5.3 M	$5.6 M	$0.2 M
10	Capital and O&M cost	$5.9 M	$8.4 M	$2.5 M
20	Capital and O&M cost	$6.9 M	$15 M	$8.4 M
30	Capital and O&M cost	$7.9 M	$22 M	$14 M
40	Capital and O&M cost	$8.9 M	$29 M	$20 M
50	Capital and O&M cost	$9.8 M	$36 M	$26 M

(a) Details of cost calculations provided in Table G-3 in Appendix G.
(b) Construction cost is higher at Moffett Field compared to other sites because of the greater depth involved.
(c) Based on modified estimates prepared by NFESC and site representatives for an example scenario.

method, the permeable barrier breaks even in approximately 6 years—2 years sooner than predicted using the present value method (see Table 5-4). More significantly, actual cost savings are much greater by the total cost method than by the present value method. After 50 years, the cost savings are estimated at $26 M.

In general, given the uncertainties in the estimates, if the barrier can retain its performance for approximately 8 years without requiring any maintenance, it will be more cost-effective than an equivalent pump-and-treat system. The oldest running barrier at Borden has been operating for 7 years without any sign of declining performance. Similarly, monitoring data from the Intersil Semiconductor Site in Sunnyvale, California, indicate that the full-scale barrier there continues to operate at design performance specifications since it was installed in January 1995. The permeable barrier replaced an existing pump-and-treat system that was installed in 1987, and was being maintained at significant cost. The permeable reactive barrier was shown to have recovered its capital cost of $770,000 in less than 3 years.

At the Moffett Field pilot barrier, so far, there is no indication of any impending decline in performance. For plumes that persist for long periods of time (several years or decades), the permeable barrier technology offers a promising option.

Moreover, the above cost-benefit analysis does not take into account the value of the intangible benefits to be gained from using the permeable reactive barrier technology, such as the total absence of aboveground structures, and the ability to continue using the site as a parking lot. These added benefits increase the attractiveness of the permeable barrier technology.

6. Implementation Issues

This section examines the lessons learned from this demonstration and their implications for full-scale application at Moffett Field and other sites.

6.1 Cost Observations

The demonstration results indicate that the cost of a permeable barrier is closely linked to the selected design and construction method. The following issues should be considered to optimize barrier application costs:

- Conducting adequate site characterization and modeling to improve the design and lower capital cost. This is because the greater the certainty in the hydrogeologic parameter estimates, the better the capability of reducing the dimensions and applying smaller safety factors in the barrier design. Also, although the barrier offers a more cost-effective option compared to a pump-and-treat system, the risk and consequences of an inadequate design are greater for the barrier, because of the complexity of the subsurface and the permanent nature of the installation.

- The relative cost of using a continuous barrier versus a funnel-and-gate system should be evaluated at every site based on site characteristics and geotechnical considerations. With the cost of iron falling to $350/ton over the last few years, the cost differential between installing a continuous reactive barrier versus installing an intervening slurry wall or sheet pile funnel walls may be favorable for the continuous reactive barriers at some sites.

- Different construction methods may be cost-effective for different sites. All these techniques should be considered for the construction. Innovative techniques, such as caisson installations and continuous trenchers, offer potential for monetary savings. The choice of slurry wall versus sheet pile for funnel walls should also be evaluated at every site.

- The monitoring network for the barrier should be discussed with regulators as early as possible in the process. Indications from Moffett Field and other sites are that both the number of monitoring points and the monitoring frequency requirements of the barrier are relatively low, and can be reduced further over the years.

- Research is underway for investigating acids or chelating agents as flushing agents to regenerate the reactivity and hydraulic properties of barriers after long-term exposure to groundwater. If successful, this research holds the promise of lower maintenance costs in the future. Otherwise, there is some uncertainty about eventual maintenance costs.

- The comparison of the barrier cost with the cost of other options, such as pump-and-treat systems, should be carefully evaluated. Intangible benefits, such as the absence of aboveground structures with the permeable barrier option, should be considered.

6.2 Performance Observations and Lessons Learned

The Moffett Field demonstration provided several key indications of the site and technology factors driving barrier performance. It is important to take these factors into account when planning a full-scale permeable barrier at Moffett Field or other sites.

The following factors drive the performance of the barrier and should be taken into consideration during design and implementation at this and other sites:

- **Nature of the Aquitard**. A competent aquitard is required so that the barrier can be properly keyed in. If a full-scale barrier at Moffett Field is installed down to the bottom of the A2 aquifer zone, the aquitard encountered is more competent than the A1/A2 aquitard underlying the pilot barrier. At other sites, site characterization should be used to ensure that the barrier can be keyed at least 1 foot into the aquitard.

- **Target Contaminants**. Bench-scale testing was a good predictor of field performance for this demonstration. Bench-scale column tests should be used to ensure that the target contaminant at the site can be degraded with the reactive medium used, and that contaminant half-lives, in conjunction with the groundwater velocity (or residence time) estimates, provide an economically feasible option. In other words, the half-life and residence time estimates should indicate a reasonable reactive cell thickness. The uncertainties in estimating groundwater velocities should be taken into account by incorporating appropriate ranges and safety factors.

- **Aquifer Heterogeneities**. No aquifer is truly homogeneous. However, at some sites (such as Dover AFB, Denver Federal Center, etc.), heterogeneities may have a limited impact on the flow system. At such sites, the flow system can be successfully modeled during design on the basis of limited site characterization and a simple 2-D flow model. However, at some sites, such as Moffett Field, heterogeneities play a key role in groundwater movement and contaminants transport. At such sites, adequate site characterization should be done to enable a multi-layered simulation of the flow system. This involves a good understanding of the geologic, hydrologic, and chemical distribution in the subsurface. A better model would allow more optimal design of the location, configuration, and dimensions of the barrier. At Moffett Field, given the fact that the full-scale barrier may be implemented at a different location from the pilot, the new location(s) will have to be adequately characterized to identify the exact extent of the sand channels. Existing site-wide sand channel maps do not have the localized resolution needed for a good barrier design. New site characterization techniques that use a CPT rig or GeoProbe™ are an efficient way of sampling a large number of locations in a relatively short time.

- **Geotechnical Considerations.** The presence of aboveground buildings and subsurface utilities in several areas of Moffett Field overlying the plume limits the possible locations of the barrier. Such areas need to be identified. On the other hand, the barrier can be designed to overcome some of these challenges through appropriate configuration and construction techniques. In terms of configuration, the use of a funnel-and-gate system versus a continuous reactive barrier should be reexamined. In the absence of subsurface utilities, a continuous reactive barrier may prove to be more cost-effective compared to a funnel-and-gate system, although the reactive medium may not be optimally used. A funnel-and-gate system may be more suitable if there are intervening utilities at the desired location. On the other hand, a funnel-and-gate system involves funnel-gate transitions that increase the complexity of construction.

- **Groundwater Velocity Estimation**. Due to the heterogeneous nature of the site and because of the limitations of the measurement methods, the groundwater velocity for the Moffett Field demonstration was estimated within a relatively wide range. This may continue to be a challenge at Moffett Field because of the nature of the site. However, a narrower range may provide a more cost-effective design if the safety factors can be minimized. For example, at the current location of the pilot barrier, if the velocity range can be narrowed down from 0.2 to 2 feet/day to a narrower range of about 0.2 to 1.5 feet/day, then a lower safety factor and therefore a lower thickness of the reactive cell may be possible.

- **Projections of Contaminant Concentrations Reaching the Barrier**. The pilot barrier design at Moffett Field was based on maximum concentrations of up to 3,000 µg/L of TCE and 600 µg/L of *cis*-1,2-DCE that were present in the vicinity of the barrier at the time of the site characterization. However, if the barrier is expected to be operational over a period of 15 or 30 years, and the plume continues to develop during this period, the concentrations encountered at the barrier could be much higher. It is important to ensure that there is a sufficient safety factor incorporated in the design thickness of the reactive cell to account for the increased concentrations. This is especially the case if the increased concentrations relate to *cis*-1,2-DCE or vinyl chloride or some other relatively recalcitrant contaminant.

- **Role of the Pea Gravel.** In the pilot barrier, the pea gravel was helpful in homogenizing the flow and the influent contamination, providing a well-mixed location for monitoring influent and effluent concentrations, and increasing the porosity and hydraulic conductivity of the gate. However, during the demonstration, water in the downgradient pea gravel had higher concentrations of target contaminants than were measured in the reactive cell. This has been explained by admixture of untreated water from beneath the reactive call and around the wing walls with treated water flowing out of the reactive cell. Furthermore, desorption of contaminants from clayey particles in the downgradient aquifer also probably account for the increase in contaminants in the downgradient pea gravel. This may not be a concern if the barrier is placed outside the boundary of the plume and it is capturing the entire

plume. Additionally, the presence of the pea gravel does tend to make the flow system more complex by introducing several sharp conductivity and porosity contrasts (aquifer-pea gravel-iron-pea gravel-aquifer). For example, there was some indication during the demonstration that groundwater flows more easily into the pea gravel than out of it, leading to some possibility of water accumulation during transient high flow conditions (e.g., after a rainfall event). The pea gravel sections could be avoided during construction, with associated cost savings. Alternatively, coarse sand in a size range similar to that of the iron may be used to homogenize flow and contaminant loading.

- **Monitoring Network.** The monitoring network need not be as extensive as the one used for the demonstration. Based on the lessons learned from this demonstration and the guidance in other references (Gavaskar et al., 1998a; ITRC, 1997), the monitoring network needs to include sufficient wells to be able to evaluate the following:

  - Possible breakthrough of contaminants through the reactive cell (wells in the last 6 inches of the iron or in the aquifer downgradient from the reactive cell or gate)
  - Possible plume bypass around or over the barrier (wells at the tips of the funnel wing walls and in the downgradient aquifer)
  - Possible breakthrough of contaminants through the funnel walls (wells upgradient and downgradient of the funnel walls).

- **Monitoring Frequency.** Monitoring once a year seems adequate based on the trends observed during this demonstration. Water levels and target contaminants may be monitored more frequently in the first quarter or first year until the performance of the barrier is established.

- **Geochemical Characteristics of the Site Groundwater.** In general, sites with high DO or high TDS in the groundwater are likely to exhibit a higher potential for precipitate formation. However, other factors, such as level of alkalinity buffer and size of precipitate particles formed, may affect the degree to which DO and TDS affect barrier performance over the long term. Colloidal precipitate particles could flow out of the reactive cell with the groundwater flow. At the Dover AFB barrier site, instead of using upgradient pea gravel, the gate includes a pretreatment zone (PTZ) consisting of a 10:90 iron-sand mixture (Gavaskar et al., 1997b). At this high-DO site, the PTZ scrubs out the DO from the water before it enters a reactive cell containing 100% iron. The iron-sand zone allows front-end precipitates (formed by the fast reaction between iron and oxygen) to be spread out over a longer path. This avoids the kind of front-end precipitate buildup observed in laboratory column tests. This front-end precipitation in the first few inches of the iron may cause the reactive cell to clog much faster than if the precipitates were spread over a longer path. Carbonate precipitates are formed by slower reactions than the reaction between iron

and oxygen; thus, carbonate precipitates tend to be distributed over the bulk of the iron in the reactive cell, rather than in the first few inches.

6.3 Regulatory Issues

The predominance of groundwater contamination and the lack of methods to treat the contamination in an effective and economical manner is a problem of great concern to the U.S. EPA and the regulated community. The regulators are especially concerned about the issue of chlorinated solvent contamination in groundwater and its potential for persisting for hundreds of years despite efforts to pump and treat it. The U.S. EPA has identified six abiotic technologies that are emerging as possible cleanup remedies for recalcitrant sites (U.S. EPA, 1995). Treatment walls or permeable barrier technology is one of them.

At the Remediation Technologies Development Forum (RTDF), Permeable Reactive Barriers (PRB) Action Team meetings in December 1997 and April 1998, the group was optimistic about the growing acceptance of the permeable barrier technology by the regulators. The first field barrier at Borden has been operating now for more than 7 years without exhibiting any signs of declining performance. At a former semiconductor manufacturing facility (Intercil, Inc.) in Sunnyvale, California, regulators allowed the installation of a full-scale iron permeable barrier to address a chlorinated solvent plume. The barrier has been in operation since December 1994 without any breakthrough of contaminants or their byproducts. Compliance monitoring is conducted at the Intercil site in accordance with regulatory requirements established by the California Regional Water Quality Control Board. At least three other full-scale barriers are now under construction (ETI, 1998).

The Interstate Technology and Regulatory Cooperation (ITRC) Working Group, a group that includes regulators from various states interested in certifying innovative technologies, has formed a subgroup to review permeable barrier applications. This subgroup held its first meeting in Philadelphia in September 1996. The ITRC subgroup recently published a regulatory guidance for permeable barriers designed to remediate chlorinated solvents (ITRC, 1997).

In December of 1993, the Navy and EPA reached an agreement in which the Moffett Field (West Side) contaminant plume was considered part of a regional plume. A pump-and-treat system is being installed in 1998 to remediate the contaminant plume as a requirement of the Record of Decision (ROD). With the successful demonstration of the pilot permeable barrier at Moffett Field, technical and cost hurdles have been mostly overcome. However, administrative hurdles remain because each of the more than ten potentially responsible parties (PRPs) subject to the ROD will now have to agree to a permeable barrier remedy instead, and the EPA will have to reopen the ROD to public scrutiny. The Navy's goal is to implement the permeable barrier in coordination with the existing pump-and-treat system. Once the effectiveness of the permeable barrier has been demonstrated, the pump-and-treat system will be shut down in favor of the long-term cost savings in reduced operation and maintenance offered by the permeable barrier. The shutdown of the pump-and-treat system will be done in coordination with U.S. EPA and the other PRPs.

In general, most regulators and site managers are convinced about the contaminant degradation capabilities of permeable reactive barriers. Given sufficient residence time, the reactive medium does degrade target contaminants to desired levels. This can be backed up with bench-scale column tests. Hydraulic performance and longevity are the two issues that continue to generate some uncertainty. Flow (plume) bypass around and above the barrier has been experienced at some sites (Denver Federal Center and Somersworth sites), at least under transient conditions. Although adequate site characterization and a good design can minimize the potential for such occurrences, some uncertainty remains. There are also limitations based on the amount sites are willing to spend to characterize subsurface complexities. On the other hand, there is a growing realization that pump-and-treat systems may have limitations too, and are likely to cost more in the long term at many sites.

6.4 Research Needs

Based on some issues that were difficult to resolve during the Moffett Field demonstration, the following areas may benefit from further investigation:

- Hydraulic performance of barriers. Although the Moffett Field demonstration has contributed to a better understanding of how subsurface characteristics can be defined and used to design a suitable barrier system, ensuring the hydraulic capture of the plume and providing sufficient residence time in the reactive cell continue to be a challenge. Similar evaluations at a number of different sites may help to generate a larger database of the relationship between the aquifer characteristics and the design features of a permeable barrier. Methods to better define localized groundwater flow velocity and direction, especially at sites with slow-moving groundwater, may enable a better design. Design configurations and safety factors required to handle these and other uncertainties, such as seasonal variations in flow, need to be studied at several sites.

- Longevity of the barrier. Actual field data showing a decline in performance for an existing barrier are lacking. It is hoped that performance data for existing barriers will continue to be collected, so that in several more years any changes in performance of these barriers will be recognized. For a better understanding of the economics of the reactive barrier technology and for greater acceptance by site managers, it would be beneficial to improve the level of understanding in this area. The Moffett Field demonstration indicates that although precipitation is taking place along expected lines, not all the precipitate particles stay within the barrier. If this characteristic can be confirmed, it would have positive implications for the technology. A more focused effort, perhaps by examining appropriately filtered and unfiltered samples of the groundwater exiting field reactive barriers, would help confirm these preliminary indications. Accelerated column tests have been proposed but they do not have the same dynamics as a field system for the study of colloidal transport. Additional iron cores could be collected at Moffett Field and other sites on an annual or biannual basis to evaluate changes in iron surface deposits. Continued water level and selected

chemical measurements on a semi-annual or annual basis could be another way of tracking any effects due to a buildup of precipitates.

- Regeneration of the reactive medium. Although site managers expect that some type of barrier maintenance will eventually be required, it is not yet clear what form this effort will take. Excavation and replacement of the iron medium may be a relatively expensive option. A better option, if it works, would be to flush the reactive medium with an appropriate solution that dissolves the precipitates and regenerates the reactivity and hydraulic characteristics of the medium. Some initial research has been undertaken (Gavaskar et al., 1998b; Focht, 1998), but this issue will have to be examined further.

- Bimetallic media. Degradation rates for CVOCs may be increased by certain bimetallic media in which zero-valent iron is contacted with other metals. Some bimetal systems, such as a mechanical mixture of iron and copper, act as galvanic couples and enhance the degradation rate by increasing electron activity. Other systems, such as iron sputtered with palladium, enhance degradation through the catalytic effect of the palladium. Nickel also appears to catalyze CVOC degradation when in contact with iron. However, all bimetallic systems are subject to much greater costs than granular iron, so there will always be a trade-off between reduced construction costs for a smaller reactive cell, and a higher materials cost (relative to granular iron) for a more highly reactive medium.

7. References

7.1 Key References

(Instrumental to completion of project)

Battelle. 1996a. *Groundwater Modeling for Evaluation of a Pilot-Scale Permeable Barrier at Moffett Federal Airfield.* Prepared for NFESC. November.

Battelle. 1996b. *September 1996 Monitoring Report for the Pilot Permeable Barrier at Moffett Field.* Prepared for NFESC. December.

Battelle. 1997a. *Performance Monitoring Plan for a Pilot-Scale Permeable Barrier at Moffett Federal Airfield in Mountain View, California.* Prepared for the Naval Facilities Engineering Service Center. July.

Battelle. 1997b. *June 1996 Monitoring Report for the Pilot Permeable Barrier at Moffett Field.* Prepared for NFESC. January.

Battelle. 1997c. *January 1997 Monitoring Report for the Pilot Permeable Barrier at Moffett Field.* Prepared for NFESC. May.

Battelle. 1997d. *April 1997 Monitoring Report for the Pilot Permeable Barrier at Moffett Field.* Prepared for NFESC. September.

Battelle. 1997e. *Field Tracer Application to Evaluate the Hydraulic Performance of the Pilot-Scale Permeable Barrier at Moffett Federal Airfield.* Prepared for NFESC, Port Hueneme, CA. October.

Battelle. 1998a. *Field Tracer Application to Evaluate the Hydraulic Performance of the Pilot-Scale Permeable Barrier at Moffett Federal Airfield.* Prepared for NFESC, Port Hueneme, CA. February.

Battelle. 1998b. *Core Testing Report for the Pilot Permeable Barrier at Moffett Field.* Prepared for NFESC. February.

Battelle. 1998c. *October 1997 Monitoring Report for the Pilot Permeable Barrier at Moffett Field.* Prepared for NFESC. April.

International Technology Corporation. 1993. *West Side Groundwater Characterization Report, NAS Moffett Field, California.* March.

IT Corporation, see International Technology Corporation.

McDonald, M.G. and A.W. Harbaugh. 1988. *A Modular Three-Dimensional Finite-Difference Ground-Water Flow Model.* Techniques of Water-Resources Investigations 06-A1, U.S. Geological Survey.

Naymik, T.G. and N.J. Gantos. 1995. Solute Transport Code Verification Report for RWLK3D. Internal Draft. Battelle Memorial Institute, Columbus, OH.

PRC Environmental Management, Inc. 1993. Draft West Side Aquifers Field Investigation Technical Memorandum, Naval Air Station Moffett Field, California. March.

PRC Environmental Management, Inc. 1995. *Iron Curtain Bench-Scale Study Report, Moffett Federal Airfield, California.* Prepared by PRC Environmental Management, Inc. for the Department of the Navy, Contract No. N62474-88-D-5086, Task Order No. 0237. October.

PRC Environmental Management, Inc. 1996a. *Naval Air Station Moffett Field, California, Iron Curtain Area Groundwater Flow Model.* June.

PRC Environmental Management, Inc. 1996b. *Moffett Federal Airfield California West-Side Aquifers Treatment System Phase 2 Cost Opinion.* Prepared for the Department of the Navy under Comprehensive Long-Term Environmental Action Navy (CLEAN I).

PRC Environmental Management, Inc. and Montgomery Watson. 1996. August 1995 Draft Quarterly Report, Moffett Federal Airfield, California. June.

PRC, see PRC Environmental Management, Inc.

7.2 Associated DoD Contracts and Records and Their Locations

Gavaskar, A., N. Gupta, B. Sass, T. Fox, R. Janosy, K. Cantrell, and R. Olfenbuttel. 1997a. *Design Guidance for Application of Permeable Barriers to Remediate Dissolved Chlorinated Solvents.* Prepared for Armstrong Laboratory/Environics Directorate. Contract No. F08637-95-D-6004.

Gavaskar, A., N. Gupta, B. Sass, R. Janosy, T. Fox, J. Hicks, and W-S. Yoon. 1997b. *Design/Test Plan Permeable Barrier Demonstration at Area 5, Dover AFB.* Strategic Environmental Research and Development Program, Washington, DC.

7.3 General References

Burris, D.R., T.J. Campbell, and V.S. Manoranjan. 1995. "Sorption of Trichloroethylene and Tetrachloroethylene in a Batch Reactive Metallic Iron-Water System." *Environ. Sci. Technol. 29* (11): 2850-2855.

Deng, B., T.J. Campbell, and D.R. Burris. 1997. "Hydrocarbon Formation in Metallic Iron/Water Systems." Accepted for publication in *Environ. Sci. Technol.*

EPA, see U.S. Environmental Protection Agency.

ETI. 1998. Personal communication from John Vogan.

Focht, R.M. 1998. "Enhanced Zero-Valent Iron Degradation of Chlorinated Solvents Using Ultrasonic Energy." In *Proceedings of the First International Conference on Remediation of Chlorinated and Recalcitrant Compounds.*

Gavaskar, A., N. Gupta, B. Sass, R. Janosy, and D. O'Sullivan. 1998a. *Permeable Barriers for Groundwater Remediation.* Battelle Press, Columbus, OH.

Gavaskar, A., B. Sass, E. Drescher, L. Cumming, D. Giammar, and N. Gupta. 1998b. "Enhancing the Reactivity of Permeable Barrier Media." In *Proceedings of the First International Conference on Remediation of Chlorinated and Recalcitrant Compounds.* In press.

Gillham, R.W. 1993. Cleaning Halogenated Contaminants from Groundwater. U.S. Patent No. 5,266,213, Nov. 30.

Gillham, R.W. 1996. "In-situ Treatment of Groundwater: Metal-Enhanced Degradation of Chlorinated Organic Contaminants." In M.M. Aral (Ed.), *Advances in Groundwater Pollution Control and Remediation*, pp. 249-274. Kluwer Academic Publishers.

Hardy, L.I. and R.W. Gillham. 1996. "Formation of Hydrocarbons from the Reduction of Aqueous CO_2 by Zero-Valent Iron." *Environ. Sci. Technol. 30*(1): 57-65.

International Technology Corporation. 1991. *Phase I Characterization Report, Naval Air Station Moffett Field, Vols. 1-5.* April.

International Technology Corporation. 1992. *Remedial Investigation Report, Operable Unit 4, NAS Moffett Field, CA.* August.

Interstate Technology & Regulatory Cooperation. 1997. *Regulators Guidance for Permeable Barrier Walls Designed to Remediate Chlorinated Solvents.* December.

ITRC, see Interstate Technology & Regulatory Cooperation.

Naval Facilities Engineering Service Center. 1998. Locations of sand channels at Moffett Field based on *unpublished* documents obtained from NFESC.

NFESC, see Naval Facilities Engineering Service Center.

Orth, W.S. and R.W. Gillham. 1996. "Dechlorination of Trichloroethene in Aqueous Solution Using Fe(0)." *Environ. Sci. Technol. 30*(1): 66-71.

Parkhurst, D.L. 1995. *User's Guide to PHREEQC-A Computer Program for Speciation, Reaction-Path, Adjective-Transport, and Inverse Geochemical Calculations.* Water-Resources Investigations Report 95-4227. U.S. Geological Survey.

Puls, R.W., R.M. Powell, and C.J. Paul. 1995. "In Situ Remediation of Ground Water Contaminated with Chromate and Chlorinated Solvents Using Zero-Valent Iron: A Field Study." 209th National Meeting Anaheim, CA. Preprint Extended Abstracts, Division of Environmental Chemistry, *35*(1):788-791.

Roberts, A.L., L.A. Totten, W.A. Arnold, D.R. Burris, and T.J. Campbell. 1996. "Reductive Elimination of Chlorinated Ethylenes by Zero-Valent Metals." *Environ. Sci. Technol.30*(4):2654-2659.

Remediation Technologies Development Forum. 1998. Web site for Permeable Reactive Barriers Action Team. Available from http://www.rtdf.org/barriers.htm

RTDF, see Remediation Technologies Development Forum.

Sivavec, T.M. 1997. Personal communication from T. Sivavec, General Electric Corporate Research and Development, Schenectady, NY.

Sivavec, T.M., and D.P. Horney. 1995. "Reductive Dechlorination of Chlorinated Ethenes by Iron Metal." Presented at the 209th ACS National Meeting, Anaheim, CA. April 2-6.

U.S. Environmental Protection Agency. 1995. *In-situ Remediation Technology Status Report: Treatment Walls.* EPA 542-K-94-004. U.S. EPA, Office of Solid Waste and Emergency Response, Washington, DC. April.